AD_____

Award Number: W81XWH-11-1-0356

TITLE: *New Treatments for Drug-Resistant Epilepsy that Target Presynaptic Transmitter Release*

PRINCIPAL INVESTIGATOR: Emilio R. Garrido Sanabria, MD, PhD

CONTRACTING ORGANIZATION: University of Texas at Brownsville
Brownsville, TX 78520-4956

REPORT DATE: July 2015

TYPE OF REPORT: Addendum to Final

PREPARED FOR: U.S. Army Medical Research and Materiel Command
Fort Detrick, Maryland 21702-5012

REPORT DOCUMENTATION PAGE

Form Approved
OMB No. 0704-0188

1. REPORT DATE : July 2015

2. REPORT TYPE:
Addendum to Final

3. DATES COVERED
15 April 2014 - 14 Apr 2015

4. TITLE AND SUBTITLE
New Treatments for Drug-Resistant Epilepsy that Target Presynaptic Transmitter Release

5a. CONTRACT NUMBER
W81XWH-11-1-0356

5b. GRANT NUMBER **W81XWH-11-0356**

5c. PROGRAM ELEMENT NUMBER

6. AUTHOR(S)
Emilio Garrido-Sanabria, MD, PhD

E-Mail: emilio.garrido@utb.edu

5d. PROJECT NUMBER

5e. TASK NUMBER

5f. WORK UNIT NUMBER

7. PERFORMING ORGANIZATION NAME(S) AND ADDRESS(ES)

University of Texas at Brownsville
One West University Blvd.
Brownsville, Texas 7852

8. PERFORMING ORGANIZATION REPORT NUMBER

9. SPONSORING / MONITORING AGENCY NAME(S) AND ADDRESS(ES)
U.S. Army Medical Research and Materiel Command
Fort Detrick, Maryland 21702-5012

10. SPONSOR/MONITOR'S ACRONYM(S)

11. SPONSOR/MONITOR'S REPORT NUMBER(S)

12. DISTRIBUTION / AVAILABILITY STATEMENT
Approved for Public Release; Distribution Unlimited

13. SUPPLEMENTARY NOTES

14. ABSTRACT

We developed electrophysiological and pharmacological studies to investigate the effects of levetiracetam, topiramate and carbamazepine in excitatory (glutamatergic) synaptic transmission onto granule cells in the dentate gyrus from slices of control and pilocarpine-treated epileptic rats and mice. We discover a novel presynaptic action of topiramate reducing the frequency of mEPSC in a dose-dependent manner while the inhibitory action on mEPSC amplitude was also present in both control and epileptic slices. Hence, our findings indicate that topiramate exert, at least in part a presynaptic action inhibiting the release of glutamate.We detected that levetiracetam inhibits the spontaneous glutamate release (mEPSC frequency) in control and epileptic rats and mice. In addition, levetiracetam was more effective in reducing excitatory synaptic transmission onto dentate granule cells in slices from chronically epileptic rats while no effect was detected on the amplitude of mEPSC indicating no action of post-synaptic AMPA receptors. We also detected that LEV increase the GABAergic inhbnitory transmission onto dentate granule cells by increasing the frequency of mIPSCs. These data indicate that presynaptically acting drugs as levetiracetam may become a key piece in the arsenal of antiepileptic drugs in mesial temporal lobe epilepsy. Thereby, screening for a presynaptic action site may be part of the strategy to discover novel and effective antiepileptic drugs.

15. SUBJECT TERMS
Epilepsy, Presynaptic, antiepileptic drugs, levetiracetam, topiramate, carbamazepine, synaptic vesicle proteins, seizures.

16. SECURITY CLASSIFICATION OF:			**17. LIMITATION OF ABSTRACT**	**18. NUMBER OF PAGES**	**19a. NAME OF RESPONSIBLE PERSON**
a. REPORT	**b. ABSTRACT**	**c. THIS PAGE**			USAMRMC
U	U	U	UU	**144**	**19b. TELEPHONE NUMBER** *(include area code)*

Table of Contents

1. Introduction

Post-traumatic epilepsy (PTE) is a major long-term complication of traumatic brain injuries (TBIs), which are often suffered by members of the Armed Forces. PTE usually develops within five years of a head injury, and it is often expressed as medically intractable hippocampal epilepsy. Although there are a variety of causes of traumatic epilepsy, the resulting chronic neurological condition is characterized by common features, including recurrent spontaneous seizures, neuronal damage, mesial temporal lobe epilepsy (MTLE) in ~30% of patients, and resistance to available anticonvulsant drugs. Therefore, it is of critical importance to develop novel models to study post-traumatic epilepsy in order to facilitate the discovery of new treatments. **Background:** during epileptogenesis, seizure-related functional and structural reorganization of neuronal circuits leads to both hyperexcitability of glutamatergic neurons and defective inhibition. While many postsynaptic alterations have been demonstrated, there is surprisingly little known concerning dysfunction of presynaptic transmitter release machinery in epilepsy. The recent successful introduction of the antiepileptic drug levetiracetam (LEV), which acts on presynaptic molecular targets, suggests that controlling dysregulation of presynaptic function could be a promising new therapeutic target for the treatment of unresponsive epilepsies. While LEV has been shown to bind to both the synaptic vesicle protein SV2a and N-type Ca^{2+} channels, its precise mechanism of action is not understood. Recent studies have found that severe seizures can down-regulate the expression of both SV2a and the group II metabotropic glutamate (mGluRII) autoreceptor that normally control glutamate release from presynaptic terminals. **Objectives:** we propose to (1) investigate whether down-regulation of SV2a is responsible for reducing the anticonvulsant efficacy of LEV (this phenomenon is known as tolerance and has limited the use of LEV in the treatment of epilepsy), and (2) search for ways to circumvent tolerance. We will compare the effects of LEV with those of other antiepileptic drugs that could potentially modulate presynaptic transmission in epilepsy. The long-term goals of this collaborative proposal are to (1) identify the most effective antiepileptic drugs, which modulate presynaptic glutamate release, and (2) assess the presynaptic mechanism of action of the new antiepileptic drug LEV.

HYPOTHESIS AND OBJECTIVES: During periods of intense neuronal activity such as seizures, a larger pool of vesicles could result in more glutamate being released and long-lasting aberrant excitation. We propose to explore the effects of seizures on transmitter release and the presynaptic action of AEDs on these changes. We will use electrophysiology and multiphoton confocal microscopy. Preliminary data indicate that SE induces long-lasting potentiation of synaptic vesicle release in epileptic rats. We hypothesize that successful AED treatment might prevent or reverse these seizure-induced molecular deficiencies (reduction of N-type VGCC, mGluR II and SV2a expression), and be antiepileptogenic as well. Our **central hypothesis** is that pharmacological regulation of glutamate transmitter release at presynaptic sites will be an effective, novel therapeutic strategy to ameliorate epileptogenesis and excessive synaptic excitation in epilepsy. The **long-term objectives** of this collaborative proposal are to: (1) identify the most effective AEDs which modulate presynaptic glutamate release, and (2) determine the presynaptic mechanism of action of the new AED LEV to modulate vesicular release properties. *Our central hypothesis is that pharmacological regulation of glutamate transmitter release at presynaptic sites will be an effective, novel therapeutic strategy to treat many cases of drug-resistant epilepsy, especially epileptogenesis following traumatic brain injury.* The **long-term goals** of this collaborative proposal are to: (1) identify the most effective antiepileptic drugs amongst compounds that modulate presynaptic glutamate release and (2) determine the presynaptic mechanism of action of the new antiepileptic drug **levetiracetam** (LEV).

2. Keywords

Levetiracetam, antiepileptic drugs, epilepsy, synaptic vesicle proteins, presynaptic, seizures

3. Accomplishments

Description of Research Accomplishments toward accomplishing the aims during Year 1.

Specific Aim 1: *Determine which antiepileptic drugs are most effective at reducing glutamate release from mossy fiber presynaptic boutons (MFBs) in the pilocarpine model of mesial temporal lobe epilepsy (MTLE)* (months 1-12). **Working hypothesis:** Drugs acting on presynaptic Ca^{2+} channels, autoreceptors, and SV2a will be more effective in reducing vesicular glutamate release at excitatory presynaptic terminals in the hippocampus.

1. Task 1. Evaluate the effects of different concentrations of "classical" (*e.g*. carbamazepine, lamotrigine, and topiramate, and "new generation" antiepileptic drugs (*e.g.* LEV) on presynaptic glutamate release by using two-photon imaging of vesicular release of the fluorescent dye FM1-43 from individual mossy fiber terminals in *in vitro* hippocampal slices.

1.1.a.b Development of the pilocarpine model of epilepsy in mice and rats at both institutions:

Colonies of chronically epileptic Sprague Dawley rats, SynaptopHlourin (SpH) mice were established at both Institutions University of Texas at Brownsville (UTB) and New York Medical College (NYMC) using protocols validated in Dr. Garrido's laboratory. In addition, the pilocarpine model of mesial temporal lobe epilepsy (MTLE) was also developed in the SV2A/SV2B knockout mice at the laboratory of Dr. Garrido. During the period of the first year of the grant, Dr. Garrido's laboratory was relocated to the new biomedical research building with fully equipped state-of-the art *vivarium*. Hippocampal slices for multiphoton laser scanning confocal imaging analysis of presynaptic release (Dr. Stanton, NYMC) and *in vitro* electrophysiology (Dr. Garrido, UTB) were obtained from control and epileptic rats and transgenic mice (Subtask 1b).

<u>The pilocarpine model in mice:</u> Previous studies have reported differential susceptibility of mouse strain to pilocarpine-induced *status epilepticus* and seizure-induced excitotoxic cell death[1]. Therefore, we optimized and fully characterized the pilocarpine model in the SpH mice (Sp21 variant) obtained expressing the fusion protein of vesicle-associated membrane protein 2 (*Vamp2*) and pH-sensitive green fluorescence protein), under the control of the mouse thymus cell antigen 1 (*Thy1*) promoter which direct the expression in granule cell of dentate gyrus and subsequent expression and trafficking to mossy fiber axons and mossy fiber boutons in the *stratum lucidum* of the hippocampus. Breeders were obtained from Jackson Laboratories *i.e.* B6.CBA-Tg(Thy1-spH)21Vnmu/J, C57BL/6J (Stock Number: 014651) to establish the colony Dr. Garrido's laboratory while this same strain was already available at Dr. Stanton's Laboratory (obtained from Dr. V. Murphy's lab, Harvard University). For the induction of *status epilepticus* animals received methylscopolamine nitrate (0.1 mg/kg in saline, s.c.) thirty minutes before pilocarpine to minimize peripheral effects of cholinergic stimulation[2]. Then, pilocarpine hydrochloride (prepared as 1%) was intraperitoneally injected using different doses (300, 320, 350 and 380 mg/kg of body weight, 5 animals per group). The dose of 350 mg/kg was the more efficient yielding 90% of animals entering *status epilepticus* and 80% survival rate. After animals entered *status epilepticus*, a second dose of methylscopolamine was subcutaneously injected and animals were led to seize during 1 hour following published protocol [3] and motor seizures were terminated with one diazepam injection (10 mg/kg in saline *i.p.*). Only animals experiencing continuous SE during these periods were studied. Controls animals received methylscopolamine and saline instead of pilocarpine. D<u>evelopment of the pilocarpine model in the SV2A knockout mice</u>: The model of mesial temporal love epilepsy was also developed in wild type, heterozygous and knockout SV2A mice obtained from Jackson Laboratories (Stock number: 006383, B6; 129P2-*Sv2a*^{tm1Sud} *Sv2b*^{tm1Sud}/J). These animals were developed with the same genetic background (C57BL/6J) of the SpH21 mice. Accordingly, the same concentrations of methylscopolamine and pilocarpine were used following the same protocol as describe above.

1.1.2. Pilocarpine-induced *status epilepticus* causes disorganization of dentate gyrus and CA3 cytoarchitecture in SpH mice.

In the hippocampal CA3 region of both control (Fig. 1a, top panel) and post-SE (Fig. 2b, bottom panel), immunostaining for the presynaptic glutamate transporter VGluT1 was intense in the mossy fiber projection area in *stratum lucidum*, where it co-localized with native SpH fluorescence (Fig. 2a merged), consistent with the glutamatergic nature of presynaptic terminals expressing SpH in the SpH21 mice [4,5]. There was also a striking decrease in the density of neurons in CA3 *stratum pyramidale* of post-SE mice that stained positively for the neuronal marker NeuN, compared to age-matched controls (Fig. 1a, merged bottom panel) consistent with seizure-induced loss of CA3 pyramidal neurons following pilocarpine-induced SE [6]. Data was recently published in Brain[7] (see appendix 2)

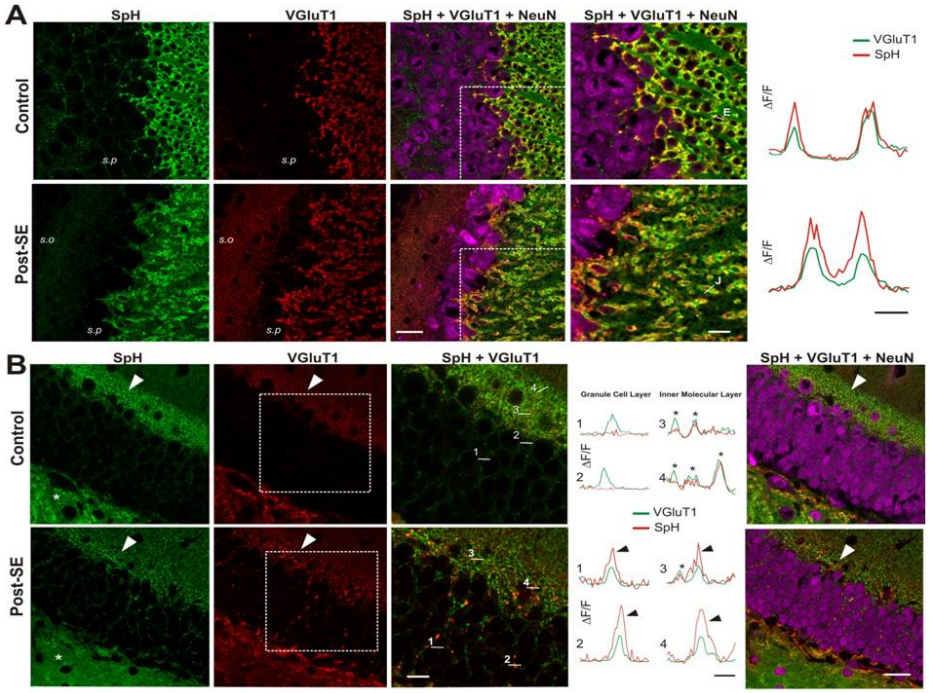

Fig. 1. Confocal images of SpH, VGluT1 and NeuN expression in CA3 and DG of control and post-SE SpH transgenic mice. **(A)** In control and post-SE mice, native SpH fluorescence image (green), VGluT1 immunofluorescence image (red) and NeuN immunofluorescence image (purple), showing co-localization of SpH with VgluT1 labeling in MFB (merge). A dramatic loss of cells was noticed in CA3 stratum pyramidale by NeuN staining (third column, compare control and post-SE) and SpH and VGluT1-positive terminals appear disorganized in stratum lucidum of post-SE compared to control (fourth column). Punctate SpH signals were also scattered through the pyramidal cell layer (s.p) surrounding cell somata that were stained with NeuN antibody. Last column shows fluorescence intensity profile and colocalization along line scans (E: control and J: post-SE, fourth column respectively) through single MFB indicated in the respective X2 magnification images (fourth column, scale bar = 25 µm) of the rectangular boxes seen in third column (scale bar = 50 µm). Scale bar for line scans in last column = 2µm **(B)** In DG cell layer of control and post-SE, (NeuN labeling), SpH fluorescence (green) and VGluT1 staining (red) were intense in the hilus (*) and in the inner molecular layer (arrow head). In control (upper panel) SpH-positive puncta around putative granule cell somata were devoid of VGluT1 expression (merged panel: lines 1 and 2), while SpH and VGluT1 signals did colocalize in the inner molecular layer (lines 3 and 4), as shown by respective line scans (fourth panel) of fluorescence intensity through puncta in the granule cell layer (1 and 2) versus the inner molecular layer (3 and 4). In post-SE (lower panel) SpH and VGluT1 colocalize in both the DG cell layer (third column and line scans 1 and 2 in the fourth column) and inner molecular layer (line scans 3 and 4, fourth column). NeuN immunofluorescence illustrates a lack of marked granule cell loss in post-SE DG (bottom panel, last column). Scale bar for line scans in last column = 2µm

In the dentate gyrus (DG) (**Fig. 1b**), robust SpH fluorescence was detected in the inner molecular layer (arrow heads) and hilus (*) of both control and post-SE mice (Fig. 1b, SpH), closely colocalized with VGluT1 immunofluorescence (**Fig. 1b** merged). VGluT1 punta positive for SpH fluorescence in the inner molecular layer exhibited 39.5% larger cross-sectional diameter (Fig. 1b, 1.84 ± 0.54µm, Student t-test, *P*<0.001) and 47.5% higher normalized mean fluorescence intensity (**Fig. 1b**, post-SE: VGluT1) relative to background-subtracted baseline intensity (204.8 ± 35.5 arbitrary units (a.u), n=29, Student's t-test, *P*<0.0001) in pilocarpine-treated post-SE mice when compared to control group (Fig. 2b, control: VGluT1 138.8 ± 32.2 a.u and mean diameter of puncta: 1.31 ± 0.37µm, n=29). Interestingly, SpH puncta in granule cell somata in the control DG (Fig. 1b upper panel) exhibited little immunostaining for VGluT1 (**Fig. 1b** control, merged and line scans 1 and 2) whereas the granule cell layer of post-SE hippocampus showed strong co-immunolabeling for VGluT1 (**Fig. 1b** lower panel, merged and line scans 1 and 2), suggesting either a possible up-regulation of VGluT1 expression in existing terminals or neo-synaptogenesis manifested by the appearance of ectopic glutamatergic (VGluT1 positive) terminals in both inner molecular layer and granule cell layer during epileptogenesis, as previously reported in animal models of TLE [6,8-11].

In addition to the characterization of neuropathological features of the SPH21 mice, we also investigate whether this model exhibits additional abnormalities in the hippocampus that may be related to the pathogenesis of epilepsy. Several mechanisms regulating presynaptic function are disturbed in epilepsy, including the expression of Ca^{2+}-binding protein Calbindin-D28K, mGluR2[12,13] and SV2A[14-18]. As previously reported we detected a down-regulation of the Calbindin-D28K (**Fig. 2**).

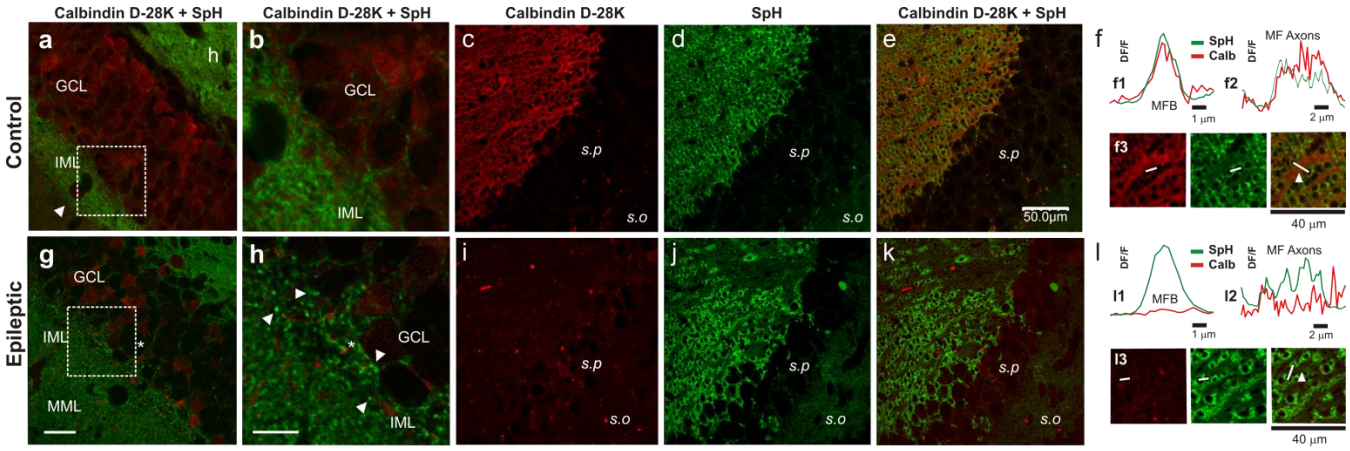

Fig. 2. Down-regulation of Ca^{2+}-binding protein CalbindinD-28K epileptic SpH Mice. In control SpH mice (3 month) **a-b**. Representative Calbindin D-28K immunefluorescence staining show that Calb (red channel) is heavily expressed in granule cell layer (GCL) (**a-b**) and mossy fibers and MFBs (**c-f**) of control SpH-expressing mice (green channel) while Calbindin D-28K expression was dramatically reduced in GCL (**g-h**), mossy fibers and MFBs (**g-l**) of chronically epilepotic SpH mice. Fluorescence intensity along a line indicate a good co-localization of Calb and SpH at MFBs (**f1**) and axons (**f2**, **f3** arrow) in control compared with a lower Calb expression in SpH-positive MFBs (**l1**, **l3**) and axons (**l2**, **l3** arrow). Scale bar for **c-e**, **i-k** in **e**.

1.1.3. Expression of Calbindin D-28K in mossy fibers in the pilocaprine model of epilepsy.

Whether increase in stimulus evoked release in post-SE state results from alterations in Ca^{2+} influx, release of $Ca^{2+}$from internal stores *per se*, or whether there are downstream changes in SNARE protein sensitivity to Ca^{2+} is not known. A previous study [19] found that pilocarpine seizures also cause down-regulation of BK potassium channels in MFBs, reductions that could slow hyperpolarization and increase terminal Ca^{2+} influx. Levels of the Ca^{2+}buffer Calbindin D-28K are also lowered in MFBs after pilocarpine seizures [20], a change that could further increase presynaptic Ca^{2+} influx, dysregulate Ca^{2+} homeostasis and promote multi vesicular release [21].

1.1.4. Structural and molecular characterization of the pilocarpine model of epilepsy in transgenic Sp21 mice. *A unique model to investigate the presynaptic function in epilepsy.*

In a recent manuscript published in *Brain, Journal of Neurology, 135: 869-85, 2012* (see appendix), we described long-term alterations in presynaptic morphology and synaptic vesicle recycling at mossy fiber-CA3 terminals of mice and rats subjected to pilocarpine-induced SE, a seizure model that produces a chronic epileptic state associated with spontaneous generalized seizures in 100% of animals [3]. These changes include increases in 1) mossy fiber bouton (MFB) size, 2) number of release sites per MFB, 3) number of vesicles in RRP and RP, 4) active zone length, 5) action potential-driven vesicular release rate measured with either FM1-43 or in synaptopHluorin-expressing transgenic mice, and 6) enhanced vesicle endocytosis. These alterations persisted for at least 1-3 months following a single sustained *status epilepticus*.

Characterization of mossy fiber boutons in the SpH21 transgenic mice: Representative two photon laser scanning image of the CA3 region of an acute hippocampal slice from this mouse (Fig. 3a) contains bright GFP positive boutons >2µm in diameter, proximal to CA3 pyramidal cell bodies in the region innervated by MF axons of dentate granule cells [22,23]. Associational-commissural CA3 synapses are significantly smaller (<1µm in diameter) and more distal to our region of interest (rectangular box, Fig. 3a). These data was obtained in Dr. Stanton's laboratory.

SpH is a fusion protein that consists of a pH sensitive eGFP (pHluorin) fused to the C-terminus luminal domain of the vesicle SNARE protein synaptobrevin [24]. Under resting conditions, the luminal pH of the synaptic vesicle is acidic (pH~5.5), resulting in proton dependent quenching of SpH fluorescence. When vesicle exocytosis is triggered and glutamate released, the lumen of the vesicle is exposed to the more alkaline pH of the extracellular space (pH~7.2), resulting in a 20-fold increase in SpH fluorescence. When the vesicle membrane is retrieved by endocytosis and the vesicle reformed, it undergoes rapid reacidification by the vesicular ATPase, which returns SpH to its quenched state. The SpH21 transgenic mice line we used in this study, expresses SpH preferentially at glutamatergic synapses [4,5,25].

1.4. Pilocarpine-induced *status epilepticus* state increases size and vesicular release rate of mossy fiber boutons in SpH-expressing mice

Data from Dr. Stanton's laboratory confirmed that large SpH expressing boutons were mossy fiber terminals. Briefly, anterograde, bulk labeling of mossy fibers was performed using Alexa Fluor 594 dextran introduced into the granule cell layer of the dentate gyrus (Fig. 3b). During a 1.5-2 hour incubation, Alexa Fluor 594 dextran was taken up by granule cells and transported anterogradely to label MF axons and presynaptic boutons (Fig. 3c). Figures 3e and 3f illustrate that some (solid arrows) but not all (broken arrows) SpH and Alexa Fluor 594-positive boutons were co-labeled confirming that, indeed, the large (>2µm in diameter) SpH fluorescent puncta within the proximal 60µm of the CA3 cell body are the excitatory mossy fiber boutons (Figure 3d). Incomplete co-localization is likely because Alexa Fluor 594-labeled a subset of mossy fiber axons in *stratum lucidum* in addition to sparse SpH expression in the excitatory terminals[4,5].

Collaborative data published in *Brain* (2012)[7] indicate a long-lasting abnormality of presynaptic structural and function in epilepsy. Multiphoton microscopy data was obtained by Dr. Stanton's group. To directly measure prospective changes in vesicular recycling properties from hippocampal mossy fiber presynaptic boutons (MFBs), control and pilocarpine-treated chronic epileptic SpH21 transgenic mice expressing SpH preferentially at glutamatergic synapses were used. There were significant increases in MFB size, faster rates of action potential-driven vesicular release and endocytosis1-2 months after pilocarpine-induced *status epilepticus*,. Furthermore we also analyzed the ultrastructure of MFB's synapsing on the thorny excrescences using transmission electron microscopy (TEM) (see below). *Status epilepticus* lead to a significant increase in the number of release sites, active zone length, postsynaptic density area, and more vesicles in the readily releasable and recycling pools, all correlated with increased release probability of synaptic vesicles. These data suggests that presynaptic release machinery is persistently altered in structure and function by *status epilepticus*, which could contribute to the development of the epileptic state and may represent a potential new target for antiepileptic therapies.

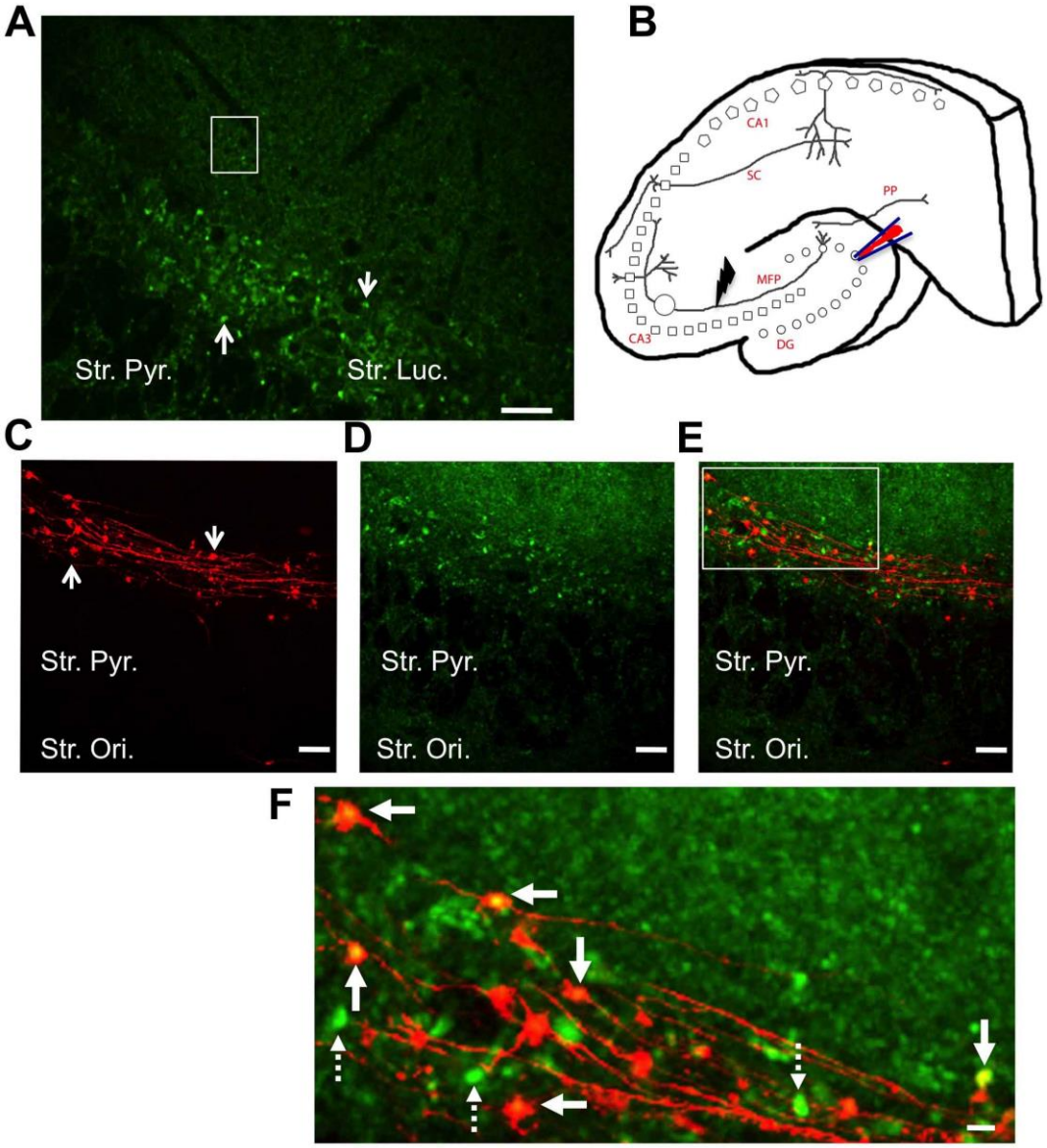

Fig. 3. Visualizing mossy fiber boutons (MFBs) in acute hippocampal slices from SpH21 transgenic mice line. **(A)** Live cell two photon laser scanning image of field CA3 of synaptopHluorin expressing glutamatergic terminals in a control hippocampal slice (postnatal 60 days). The arrows depict representative fluorescence puncta (about 4-5µm in diameter) in the proximal (*stratum lucidum*) region of CA3 pyramidal cells (seen here as a ghost layer) that are likely to be giant MFBs. Distal puncta shown within the rectangular box are notably smaller in size and likely represent the associational-commissural synapses in the *stratum radiatum*. *Stratum pyramidale* (Str. Pyr.) and *Stratum Oriens* (Str. Ori.). Scale bar = 20 µm. **(B)** Cartoon representing the hippocampal circuitry with the circle in the mossy fiber pathway (MFP) depicting the area of imaging, arrow the depicts the area of local stimulation and the pipette in the dentate granule cell layer (DG) shows the area of Alexa Fluor 594 dextran containing pipette insertion. (PP: perforant path, SC: Schaffer collaterals, squares and pentagons depict CA3 and CA1 pyramidal cell layers respectively). **(C)** Alexa Fluor 594 dextran filled MF axons and giant MFB (arrows) showing characteristic en-passant arrangement along the axonal projections, visualized using 825nm excitation. **(D)** Same region as (c) but visualized with 890nm excitation to see synaptopHluorin native fluorescence. CA3 pyramidal cell bodies can be seen as ghost cells in stratum pyramidal (Str. Pyr), and bright giant MFB in *stratum lucidum*. Scale bar = 20 µm (c-e). **(E-F)** Merged images of (c) and (d) showing colocalization (f: arrows) between SpH and Alexa Fluor 594 dextran-labeled puncta. (**F**) Digital zoom of image from the inset box in (**E**), scale bar = 4 µm. Note not all SpH-positive puncta colocalize with Alexa Fluor 594 puncta (F: broken arrows).

1.5. SE elicits long-term ultrastructural reorganization of active zones in MFBs.

Previous literature has demonstrated clear correlations between release probability and synapse morphological parameters such as sizes of the RRP [26] and rapidly-recycling pools [27], active zone (AZ) [28,29] also known as 'release sites', postsynaptic density (PSD) [29] and presynaptic bouton [28]. Since we found increased release probability post-SE as measured by both SpH and FM1-43 destaining[7], we examined possible ultrastructural rearrangements in MFBs in CA3 *stratum lucidum* in post-SE and age-matched non-seizure Sprague-Dawley rats (Fig. 4a). Electron microscopy study was performed in collaboration with Dr. Dwight Romanovicz and Dr. Theresa Jones from University of Texas at Austin, Texas. Transmission electron microscopy (TEM) of large MFBs (2-5 μm in diameter) revealed multiple AZs facing PSDs, contained mitochondria of various sizes, and were filled with numerous small and large clear synaptic vesicles distributed throughout the terminal, as described previously [30-32]. Asymmetric AZs were distinguished in MFB synapses, by the dense accumulation of synaptic vesicles in close proximity to the presynaptic density and characteristic widening of the synaptic cleft[8]. There was a significant increase in number of AZ per MFB in post-SE rats (130 AZs in 6 control rats, 5.1 ± 1.36 AZs per MFB; 286 AZs in 7 post-SE rats, 7.7 ± 3.05 AZs per MFB, Student's t-test, $P<0.05$). The majority of EM variables failed to follow normal distributions, necessitating use of a nonparametric Kolgomorov-Smirnov two-sample test to assess between group differences in distributions. As reported previously[31,32] individual AZs varied substantially in shape and size; both very large and very small AZs were found in control (104-887nm) and post-SE (105-1837nm). Frequency distributions revealed the presence of a distinct group of synapses of larger length in epileptic animals that was not present in controls (Fig. 5b, panel a). A cumulative histogram indicated a significant leftward shift towards larger individual AZ lengths in MFBs post-SE (Fig. 5c), compared to controls (Table 1, Kolgomorov-Smirnov test, $P<0.005$). There was also a significant increase in mean PSD area in the post-SE group (Table 1) compared to controls (Table 1, Kolgomorov-Smirnov test $P<0.005$, an ~37% increase). In contrast, no significant changes were detected in average synaptic cleft width between control and post-SE AZs (Table 1).

***Table 1**. Summary of quantitative analysis of structural variables in AZs of MFBs.*

	Control	**Post-SE**		
AZ Ultrastructural Variables	Mean ± SD	Mean ± SD	% of Control	K-S *P*
Length of AZ (nm)	364.91 ± 44.81	485.27 ± 59.63	133.5	*P<0.005*
Length of synaptic cleft (nm)	26.93 ± 3.91	29.95 ± 2.46	107.4	*P=0.31*
PSD area (μm^2)	12.31 ± 3.03	16.90 ± 3.31	136.9	*P<0.005*
Number of SVs in RRP	7.43 ± 3.12	8.94 ± 1.78	120.3	*P<0.001*
Number of SVs in the RP	31.07 ± 6.05	33.44 ± 7.13	107.6	*P<0.05*
Number of docked SVs per AZ	1.96 ± 0.68	2.63 ± 0.56	134.2	*P<0.0005*
Docked SVs per AZ length (SV/μm)	5.48 ± 1.75	5.88 ± 0.90	108.9	*P<0.05*
% of Docked SVs of RRP	27.92 ± 6.45	29.56 ± 3.24	105.85	*P=0.59*

Measurements were obtained from analysis of active zone (AZ) variables in MFBs. Statistical comparisons were made by the Kolgomorov-Smirnov (K-S) two-sample test. Statistical significance was set at $P<0.05$. Values are presented as means ± SEM. PSD, postsynaptic density, SVs, synaptic vesicles, RRP, readily releasable pool.

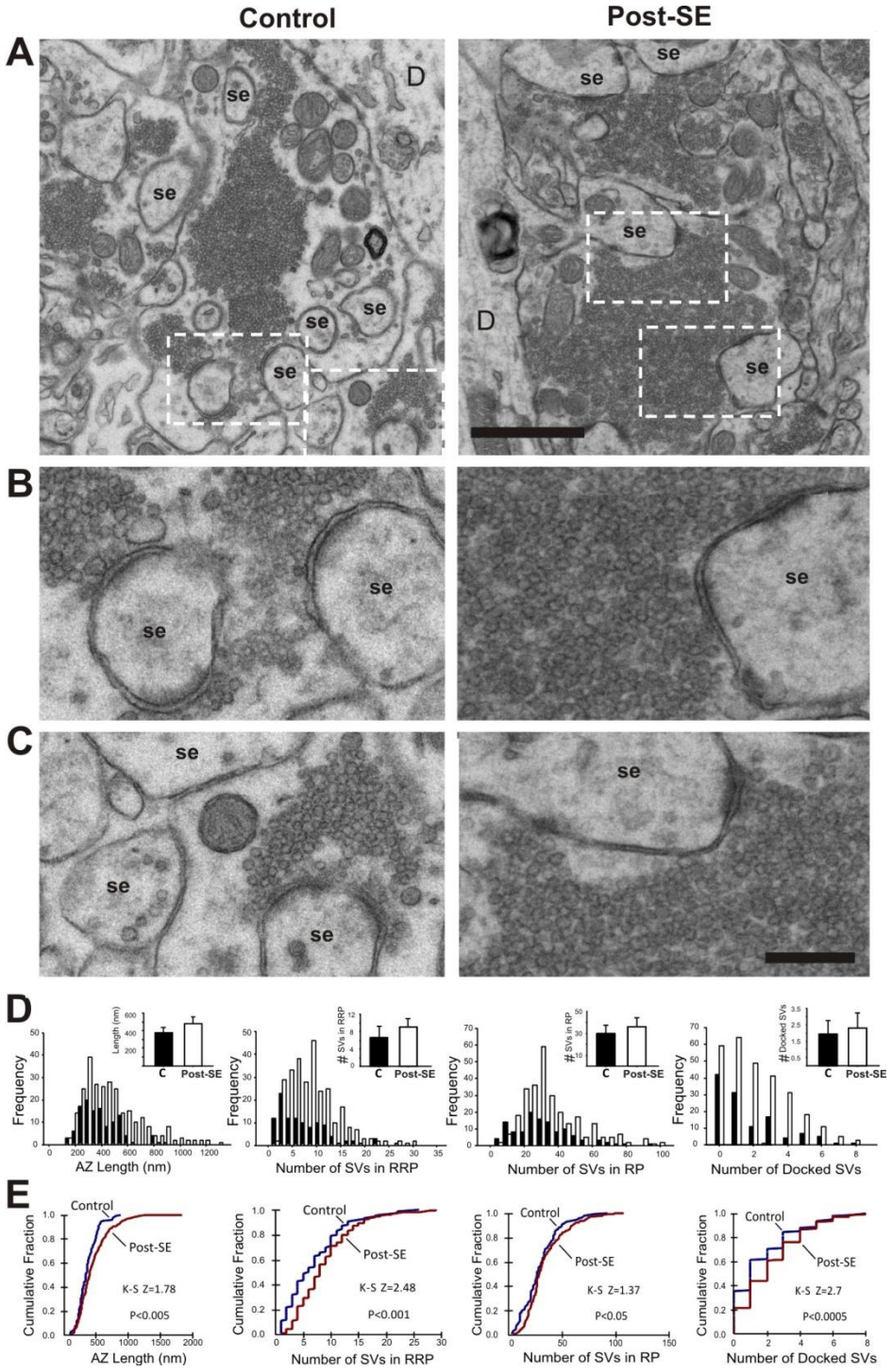

Fig. 4. Transmission electron microscopy (TEM) of active zones (AZs) in MFBs of control and post-SE rats. **(A)** Representative TEM images of control (Left column) and post-SE (right column) MFBs illustrating AZs on synaptic excrescences (se) showing an apparent increase in synaptic vesicle density in post-SE MFB. Boxed areas are depicted at higher magnification (x4) images **(B).(C)** showing arrangement of vesicles in the AZs of control and epileptic MFBs. Notice a larger density of vesicles and length of AZ in post-SE MFBs. Scale bar 2mm for a and 500 nm for all others, D=dendrite. **(D)** Frequency histograms and bar graph representation of data for AZ length, number of synaptic vesicles in RRP and RP, and number of docked synaptic vesicles. Notice appearance of increase number of AZs exhibiting larger lengths in post-SE (>800nm). **(E)** Cumulative histograms for these variables in control versus post-SE groups revealed significant rightward shifts toward the larger-size bins by Kolgomorov-Smirnov two-sample test (K-S).

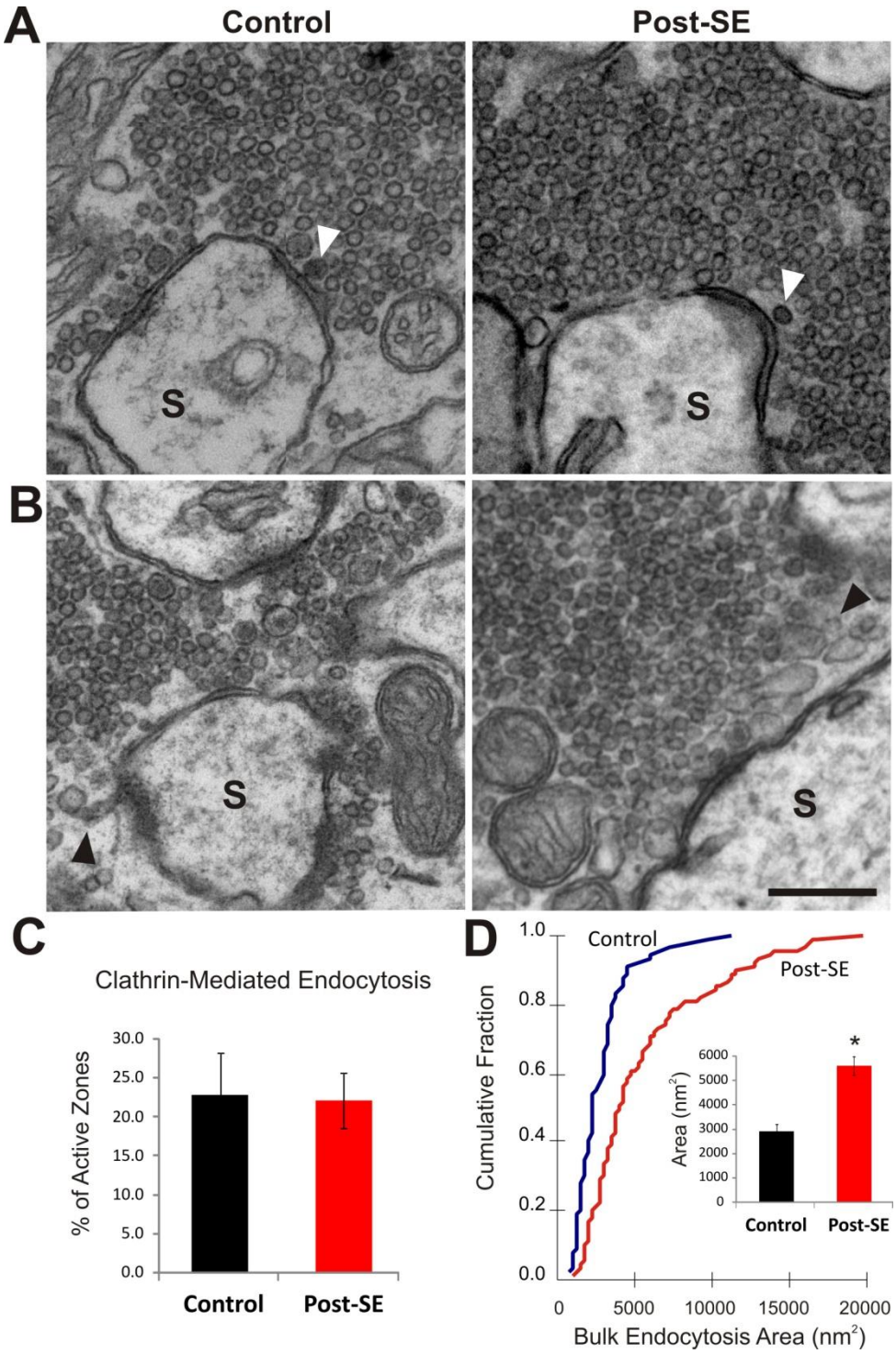

Fig. 5. Representative TEM images of active zones (AZs) in MFBs exhibiting structural signs of clathrin-mediated endocytosis and "bulk endocytosis" in control and epileptic rats. Putative clathrin-coated (dark) vesicles (white arrows) located proximal to presynaptic membrane AZs synapsing on spines (S) of Control **(A)** and post-SE **(B)** MFBs. Irregular membranous structures (black arrows) near AZs on spines (S) were observed in Control **(C)** and post-SE **(D)** MFBs. Note these structures were larger in post-SE rats. (Scale bar in **d** 500nm) **(E)** Mean ± SEM % AZs positive for clathrin-coated vesicles, showing no difference in control versus post-SE rats (P>0.20, Student's t-test). **(F)** Cumulative histogram plot of bulk endocytosis area showing a significant rightward shift on the size distribution towards larger values in post-SE MFBs (red) compared to Controls (blue, P<0.001, Kolgomorov-Smirnov test). (Inset: mean area of bulk endocytosis in Control (black) versus post-SE (red) rats (*, P<0.05, Student's t-test).

It has been previously suggested that a rapid refilling of the RRP from a larger releasable vesicle pool (RP) is a key mechanism in ensuring fidelity of mossy fiber-CA3 pyramidal cell neurotransmission[33]. To determine whether ultrastructural organization of synaptic vesicle pools is altered post-SE, we measured the number of vesicles docked, within 60nm of the AZ, 60-200nm from an AZ, and >200nm from an AZ, in MFBs of control versus epileptic animals. The RRP was defined as the sum of docked vesicles and those within 60 nm of the AZ, while the releasable pool (RP) was defined as vesicles 60 to 200 nm away from an AZ [33] (Fig. 5a, panel 2 and 6). Compared to controls, post-SE increased number of docked (+34.2%), RRP (+20.3%), and RP (+7.6%) synaptic vesicles (Table 1). A significant difference was detected in the analysis of the cumulative distributions of these variables by Kolmogorov-Smirnov test (Fig. 5c and Table 1). Although the percentage of docked vesicles relative to RRP size was not significantly different (Table 1), the average number of docked vesicles per length of AZs was significantly higher for post-SE (+8.9%, Table 1). Additionally, the number of synaptic vesicles in each of these pools was significantly correlated with the length of individual AZs in both control (RRP: r = 0.33, P<0.001 and RP: r =0.41, P<0.001) and post-SE MFB (RRP: r =0.57, P<0.001 and RP: r=0.55, P<0.001).

In order to assess endocytosis, we measured (a) the number and percent of clathrin-coated vesicles 0-200 nm from an AZ (Fig. 5a and b) and the area of membranous regions apparently internalized at the AZ, indicative of "bulk endocytosis" (Fig. 5c and d), in MFBs of control and post-SE. There were no statistical differences in percent of synapses exhibiting 1 or 2 putative clathrin-coated vesicles at AZ between control (22.7 ± 10.1%) and post-SE (22.0 ± 7.1%, Fig. 5e) animals, or percent synapses exhibiting bulk endocytosis (control: 48.7 ± 13.1%, epileptic: 40.7 ± 15.8%). In contrast, the area of large elliptical or irregular membranous structures at the AZ was significantly higher at MFB synapses post-SE (5662 ± 385 nm^2) compared to controls (2917 ± 287 nm^2, Kolmogorov-Smirnov test, P<0.001, Fig. 5f). Taken together, our EM data show pilocarpine-induced SE leads to profound and long-lasting rearrangement of MFB transmitter release sites, resulting in significant increases in number of release sites per MFB, length of individual release sites, and RRP and RP vesicle pools sizes that may underlie persistent increases in functional transmitter vesicular release rates, magnitude, and recycling properties. The pilocarpine model of epilepsy in the SpH21 transgenic mice is thereby an invaluable tool to investigate the presynaptic function using advanced imaging methods.

Task 2. Evaluate the effects of different concentrations of "classical" (e.g. carbamazepine and topiramate), and "new generation" antiepileptic drugs (e.g. LEV) on patch-clamp electrophysiological recordings from dentate granule cells that give rise to mossy fibers. This data will be used to assess the effects of antiepileptic drugs on spontaneous miniature excitatory postsynaptic currents (mEPSC) in control versus pilocarpine treated rats. Subtask 2a. Develop chronic epileptic rats with a single injection of pilocarpine (Dr. Garrido, Dr. Pacheco; months 1-12). Horizontal hippocampal slices were prepared from control and epileptic rats (Subtask 2b) using previous protocols established in Dr. Garrido's laboratory. Patch-clamp recordings were obtained from granule cells to record spontaneous mEPSCs and mIPSCs in slices from control and epileptic rats and mice (Subtask 2c.)

As proposed in the revised Statement of Work, we have evaluated the effect of levetiracetam on inhibitory synaptic transmission by assessing the LEV effect on miniature inhibitory postsynaptic currents in control versus epileptic animals (Subtask 2d).

Different antiepileptic drugs were tested on their effectiveness to modify the frequency and amplitude of mEPSCs in granule cells in control versus epileptic rats (Subtask 2d.). Statistical comparisons were performed to analyze the electrophysiology data (Subtask 2e) and compare the effectiveness and presynaptic action of different antiepileptic drugs in modifying the excitatory and inhibitory transmission.

2.1. Intrinsic properties, firing pattern and spontaneous activity dependent excitatory currents in control *versus* epileptic rats.

Analysis of intrinsic properties in different groups of dentate granule cells revealed no significant changes in the resting membrane potential (RMP, control 64.2 ± 5.2 vs epileptic 66.2 ± 4.1 mV), input resistance (control 354.2 ± 53.6 mΩ vs epileptic 371.5 ± 49.1 mΩ), membrane time constant (control= 27.1 ± 3.1 ms vs epileptic 26.5 ± 4.2 ms) or threshold to action potentials (control=42.5 ± 4.1 mV vs epileptic 46.0 ± 3.9 mV) in control (n=24) *versus* granule cells in epileptic rats sacrificed 2-4 months after *status epilepticus* (n=17). Statistical analysis was performed using student t-test and statistical significance set at p=0.05. Analysis of firing modes revealed that the

majority of control granule cells (22 out of 24 cells) responded with regular spike firing to increasing steps of depolarizing currents while 2 cells fired initial burst of 2-3 action potentials at supra-threshold current injection). In contrast, 12 out 17 cells in slices from epileptic rats respond with regular spiking while 5 neurons fired burst of action potentials in respond to supra-threshold current stimulus. No low-threshold or spontaneous burst firing was detected in control neither in epileptic granule cells. Analysis of spontaneous activity dependent sEPSC revealed that the frequency of spontaneous excitatory drive onto granule cells was significantly higher 64% in dentate gyrus of chronically epileptic rats (3.17 ± 0.7, n=4) when compared to age-matched controls (1.92 ± 0.6, n=8) (Student t-test, $p<0.05$). These data indicate that epileptogenesis do not affect the intrinsic properties of granule cells but increased the excitatory drive. It has been widely reported that mossy fibers from granule cells form newly recurrent excitatory synapses onto dendritic arborizations of local granule cells[9,34]. This type of synaptic reorganization has been considered a major contributor to increased excitatory drive on granule cells[35-37] summating to the glutamatergic inputs originating in the entorhinal cortex (perforant path synapses). Enhanced excitatory drive can play a pro-epileptic role, especially in conditions of transient or partial disinhibition leading to seizure generation of facilitation of seizure propagation throughout the hippocampus.

2.1. Effect of antiepileptic drugs on excitatory and inhibitory synaptic transmission

The precise mechanism of action of LEV interaction with SV2A receptors to exert an antiepileptic effect is an unsolved enigma in epilepsy research. Experiments in this project investigated the mechanisms of action of LEV in modulating presynaptic function in animal models of MTLE induced by pilocarpine. Specifically, we assessed the effect of different concentrations of LEV (5, 50 and 100 μM) in control versus pilocarpine-treated epileptic Sprague Dawley rats sacrificed 2-4 months after *status epilepticus.* Additional experiments were performed in the SV2A/SV2V knockout transgenic mice obtained from Jackson laboratories to assess the role of SV2A gene dosage and epileptogenesis on the action of LEV on both excitatory and inhibitory transmission in dentate gyrus.

2.1.1. Effect of Levetiracetam (LEV) on excitatory synaptic transmission onto granule cells in the dentate gyrus of epileptic rats compared to age-matched controls.

Epileptic rats were obtained by the pilocarpine model of mesial temporal lobe epilepsy using protocols established a PI's laboratory[7,13,19,38-41]. Whole-cell patch recordings were performed in Diferential interference contrast (DIC)-visualized granule cells in dentate gyrus of age-matched controls and epileptic Sprague Dawley rats. After recording the intrinsic membrane properties and firing patterns in the current-clamp configuration, the recording mode was switched to voltage-clamp to record activity-dependent spontaneous excitatory postsynaptic currents (sEPSCs) to compare whether the spontaneous action potential excitatory drive onto granule cells change during the course of epileptogenesis. Tetradotoxin (TTX) was added to the artificial cerebrospinal fluids (ACSF) to block TTX-sensitive sodium channels and assess the effect of LEV on miniature EPSCs (mEPSCs).

The electrophysiology/pharmacology paradigm is illustrated in **Fig. 6**. Recordings of mEPSCs were performed in AP-5 and GABAzin to block NMDA-mediated glutamatergic currents and $GABA_A$ receptors respectively. Biocytin was added to the patch pipette solution for post-hoc identification of the recorded cells after recordings. Neurons were reconstructed using Neurolucida (MicroBrightField, Inc) and morphological features of recorded granule cells in slices from control and epileptic rats were analyzed (see section 1.2.6 below).

A sample of reconstructed cells is illustrated in Appendix #3.

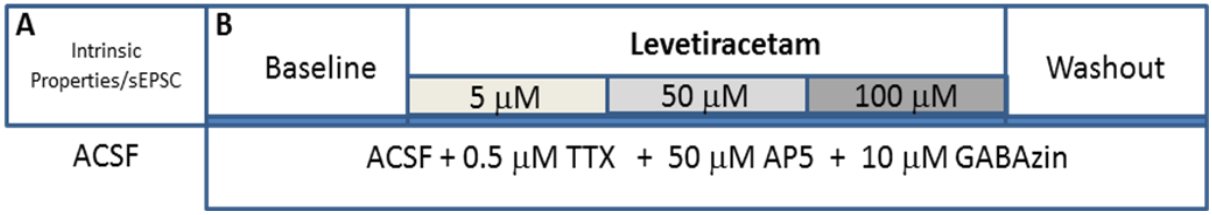

Fig. 6. Experimental paradigm to evaluate the effect of levetiracetam (LEV) on excitatory transmission in the dentate gyrus. **A.** Visualized whole-cell patch clamp recordings were performed in standard artificial cerebrospinal fluid (ACSF) from granule cells in the dentate gyrus of horizontal hippocampal slices obtained from pilocarpine-treated Sprague Dawley rats compared to age-matched controls. In current clamp we measured intrinsic properties (*i.e.* resting membrane potential, membrane time constant and input resistance) and firing pattern phenotype and in voltage clamp we recorded activity-dependent spontaneous excitatory postsynaptic currents (sEPSCs). **B**. Slices were then bathed in ACSF containing: (1) tetradotoxin (TTX) to block TTX-sensitive sodium channels and measure spontaneous miniature EPSCs (mEPSC), (2) 5-aminophosphovaleric acid (AP-5) to block NMDA receptor-mediated currents and isolate AMPA/kainate mediated mEPSCs, and (3) GABAzin to inhibit $GABA_A$ receptors-mediated inhibitory currents. After a recording of 10 minute baseline period, increasing concentrations of LEV were applied for 10 minute period each while recording mEPSCs. Then, LEV was removed from the bath ACSF while recording the washout effect to assess whether LEV effects on mEPSC are reversible (recovery).

2.1.1.1. Effect of different concentrations of LEV on mEPSC frequency in granule cells of dentate gyrus in control vs epileptic rats.

Incubation of slices in LEV induced a significant change in the frequency of mEPSCs recorded in dentate granule cells in control and slices from chronically epileptic rats (Fig. 7 and 8, Table 2). The action of LEV was characterized by a dose-dependent inhibition of mEPSC frequency. In control slices, 10 min incubation in 5 μM LEV significantly inhibited mEPSC to 77.8% of baseline (22.2% reduction, paired Student t-test, $p<0.05$). Subsequent 10 min incubation with 50 μM LEV induced additional 20.9% inhibition of frequency (paired Student t-test, $p<0.05$) while 100 μM incubation inhibited mEPSC frequency to 78.4% of 50 μM effects (21.5% reduction). The maximal effect detected during 100 mM LEV was 51.7% reduction of mEPSC frequency of baseline period. The estimated IC_{50} for LEV inhibition of mEPSC frequency was 12.5 μM. This LEV action on mEPSC frequency was not reversible after 10 minutes washout of the drug (Fig. 7).

In slices from epileptic rats, LEV reduced the mEPSC frequency after 10 min 5 μM incubation to 47.3% of baseline (52% reduction, paired t-test, $p<0.01$) while subsequent incubation with 50 μM for 10 min further reduced the frequency by 6.51% (but effect was not significant when compared to 5 μM LEV, paired t-test $p>0.05$). However, further incubation in 100 μM LEV induced an additional 17% significant reduction in mEPSC frequency (paired t-test, $p<0.05$) when compared to 50 μM LEV (Fig. 8). Maximal effect of 100 mM LEV was 63% reduction of baseline mEPSC frequency. Estimated IC_{50}= 8.67 μM was 30% lower than effective concentration calculated for LEV effect on control slices. In contrast to experiments in control slices, effect of LEV on mEPSC frequency exhibited a partial recovery to 59% of baseline response.

Table 2. *Effect of levetiracetam on mEPSC amplitude in granule cells of dentate gyrus.*

		Levetiracetam				
Groups	Baseline	5 μM	50 μM	100 μM	Washout	ANOVA
Control (n=8)	1.92 ± 0.6 Hz	1.50 ± 0.3 Hz	1.18 ± 0.2 Hz	0.93 ± 0.2 Hz	0.83 ± 0.3 Hz	*P<0.001*
Epileptic (n=4)	3.17 ± 0.6 Hz	1.50 ± 0.2 Hz	1.41 ± 0.2 Hz	1.17 ± 0.2 Hz	1.87 ± 0.4 Hz	*P<0.05*

Statistical comparisons were made by one-way ANOVA. Statistical significance was set at *P*<0.05. Values are presented as means ± SEM.

2.1.1.2. Effect of different concentrations of LEV on mEPSC amplitude in granule cells of dentate gyrus in control *vs* epileptic rats.

As predicted, experiments performed in control and epileptic slices revealed that incubation with LEV reduce frequency of mEPSC without affecting the amplitude of mEPSC (Table 3) indicating that LEV site of action in primarily presynaptic (Fig. 7e and Fig. 8e).

***Table 3**. Effect of levetiracetam on mEPSC amplitude in granule cells of rat dentate gyrus.*

		Levetiracetam				
Groups	Baseline	5 μM	50 μM	100 μM	Washout	ANOVA
Control (n=8)	4.5 ± 0.5 pA	4.6 ± 0.4 pA	4.4 ± 0.3 pA	4.5 ± 0.4 pA	4.4 ± 0.5 pA	n.s.
Epileptic (n=4)	4.7 ± 0.4 pA	4.8 ± 0.3 pA	4.4 ± 0.5 pA	4.5 ± 0.6 pA	4.3 ± 0.7 pA	n.s.

Statistical comparisons were made by one-way ANOVA. Statistical significance was set at $p<0.05$. Values are presented as means ± SEM.

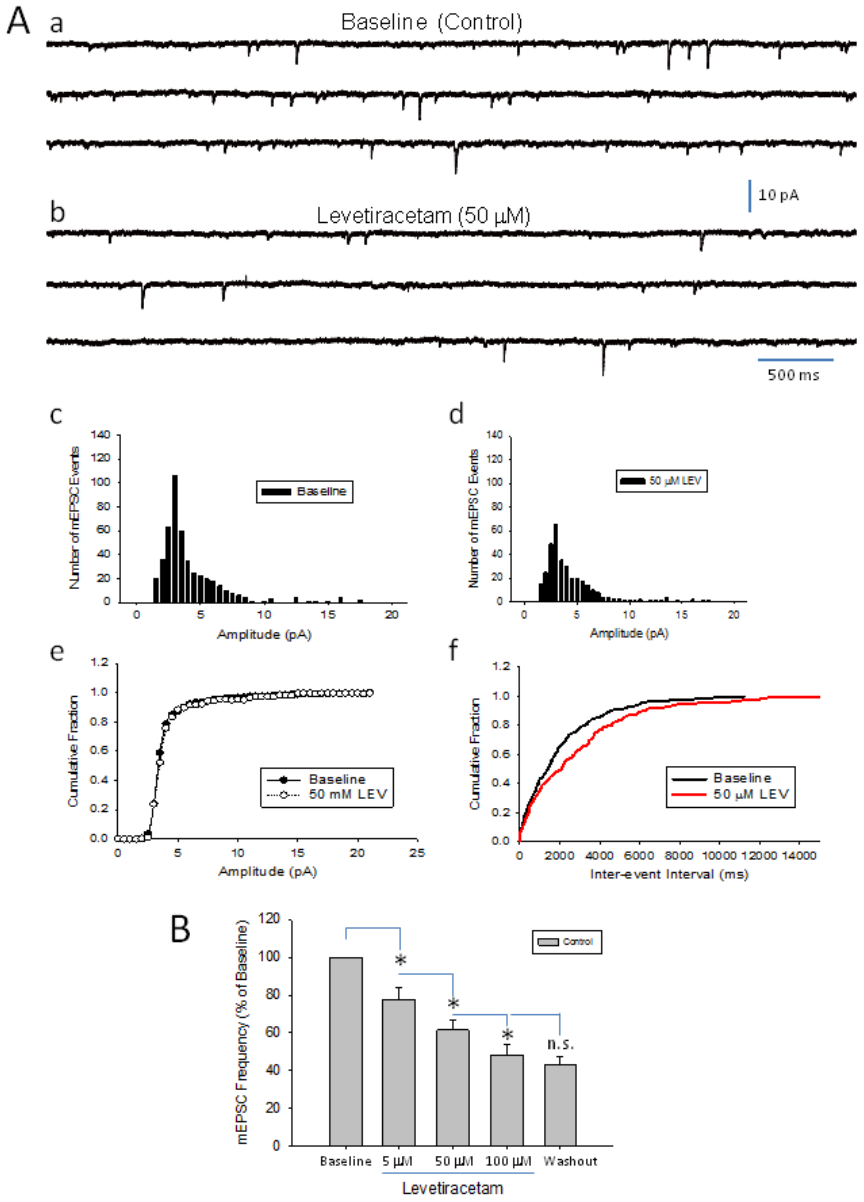

Fig. 7. ***Levetiracetam inhibits excitatory transmission in dentate granule cells in slices from control rats.*** **A.** Representative experiments assessing the effect of levetiracetam (LEV) on mEPSCs. a. Traces from a control (baseline) period of mEPSC recordings. b. traces from a period of incubation with 50 µM levetiracetam. Notice a reduction in the frequency of mEPSCs. c,d. Frequency histograms of mEPSC amplitude during baseline and LEV incubation respectively. e. Graph of cumulative fraction histograms shows no difference in cumulative fractions of amplitude in baseline compared to LEV (Kolgomorov-Smirnov test, $p>0.05$). f. Graph representing the analysis of cumulative histograms for inter-event of baseline period compared to LEV application. Notice a right-shift of curve after LEV indicating longer inter-event intervals. Difference was significant by the Kolgomorov-Smirnov test, $Z=4.4$, $p<0.05$). **B**. Bar graph illustrating the mean percent change in mEPSC frequency relative to baseline period. * Statistical significance $p<0.05$, Paired student t-test compared to preceding concentration. One-way ANOVA statistical comparisons was significant, $p<0.05$.

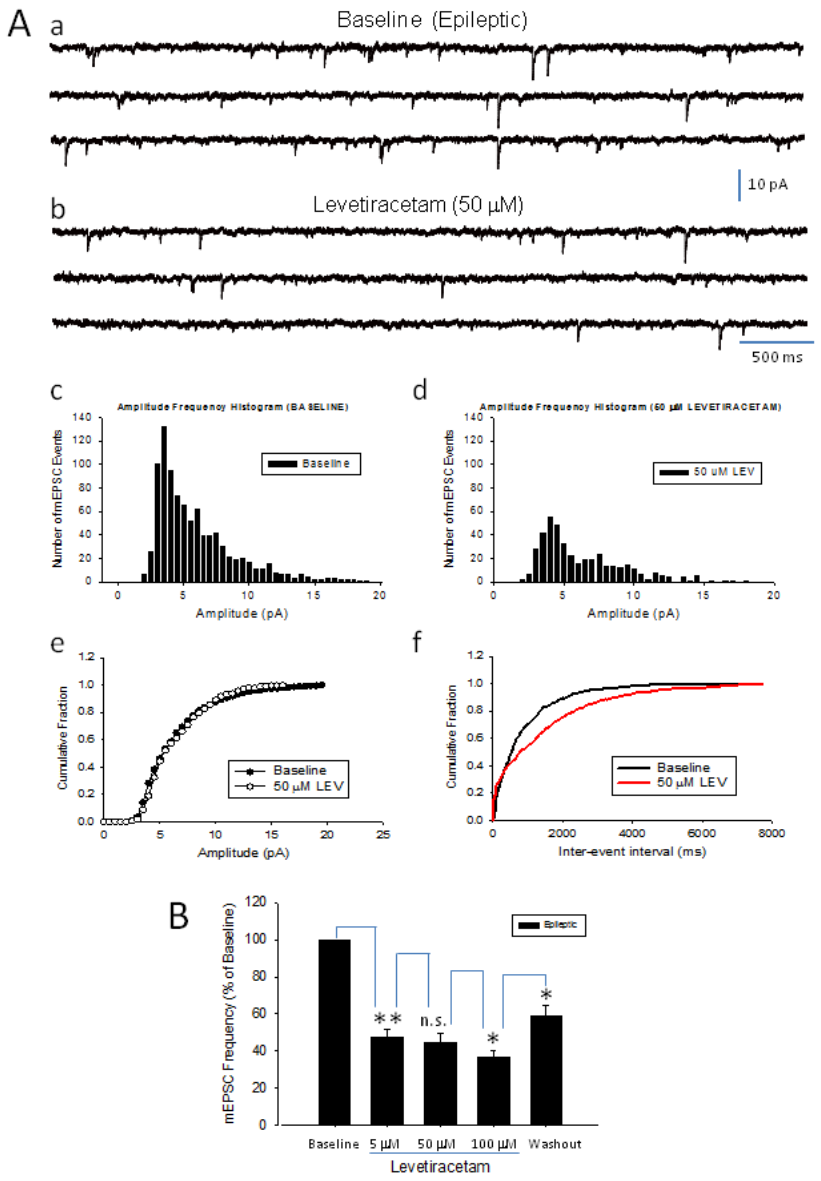

Fig. 8. Levetiracetam inhibits excitatory transmission in dentate granule cells in slices from epileptic rats. **A.** Representative experiments assessing the effect of levetiracetam (LEV) on mEPSCs. a. Traces from a control (baseline) period of mEPSC recordings. b. traces from a period of incubation with 50 µM levetiracetam. Notice a reduction in the frequency of mEPSCs. c,d. Frequency histograms of mEPSC amplitude during baseline and LEV incubation respectively. e. Graph of cumulative fraction histograms shows no difference in cumulative fractions of amplitude in baseline compared to LEV (Kolgomorov-Smirnov test, $p>0.05$). f. Graph representing the analysis of cumulative histograms for inter-event of baseline period compared to LEV application. Notice a right-shift of curve after LEV indicating longer inter-event intervals. Difference was significant by the Kolgomorov-Smirnov test, $Z=4.01$, $p<0.05$). **B**. Bar graph illustrating the mean percent change in mEPSC frequency relative to baseline period. * Statistical significance $p<0.05$, ** Statistical significance $p<0.05$, Paired student t-test compared to preceding concentration. One-way ANOVA statistical comparisons was significant, $p<0.01$.

It has been recently reported that levetiracetam inhibit presynaptic Ca2+ channels to reduce transmitter release and excitability[42]. In addition, whole-cell patch-clamp recordings of AMPA and NMDA-mediated excitatory post-synatic currents in granule cells of dentate gyrus of Wistar rats showed that levetiracetam (100 μM) inhibited both evoked $EPSC_{AMPA}$ and $EPSC_{NMDA}$ to an equal extent (80%), altered the paired-pulse ratio (from 1.39 to 1.25), decreased the frequency of asynchronous EPSC and prolonged the inter-event interval of miniature $EPSC_{AMPA}$ (from 2.7 to 4.6 s) without changing the amplitude, suggesting a presynaptic action of levetiracetam[43]. Furthermore, action of levetiracetam was mediated by presynaptic P/Q-type voltage-dependent calcium channel to reduce glutamate release. In a different study, local perfusion with LEV (10, 30 and 100μM) alone did not affect the extracellular levels of all neurotransmitters whilst the release of neurotransmitters induced by K^+-evoked stimulation was inhibited by perfusion with LEV in a concentration-dependent manner, and those induced by agonists of RyR and IP3R were also inhibited by LEV[44]. Specifically, the RyR-induced release was inhibited by 10 μM LEV, whereas the IP3R-induced release was inhibited by 100 μM LEV, but not by 10 or 30 μM LEV. The above results suggest that LEV has little effect on the components of normal synaptic transmission but selectively inhibits transmission induced by neuronal hyperactivation. These data is in agreement with our results since we have now demonstrated that LEV is more effective on epileptic tissue.

2.1.2. Effect of Levetiracetam on excitatory transmission (spontaneous mEPSC) onto granule cells in the dentate gyrus of epileptic mice compared to age-matched controls: effects of gene dosage on the effectiveness of Levetiracetam.

LEV is a new type of antiepileptic drug (AED) exhibiting selective seizure protection in chronic animal models of epilepsy. LEV binds to the synaptic vesicle protein SV2A indicating a presynaptic site of action to counter hyperexcitability. In this study, we evaluated the *in vitro* effects of LEV on excitatory synaptic transmission in the pilocarpine model of mesial temporal lobe epilepsy (MTLE). It has been reported that expression levels of SV2A decline during the course of human epilepsy and in experimental MTLE. We hypothesized that LEV action may be differentially affected during epileptogenesis and in transgenic mice with altered SV2A expression. For this purpose, we also assessed LEV effects on excitatory synaptic transmission in slices from pilocarpine-treated epileptic and control mice with different SV2A genotypes. The pilocarpine model of epilepsy was induced in SV2A/SV2B double knockout (KO) mice obtained from Jackson Laboratories. AMPA receptor-mediated miniature excitatory postsynaptic currents (mEPSCs) were recorded in dentate granule cells using the whole cell patch-clamp configuration in saline-injected control SV2A KO (-/-)/SV2B+/+ mice, SV2A heterozygous (+/-)/SV2B+/+ and in wild type SV2A (+/+)/SV2B+/+. Different concentrations of LEV (5, 50 and 100 microM) were bath applied to evaluate effects on mEPSC frequency and amplitude. Double SV2A/SV2B KO mice were not included in this study due to early life mortality. All SV2A KO/SV2B +/+ mice exhibited seizures while handled or cage cleaning. Moreover, 14% of SV2A heterozygous mice exhibited spontaneous seizures (genetically epileptic). The amplitude of mEPSC was not significantly different among groups. These data indicate that in SV2A KO mice, action potential dependent synaptic drive onto granule cells is abnormally exaggerated while spontaneous release from readily releasable pool (RRP) may be preserved. It is possible that compensatory changes in other SV2 proteins may maintain control of quantal release from RRP while SV2A may play a critical role in activity dependent synaptic vesicle release.

LEV induced a significant decrease of mEPSC frequency in granule cells from SV2A wild-type (26% reduction) and heterozygous mice (37% reduction) when compared to pre-drug baseline (***Fig. 9,*** Table 4). LEV (100 μM) failed to modify mEPSC frequency in ~ 60% of the slices from SV2A KO/SV2B wild control mice while a paradoxical increase of mEPSC frequency was detected in the rest of the slices (***Fig. 10***). In addition, LEV induced a significant decrease of mEPSC frequency (51.7% reduction, Paired T-test, $p<0.05$) in slices from SV2A/SV2B (wild-type) mice sacrificed 2-4 months after *status epilepticus*. LEV exerted no significant effects on mEPSC amplitude in all experimental groups. Our findings indicate that LEV acts presynaptically to inhibit the glutamatergic drive onto dentate granule cells in control and chronically epileptic mice but this effect was more pronounced in epileptic slices. Lack of SV2A expression (SV2A KO) occluded the inhibitory effect of LEV on excitatory transmission in a subset of animals while a paradoxical increase of glutamate release was detected in another group. Although LEV selectively binds SV2A in normal brain, it is possible that compensatory changes (*i.e.* abnormal splicing) of remaining SV2B and SV2C proteins may provide additional non-SV2A LEV binding sites in SV2A KO and in epileptic mice with significant implications for the development of novel LEV-like antiepileptic drugs.

***Table 4**. Effect of levetiracetam on mEPSC frequency in granule cells of rat dentate gyrus.*

Groups	Baseline	LEV	Washout	ANOVA
Control SV2A +/+ Mice (n=13)	1.14 ±0.5 Hz	0.84 ± 0.3 Hz	0.77 ± 0.2 Hz	p<0.05
Control SV2A +/- Mice (n=4)	1.15 ±0.4 Hz	0.72 ± 0.6 Hz	0.90 ± 0.3 Hz	p<0.05
Control SV2A KO Mice (n=3)	0.28 ±0.1 Hz	0.37 ± 0.1 Hz	0.22 ± 0.1 Hz	p<0.05
Epileptic SV2A +/+ Mice (n=4)	0.39 ±0.2 Hz	0.18 ± 0.1 Hz	0.23 ± 0.1 Hz	p<0.05

Statistical comparisons were made by one-way ANOVA. Statistical significance was set at p<0.05. Values are presented as means ± SEM.

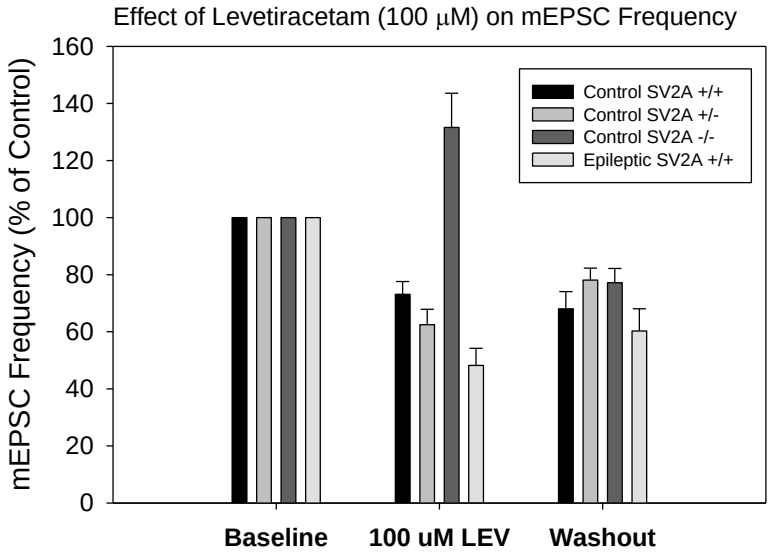

Fig. 9. Effect of levetiracetam (LEV) on mEPSC recorded from dentate granule cells in SV2A/SV2B transgenic mice. LEV inhibited mEPSC frequency in saline-injected control SV2A +/+ and SV2A +/- (paired Student t-test, p<0.05 in each case compared to baseline pre-drug period). In a subset of SV2A -/- LEV exerted a paradoxical effect increasing the frequency of mEPSCs.

***Table 5**. Effect of levetiracetam on mEPSC amplitude in granule cells of rat dentate gyrus.*

Groups	Baseline	LEV	Washout	ANOVA
Control SV2A +/+ Mice (n=13)	6.01 ±0.8 pA	5.62 ± 0.6 pA	5.72 ± 0.5 pA	n.s
Control SV2A +/- Mice (n=4)	5.82 ±0.4 pA	5.65 ± 0.7 pA	5.40 ± 0.8 pA	n.s
Control SV2A KO Mice (n=3)	4.84 ±0.7 pA	5.10 ± 0.5 pA	4.41 ± 0.7 pA	n.s
Epileptic SV2A +/+ Mice (n=4)	4.75 ±0.5 pA	4.23 ± 0.4 pA	5.10 ± 0.5 pA	n.s

Statistical comparisons were made by one-way ANOVA. Statistical significance was set at p<0.05. Values are presented as means ± SEM.

2.3. Effect of topiramate oan synaptic transmission (spontaneous mEPSC) onto granule cells in the dentate gyrus of epileptic rats compared to age-matched controls.

Topiramate is a widely used antiepileptic drug that exhibits effectiveness in most seizure types except perhaps for absence. Studies have found it useful for intractable epilepsy[45,46]. Although the exact mechanism of action of topiramate is not fully understood it has been reported that the antiepileptic properties of topiramate may result, at least in part, from the interaction and inhibition of AMPA (α-amino-3-hydroxy-5-methylisoxazole-4-propionic acid)/kainate glutamate receptors/kainate-induced inward currents without effect on NMDA-evoked currents[47]. For instance, in whole-cell voltage-clamp recordings from principal neurons of the rat basolateral amygdala, topiramate at low concentrations (IC50, approximately 0.5 μM) selectively inhibited pharmacologically isolated excitatory synaptic currents mediated by kainate receptors containing the GluR5 subunit[48,49]. However, controversial electrophysiological studies have shown that topiramate also exerts a direct membrane action to reduce neuronal excitability. For instance, in cultured hippocampal neurons, topiramate reduced the duration of spontaneous epileptiform bursts and limited repetitive firing of Na^+-dependent action potentials elicited by a depolarizing current pulse[50]. These effects were generally credited to an ability of this drug to act as state-dependent Na^+ channel blocker[51]. In addition, Zona et al, reported that Topiramate attenuates voltage-gated sodium currents in rat cerebellar granule cells[52]. In a recent study, application of topiramate reduced the duration of paroxysmal depolarization shift and later spikes with less effect on the initial action potential. These results suggest that frequency-dependent inhibition of neuronal activity due to blockade of sodium channels may account largely for the anticonvulsant efficacy of topiramate[53]. However, electrophysiological analysis of topiramate on sodium currents in mouse spinal cord neurons in cell culture failed to support the notion that topiramate act via inhibition of sodium currents[54]. In favor of a presynaptic action site, it has recently reported that the presynaptic fiber spike was depressed by topiramate (100 μM) at the stimulation frequency of 0.2 Hz but not at 0.05 Hz[53]. The frequency-dependent inhibition of excitatory potentials and presynaptic fiber spike suggests that topiramate may block Na^+ channels thereby stabilizing presynaptic membranes and decreasing the release of transmitter. However, these authors did not observe a significant effect of topiramate on the paired-pulse facilitation suggesting that inhibition induced by topiramate does not interfere with the presynaptic mechanisms involved in this kind of facilitation. As alternative explanation, these authors suggested that topiramate-induced inhibition occurs via reduction axon excitability. In support of a presyanptic site of action, it has been reported that topiramate induced a 27% decrease in Ca^{2+} channel-mediated release of [^{3}H]Glutamate evoked by high K^+ in hippocampal isolated nerve endings[55]. In our experiments, we recorded mEPSC from granule cells in the dentate gyrus of control and epileptic rats. We tested different concentrations of topiramate (5, 50 and 100 μM) on the frequency and amplitude of mEPSC recorded in an ACSF containing TTX (0.5 μM) to block action potential-mediated release of glutamate, GABAzin (10 μM) to inhibit GABAa receptors and AP-5 (50 μM) to block NMDA-mediate currents. The experimental paradigm for these experiments is depicted in **Fig. 10**. The inhibitory concentration (IC_{50}) was calculated fitting the dose-response curve in SigmaPlot with the function: *f1 = min + (max-min)/(1 + (x/IC50)^(-Hillslope)) where f = if(x<=0, if(Hillslope>0,min,max), f1).*

Results: Consisting with previous reports on the effect of topiramate on excitatory synaptic transmission, we detected a significant inhibitory effect of topiramate (50 and 100 μM) on mEPSC amplitude in control slices (baseline= 5.2 ± 0.6 pA *versus* 50 μM topiramate=3.36 ± 0.6 pA, a 31.5% reduction and 100 μM topiramate= 3.48 ± 0.7 pA, 29% reduction, Paired t-test, $p<0.05$, n=6) and slices from pilocarpine-treated chronically epileptic Sprague Dawley rats (baseline=4.9±0.8 pA *versus* 50 μM topiramate=3.8 ± 0.4 pA, only 5.7% reduction and 100 μM topiramate=3.6 ± 0.6 pA, 11.4% reduction, Paired t-test, $p<0.05$, n=4). Although topiramate's inhibitory action on mEPSC amplitude was still present on slices from epileptic rats, the relative effectiveness was reduced in rats sacrificed 2-4 month after pilocarpine-induced *status epilepticus* ***(Fig. 11)***. For instance, 50 μM Topiramate induced a non-significant 5.7% reduction of mEPSC amplitude while 100 μM topiramate was approximately 3 times less effective in epileptic than in control tissue). These data indicate that the post-synaptic action of topiramate, putatively on AMPA/kainate (*i.e.* GluR5 receptors) may be partially affected during epileptogenesis yielding incomplete protection against seizures. In part, this notion may explain, at least in part, the pharmacoresistance observed in a subset of some patients to topiramate treatment.

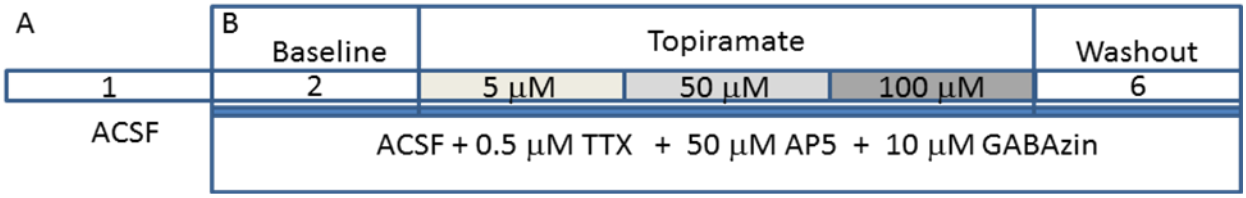

Fig. 10. Experimental paradigm to evaluate the effect of topiramate on excitatory transmission in the dentate gyrus. **A.** Visualized whole-cell patch clamp recordings were performed in ACSF from granule cells in the dentate gyrus of horizontal hippocampal slices obtained from pilocarpine-treated Sprague Dawley rats compared to age-matched controls. In current clamp we measured intrinsic properties (i.e. resting membrane potential, membrane time constant and input resistance) and firing pattern phenotype and in voltage clamp we recorded activity-dependent spontaneous EPSCs. **B**. Slices were then bathed in ACSF containing: (1) TTX to block TTX-sensitive sodium channels and measure spontaneous mEPSC), (2) 5-amino-phosphovaleric acid (AP-5) to block NMDA receptor-mediated currents and isolate AMPA/kainate mediated mEPSCs, and (3) GABAzin to inhibit $GABA_A$ receptors-mediated inhibitory currents. After a recording of 10 minute baseline period (1), increasing concentrations of topiramate were applied for 10 minute period each while recording mEPSCs. Then, topiramate was removed from the bath ACSF (period 6) while recording the washout effect to assess any recovery of topiramate effects on mEPSC.

Additional studies are in progress to determine the time-course of these abnormalities after *status epilepticus*. We predict that action of topiramate will be further impaired as the epileptogenic process progress. Topiramate inhibition of mEPSC amplitude in control and epileptic slices is consistent with the current notion that topiramate inhibits GluR5 kainate receptors[48,49,56] as a key antiepileptic mechanism to increase the threshold for seizures. We also detected a dose-dependent effect of topiramate on the mEPSC frequency indicating a presynaptic action site of topiramate. In control slices, this effect was significant with 5 and 50 μM topiramate (Paired t-test, $p<0.05$ respectively) (**Fig. 11B**) but was not significant at 100 μM. In contrast, topiramate induced a dose-dependent reduction of mEPSC frequency in slices from epileptic rats sacrificed 2-4 months after *status epilepticus* but this effect was only significant at 50 μM (1.89±0.4 Hz) and 100 μM topiramate concentration (1.47±0.4 Hz) compared to baseline period frequency (2.21±0.5 Hz) for a 14.4 and 33.1% *reduction respectively*. Interestingly, this inhibitory effect on mEPSC frequency was reversible during the washout of the drug. Our findings indicate that topiramate at 50 and 100 μM may act presynapticaly to reduce the release of glutamate and excitability in slices from epileptic rats.

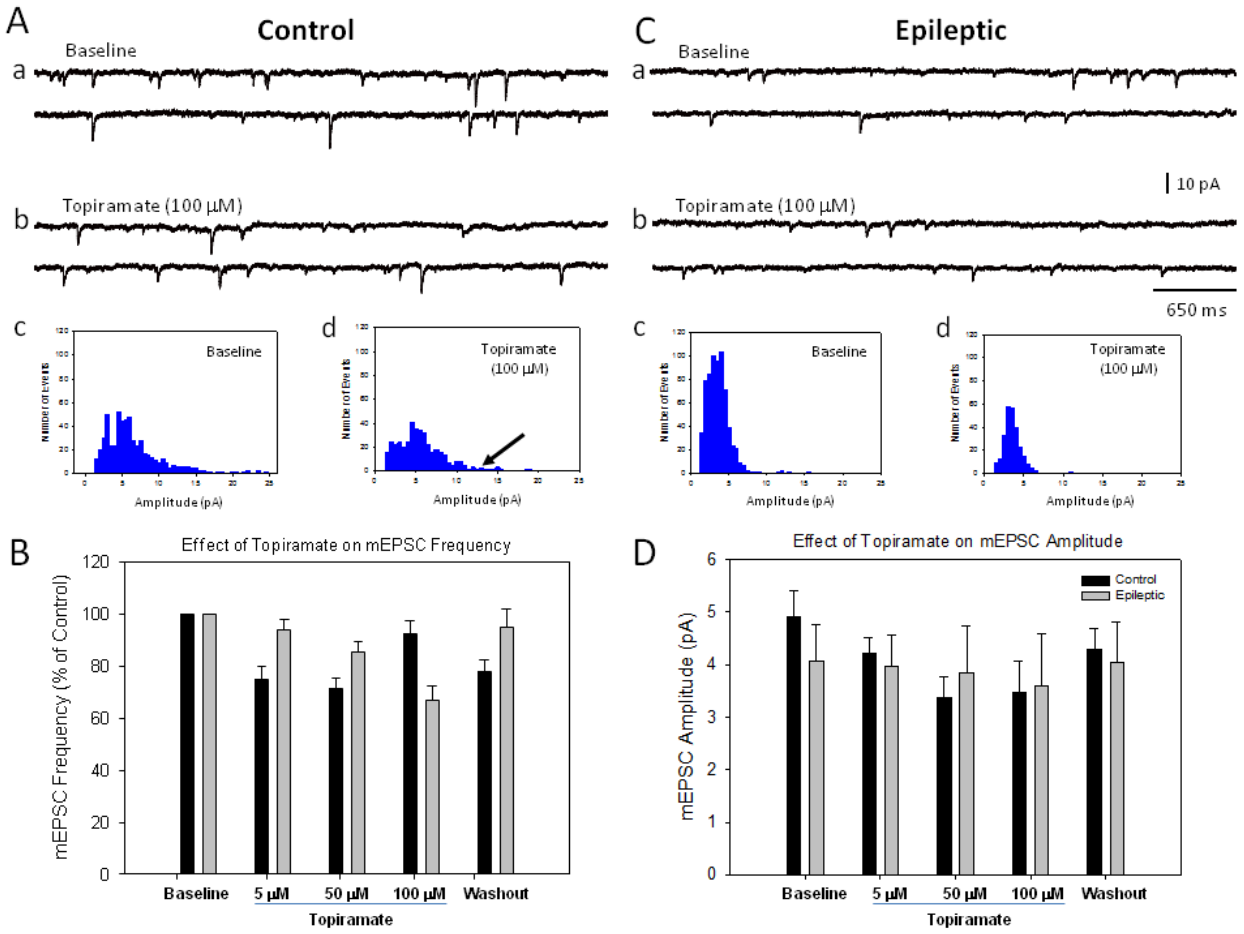

Fig. 11. Topiramate is effective in reducing the frequency and amplitude of mEPSCs in control (A) and epileptic rats (B). **Panel A.** Representative mEPSC traces recorded from a granule cell in control rat before (baseline) (a) and after 100 □M Topiramate bath application (b). Frequency histogram of mEPSC amplitude is represented in the bar graph of baseline (c) and after Topiramate application (d). Notice a general reduction in the number of events, but effect was more accentuated in events ranging 10 -25 pA amplitude (arrow) in (d). **B**. Similar results were obtained in the analysis of mEPSC in epileptic rats sacrificed 2-4 months after *Status Epilepticus*. Analysis of pooled data for different experiments comparing increasing concentrations of Topiramate indicate a significant effect of on the frequency (ANOVA, $p<0.05$) (**C**) and amplitude of mEPSCs (**D**) (ANOVA, $p<0.05$). For epileptic tissue, topiramate-induced changes in frequency of mEPSC was only significant (when compared to baseline) during 5 and 50 □M of Topiramate while effect on amplitude exhibited similar pattern in control and epileptic and maximal effect was reached at 50 □M with partial recovery. We tested different concentrations of topiramate (5, 50 and 100 □M) on the frequency and amplitude of mEPSC recorded in an ACSF containing tetradotoxin (0.5 uM) to block action potential-mediated release of glutamate, GABAzin (10 □M) to inhibit GABAA receptors and AP-5 (50 □M) to block NMDA-mediate mEPSCs.

Several mechanisms have been postulated to explain the antiepileptic effects of topiramate, however, the relevance of these actions to the antiepileptic and anti-epileptogenic efficacy remained unclear. Our findings indicate that topiramate exert, at least in part a presynaptic action inhibiting the release of glutamate in the dentate gyrus. In epileptic rats, the presynaptic action of topiramate followed a dose-dependent effect with maximal inhibitory action at 100 µM (IC_{50}=37µM) in contrast to responses in control tissue where the presynaptic inhibitory effect disappeared at that dose. We also detected a dose-dependent effect on the amplitude of non-NMDA-mediated excitatory currents supporting previous studies that suggest topiramate act by inhibiting AMPA or

Kainate receptors. In addition, the inhibitory effect of topiramate on excitatory transmission was preserved but reduced when compared to controls in chronically epileptic Sprague Dawley rats. We also detected a dose-dependent effect of topiramate on the mEPSC frequency indicating a novel presynaptic action site.

2.4. Effect of carbamazepine on synaptic transmission (spontaneous mEPSC) onto granule cells in the dentate gyrus of epileptic rats compared to age-matched controls.

Compelling number of studies have demonstrated that carbamazepine (CBZ) binds and block sodium channels in an activity dependent manner to reduce action potential firing and consequentially reduce hyperexcitability[57-59]. However, the presynaptic action of CBZ has remained unexplored. In order to evaluate whether CBZ affect the amplitude and frequency of mEPSCs onto granule cells, different concentrations where bath applied in slices from control and chronically epileptic rats. We notice that CBZ induced no changes in the frequency of mEPSC in slices from control (Baseline= 0.83 ± 0.2 Hz, 3μM=0.78 ± 0.3 Hz, 30 μM= 0.81 ± 0.2 Hz, 300 μM=0.71 ± 0.1 Hz, ANOVA, $p>0.05$, n=7) or pilocarpine-treated chronically epileptic rats (Baseline= 0.92 ± 0.3 Hz, 3μM=0.9 ± 0.4 Hz, 30 μM= 0.87 ± 0.2 Hz, 300 μM=0.85 ± 0.2 Hz, n=7, ANOVA, $p>0.05$) n=9). CBZ did not affect mEPSC amplitude.

2.5. Effect of antiepileptic drugs on GABAergic transmission

Recent studies indicate that in control tissue LEV inhibit inhibitory synaptic transmission in a frequency dependent manner[60]. These authors found that LEV reduces inhibitory currents in a frequency-dependent manner, with the largest relative effect on the later IPSCs in the highest frequency trains. However, in contrast to excitatory postsynaptic currents (EPSCs), LEV reduced IPSC trains after a briefer, 30 min incubation. In order to elucidate the action of levetiracetam in presynaptic inhibitory transmission were recorded miniature inhibitory postsynaptic currents mEPSC (of GABAergic nature) in granule cells in the dentate gyrus of control rats and in the SV2A/SV2B transgenic mice with different SV2A genotypes (SV2A+/+ and SV2A-/- KO). In addition, we recorded mIPSC from granule cells in pilocarpine-treated SV2A+/+ mice 2 months after induction of *status epilepticus*.

2.5.1. Effect of Levetiracetam on spontaneous miniature inhibitory postsynaptic currents (mIPSC) onto granule cells in the dentate gyrus of epileptic rats and mice.

Our data revealed that LEV induced a significant reduction in the frequency of baseline mIPSCs (1.58±0.5 Hz) to 0.4±0.15 Hz (75% reduction, Paired t-test, $p<0.01$, n=6) in Sprague Dawley rats (**Fig. 12**). Action of LEV on mIPSC frequency did not recover after 10 minute washout. Incubation of slices in 100 μM LEV for 10 minutes induced a significant reduction of mIPSC to 35% of control in saline-injected control SV2A+/+ mice (n=4) (baseline=1.59±0.2 Hz compared to LEV=0.56 ±0.17 Hz, a 65% reduction, Paired Student-t test, $p<0.01$) with partial recovery (**Fig. 13**). Interestingly, LEV was also effective in reducing mIPSC frequency in SV2A KO mice (baseline= 2.44 ± 0.6 Hz versus LEV=1.48 ± 0.7 Hz, a 40% reduction, Paired Student t-test, $p<0.05$) with no recovery (**Fig. 14**). These results indicate that other LEV can bind or interact with other presynaptic targets in the SV2A-/- mice. It is possible that SV2A KO may trigger compensatory changes in other SV2 proteins (i.e. SV2B or SV2C) that may facilitate binding to LEV (i.e. alternative splicing). Incubation of slices from pilocarpine-treated epileptic SV2A+/+ mice in LEV (100 μM) revealed a significant 46% increase in the frequency of mIPSCs (**Fig. 15**) with a complete recovery of the LEV effect after washout of the drug. Changes in mIPSC frequency were not associated with significant changes in mIPSC amplitude indicated a presynaptic site of action to control GABA release onto dentate gyrus granule cells.

A recent study reported that LEV reduces inhibitory currents in a frequency-dependent manner, with the largest relative effect on the later IPSCs in the highest frequency trains[60] . These authors demonstrated that in contrast to excitatory postsynaptic currents (EPSCs), LEV reduced IPSC trains after a briefer, 30 min incubation. However, if synaptic activity was limited by treating with excitatory transmitter antagonists, after the initial LEV exposure, LEV still diminished trains of IPSC. The concentration required to diminish IPSC trains was lower than for EPSCs. Our data are in agreement with these findings indicating that LEV can also modulate inhibitory transmission. Although the reduction of IPSC trains by LEV initially seems counterintuitive for an antiepileptic drug,

there are multiple reasons that disruption of γ-aminobutyric acid (GABA) release could ultimately attenuate pathologic discharges. Interestingly, we also discover that in contrast with control tissue, LEV enhanced inhibitory (i.e. GABAergic) transmission by increasing the frequency of mIPSC in dentate gyrus. To the best of our knowledge this action of LEV has not been described yet, we will perform additional experiments to confirm and fully characterize this novel action of LEV in the epileptic brain. It is important to highlight that LEV is a drug with a unique antiepileptic profile. LEV failed to block seizures in acute models of epilepsy while exhibited a potent antiepileptic effect in chronic experimental models of epilepsy as the kainate, kindling and pilocarpine models. This antiepileptic profile may be related to molecular changes that are specific for tissue undergoing epileptogenesis (i.*e.* abnormal binding sites for LEV, in addition to the already reported SV2A).

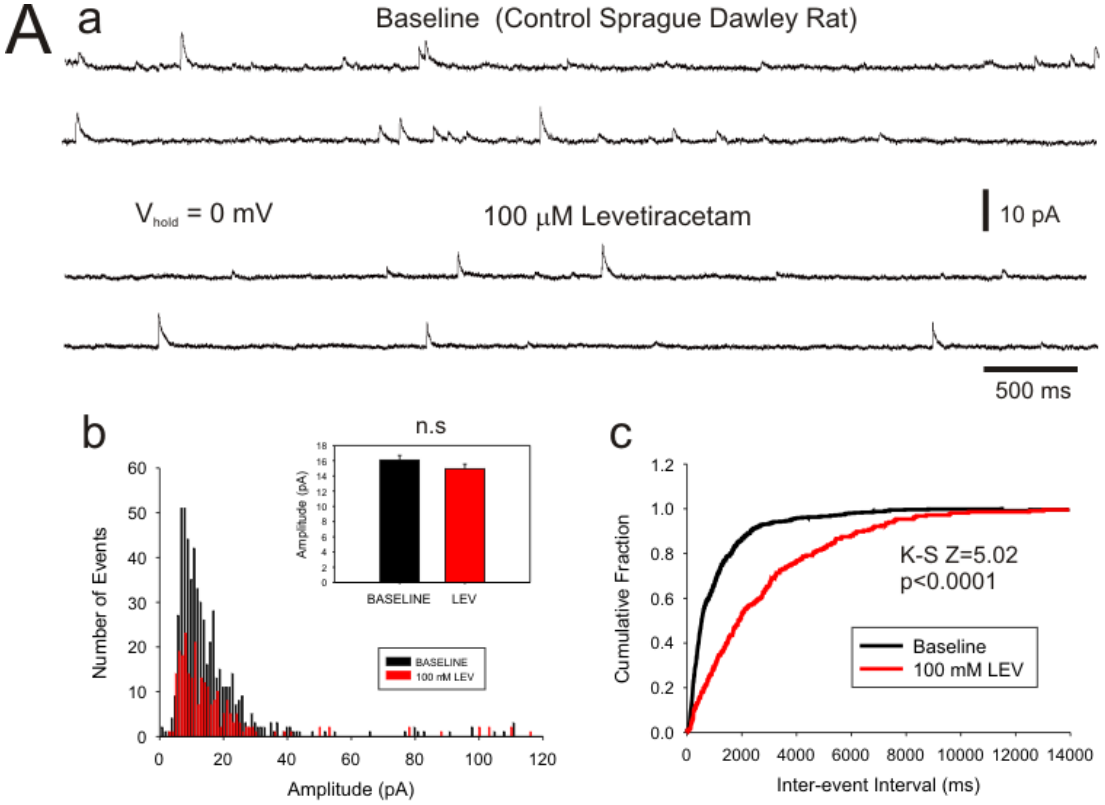

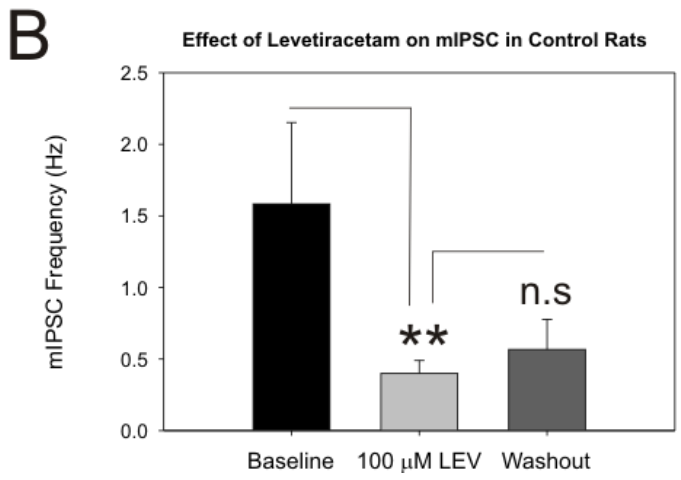

Fig. 12. Levetiracetam (LEV) inhibits GABAergic synaptic transmission onto dentate granule cells from Sprague Dawley rat. **A**. Representative experiment illustrating the inhibitory effect of LEV on mIPSC frequency. a. Upper traces: mIPSC recordings from baseline period, Lower traces: mIPSC during 100 mM LEV treatment. B. Frequency of histogram of mIPSC amplitude. *Inset*: Bar graph showing no significant LEV effect on mIPSC amplitude (n.s, paired t-test, p>0.05). c. Cumulative frequency distributions for mIPSC inter-event intervals obtained before and during LEV application show a right-shift towards longer intervals. Plot distributions were significantly different by Kolmogorov-Smirnov (K-S) stat (inset). mIPSC frequency from 1.2 Hz during baseline and was reduced to 0.6 Hz after LEV. **B**. Bar graph of pool data for mean frequency depicting LEV inhibitory action on mIPSC frequency. **Statistical significance, p<0.01, Student paired T-test.

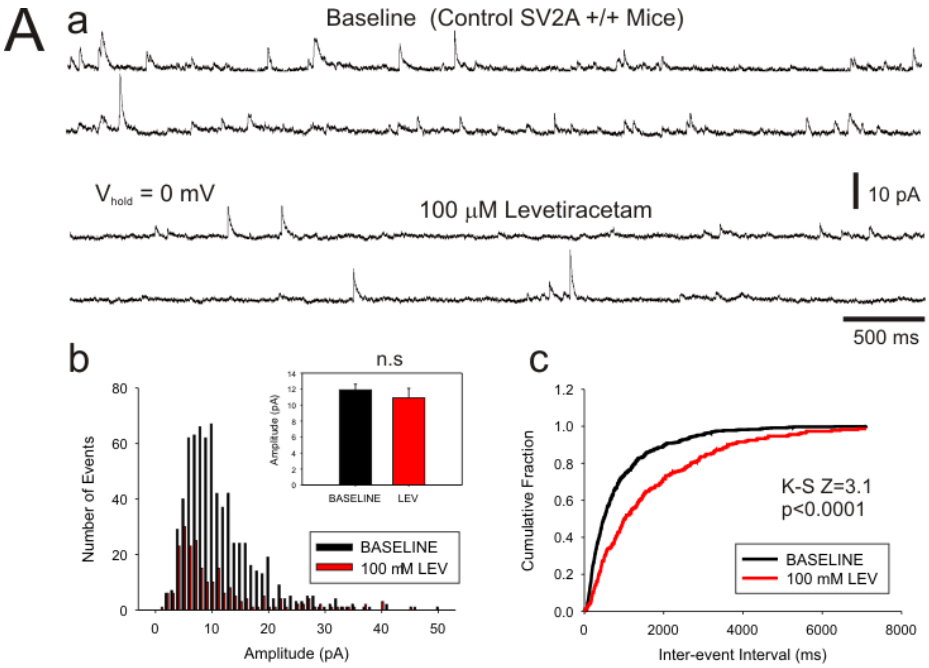

Fig. 13. Levetiracetam (LEV) reduce inhibitory transmission onto dentate granule cells in adult control SV2A+/+ /SV2B+/+ mice. **A**. Representative experiment illustrating the inhibitory effect of LEV on mIPSC frequency. a. Upper traces: mIPSC recordings from baseline period, Lower traces: mIPSC during 100 mM LEV treatment. B. Frequency of histogram of mIPSC amplitude. *Inset*: Bar graph showing no significant LEV effect on mIPSC amplitude (n.s, paired t-test, p>0.05). c. Cumulative frequency distributions for mIPSC inter-event intervals obtained before and during LEV application show a right-shift towards longer intervals. Plot distributions were significantly different by Kolmogorov-Smirnov (K-S) stat (inset). mIPSC frequency from 2.1 Hz during baseline and was reduced to 1.2 Hz after LEV. **B**. Bar graph of pool data for mean frequency depicting LEV inhibitory action on mIPSC frequency. Statistical significance * and **, p<0.05 and p<0.01 respectively, Student Paired T-test.

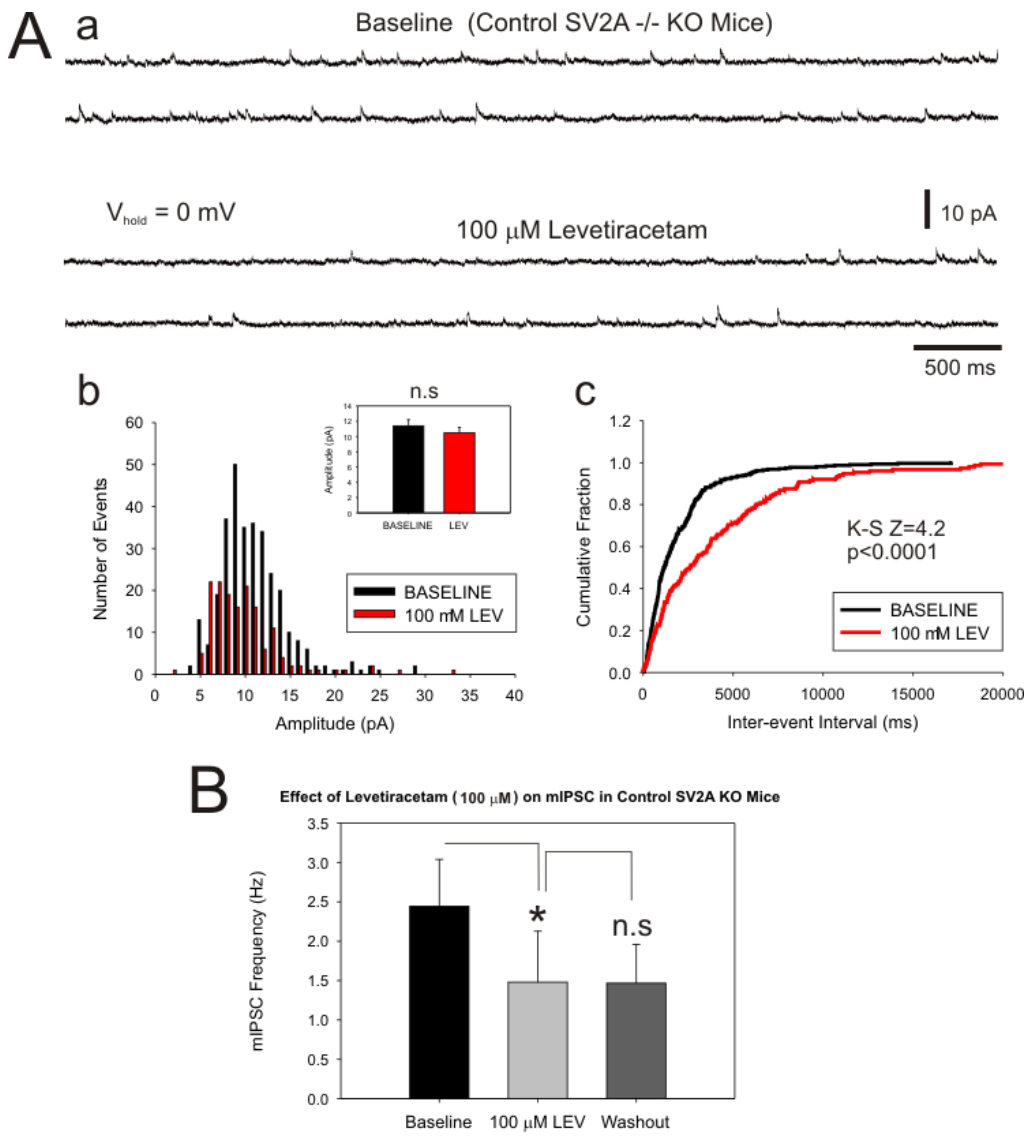

Fig. 14. Effect of levetiracetam (LEV) on mIPSC recorded in dentate granule cells from adult control SV2A-/- / SV2B+/+ mice. **A**. Representative experiments illustrating the inhibitory effect of LEV on mIPSC frequency. a. Upper traces: mIPSC recordings from baseline period, Lower traces: mIPSC during 100 mM LEV treatment. B. Frequency of histogram of mIPSC amplitude. *Inset*: Bar graph showing no significant LEV effect on mIPSC amplitude (n.s, paired t-test, p>0.05). c. Cumulative frequency distributions for mIPSC inter-event intervals obtained before and during LEV application show a right-shift towards longer intervals. Plot distributions were significantly different by Kolmogorov-Smirnov (K-S) stat (inset). mIPSC frequency from 0.85 Hz during baseline and was reduced to 0.55 Hz after LEV. **B**. Bar graph of pool data for mean frequency depicting LEV inhibitory action on mIPSC frequency. Statistical significance * = p<0.05, Student Paired T-test. n.s, no significance.

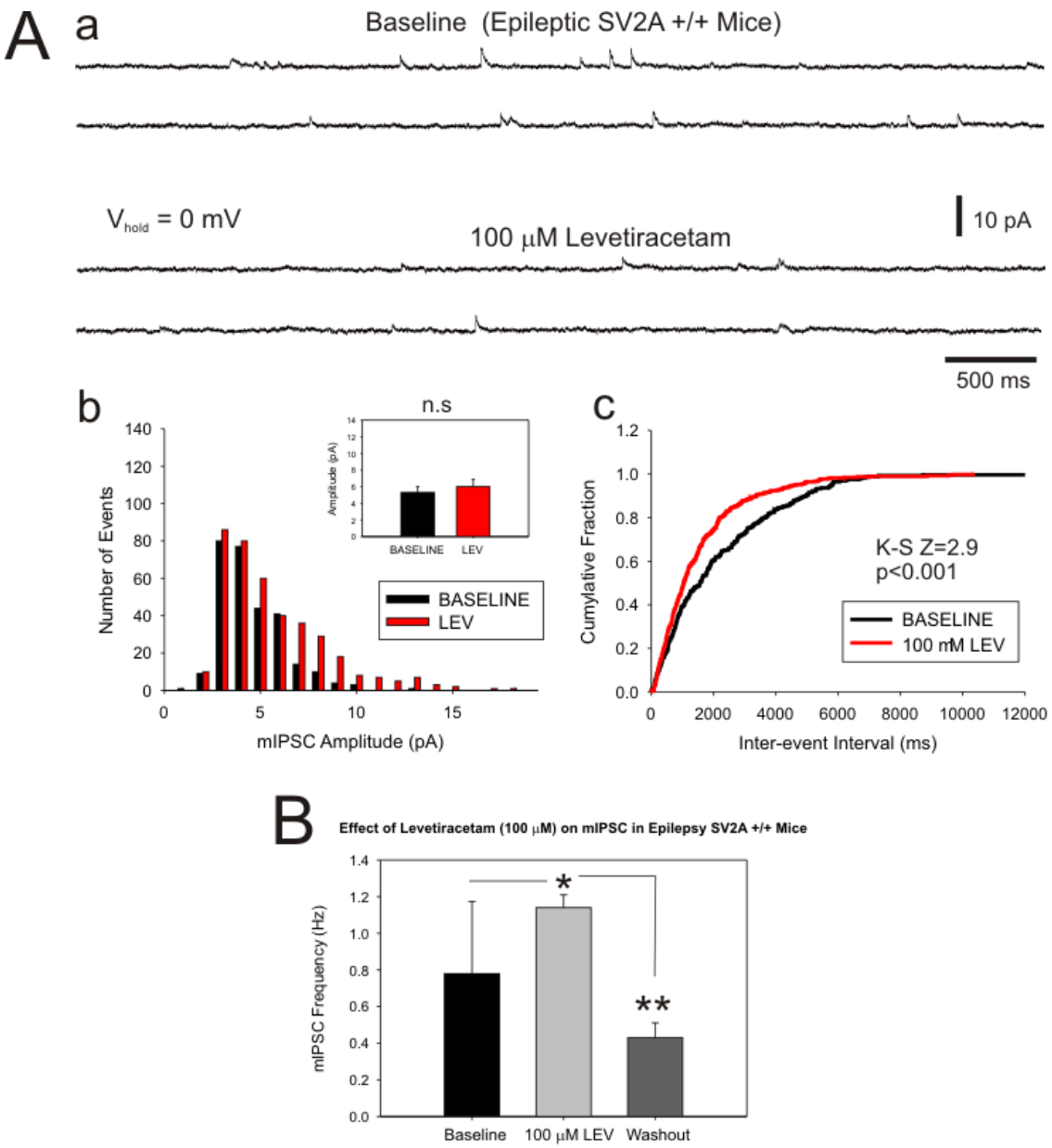

Fig. 15. Levetiracetam (LEV) enhances inhibitory synaptic transmission onto dentate granule cells in pilocarpine-treated chronic epileptic SV2+/+ /SV2B+/+ mice. **A**. Representative experiment illustrating action of LEV on mIPSC frequency. a. Upper traces: mIPSC recordings from baseline period, Lower traces: mIPSC during 100 mM LEV treatment. B. Frequency of histogram of mIPSC amplitude. *Inset*: Bar graph showing no significant LEV effect on mIPSC amplitude (n.s, paired t-test, p>0.05). c. Cumulative frequency distributions for mIPSC inter-event intervals obtained before and during LEV application show a left-shift towards shorter intervals. Plot distributions were significantly different by Kolmogorov-Smirnov (K-S) stat (inset). mIPSC frequency from 0.35 Hz in baseline was increased to 0.65 Hz after LEV incubation for 10 min. **B**. Bar graph of pool data for mean frequency depicting a significant pro-inhibitory action of LEV (increasing mIPSC frequency). Statistical significance * = p<0.05 and *=p<0.01, Student paired T-test. n.s, no significance.

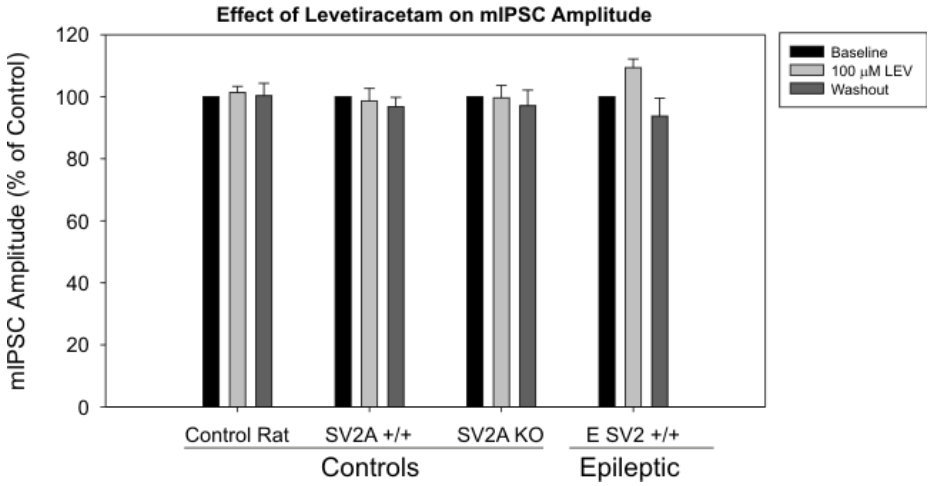

Fig. 16. Effect of levetiracetam (LEV) in mIPSC in granule cells from control Sprague Dawley rats (A), control SV2A+/+/SV2B+/+ mice (B), control SV2A KO/SV2B+/+ mice (C) and pilocarpine-treated epileptic SV2A+/+ /SV2B mice (D). LEV (100 μM) incubation resulted in no significant changes in the mIPSC amplitude for any of the experimental groups. Statistical analysis before and after-drug by paired Student t-test.

2.6. Morphological reconstructions and analysis of biocyting filled granule cells in control versus epileptic rats and SV2A/SV2B transgenic mice.

Biocytin was injected during patch-clamp recordings to assess the morphological characteristics of the cells and identify that the recorded neurons was in fact a granule cell. This procedure did not affected the number of animals used in the study but will provide additional information about the morphological features of recorded neurons. We have now optimized the protocol after troubleshooting issues with biocytin concentration and histochemistry assays to detect biocytin. Thereby, no all the recorded cells in our data (above) were filled with biocytin, but, all the filled neurons were identified as granule cells. In addition, we plan to analyze and correlate the frequency of spontaneous and miniature EPSC with the complexity of the recorded neurons. We hypothesize that the level of dendritic complexity will positively correlate with the excitatory and/or inhibitory drive. We plan in the next year to increase the number of biocytin-labeled neurons to perform statitical analysis and correlations.

Table 6. *Morphological characteristics of biocytin-labeled granule cells recorded in control and epileptic rats and mice.*

Morphological features	Sprague Dawley Rats		SV2A/SV2B Transgenic Mice	
	Control (n=2)	Epileptic (n=8)	Control (n=13)	Epileptic (n=2)
Soma				
Area (μm²)	68.81±9.24	130.94±37.44	86.47±11.18	88.56±26.53
Perimeter (μm)	33.80±3.70	46.55±4.98	36.94±2.53 (n=13)	39.650±9.45 (n=
Dentrites				
Quantity	1.50±0.50	2.25±0.31	1.92±0.34	1.50±0.50
Nodes	13.50±6.50	15.25±1.76	10.92±1.43	8.00±1.00
Ends	15.50±6.50	16.62±1.38	12.33±1.22	10.00±1.00
Mean Length (μm)	1765±194.15	1430.98±216.16	1094±186.19	971.10±507.20
Total Length (μm)	2550.65±591.35	2906.01±298.17	1566.96±164.61	1203.05±275.25

Values are presented as means ± SEM.

Several examples of biocytin-filled neurons are illustrated in the Appendix 3.

Milestones: The following milestones were accomplished during year 1.

(a) We have discovered that levetiracetam is more effective in inhibiting mEPSC frequency in slices from chronically epileptic rats (lower IC50), compared to age-matched controls, indicating that the epileptic condition does modify the function of the vesicular protein SV2A and its response to levetiracetam.

(b) Our data indicate that levetiracetam is more effective than topiramate or carbamazepine in reducing glutamate release in epileptic rats.

(c) In addition, we also found that topiramate can also act presynaptically to reduce glutamate release, while carbamazepine had no presynaptic effect on spontaneous quantal release.

(d) We demonstrated that levetiracetam also reduce the frequency of mIPSC, thereby altering the GABAergic inhibitory synaptic transmission but only in control animals. As a novel finding, LEV was still effective in reduce mIPSC frequency in SV2A KO mice suggesting that other LEV targets may become available in SV2A-/-. In addition, we also demonstrated that LEV increase the frequency of mIPSC in epileptic SV2A+/+ mice. To the best of our knowledge this effect of LEV in enhancing inhibitory synaptic transmission (augmented release of GABA) in chronically epileptic hippocampus has not been described yet, and may provide the basis for a novel mechanism of action of LEV to reduce hyperexcitability in chronically epileptic tissue.

During Year 1, we discovered that pilocarpine-induced status epilepticus causes disorganization of dentate gyrus and CA3 cytoarchitecture in mice. *Status epilepticus* also induced abnormal increases in the size and vesicular release rate of mossy fiber boutons in SpH-expressing mice that correlated with long-term ultrastructural reorganization of active zones in MFBs, including an increase in size of the active zone and the readily-releasable pool of vesicles. We performed electrophysiological and pharmacological studies to investigate the effects of levetiracetam, topiramate and carbamazepine on excitatory (glutamatergic) synaptic transmission onto granule cells in the dentate gyrus in slices from control vs. pilocarpine-treated epileptic rats and mice. We found that levetiracetam inhibits spontaneous glutamate release (mEPSC frequency) in control and epileptic rats and mice. In addition, levetiracetam was more effective in reducing excitatory synaptic transmission onto dentate granule cells in slices from chronically epileptic rats, while the lack of effect on mEPSC amplitude indicated it had no action on postsynaptic glutamate receptors. We also found that LEV increased the frequency of mIPSCs, enhancing GABAergic transmission via a presynaptic action. These data indicate that presynaptically acting drugs such as levetiracetam may become a key piece in the arsenal of antiepileptic drugs in drug-resistant mesial temporal lobe epilepsy. Thereby, screening for a presynaptic action site may be part of the strategy to discover novel and effective antiepileptic drugs.

We also uncover a novel presynaptic action of topiramate to reduce frequency of mEPSC in a dose-dependent manner, while inhibition of mEPSC amplitude was also present in both control and epileptic slices. In epileptic rats, the presynaptic action of topiramate followed a dose-dependent effect with maximal inhibitory action at 100 μM (IC50=37μM). We also detected a dose-dependent effect on the amplitude of non-NMDA-mediated excitatory currents, supporting previous studies that suggest topiramate inhibits AMPA or Kainate glutamate receptors. Interestingly, the inhibitory effect of topiramate on excitatory transmission was preserved in chronically epileptic rats. Consistent with previous studies, our data indicate that carbamazepine exerts no effect on either postsynaptic receptors or in the presynaptic release machinery. However, since carbamazepine inhibits sodium channels, it is still possible that inhibition of presynaptic sodium channels may reduce axonal and presynaptic bouton excitability during seizures or activity-dependent glutamate release. In the next year, we will assess whether antiepileptic drugs acting on presynaptic sites can reduce or prevent seizure-induced effects on basal vesicular release, and plasticity of release, from mossy fiber boutons in MTLE.

KEY RESEARCH ACCOMPLISHMENTS:

Data from our experiments in year 01 revealed that:

- Pilocarpine-induced *status epilepticus* causes disorganization of dentate gyrus and CA3 cytoarchitecture in SpH mice.

- Pilocarpine-induced *status epilepticus* state increases size and vesicular release rate of mossy fiber boutons in SpH-expressing mice

- *Status epilepticus* elicits long-term ultrastructural reorganization of active zones in MFBs.

- Levetiracetam is effective in inhibiting spontaneous glutamate release (mEPSC frequency) in both control and epileptic rats and mice.

- Levetiracetam was more effective in reducing excitatory synaptic transmission onto dentate granule cells in slices from chronically epileptic rats (IC_{50}= 8.67 μM) when compared to control rats (IC_{50}=12.5 μM).

- Levetiracetam failed to modify the amplitude of mEPSCs, indicating no action on postsynaptic AMPA receptors.

- Levetiracetam reduced GABAergic synaptic transmission on granule cells in control hippocampus. Specifically, LEV reduced the frequency of mIPSCs in control Sprague Dawley rats, SV2A+/+ and SV2A-/- mice, while increasing mIPSC frequency in dentate granule cells from epileptic SV2+/+ mice, without affecting the amplitude of mIPSCs.

- Topiramate reduced both amplitude and frequency of mEPSCs, indicating it also has a postsynaptic inhibitory effect on AMPA-mediated postsynaptic currents, along with a presynaptic effect on release of glutamate.

- Carbamazepine failed to modify either amplitude or frequency of mEPSCs, indicating that this drug does not alter postsynaptic glutamatergic receptor sensitivity or presynaptic transmitter release.

Description of Research Accomplishments toward accomplishing the aims during Year 2.

Specific Aim 2: *Assess whether antiepileptic drugs acting on presynaptic sites can reduce or prevent seizure induced long-term potentiation of vesicular release from mossy fiber boutons in MTLE.* **Working hypothesis:** Epileptic rats exhibit enhanced pool size and release probability from the rapidly-recycling vesicle pool, and SV2a down-regulation contributes to this enhanced release. Chronic treatment with LEV or other presynaptic antiepileptic drugs during epileptogenesis will protect presynaptic function and normal glutamate release, reducing or preventing hyperexcitability and seizures (months 13-24).

Infrastructure upgrade at Dr. Garrido's site

*New Laser Scanning Confocal Microscope for functional imaging and physiology***:** During the period of the second year of the grant, infrastructure for research at Dr. Garrido's site was further enhanced with a significant upgrade of the Imaging Core facilities. The imaging core acquired a new imaging and physiology workstation with a spectrum-based laser scanning confocal microscope TSC SP2 (Leica) to add to the resources available for this project. This core facility is conveniently located in front of Dr. Garrido's laboratory. This microscope is suitable for functional imaging including analysis of stimulus-evoked changes in fluorescence of SynaptopHlourin (SpH) in transgenic mice and it will positively contribute to the overall performance of this project since confocal capabilities are now excellent at both sites.

2.2. Development of the pilocarpine model of epilepsy in mice and rats

Model of epilepsy in SPH mice: During the second year, we continued developing and improving the pilocarpine model of epilepsy in mice and rats at both institutions. During year 1, we acquired SpH transgenic mice from Jackson Laboratories to establish a newly refreshed colony and and develop the pilocarpine model of epilepsy in parallel with Dr. Stanton's laboratories. For our surprise, animals obtained from Jackson laboratories, Inc exhibited an increased resistance to enter status epilepticus in contrast to colonies established at Dr. Stanton's laboratories based in animals originally provided by Dr. Venkatesh N. Murphy (Harvard University). These negative results contrasted with our collaborative studies performed at Dr. Stanton's lab using SpH mice. Thereby, we further investigated the source of this variability. For developing the SpH pilocarpine model of epilepsy at Dr. Garrido's site, breeders were obtained from Jackson Laboratories *i.e.* B6.CBA-Tg(Thy1-spH)21Vnmu/J (Stock Number: 014651). The difference of these mice with Dr. Stanton SpH mice was that at Jackson Laboratories original SPH mice (donated by Dr. Murphy) were cross-bred with C57BL/6J (Stock No.o 000664). In recent studies, C57BL/6J mice have been found to be highly resistance to pilocarpine-induced seizures and status epilepticus[61]. To address this problem, Dr. Stanton sent original SPH mice in his colony to Dr. Garrido's site. Breeding of those mice has been successful and we are now expanding the colonies to increase the number of animals to continue the imaging studies, specially using the new imaging capabilities.

Model of chronic epilepsy in rats: All experiments were performed in accordance with the National Institutes of Health Guidelines for the Care and Use of Laboratory Animals and with the approval of The University of Texas at Brownsville Institutional Animal Care and Use Committee (Protocol #2004-007-IACUC-1). Male Sprague–Dawley rats were maintained in a temperature- and humidity-controlled vivarium, with water and standard laboratory chow ad libitum. All efforts were made to minimize the number of animals in the study. A subset of the animals was made chronically epileptic by the systemic injection of pilocarpine, as described elsewhere[7,11,19,38,40].

2.3 Effect of LEV in network excitability and excitatory transmission in control and chronically epileptic rats.

We investigated whether acute or chronic treatment of slices with LEV will affect the excitability in hippocampal slices obtained from control and chronically epileptic rats. For this purpose, we performed extracellular recordings of population spikes in CA1 area of hippocampus and field excitatory postsynaptic potentials in dentate gyrus. In

previous year, we demonstrated that LEV significantly reduced the frequency of excitatory postsynaptic currents onto granule cells of dentate gyrus in both mice and rats.

Brief description of methods for hippocampal slice preparation: Brains from >60 days of status epileptic or control Sprague Dawley rats were used for all experiments, and procedures were approved by The University of Texas at Brownsville Institutional Animal Care and Use Committee (Protocol 2011-001-IACU). After isoflurane anesthesia, rats were decapitated and their brains were quickly removed and submerged in 0 C artificial cerebral spinal fluid (ACSF) solution containing (in mM) 124 NaCl, 3 KCl, 2 $CaCl_2$, 1.3 $MgSO_4$, 1.25 NaH_2PO_4, 25 $NaHCO_3$ and 10 glucose. For preparation the hippocampal slices, the whole brain excluding the olfactory bulbs was rapidly removed after decapitation and immediately in cooled in oxygenated ice-cold ACSF. Horizontal hippocampal slices were cut at 350 μm using Leica Vibratome. The experiments were performed in slices from control and epileptic rats. To assess the effect of LEV in excitability and the antiepileptic action, slices were pre-incubated for 3 hours in ACSF solution containing 50μM AP5 to block NMDA receptors. A group of slices (Non-treatment) was incubated with this baseline sACSF solution while another group of slices from same animal was incubated with a treatment ACSF solution containing 300 μM LEV (Sigma Aldrich). After 3 h incubations slices were transferred to recording chamber (32^0C) and perfused at 2ml/min with oxygenated ACSF, or 300μM LEV (treatment).

2.3.1. Effects of LEV on population spikes evoked in CA1 area of hippocampal slices.

In these experiments LEV treatment resulted in a reduction of the amplitude of CA1 population spikes in both control and epileptics but this effect was not significant at least for our sample size. The effect of LEV in CA1 excitability of epileptic group was more pronounced (28.5% reduction, Fig. 17b2, Table 7.2) in contrast to effect on controls (20.7% reduction, Figure 17a2, Table 7.1). Population spikes in CA1 evoked for stimulation of the Shaffer collaterals were recoded and averaged in the Fig 17A and Fig 17B for the control and epileptic group respectively. The test stimulus intensity was adjusted to evoked 40% the maximal response of the input output (I/O). Levetiracetam did not have any significant effect on the mean population spike amplitude, slope and coastline in the control group (n=10) or in the chronic epileptic group (n=3). Synaptic responses in slices from the control and epileptic group were clearly altered after treatment with LEV (Figure 17A-a2 and 17B-b2) respectively. Although the inhibitory effect of LEV was very pronounced, analysis failed to reveal a statistical significance in neither of both groups. Paired t test analysis revealed, no significant effect were found in control group (n=10) in the amplitude (t=-09396, df=9, p= 0.37195), Coastline (t= 1.35339, df =9 p= 0.20894) and Slope (t=-100405, df=9 , p= 0.34159) before or after the application the 300μM the LEV. In addition, no significant effect in the effect of LEV treatment in slices from the epileptic group (SE-LEV) (n=3) was found in the analysis of the amplitude (t=-0.856, df=2, p=0.48868), coastline (t=0.24009, df=2, p=0.83262) or slope (t=-1.84803, df=3, p=0.20585) when compared with effect of LEV in slices of control group. These data indicate that potential antiepileptic action of LEV in chronically epileptic tissue is preserved despite seizure-mediated down-regulation of SV2A proteins as measured by immunohistochemistry, Western blotting and real-time quantitative PCR (see below). Understanding the antiepileptic effect of LEV despite down-regulation of pharmacological targets is important to design similarly effective drugs acting on presynaptic sites.

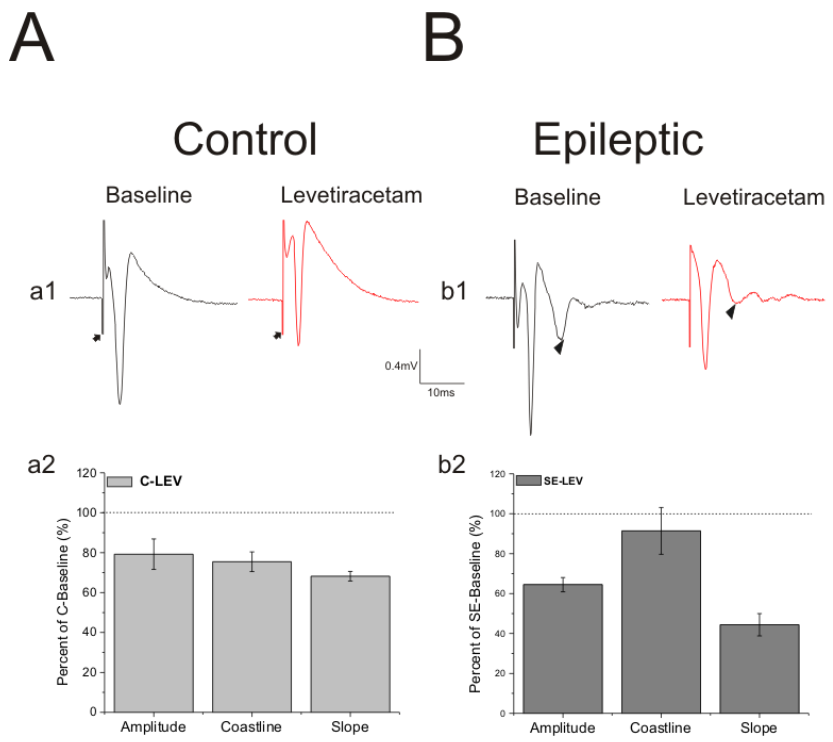

Figure 17. *LEV reduced amplitude of population spike responses evoked in the CA1 area of hippocampal slices.* (1A-1B). Representative recordings of population spikes show a reduction in amplitude after LEV treatment in control group (a1) control-baseline (black trace) compared to control-LEV (red trace) and (b1) epileptic(SE)-group where baseline (black trace) is compared to LEV treatment (SE-LEV, red trace). Graphs in a2 and b2 summarize percent changes of population spike amplitude, coastline and slope after LEV treatment in control and epileptic group respectively. Note reduction in the second population spike in chronic epileptic rat is observed (black triangle). Arrow shows stimuli artifacts.

Table 7.1 Paired samples *t*-test analysis for population spikes in CA1 area in control group

Population spikes Control (CA1)

		N	Mean	SD	SEM	t Stat	DF	Prob>|t|	% change
Amplitude	**C-Baseline**	10	-0.9877	0.48505	0.15339	-0.9396	9	0.37195	20.70%
	C-LEV	10	-0.7823	0.36989	0.11697				
	Difference		-0.2054						

		N	Mean	SD	SEM	t Stat	DF	Prob>|t|	% change
Coastline	**C-Baseline**	10	4.4394	2.17127	0.68662	1.35339	9	0.20894	24.55%
	C-LEV	10	3.3495	1.07123	0.33875				
	Difference		1.0899						

	N	Mean	SD	SEM	t Stat	DF	Prob>|t|	% change

	C-Baseline	10	-1.4337	1.38163	0.43691	-1.00405	9	0.34159	31.17%
Slope	**C-LEV**	10	-0.9779	0.33317	0.10536				
	Difference		-0.4558						

Table 7.2 Paired t-test analysis for population spikes in CA1 area in epileptic group

Population spikes Epileptic Group (CA1)

		N	Mean	SD	SEM	t Statistic	DF	Prob>|t|	% change
	SE-Baseline	3	-0.856	0.62521	0.36097	-0.84143	2	0.48868	28.5
Amplitude	**SE-LEV**	3	-0.612	0.19948	0.11517				
	Difference		-0.244						

		N	Mean	SD	SEM	t Statistic	DF	Prob>|t|	% change
	SE-Baseline	3	3.697	1.97978	1.14302	0.24009	2	0.83262	7.3
Coastline	**SE-LEV**	3	3.426	1.29803	0.74942				
	Difference		0.271						

		N	Mean	SD	SEM	t Statistic	DF	Prob>|t|	% change
	SE-Baseline	3	-1.083	0.97686	0.56399	-1.84803	2	0.20585	39.5
Slope	**SE-LEV**	3	-0.558	0.49915	0.28818				
	Difference		-0.525						

2.3.2 Effect of LEV on excitatory transmission in dentate gyrus in hippocampal slices from control and epileptic rats.

In this part of the study, we developed electrophysiology experiments to correlate data and understand mechanisms of inhibitory effect of LEV in presynaptic as detected by two-photon imaging of presynaptic release in SpH mice and patch-clamp analysis of excitatory postsynaptic currents. Our previous study indicates a long-term enhancement of presynaptic glutamatergic transmission in chronically epileptic mice and rats[7]. In this project, we are investigating if LEV can restore normal levels of presynaptic transmission at excitatory synapses by reducing release of glutamate. Accordingly, in order to assess the frequency-dependent action of LEV on presynaptic transmission, we implemented a paradigm consisting on recording field excitatory postsynaptic potentials (fEPSPs) during repetitive stimulation at a frequency of 20 Hz (10 stimuli) of perforant path afferents to granule cells in dentate gyrus of hippocampal slices maintained in vitro.

LEV significantly reduced the amplitude of fEPSPs in dentate gyrus of slices from both control (Fig. 18A) and epileptic groups (Fig. 18B) in response to repetitive stimulation (10 stimuli train at 20 Hz). The fEPSP responses were averaged for 10 min in two conditions: (a) 3h pre-incubation and perfusion with ACSF containing 50 μM AP5 (black traces) and (b) 300 μM LEV solution containing 50M AP5 (red traces) (Fig. 18 a1,b1). As previously reported for dentate gyrus[62,63], stimulation of the perforant path induced a paired pulse depression of subsequent fEPSP responses at 50 ms intervals, a phenomenon that was more evident during the first 4 fEPSPs in the train (Fig. 18 a1). Pre-incubation (3h) and perfusion with LEV (300 μM) induced a significant reduction of fEPSP amplitudes in the train in control slices (Fig. 18 a2). The summated data of all fEPSPs in the train revealed a significant 37.6 % reduction of mean summated fEPSP amplitudes after LEV treatment compared to slices (n=6) exposed to only ACSF and 50 μM AP5 (Graph inset in Fig. 18 a2, Table 2.1). The statistical analysis comparing

relative changed in baseline versus LEV treatment for each fEPSP in the train revealed that LEV significantly reduced the amplitude for all individual fEPSPs in the train (Table 2.2). In contrast to control fEPSP responses, 2 slices out 6 from epileptic group exhibited paired pulse facilitation of second fEPSP ($fEPSP_2$) (see Fig. 18 b1) while 4 slices exhibited paired-pulse depression (Fig. 19). However, the analysis of the mean fEPSP amplitude revealed an overall depression of second fEPSP in the epileptic group (Fig. 18 b2, black squares). Similarly to controls, LEV treatment resulted in a significant decrease in the amplitude of the fEPSP in treated slices when compared untreated slices (Fig. 18 b1, b2). This inhibitory action of LEV on fEPSP amplitude was detected in (a) the mean summated amplitude of fEPSPs in the train (a significant 49% reduction, paired student t-test, $p<0.0001$, Fig. 18. B2 inset graph, Table 8.1) and (b) for each individual fEPSPs in the train (Table 8.2). Statistical analysis revealed that LEV induced a significant 33.6% more reduction of fEPSP's amplitudes in slices from epileptic rats (Student t-test, $p<0.01$) when compared to the effect of LEV in fEPSPs in control group.

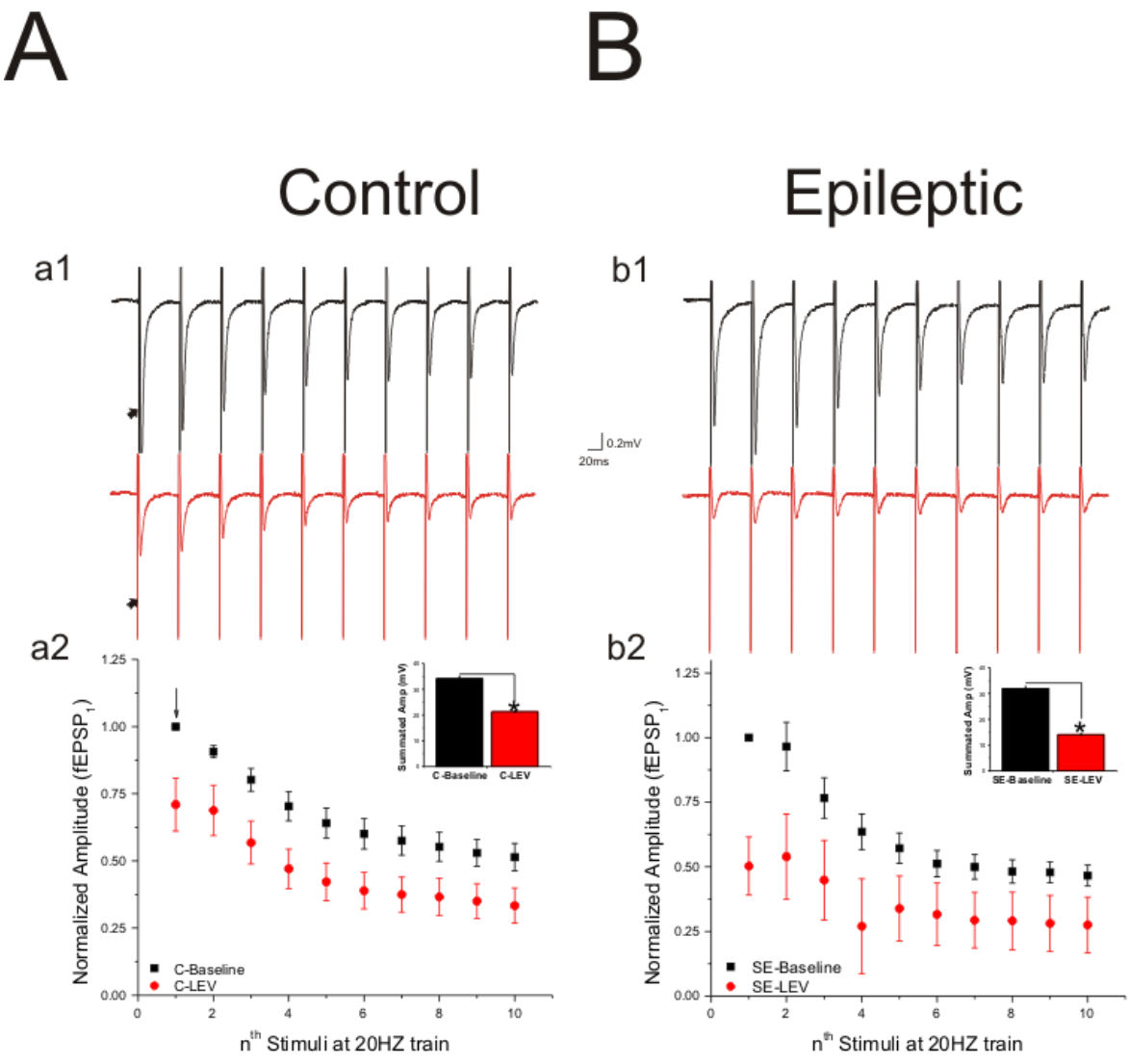

Figure 18. *LEV reduce excitatory transmission of perforant path to dentate gyrus in both control (A) and epileptic groups (B)*. Upper raw illustrate representative traces of dentate gyrus fEPSP responses to 20Hz stimulation (10 stimuli) in untreated (black) and 300 μM LEV treated (red) slices from control (a1) versus epileptic (b2) rat. Notice

a marked reduction in fEPSP amplitudes during the train after LEV treatment. Graph representation of normalized mean fEPSP amplitude in untreated and LEV treated slices (Red symbols) show a significant reduction of amplitude of fEPSP in the train after LEV treatment in slices obtained from both control (Aa2) and epileptic group (Bb2).

Table 8.1 Paired samples *t*-test analysis for summered amplitudes of dentate gyrus repetitive stimulation on control and chronic epileptic rat

	N	Mean	SD	SEM	t Statistic	DF	Prob>|t|	% change
C-Baseline	10	-0.5684	0.15658	0.04951	-14.0109	9	0.0000002	**37.6**
C-LEV	10	-0.35439	0.11041	0.03492				
Difference		-0.21401						

	N	Mean	SD	SEM	t Statistic	DF	Prob>|t|	% change
SE-Baseline	10	-0.53226	0.13954	0.04413	-9.25131	9	0.0000068	**49**
SE-LEV	10	-0.27143	0.06196	0.01959				
Difference		-0.26084						

Table 8.2 Balance Two-Way Repeated Measures ANOVA to analyze the effect of LEV on individual fEPSPs in train evoked by 20Hz stimulation in control and epileptic groups.

Control Group	peaks	Mean Difference	Std. Error	DF	|t|value	Prob>|t|	Alpha	Sig Flag	% change
Baseline LEV	2	0.21904	0.04856	40	6.37969	0.0000554	0.05	1	**24.15**
Baseline LEV	3	0.23372	0.04856	40	6.80721	0.0000214	0.05	1	**29.15**
Baseline LEV	4	0.23269	0.04856	40	6.77716	0.0000229	0.05	1	**33.09**
Baseline LEV	5	0.2187	0.04856	40	6.36978	0.0000566	0.05	1	**34.13**
Baseline LEV	6	0.21206	0.04856	40	6.17644	0.0000866	0.05	1	**35.28**
Baseline LEV	7	0.2011	0.04856	40	5.85709	0.0001732	0.05	1	**34.94**
Baseline LEV	8	0.18643	0.04856	40	5.42987	0.0004299	0.05	1	**33.73**
Baseline LEV	9	0.17949	0.04856	40	5.22763	0.0006553	0.05	1	**33.88**
Baseline LEV	10	0.18088	0.04856	40	5.2684	0.0006022	0.05	1	**35.17**

Epileptic- Group	peaks	Mean Difference	Std. Error	DF	|t|value	Prob>|t|	Alpha	Sig Flag	% change
Baseline LEV	2	0.42612	0.06684	48	9.01562	0.0000002	0.05	1	**44.14**
Baseline LEV	3	0.31758	0.06684	48	6.71918	0.0000188	0.05	1	**41.44**
Baseline LEV	4	0.26813	0.06684	48	5.67294	0.0002104	0.05	1	**42.19**
Baseline LEV	5	0.23293	0.06684	48	4.92829	0.0010600	0.05	1	**40.70**
Baseline LEV	6	0.19558	0.06684	48	4.13801	0.0052300	0.05	1	**38.19**
Baseline LEV	7	0.20635	0.06684	48	4.36578	0.0033500	0.05	1	**41.29**
Baseline LEV	8	0.19119	0.06684	48	4.04502	0.0062500	0.05	1	**39.67**
Baseline LEV	9	0.19724	0.06684	48	4.17318	0.0048900	0.05	1	**41.22**

Baseline LEV	10	0.19063	0.06684	48	4.03336	0.0063900	0.05	1	**40.89**

In order to assess the effect of LEV in frequency-dependent changes in short-term synaptic plasticity of excitatory transmission we tested if LEV treatment (300 μM) on paired-pulse ratios (PPR) during the duration of the train in control versus epileptic group. Although LEV treatment reduce the overall fEPSP amplitude (Fig. 19A a2,b2), when PPR2 was analyzed ($fEPSP_2/fEPSP_1$), LEV treatment (n=6) reduced the PPR_2 (less depression) relative to the first $fEPSP_1$ when compared to baseline (no treatment, n=6) in control group (Fig. 19A a1) but this effect was not statistically significant (Fig. 19A a2) (Paired t-test, P>0.05). In the epileptic group, the effect of LEV (n=6) on PPR_2 was more complex since LEV induced less depression of PPR_2 in 5 out 6 slices, but in 1 slice, LEV induced more depression (Fig. 19B b1) when compared to basleine no treatment (n=6). Overall, there were not significant changes in PPR_2 in this group (Fig. 3B b2) (Paired t-test, P>0.05).

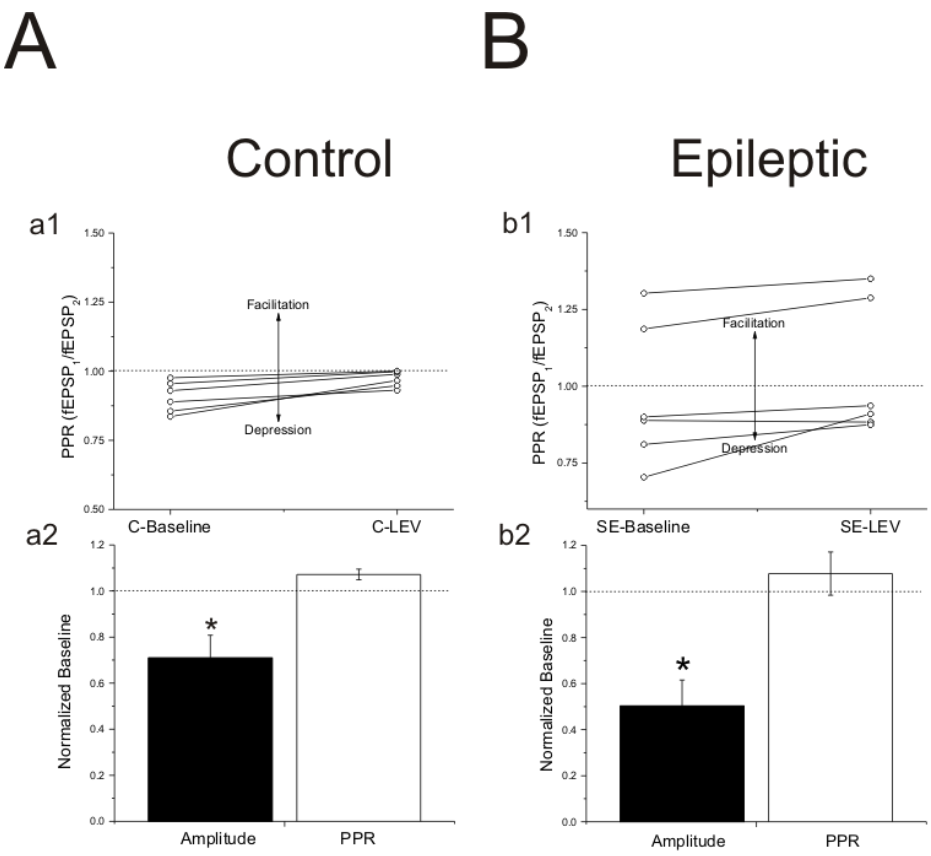

Figure 19. *Effect of LEV on paired-pulse ratio of perforant parth to dentate gyrus excitatory synapses in control (A) versus epileptic groups (B)*. Aa1. Graph representing a paired-pulse depression of PPR for first two responses (fEPSP2/fEPSP1) (in slices non treated (C-Baseline) and a reduction of depression (relative facilitation) after treatment with 300 μM LEV (C-LEV). Bb1. Graph represented a complex behavior of PPR in untreated slices (4 depression and 2 facilitation). Similarly to control slices, treatment with LEV (SE-LEV) a reduced depression (relative facilitation) was observed in all the slices. Aa2. Summary graph representing a reduction of amplitude of first fEPSP and a non-significant increase in relative facilitation in control group after treatment with LEV. Bb2. Summary graph representing a significant reduction of amplitude of first fEPSP and a non-significant increase in relative facilitation in epileptic group following treatment with LEV.

The individual analysis of depression of fEPSP2 in all slices of control group revealed that all except one slice exhibited paired-pulse depression with or without LEV treatment (Fig. 20A a1, a2). In contrast to control group, 4

out 12 slices exhibited paired-pulse facilitation *i.e.* 2 slices in baseline SE non-treated group, Fig. 20B b1) and 2 slices in LEV treated epileptic group (Fig. 20B b2) and 8 slices exhibited depression in the epileptic group.

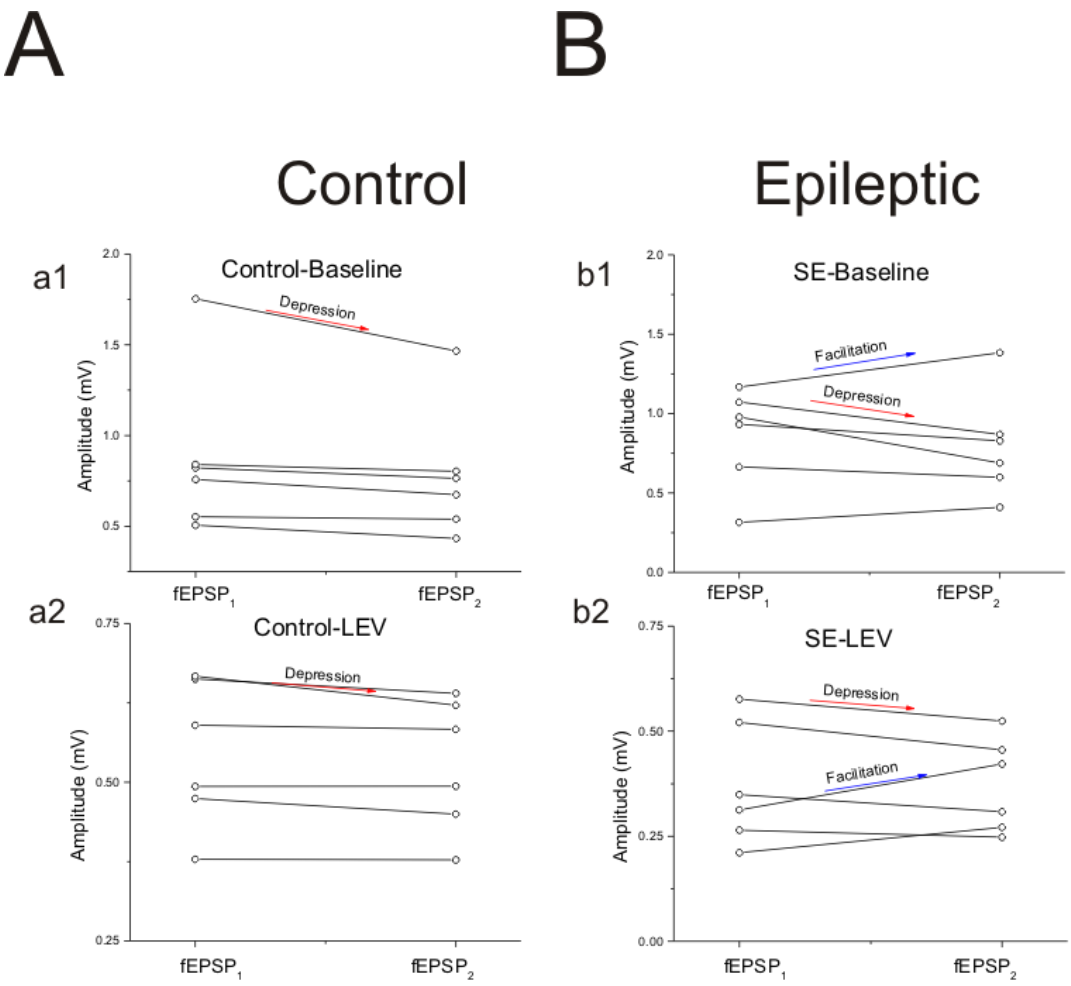

Figure 20. *Graphs representing changes in amplitude of first (fEPSP1) and second (fEPSP2) responses in the train of stimuli in both control (A) and epileptic groups (B) after treatment of slices with 300 μM LEV. A. Notice depression of fEPSP2 relative to fEPSP1 in non-treated slices and less depression after LEV treatment (a2). In contrast, slices in epileptic group exhibited both facilitation and depression*

We then normalized both fEPSPs in non-treated and LEV treated slices to the first fEPSP to investigate if the decay of depression is affected by LEV treatmen in control versus epileptic groups (Fig. 21). Analysis of the decay of fEPSP amplitudes normalized to fEPSP1 showed no significant differences (Kolgomorov-Smirnov Stat, $p>0.05$) of LEV treatment compared to baseline in control (Fig. 21A a1) and epileptic groups (Fig. 21 b1, Table 9). In addition, analysis of the decay (time constant) of depression after normalization to the first fEPSP in treated and non-treated revealed that in control group LEV treatment induced faster decay while in the epileptic group LEV induced slower decay of consecutive responses, however, these changes were not statistically significant with the current data and experiments performed (Table 10). However, after normalization to the first fEPSP, we then

analyzed the effect of LEV on the PPR on each consecutive fEPSP in the train for both control and epileptic group. *As represented in graphs of Fig. 21A a2 and 21B b2, there was a significant change after LEV treatment for only the second normalized paired-pulse ratio since LEV treatment significantly increased the ratio relative to non-treated slices in both groups (Table 11).* No significant changes were detected for all the other consecutive rations.

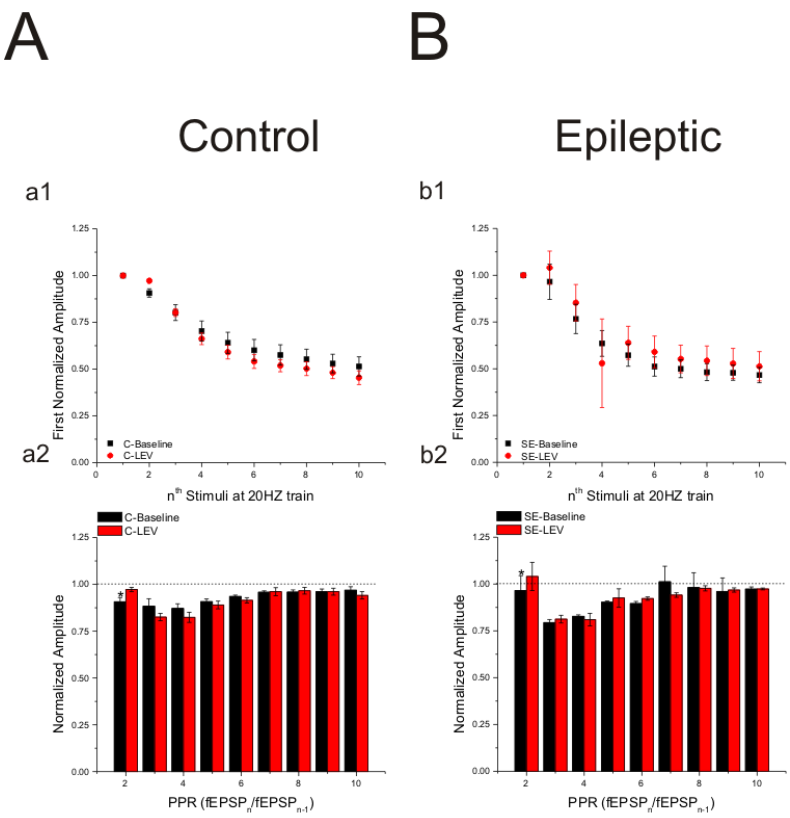

Figure 5. *Graph representing normalized data relative to first fEPSP amplitude in both control (A) and Epileptic (B) groups*. No significant changes were detected in the decay of amplitudes for subsequent fEPSP in the train of responses in groups after LEV treatment in both control (a1) and epileptic group (b1). Consecutive ratios were computed for fEPSP in the train revealing a significant increase (facilitation) for the first PPR1 in the train for both control (C-LEV, a2) and epileptic (SE-LEV, b2).

Table 9. Kolmogorov-Smirnov analysis for the amplitude of dentate gyrus repetitive stimulation on control and chronic epileptic rats (first normalization)

	N	Min	Q1	Median	Q3	Max	D	Z	Prob>|D|
C-Baseline	9	0.51433	0.54125	0.60108	0.75255	0.90692	0.33333	0.15713	0.73011
C-LEV	9	0.45405	0.49113	0.54122	0.73193	0.9723			

	N	Min	Q1	Median	Q3	Max	D	Z	Prob>|D|
SE-Baseline	9	0.65433	0.67554	0.71755	0.86937	1.0563	0.11111	0.05238	1
SE-LEV	9	0.65842	0.67034	0.69928	0.84517	1.05568			

Table 10. Paired samples *t*-test analysis for paired for Decay constant time (τ) analysis for amplitude normalized (first) of control vs SE group.

Decay constant first normalized

CONTROL

	N	Mean	SD	SEM	t Statistic	DF	Prob>|t|
Baseline	5	139.2175	45.43435	20.31886	0.54835	4	0.61262
LEV	5	122.1192	42.10787	18.83121			
Difference		17.09827					

EPILEPTIC

	N	Mean	SD	SEM	t Statistic	DF	Prob>|t|
Baseline	6	96.04301	15.37903	6.27846	-0.20467	5	0.8459
LEV	6	99.29265	39.3223	16.05326			
Difference		-3.24964					

Table 11. Analysis of LEV effect on paired pulse ratio relative to normalized first fEPSP by Student Paired *t*-test for second fEPSP ($fEPSP_2/fEPSP_1$ normalized) in control and epileptic group.

		N	Mean	SD	SEM	t Statistic	DF	Prob>|t|
C-Baseline	peak2	6	0.90692	0.05572	0.02275	-4.10992	5	0.00926
C-LEV	peak2	6	0.9723	0.02853	0.01165			
	Difference		-0.06538					

		N	Mean	SD	SEM	t Statistic	DF	Prob>|t|
SE-Baseline	peak2	7	0.96539	0.21025	0.07947	-2.9756	6	0.02478
SE-LEV	peak2	7	1.04032	0.19871	0.07511			
	Difference		-0.07493					

We then normalized fEPSP amplitudes in the train ($fEPSP_{3\text{-}10}$) relative to the second $fEPSP_2$ to analyze whether rate of decay of fEPSP amplitudes differs after treatment with LEV in both control and epileptic groups (Table. 12). No significance changes were detected by Kolgomorov Smirnov statistical analysis of distributions of normalized fEPSP relative to second fEPSP. In addition, we compared changes in decay of fEPSP amplitudes in the train without treatment (baseline in control versus epileptic group) (Fig. 6A) and in slices treated with LEV in both groups (Fig. 22B). Statistical analysis revealed that although fEPSP amplitudes decay faster in epileptic groups (both untreated and LEV treated groups) (Table 13), changes in time constant (τ) of rate of decay were not significant by student *t*-test.

Table 6. Kolmogorov-Smirnov analysis for the normalized amplitude fEPSP in train relative to second fEPSP after LEV inn control and chronic epileptic groups.

	N	Min	Q1	Median	Q3	Max	D	Z	Prob>|D|
SE-Baseline	9	0.48798	0.50167	0.53272	0.72575	1	0.55556	0.26189	0.12587
SE-LEV	9	0.58304	0.61355	0.64425	0.78486	1			

	N	Min	Q1	Median	Q3	Max	D	Z	Prob>|D|
C-Baseline	9	0.56681	0.59704	0.6629	0.82919	1	0.55556	0.26189	0.12587
C-LEV	9	0.46789	0.50597	0.55686	0.753	1			

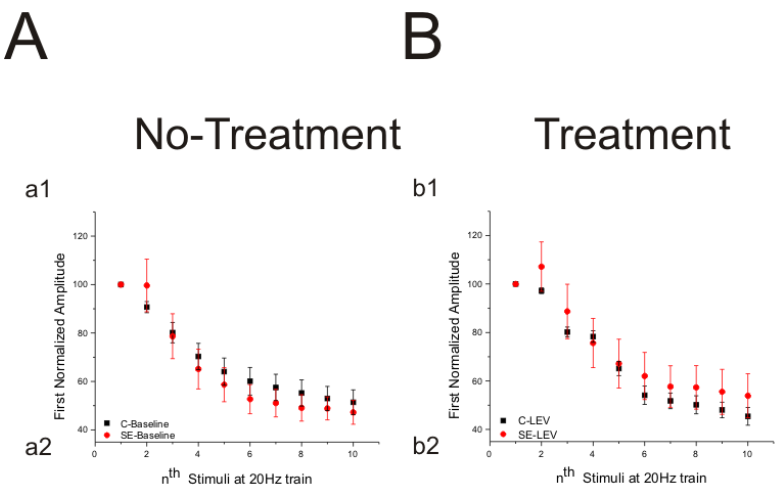

Figure 22. LEV did not affect the rate of decay of fEPSP following the second response when compared no treated slices in control versus epileptic group (A) and LEV-treated slices in control versus epileptic group (B). fEPSPs in the train were normalized to first response (fEPSP1) .

Table 13. Decay constant time (τ) analysis for amplitude normalized (first) of control vs SE group.

		N	Mean	SD	SEM	t Statistic	DF	Prob>|t|
Baseline	control	5	139.2175	45.43436	20.31886	2.5612	4	0.06256
Baseline	SE	5	92.58236	14.34652	6.41596			
	Difference		46.63509					

		N	Mean	SD	SEM	t Statistic	DF	Prob>|t|
LEV	Control	6	124.3813	38.06786	15.54114	1.09262	5	0.32439
LEV	SE	6	99.29265	39.3223	16.05326			
	Difference		25.08867					

2.4. Quantification of the plasma level of LEV for HPLC assays

In order to assess plasmatic levels of LEV after systemic intraperitoneal administration of LEV we developed High Pressure Liquid Chromatography (HPLC) assays to measure the plasma concentration of LEV in separate group of animals. LEV HPLC assays were performed using column BetaBasic-18 of particle size 5 μm (Thermo Electron Corporation) and eluent 5% Acetonitrile in water with flow 0.25 ml/min for 15 min and retention time of 8.8 min. LEV was monitored at 205 nm. For analysis of HPLC chromatogram was used Empower software (Waters). HPLC analysis was conducted using Waters 2695 separation module equipped by 2996 PhotoDiode detector. For these experiments, LEV (dissolved in saline solution) was injected intraperitoneally at doses of 100mg/kg (n=6) or 200mg/kg (n=6). Animals were sacrifice after 1, 3 or 7 days after treatment blood was collected and plasma was separated using standard procedures. Concentration of plasmatic LEV in samples were then analyzed HPLC analysis using LEV analytical grade from Sigma-Aldrich as standard for HPLC. Plasma isolated from animals injected with physiological saline (n=2) was used as control. Our results indicate that in animals injected with 100 mg/kg LEV reached highest plasma levels (0.69 μg/dl) at 5 days following injection and then declined to 0.53 μg/dl 7 days after LEV injection (Figure 23, Table 14) while at a dose of 200 mg/kg of intraperitoneal LEV, plasmatic levels reached a maximum at 5 days (0.67 μg/dl), but levels continue high after 7 days of injection (0.65 μg/dl) (Figure 23, Table 14). It is important to notice that levels at 5 days were similar with both doses of 100 mg/kg and 200 mg/kg, but higher dose 200 mg/kg induced a long-lasting increase in plasma LEV concentrations.

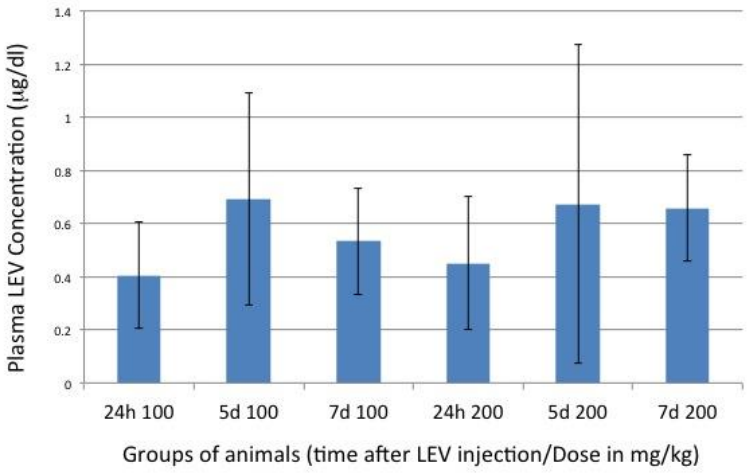

Figure 23. Graph representing plasmatic concentration of LEV after intraperitoneal injection of 100 mg/kg and 200 mg/kg. Blood samples were collected at 24hours, 5 days and 7 days after LEV administration and plasmatic LEV concentration was measured using HPLC.

Table 14. Plasmatic LEV concentration measured by HPLC.

LEV Plasmatic Concentration (□g/dl)	Experimental groups	*error*
0.404689	24h 100 mg/kg (n=3)	0.2
0.693338	5d 100 mg/kg (n=3)	0.4
0.532885	7d 100 mg/kg (n=3)	0.2
0.451048	24h 200 mg/kg (n=3)	0.25
0.673199	5d 200 mg/kg (n=3)	0.6
0.656432	7d 200 mg/kg (n=3)	0.2

2.5. Analysis of the expression of synaptic vesicle proteins during epileptogenesis.

The involvement of SV2A on epilepsy is indicated by 3 facts: (1) SV2A is the sole molecular target for the antiepileptic drug levetiracetam LEV[64], (2) SV2A knockout mice exhibit severe seizures thought to be associated with increased probability of transmitter release[65,66], and (3) down-regulation of SV2A has been reported in epilepsy. The exact antiepileptic mechanism of LEV remains elusive. Hence, the empirical use of this drug has limited the rational development of bioassays to search for other compounds displaying similar or more potent actions. Moreover, given the lack of functional assays to probe whether LEV modifies SV2A function, the exact binding site of LEV on the structure of SV2A has not been discovered yet. As described below, SV2A levels changes in both experimental models and human suffering epilepsy.[16,17,67] However, it is not clear that SV2B or SV2B levels changes in epilepsy. This is important because patch-clamp experiments during the first year revealed that LEV is still effective to reduced excitatory postsynaptic currents to granule cells in SV2A knockout mice, opening a question of whether LEV uses alternative synaptic vesicles to enter neurons or exert pharmacological effects. In order to analyze SV2A (Fig 24.1), SV2B (Fig. 24.2) and SV2C (Fig.24.3) expression changes during the epileptic process we performed immunohistochemistry, western blotting and real-time quantitative PCR using TaqMan assays and the delta-delta CT relative quantification approach with Gapdh as the normalizing gene (Fig 24). Our data revealed a significant down regulation of SV2A immunostainings in mossy fibers in *stratum lucidum* (Fig. 24.1A) and dentate gyrus of chronically epileptic rats (Fig. 24.1B) that correlate with a 61% down-regulation of SV2A proteins by Western Blotting at 10 days following *status epilepticus* (Fig. 24C). At 1 month after status epilepticus, SV2A protein levels were still significantly reduced at51% of control group. Down-regulation was also expressed in animals sacrificed at more than 2 months period after status epilepticus. Reduction of SV2A transcripts in qPCR was not as dramatic when compared to changes in protein expression (Fig. 24D) but this may indicate a compensatory change in transcript production or an increase in degradation of SV2A.

We then analyzed the expression of other proteins of the same family SV2B and SV2C exhibiting high homology to SV2A. [68-71] Immunohistochemical analysis revealed that SV2B was not expressed in mossy fibers in neither control nor epileptic slices. SV2B expression was more apparent in stratum radiatum and other areas. We observed a marked down-regulation of SV2B in epileptic rats Western blotting assays (60% reduction, Fig. 25C) that was consistent with data of real-time qPCR assays (Fig. 25D). SV2B down-regulation persisted during the entire epileptic phases of this model. Immunofluorescence assays for SV2C revealed a pattern of distribution similar to SV2A expression in that expression is high in mossy fibers and dentate gyrus in slices from control and chronically epileptic animals (Fig. 26A, B). Analysis of SV2C by Western blotting showed that despite initial reduction 24h following *status epilepticus*, SV2C, a protein that exhibit a distribution similar to SV2A exhibited an intriguing up-regulation at 10 days following status epilepticus. These findings on SV2C protein expression correlate with upregulation in the SV2C transcripts as shown by qPCR (Fig. 26D). These data indicate that down-regulation of SV2A expression contrast with up-regulation of SV2C in the pilocarpine model of epilepsy. Although, binding of LEV to SV2C has not been demonstrated, homology of these two proteins is very high and it is possible that during the epileptogenic process additional modifications of the SV2C proteins (*e.g.* alternative splicing) may allow these SV2C proteins to add as “alternative” targets for LEV and may preserve the antiepileptic effect of LEV either acting as LEV transporters or molecular pharmacological targets affecting presynaptic release of glutamate at excitatory synapses.

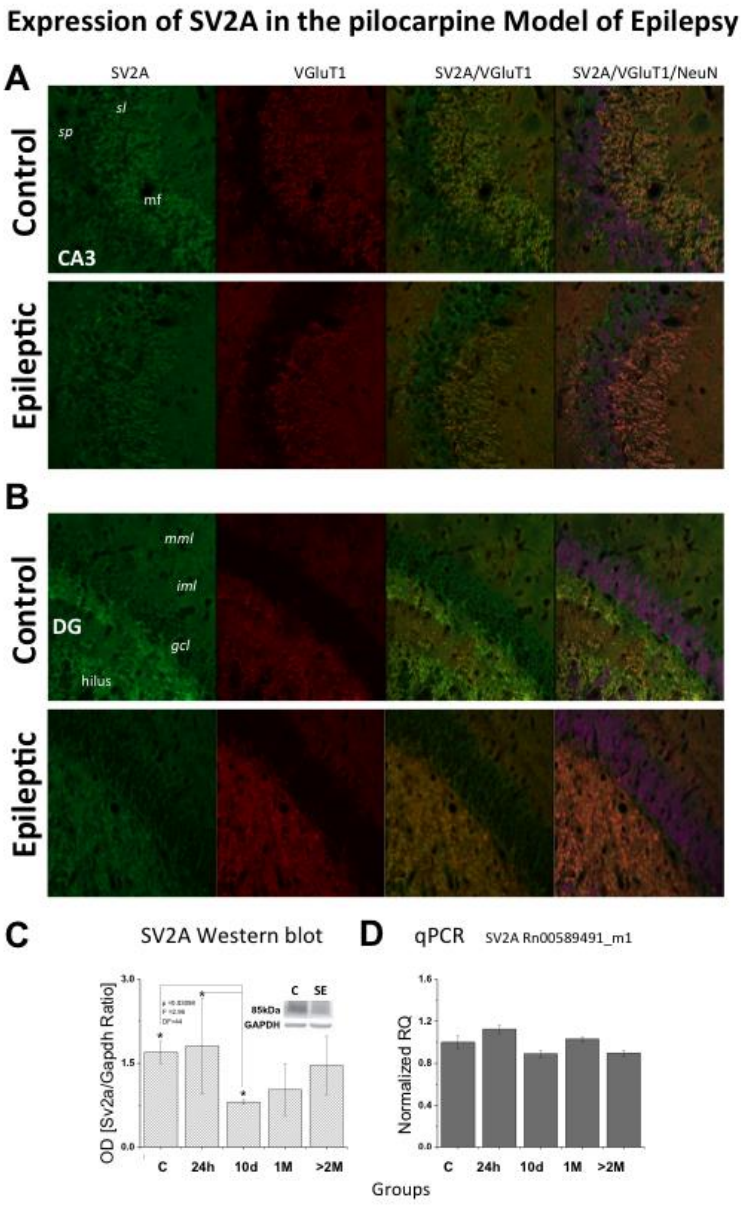

Figure 24.1. *SV2A is down-regulated in chronically epileptic rats*. A. Immunofluorescence assays indicating expression of SV2A in mossy fiber and dentate gyrus in control animal and a marked reduction of staining in epileptic rat while no detectable changes were found for expression of vesicular glutamate transporter type 1 (VGluT1). C. Western blotting showed a significant reduction of SV2A expression at 10 days and subsequent down-regulation at 1month and more than 2 months after *status epilepticus*. D. Data from real-time PCR (TaqMan assays) correlate with SV2A protein down-regulation in chronically epileptic rats. Normalizing gene: Gapdh.

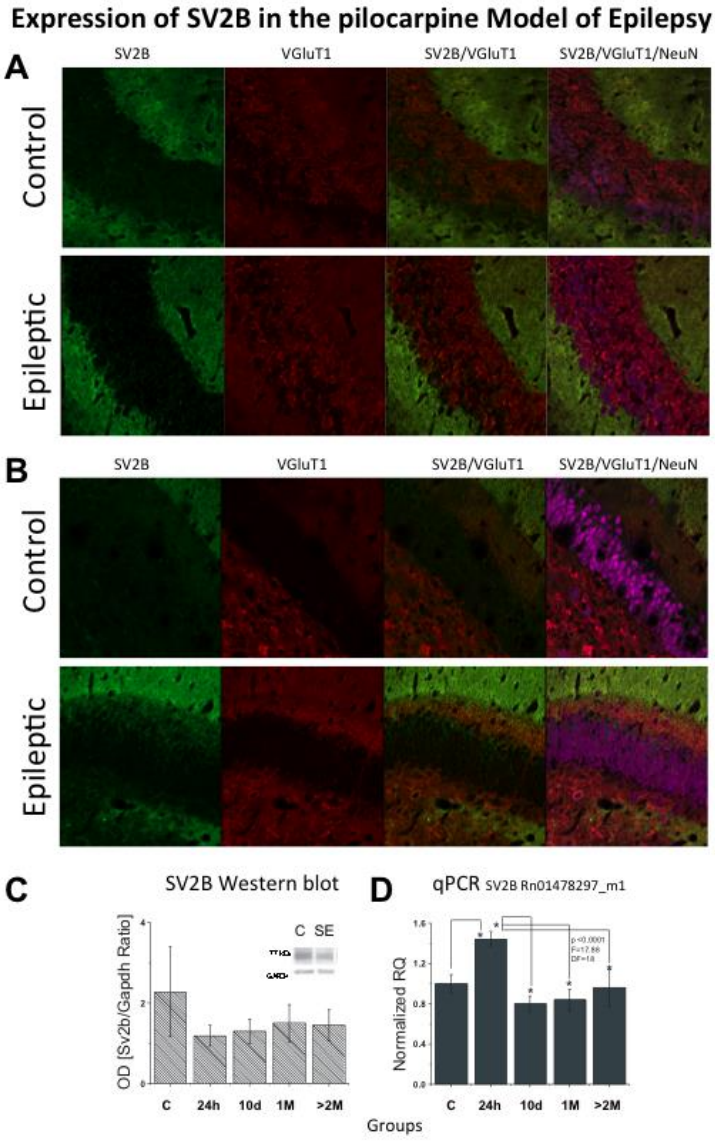

Figure 24.2. *SV2B is down-regulated in chronically epileptic rats*. A. Immunofluorescence assays indicating that SV2B is not expressed in mossy fibers in neither control animal nor epileptic rat while vesicular glutamate transporter type 1 (VGluT1) was expressed in mossy fibers (red staining). Counterstaining of granule cells in dentate gyrus was obtained using C. Western blotting showed a significant reduction of SV2A expression at 10 days and subsequent down-regulation at 1month and more than 2 months after *status epilepticus*. D. Data from real-time PCR (TaqMan assays) correlate with SV2A protein down-regulation in chronically epileptic rats. Normalizing gene: Gapdh.

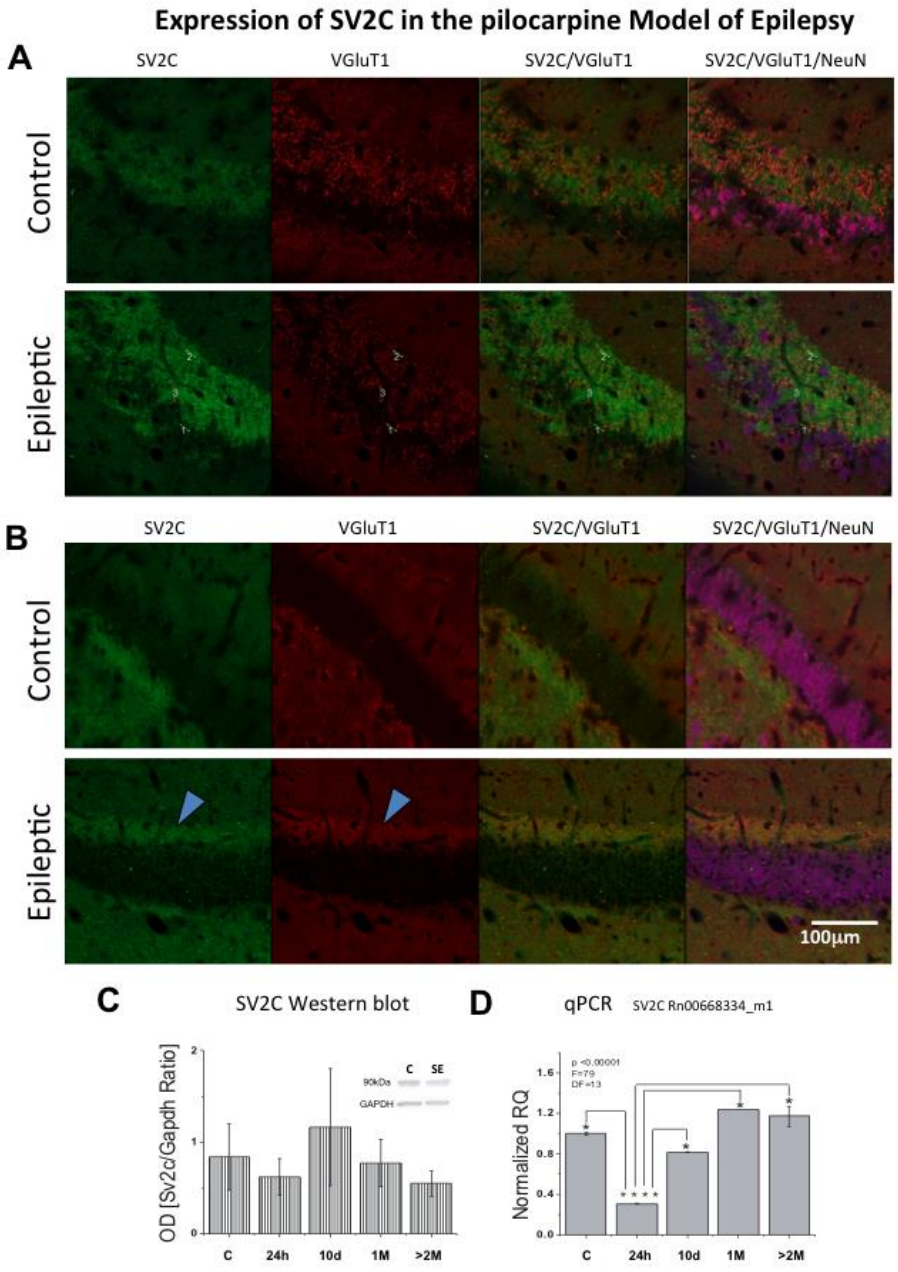

Figure 24.3. *SV2C expression was up-regulated in chronically epileptic rats*. A. Immunofluorescence assays indicating expression of SV2C is high in mossy fiber and dentate gyrus in both control and epileptic rat while no detectable changes were found for expression of vesicular glutamate transporter type 1 (VGluT1). C. Western blotting showed a significant up-regulation of SV2C expression at 10 days and subsequent down-regulation at 1month and more than 2 months after *status epilepticus*. D. Data from real-time PCR (TaqMan assays) indicate a down-regulation at 24h, but subsequent increases that were significant at 1 month and more than 2 months after *status epilepticus* (chronic epileptic phase). Normalizing gene: Gapdh.

Milestones: The following milestones were accomplished during year 2.

(e) LEV was effective in inhibiting the excitability of slices as measured by population spike amplitude in both control and epileptic rats
(f) LEV significantly reduced excitatory synaptic transmission onto granule cells in dentate gyrus.
(g) We discover that although SV2A is down-regulated SV2C is upregulated 10 days after *status epilepticus.* We discovered that SV2C expression in hippocampus followed similar distribution as SV2A. SV2C may represent novel targets for LEV in the epileptic tissue.

KEY RESEARCH ACCOMPLISHMENTS:

Data from our experiments in year 02 revealed that:

1- LEV was effective in inhibiting the excitability of slices as measured by population spike amplitude in both control and epileptic rats

2- LEV significantly reduced excitatory synaptic transmission onto granule cells in dentate gyrus.

3- We discover that whole SV2A are SV2B are down-regulated,SV2C expression is upregulated after *status epilepticus.* We discovered that SV2C expression in hippocampus followed similar distribution as SV2A and may represent addition al targets for LEV action in epilepsy.

4- LEV plasmatic concentration was measured using a newly developed assay for LEV detection using HPLC. Injection of 100 and 200 mg/kg of LEV resulted in plasmatic concentration of approximately 0.6 μg/dl 5 days after injection.

We have obtained key data indicating that chronic slice treatment with LEV can reduce excitability and reduce excitatory synaptic transmission in hippocampal slices obtained from control and epileptic rats. These are significant findings because during the course of epilepsy LEV pharmacological target SV2A is down-regulate. Therefore, current data open two possibilities: (a) remaining SV2A receptors are still functional for LEV action and their activation is still effective in control presynaptic release of glutamate, overall excitability and ultimately seizures in epilepsy and/or (b) the action of LEV is independent of SV2A binding, but SV2A may act as a carrier/transport that mediates LEV molecules to enter the interior of the presynaptic boutons and act on secondary targets. Hence, even down-regulate, SV2A can bind and internalize enough LEV to act effectively in another intracellular targets or pathways. Although LEV has been shown to act on other targets like presynaptic Ca^{2+} channels[72,73], binding experiments only confirm SV2A as a sole molecular receptor. Additional studies are necessary to pin-point and differentiate the role of SV2A in mediating the antiepileptic effect of LEV as receptor-effector versus receptor-transporter molecular targets. Our data indicate that presynaptically acting drugs such as levetiracetam reduces hyperexcitability and inhibit presynaptic transmission in mesial temporal lobe epilepsy.

Description of Research Accomplishments toward accomplishing the aims during Year 3 and non-cost extension period

Specific Aim 3: *Assess whether down-regulation of mGluR2 and SV2a at mossy fiber terminals can be prevented by chronic treatment with presynaptic acting antiepileptic drugs.*
Working hypothesis: Reduced expression of SV2A and mGluR2 results in deficient mGluR2-mediated suppression of presynaptic release and reduced anticonvulsant efficacy of LEV. To evaluate the role of altered mGluR2 and SV2a expression epilepsy, we evaluated whether treatment with levetiracetam reduce transmitter release as evaluated using SpH transgenic mice and confocal laser scanning microscopy. In addition, we investigated whether changes in transmitter release (functional data) are associated with changes in expression of mGluR2 and SV2A and related proteins SV2B and SV2C.

3.1 Imaging presynaptic transmitter release using Leica *Laser Scanning Confocal Microscope for functional imaging and physiology.* This microscope was used for functional imaging including analysis of stimulus-evoked changes in fluorescence of SynaptopHlourin (SpH) in transgenic mice. Experiments to tackle Specific Aim 3.1 (below) were performed using this technique.

3.2 Development of the pilocarpine model of epilepsy in mice and rats

Model of epilepsy in SPH mice: During the second year, we continued developing and improving the pilocarpine model of epilepsy in mice and rats at both institutions. We addressed a concern in relation to variability in the seizure patterns in transgenic SpH mice obtained from Jackson laboratories, Inc specifically B6.CBA-Tg(Thy1-spH)21Vnmu/J (Stock Number: 014651) when compared to mice animals originally provided by Dr. Venkatesh N. Murphy (Harvard University) to our collaborator Dr. Stanton (New York Medical College).

During year 1, we acquired SpH transgenic mice from Jackson Laboratories to establish a newly refreshed colony and develop the pilocarpine model of epilepsy in parallel with Dr. Stanton's laboratories. For our surprise, animals obtained from Jackson laboratories, Inc exhibited an increased resistance to enter *status epilepticus* in contrast to colonies established at Dr. Stanton's laboratory. These negative results contrasted with our collaborative studies performed at Dr. Stanton's lab using SpH mice. Thereby, we further investigated the source of this variability. For developing the SpH pilocarpine model of epilepsy at Dr. Garrido's site, breeders were obtained from Jackson Laboratories, however, the original SpH mice (donated by Dr. Murphy) were cross-bred with C57BL/6J (Stock No. 000664) at Jackson Labs. We found that these animals exhibited a different pattern of pilocarpine-induced *status epilepticus.* In recent studies, C57BL/6J mice have been found to be highly resistance to pilocarpine-induced seizures and *status epilepticus*[61]. To address this problem, Dr. Stanton sent original SpH mice from his colony to Dr. Garrido's site. Breeding of those mice has been successful and we expanded the colonies to increase the number of animals to continue the imaging studies and molecular studies, specially using the new imaging capabilities. Development of *status epilepticus* in this new breed of SpH mice from Dr. Stanton's lab was successful following the same pattern as published in our previous study[7]. However, we dedicated several months to troubleshoot this problem and getting the new colony to be productive to obtain animals for this study. This was one of the main reasons we requested a Non-cost extension period to be able to further complete all the experiments proposed in the **Specific Aim 3**. Despite this setback, we were able to obtain significant amount of data to support our hypothesis for this specific aim 3 (see sections **3.1** and **3.2** below). Additional experiments are planned for this purpose during the non-cost extension period.

Model of chronic epilepsy in mice and rats: All experiments were performed in accordance with the National Institutes of Health Guidelines for the Care and Use of Laboratory Animals and with the approval of The University of Texas at Brownsville Institutional Animal Care and Use Committee (Protocol #2004-007-IACUC-1). Male Sprague–Dawley rats were maintained in a temperature- and humidity-controlled vivarium, with water and

standard laboratory chow ad libitum. All efforts were made to minimize the number of animals in the study. A subset of the animals was made chronically epileptic by the systemic injection of pilocarpine, as described elsewhere[7,11,19,38,40].

3.3.1. Chronic levetiracetam (LEV) treatment *in vivo* ameliorated abnormal presynaptic vesicular transmitter release from mossy fiber pathway after *status epilepticus*.

To address hypothesis of specific aim 3.1, we investigated whether chronic treatment with antiepileptic drug levetiracetam (Kepra) can reduce the abnormally enhanced presynaptic release of vesicles in a glutamatergic pathway (i.e. mossy fibers). For this purpose, presynaptic transmitter (vesicle) release was investigated in 4 groups of SPH transgenic mice as follows: a) control mice injected with saline vehicle for 4 weeks (control no treatment=C-NT, n=5), b) pilocarpine-treated SpH mice that developed *status epilepticus injected* with saline (*status epilepticus* no treatment=SE–NT, n=5), c) control SpH mice injected with levetiracetam (see below) (control treated=C-T, n=4), and d) pilocarpine-treated SpH mice that suffered *status epilepticus* and were treated subsequently with levetiracetam intraperitoneally (see below) (*status epilepticus* treated= SE-T, n=4). The treatment schedule for levetiracetam and saline administration consisted of repetitive injections (100 μg/kg) in alternate days during 30 days (endpoint). After the end of the treatment period, animals were sacrificed for a preparation of brain slices to measure changes in presynaptic transmission and to collect mRNA samples. Similar groups of animals were sacrificed to obtain proteins in order to investigate change sin expression of SV2A, SV2B, and SV2C. After animals were sacrificed, blood samples were collected (at endpoint) to measure plasmatic levels of levetiracetam using high-pressure liquid chromatography (HPLC) in treated versus non-treated groups.

Brief description of methods for hippocampal slice preparation: Brains from ~60 days of status epileptic or control SpH mice were used for all experiments, and procedures were approved by The University of Texas at Brownsville Institutional Animal Care and Use Committee (Protocol 2011-001-IACU). After anesthesia, rats were decapitated and their brains were quickly removed and submerged in ~0^{o} C artificial cerebral spinal fluid (ACSF) solution containing (in mM) 124 NaCl, 3 KCl, 2 $CaCl_2$, 1.3 $MgSO_4$, 1.25 NaH_2PO_4, 25 $NaHCO_3$ and 10 glucose. For preparation the hippocampal slices, the whole brain excluding the olfactory bulbs was rapidly removed after decapitation and immediately in cooled in oxygenated ice-cold ACSF. Horizontal hippocampal slices were cut at 350 μm using Leica Vibratome. The experiments were performed in slices from control and SpH mice treated or non-treated with levetiracetam.

Analysis of presynaptic vesicular release in slices from SpH mice using laser scanning confocal microscopy: Imaging of SpH-positive mossy fiber boutons in brain slices was performed using a slightly modified protocol as the one previously described in our manuscript published in Brain[7]. Briefly, changes in SpH fluorescence upon release were visualized with a spectral Leica TCS SPE laser-scanning confocal in a Leica DM6000 FS microscope with the objective ×63/0.90 NA water immersion infrared objective lens and a multispectral Leica confocal laser scan unit. Briefly, the light source was a solid state laser (488nm/10 mW). Epifluorescence from SpH-positive mossy fiber boutons was detected with photomultiplier tubes of the confocal laser scan head and emission spectral window was optimized for signal over background. A 565-nm dichroic mirror (Chroma Technology) separated green and red fluorescence to eliminate transmitted or reflected excitation light. Although there were no signs of photodamage, we used the lowest intensity needed for adequate signal-to-noise ratios. To detect position of the slices in the recording chamber, images were obtained at low magnification (x5 objective) using DIC, a CCD camera and video monitor. After positioning the slices in the proper position with image field over the *stratum lucidum* (area of mossy fiber pathway), setting were changed to epifluorescence in the microscope to detect level of fluorescent and confirm that the transgenic animal indeed express adequate levels of SpH fluorescence for the experiments. For SpH fluorescence experiments, slices were perfused with 25 μM 6-cyano-7-nitroquinoxaline-2,3-dione (CNQX; Tocris) and 50 μM D-(-)-2-Amino-5-phosphonopentanoic acid (D-AP5; Tocris). A 600 stimulus 20-Hz train in the stratum lucidum evoked SpH fluorescence increases (imaged within 100 μm from stimulating electrode) in the proximal region (the first 100 μm) of CA3 apical dendrites and images were acquired every 30 s. As previously reported, we use SpH as a pH-sensitive indicator of vesicular release in brain slices bathed in artificial CSF (containing 25 μM CNQX and 50 μM D-AP5 to prevent synaptically driven action potentials and epileptiform activity) in our recording chamber with pH maintained at or ~7.4 [7]. To calculate half-time of post-stimulus decay of SpH peak fluorescence intensity, ($t_{1/2}$) was calculated for each punctum by single exponential

fits to destaining curves using the equation: $y_0 + A_1 e^{(-x/t_1)}$, with t_1 the decay constant. Data were analyzed with OriginPro.

Results: Four different groups of animals were analyzed to determine whether chronic treatment with levetiracetam *in vivo* may reduce presyanptic vesiclar transmitter release in the mossy fiber pathway from granule cells in hippocmapus of pilocarpine-treated epileptic SPH trasnegnic mice. Changes of SpH fluorescence were induced by a train of 600 action potentials delivered to the mossy fiber pathway using a bipolar stimulating electrode. Images of stimuli-induced SpH fluorescence changes were detected using laser scanning confocal microscopy (see above). We first compared normalized peak fluorescence changes after stimuli in control versus pilocarpine-treated (suffering status epilepticus) group of animals that were injected with saline instead of levetiracetam for 1 month (Figure 25A). As previously reported we detected a significant 4.4% increase in normalized peak fluorescence in status epilepticus (SE) group ($F_{peak} = 119.25 \pm 2.13\%$, $n = 4$, 106 boutons, 7 slices) when compared to saline-injected control group ($F_{peak} = 114.18 \pm 1.19$ %, *$n = 5$, 112 boutons, 10 slices)* (Figure 25 A, b3). These data is consistent with our previous findings that status epilepticus induce an abnortmal increase in presynaptic vesicular release as measured by SpH fluorescence changes in transgenic mice[7]. To determine if chronic treatment with levetiracetam can ameliorate or prevent such increase in presynaptic vesicular release, we treated pilocarpine-injected animals with levetirecetam (i.p, dose: 100 μg/kg) during one month immediatelly following *status epilepticus* and compared this group to control animals treated with similar drug administration protocol simultaneously. Analysis demonstrated no significant differences in of normalized peak fluorescence changes after stimulation of mossy fibers between these groups indicating that chronic treatment with levetiracetam corrected presyanptic function abnormalities previously detected after *status epilepticus* (Figure 25B).

Plasmatic concentration of levetiracetam after treatment was assessed by high-pressure chromatography (HPLC) assays. No significant changes were detected between controls (57.1± μg/ml) versus and *status eplepticus* groups (47.9±1.5 μg/ml, Student t-test,, p>0.05).

Chronic treatemend with levetiacetam after *status epilepticus* can revert abnormalities (*i.e.* abnormally enhanced vesicular release) in presynaptic function of glutamatergic (excitatory pathways (*i.e.* mossy fibers) that may be responsible for epileptogenesis and hyperexcitability in mesial temporal lobe epilepsy. Accordingly, reduction in abnormally enhanced presyanptic vesicular release is possibly the main mechanisms of action of levetiracetam. Data in subsequent experiments indicate that this effect may be mediated by levatiracetam-induced up-regulation of its own target SV2A which is pathologicall down-regulted after *status epilepticus*. However, further experiments are necessary to elucidate how levetiracetam reduce presyanptic release in epileptic synapses.

Figure 25

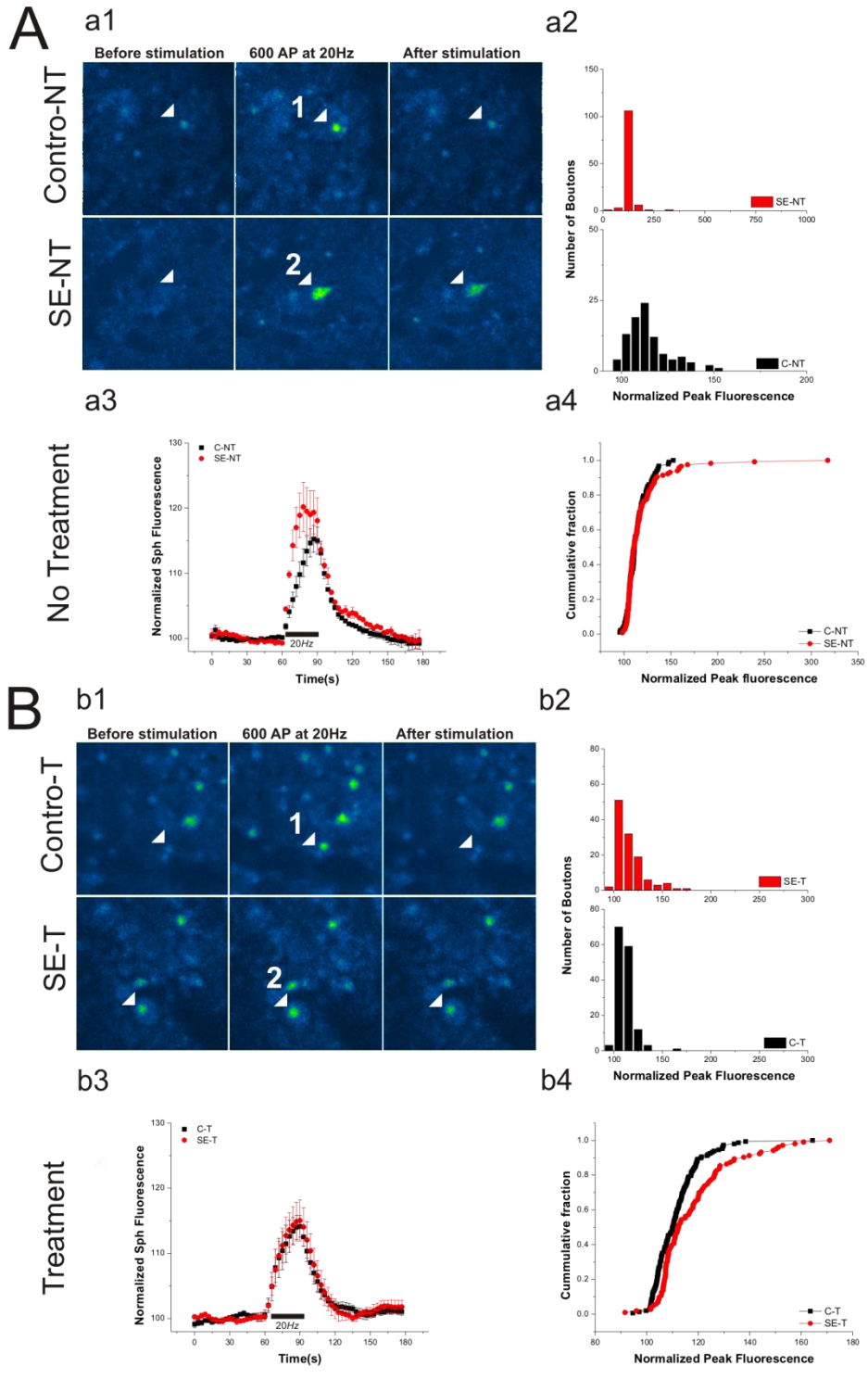
A
a1
Before stimulation
600 AP at 20Hz
After stimulation
Contro-NT
SE-NT
1
2
a2
Number of Boutons
SE-NT
C-NT
Normalized Peak Fluorescence
a3
No Treatment
C-NT
SE-NT
Normalized Sph Fluorescence
20Hz
Time(s)
a4
Cummulative fraction
C-NT
SE-NT
Normalized Peak fluorescence
B
b1
Before stimulation
600 AP at 20Hz
After stimulation
Contro-T
SE-T
1
2
b2
Number of Boutons
SE-T
C-T
Normalized Peak Fluorescence
b3
Treatment
C-T
SE-T
Normalized Sph Fluorescence
20Hz
Time(s)
b4
Cummulative fraction
C-T
SE-T
Normalized Peak Fluorescence

Figure 25. Effect of levetiracetam on the pilocarpine model to induced *status epilepticus* (SE) in SpH transgenic mice. A. *Stimuli-induced changes in presynaptic vesicular release at mossy fiber boutons in control and pilocarpine-treated SpH transgenic mice (no-treatment).* **a1**. Representative time-lapsed confocal images from control and post-*status epilepticus* SpH-expressing mossy fiber boutons MFBs in the proximal apical dendritic region of field CA3 in hippocampal slices of saline-treated control versus mouse one month after suffering SE treated with saline vehicle (lower row). First column: baseline imaging, second column: imaging during 600 action potential train stimulation, last column: recover of fluorescence changes 10 sec after end of stimulation. Notice larger increase in fluorescence changes after SE (compared arrowhead 1 to 2). **a2**. Frequency distribution histogram of normalized peak SpH fluorescence for all mossy fiber boutons after stimulation in control (black) compared to *status epilepticus* (SE) group (red). Notice a change in the distribution pattern, specifically a large group of mossy fiber boutons that release more than 200% increase of baseline after *status epilepticus* while peak fluorescence changes in mossy fiber boutons from control saline-treated animals follow a normal distribution. **a3**. Normalized, evoked SpH fluorescence increases in response to a 600 pulse/20 Hz mossy fibre stimulus train, in MFBs from control (filled black circles, $F_{peak} = 114.18 \pm 1.19$ %, *n = 5, boutons=112, 10 slices*) versus post-status epilepticus (open red circles, $F_{peak} = 119.25 \pm 2.13$%, $n = 4$, boutons=106, 7 slices). F_{peak} was significantly increased in post-status epilepticus slices ($P < 0.05$, Student's *t*-test; all values mean ± SEM). a4. Cumulative histogram distribution of normalized peak fluorescence changes in control (black) versus SE group (red) showing a left shift and a significant difference towards larger fluorescence peak changes (more release) in slices from post-*status epilepticus* animals (D= 0.23, Z= 0.0305, p<0.00197, statistical comparisons using Kolmogorov-Smirnov test). B. *Chronic treatment with Levetiracetam (30 days period) after pilocarpine-induced status epilepticus normalized abnormally enhanced vesicular release at mossy fiber boutons*. **b1**. Time-lapsed images from representative experiments in slices from levetiracetam-treated control and epileptic SpH transgenic mice. Solid arrows indicate puncta corresponding to SpH-positive mossy fiber bouton that showed activity-dependent fluorescence changes during a 600 pulse/20 Hz stimulus train. **a2**. Frequency distribution histogram of normalized peak fluorescence for pooled mossy fiber boutons in control (black) *versus* pilocarpine-treated mice (red) chronically treated with levetiracetam after *status epilepticus*. **b3**. Representative time course of normalized, evoked SpH fluorescence increases in response to a 600 pulse/20 Hz mossy fibre stimulus train, in MFBs from control (filled black circles, $F_{peak} = 115.09 \pm 0.67$ %, *n = 3, boutons=148, 9 slices*) versus post-*status epilepticus* (open red circles, $F_{peak} = 116.25 \pm 1.27$%, $n = 3$, boutons=106, 6 slices). F_{peak} was not significantly changed in levetiracetam-treated post-*status epilepticus* animals ($P > 0.05$, Student's *t*-test; all values mean ± SEM). **b4**. Cumulative frequency histogram of normalized peak SpH fluorescence between the levetiracetam-treated control and SE group (red). Kolmogorov-Smirnov two-sample test indicated a significant difference between both groups (t=2.7, DF=18 p=0.014).

3.3.2. Status epileptics-induced abnormalities in presynaptic protein expression: effect of chronic treatment in vivo with levetiracetam.

In previous studies, we have detected a down-regulation of both metabotropic glutamate receptor type 2 (mGluR2) and SV2A presynaptic after pilocarpine-induced *status epilepticus[11,12]*. This particularly relevant because mGluR2 is a presynaptic regulator of transmitter release reducing excessive glutamate release during conditions of hyperexcitability (*i.e.* epilepsy)[11-13,74-76]. SV2A is the molecular target of the antiepileptic drug levetiracetam. Previous studies in experimental animals of epilepsy and in patients with epilepsy have indicated that expression of SV2A is also chronically decreased in the epileptic tissue[16,77,78]. In this project we investigated how *status epilepticus* can alter expression of synaptic vesicle proteins (SV2A, Sv2B, and SV2C) (3.2a) and whether chronic treatment with levetiracetam can reverse those changes after *status epilepticus* to restore the presynaptic release machinery responsible for epileptogenesis (3.2b).

3.3.2a Status epileptics-induced abnormalities in presynaptic protein expression.

Using immunohistochemistry, western blotting and real-time quantitative PCR (qPCR) analysis we have previously demonstrated status-epilepticus-induced abnormalities and changes in presynaptic protein expression of SV2A, SV2B and SV2C in Sprague Daley rats (2012-2013 Progress Report). We then tested whether similar abnormalities can be reproduced in mice considering that mice were used for the levetiracetam treatment in vivo due to 2 reasons *1) data on presynaptic function (status epilepticus-induced abnormal presynaptic release of*

vesicles) and 2) rats are a larger species requiring larger amounts of drugs per kg of body weight (levetiracetam is a relatively expensive drug).

Immunohistochemical analysis of protein expression of SV2A, SV2B, SV2C. Multiple immunofluorescent staining was performed in histological sections from control and epileptic mice sacrificed 1-2 months after *status epilepticus*. We used SpH-positive (transgenic) and negative (no SpH) mice. SV2A protein expression was detected using polyclonal antibodies against SV2A (1:1000) from Synaptic System, Inc (Germany) with green channel secondary detection using AlexaFluo488 antibodies (Life Technologies). To identify the mossy fibers, antibodies against vesicular glutamate transporter type 1 (vGluT1) (1:2000, Millipore Corp, USA) were visualized with red-shifted AlexaFluo594 secondary antibodies. Neurons were labeled with anti-NeuN antibody visualized using AlexaFluo647 secondary antibodies to determine relative position of main hippocampal neuronal layers (pyramidal cell layer and granule cell layers). Imaging was performed using laser scanning confocal microscope Fluoview System in the IX81 inverted microscope (Olympus).

Results: Immunohistochemistry data revealed a down-regulation of SV2A in the chronic phase of the pilocarpine model of epilepsy in SpH mice (animals sacrificed after 2 months of *status epilepticus*) (Figure 26) while no qualitative changes were observed in the expression of SV2B (Figure 27) non-SpH mice. In addition, up-regulation of SV2C was noticeable in chronically epileptic mice, specifically, SV2C expression (intensity of fluorescent signal) was increased in the mossy fiber pathway, and in the outer layers of dentate gyrus consistent with abnormally sprouted mossy fiber bouton synapse onto granule cell dendrites forming a “recurrent excitatory pathway” the landmark of altered synaptic reorganization in this experimental model of temporal lobe epilepsy (Figure 28).

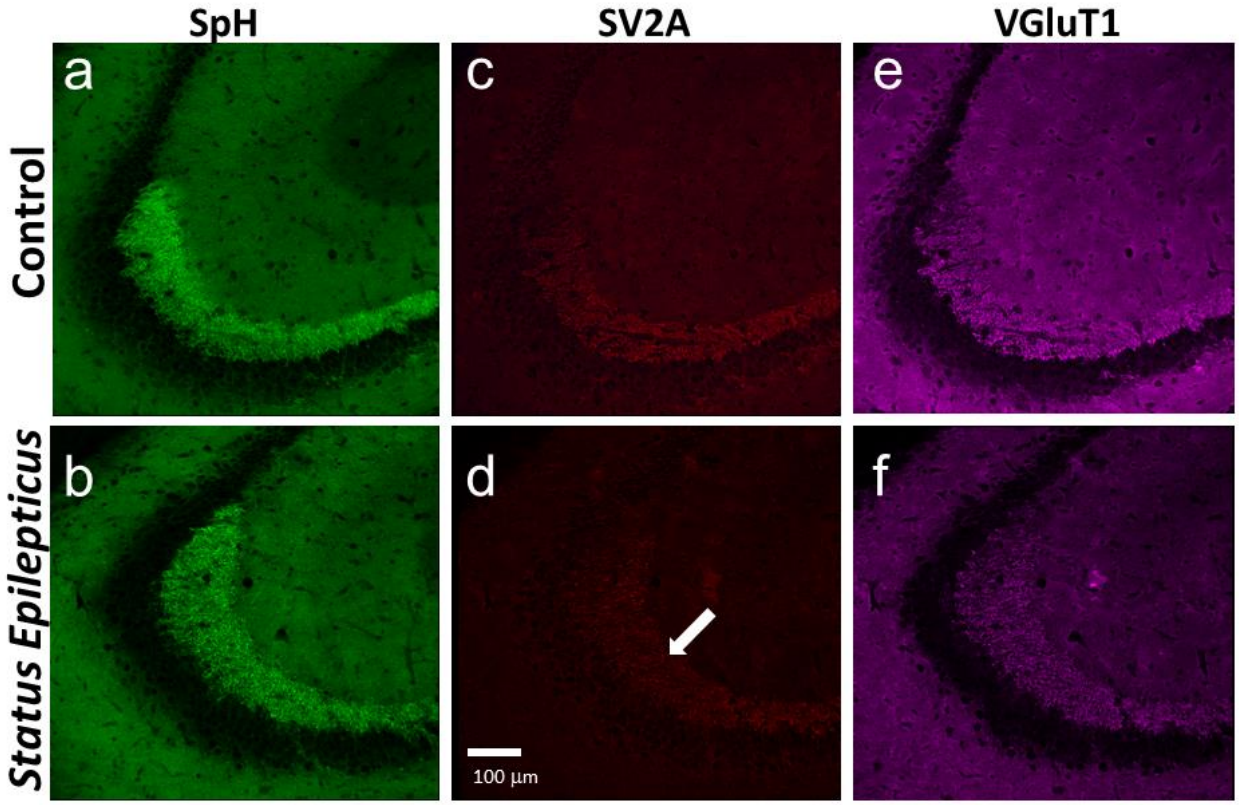

Figure 26. Immunostaining of SVA2 in transgenic SpH mice revealed a down-regulation of SV2A in the stratum lucidum (arrows) corresponding to the mossy fiber pathway in animal sacrificed 2 months after *status epilepticus*.

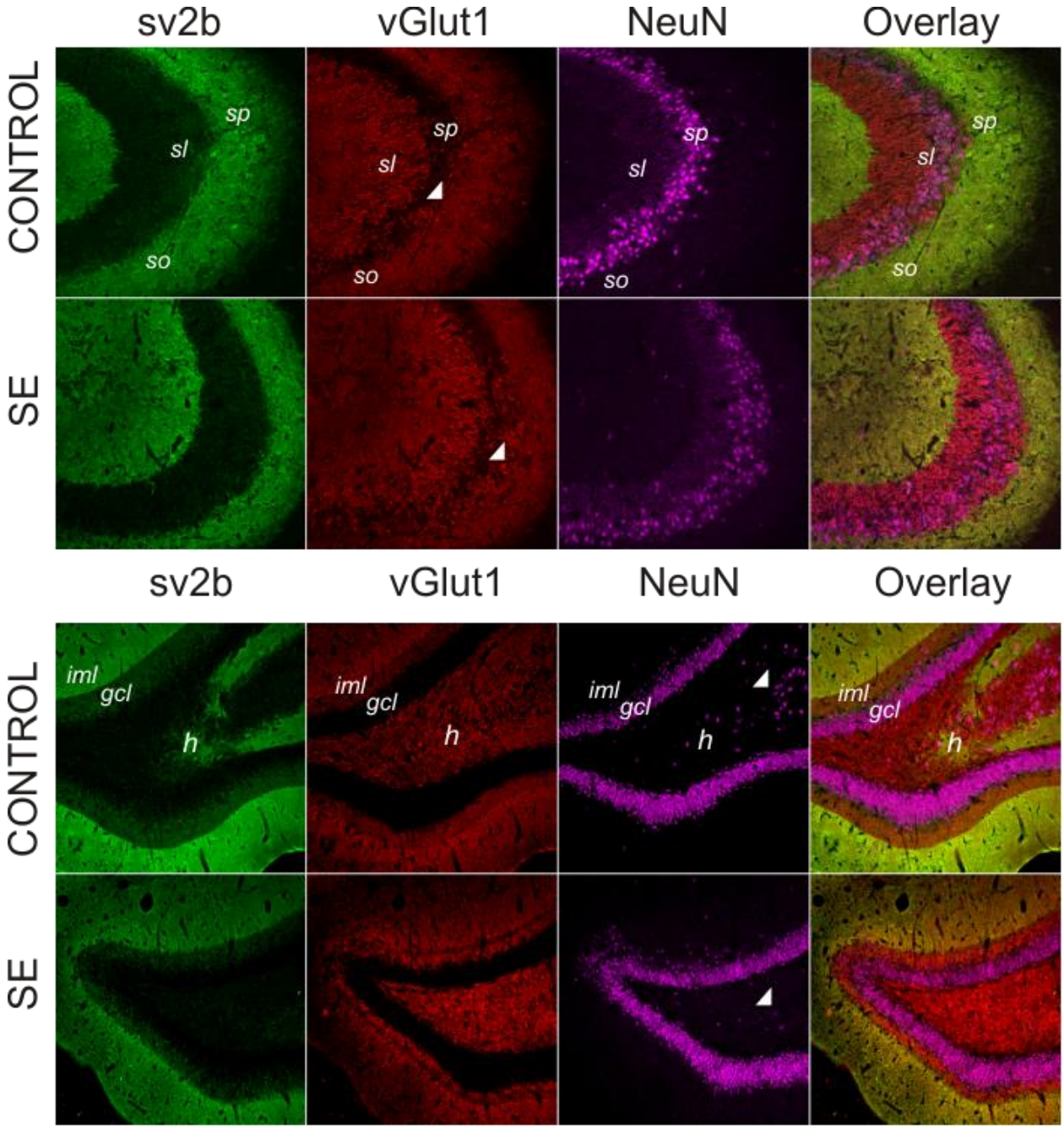

Figure 27. SV2B expression in hippocampus shows no qualitative differences after *status epilepticus*

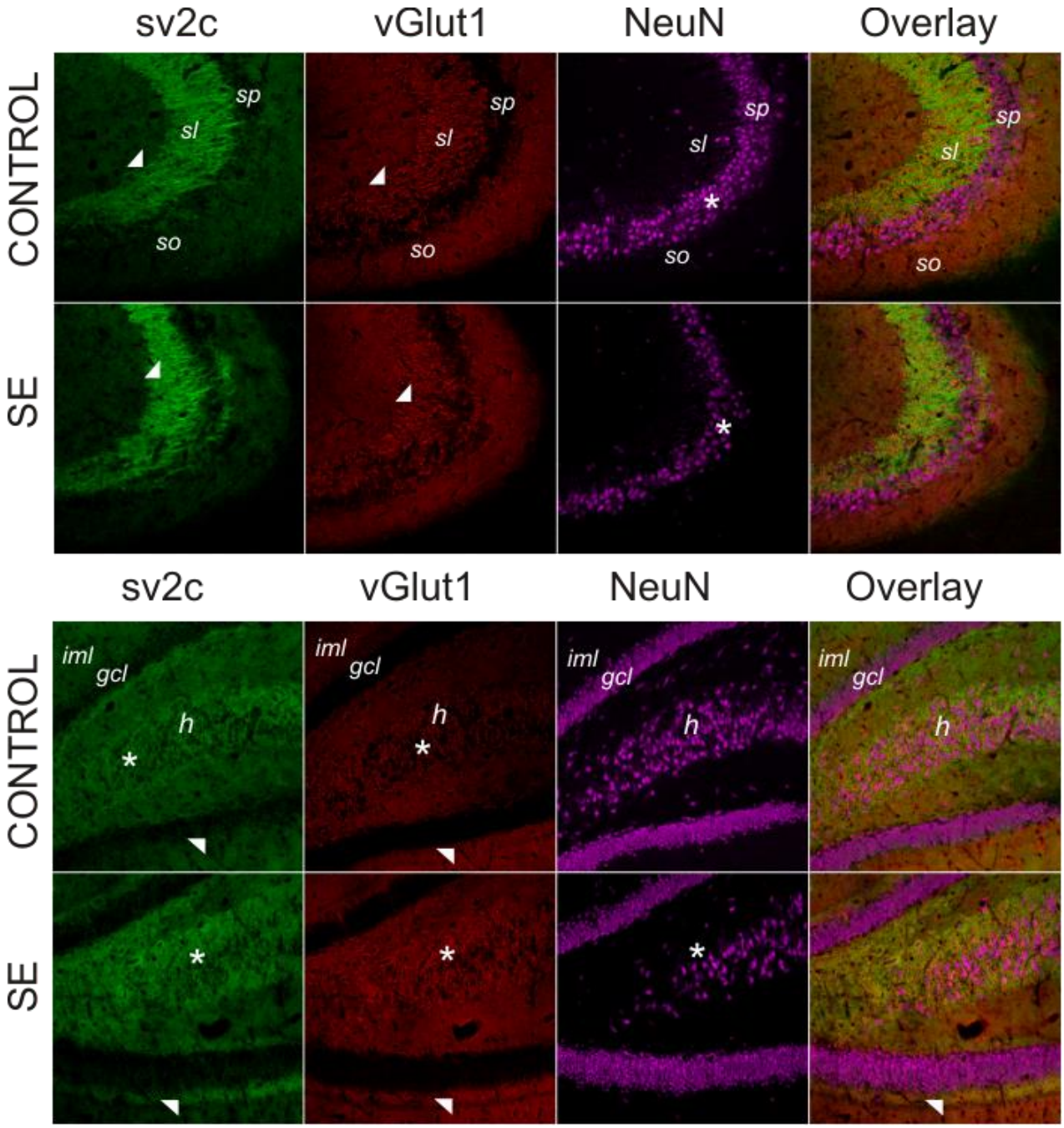

Figure 28. *Status epilepticus* (SE) induced up-regulation of SV2C in mice. Representative immunostaining experiments for SV2C, vGluT1 and NeuN in hippocampus of control and pilocarpine-treated mice that suffered *status epilepticus* (sacrificed 1 month after SE). Expression of Sv2c was increased in the mossy fiber pathway (arrows) in both panels. Top panel: Ca3 region, bottom panel: dentate gyrus. Please notice up-regulation of SV2C in the inner molecular layer of dentate gyrus just above granule cells. These Sv2c staining overlap(co-localized) to abnormally expressed vGluT1 proteins in same area indicating that SV2C is expressed in newly sprouted mossy fibers and boutons as part of the abnormal reorganization process that occurs after *status epilepticus*. This

anomalous reorganization of excitatory (VGluT1-expressing fibers) is proposed to play a major role in part in the pathogenesis of temporal lobe epilepsy.

3.3.2b. Chronic levetiracetam (LEV) treatment *in vivo* ameliorated abnormalities in presynaptic protein expression after *status epilepticus* in mice.

To determine whether chronic treatment with antiepileptic drug can modify (correct) abnormal expression of presynaptic proteins SV2A, SV2B and SV2C we used two different but complementary paradigms. A) Analysis of protein expression using western immunoblotting and B) Analysis of gene expression of SV2A, SV2B and SV2C using TaqMan-based real-time quantitative PCR. Control and experimental groups are similar as described for experiments of specific aim 3.1. Briefly, a) control SpH mice (*no status epilepticus*) injected with saline instead of levetiracetam (Control no treatment=C-NT), b) pilocarpine-treated mice that suffered *status epilepticus* injected with saline instead of levetiracetam (*status epilepticus*-no treatment=SE-NT), c) control SpH mice (*no status epilepticus)* that were injected with levetiracetam same days as post-*status epilepticus* mice (Control Treatment=C-T), and d) pilocarpine-treated mice that suffered *status epilepticus* and were injected with levetiracetam during one month 2 days after *status epilepticus* (status epileptics-treatment=SE-T).

Task 2 of Specific Aim 3. Analysis of protein expression of SV2, SV2B and SVC using western immunoblotting after *in vivo* treatment of epileptic mice with levetiracetam

Results: Data from these experiments revealed that *status epilepticus* induced a down-regulation of SV2A (25% reduction, but not significant at this time by Student t-test *p>0.05, n=5*), a no significant 24.1%increase in SV2B, and a statistically significant up-regulation of SV2C (52% increase, Student t-test, *p<0.05, n=5)* in animals that only received saline vehicle (0.9% NaCl) when compared to control saline-injected SpH mice group (Figure 29A) in a similar fashion as previously demonstrated in Sprague Dawley rats. Additional animals will be added to this data to improve power of the statistical analysis. After treatment with levetiracetam for 1 month (injections of drug 100mg/kg i.p in alternate days) the levels of SV2A significantly increased in animals that suffered *status epilepticus* (SE-T, n=4) (39.80% increased) when compared to levetirecetam-treated control group (C-T, n=4) (Student t-test, $p<0.05$) while expression of SV2B decreased 13.79% of control group ($p<0.05$). No significant change in the pattern of SV2C protein expression was observed detected (Figure 29B). These results indicated that chronic treatment with levetiracetam can revert or correct abnormalities of SV2A expression induced by *status epilepticus*, however this potentially therapeutic effect was not observed for SV2C which is abnormally increased after *status epilepticus*.

The significance of these findings are that treatment with levetiracetam may exert an antiepileptic action and neuroprotective effect by up-modulating expression of its own target SV2A, accordingly, levetiracetam-induced Sv2A up-regulation may explain why levetiracetam is selectively effective in chronically epileptic tissue with minimal effect in healthier non-epileptic brain in patients or animals models of epilepsy. It is known that levetiracetam failed to control convulsions/seizures in acute models of epilepsy while exerting a very potent antiepileptic effect in chronic models of epilepsy[79-81].

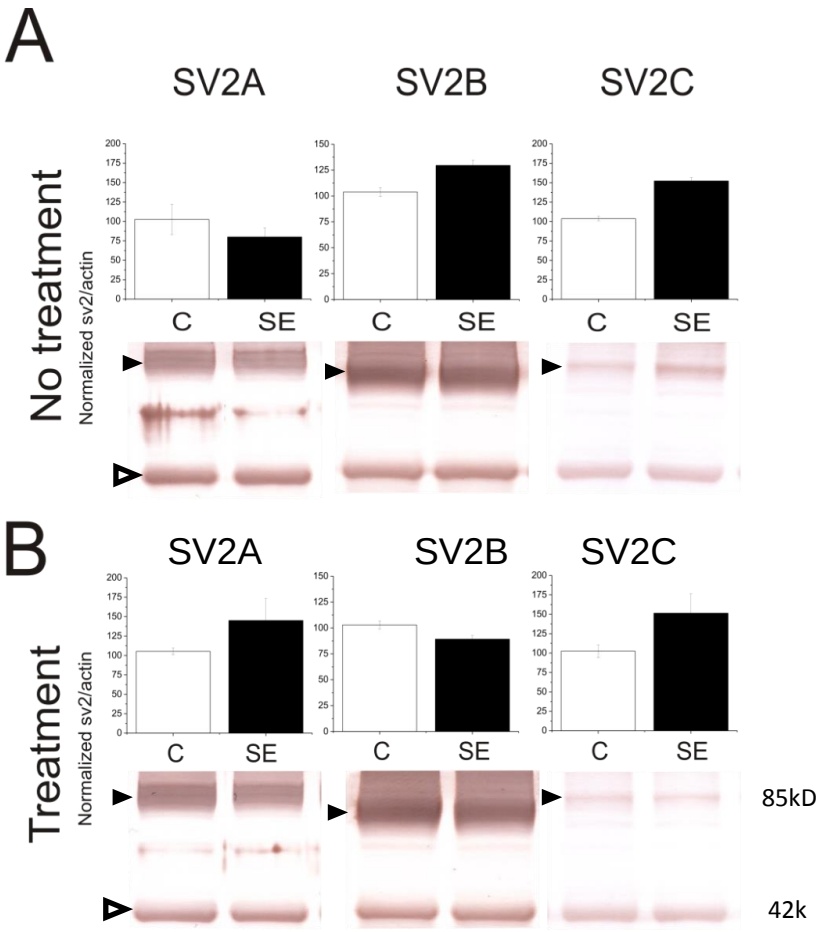

Figure 29. Effect of chronic in vivo treatment with levetiracetam (i.p) on the levels of protein expression of presynaptic vesicles SV2, SV2, and SV2C in hippocampus of SpH transgenic mice following the pilocarpine-induced *status epilepticus*. **A**. Graphs of normalized optical density for immunopositive bands show that *status epilepticus* (SE) induced a down-regulation of SV2A and up-regulation of SV2B and SV2C in no treatment groups (saline-injected). Measurements of optical density of immunopositive bands were normalized to expression of loading control β-actin (42kD) band. *Inset*: Representative immunoblottings for each of these SV proteins (black arrowheads, 85kD bands) and β-acting (white arrowhead, 42kD band). **B**. Chronic treatment with levetiracetam (100μg/Kg i.p) increased expression of SV2A (39.80% increase) and reduced expression of SV2B by 13.79% when compared to levetiracetam-treated control group (B). No significant change in the pattern the expression the SV2C was observed in the group treatment with levetiracetam.

Task 3 of Specific Aim 3: Analysis of gene expression of SV2, SV2B and SVC using TaqMan-based real-time quantitative PCR after *in vivo* treatment of epileptic mice with levetiracetam.

In order to investigate changes in gene expression of these presynaptic proteins, we used the TagMan-based real time quantitative PCR technique using protocols already described in our previous studies [12,39-41,82]. Experimental groups were described above. The rational of this experimental design was to determine whether changes in proteins expression of SV2A, SV2B and SV2C are associated with corresponding changes in gene expression (mRNA transcripts) and to assess whether levetiracetam-induced SV2A up-regulation detected in the epileptic tissue was mediated by changes in gene expression machinery/process. For this purpose, one half (hemisphere) of the brain was used for protein expression analysis (western blotting) as described above while the other hemisphere was used for mRNA extraction. As internal controls we measure expression of calbindin D-28K (*calb1*) and vGluT1 (*Slc17a7*) which are down-regulated and up-regulated respectively in chronically epileptic tissue[13,19].

Isolation of mRNA and real-time quantitative PCR analysis of gene expression.
For isolation of total RNA, control and experimental groups (as described above) of SpH mice were anaesthetized and sacrificed 1 months (endpoint) after the beginning of injection sections (saline or levetiracetam) . One hemisphere was used for protein isolation while the other hemisphere was used for total RNA isolation as previously reported[12,39-41,82]. Briefly, tissue was collected, weighed (about 20 mg), homogenized, and processed for total RNA isolation at 4°C using the RNAqueous-4PCR Kit (Foster City, California, USA), following manufacturer's instructions. The concentration and purity of total RNA for each sample was determined by the Quant-iT RNA Assay Kit and Q32857 Qubit fluorometer (Carlsbad, Invitrogen, California, USA) and confirmed by optical density measurements at 260 and 280nm using a BioMate 5 UV-visible spectrophotometer (Thermo Spectronic, Waltham, Massachusetts, USA). The integrity of the extracted RNA was confirmed by electrophoresis under denaturating condition. RNA samples from each set of control and epileptic rats were processed in parallel under the same conditions. RT were performed on an iCycler Thermal Cycler PCR System (Bio-Rad Laboratories, Hercules, California, USA), the High Capacity cDNA Reverse Transcription Kit (P/N: 4368814; Applied Biosystems, ABI, California, USA) for synthesis of single-stranded cDNA. The cDNA synthesis was carried out by following manufacturer's protocol using random primers for 1 µg of starting RNA. Each RT reaction contained 1000 ng of extracted total RNA template and RT reagents. The 20 µl reactions were incubated in the iCycler Thermocycler in thin-walled 0.2-µl PCR tubes for 10 min at 25°C, 120 min at 37°C, 5 s at 85°C, and then held at 4°C. The efficiency of the RT reaction and amount of input RNA template was determined by serial dilutions of input RNA. Each RNA concentration was reverse transcribed using the same RT reaction volume. The resulting cDNA template was subjected to quantitative real-time PCR (qrtPCR) real-time using Taqman-based Applied Biosystems gene expression assays, the TaqMan Fast Universal PCR Master Mix (ABI) and the StepOne Real-Time PCR System (ABI). Analysis of SV2A, SV2B and SV2C mRNA expression were carried out in a StepOne Real-Time PCR System using the validated TaqMan Gene Expression Assays for target genes. Gene expression analysis was performed using the TaqMan Gene Expression Assays Mm00486647_m1 for the target gene *Calb1* (RefSeq: NM_009788.4, amplicon size = 78 bp), Mm00812888_m1 for the target gene *Slc17a7* (RefSeq: NM_020309.3, amplicon size = 81 bp), Mm00491537_m1 for the target gene *Sv2a* (RefSeq: NM_022030.3, amplicon size = 79 bp), Mm00463805_m1 for the target gene *Sv2b* (RefSeq: NM_001109753.1, amplicon size = 88 bp), Mm01282622_m1 for the target gene *Sv2c* (RefSeq: NM_029210.1, amplicon size = 72 bp), and Mm99999915_g1 for the normalization gene glyceraldehyde-3-phosphate dehydrogenase *Gapdh* (RefSeq: NM_008084.2, amplicon size = 107 bp).
For qrtPCR analysis, each sample was run in triplicates. Each run included a no-template control to test for contamination of assay reagents. After a 94°C denaturation for 10 min, the reactions were cycled 40 times with a 94°C denaturation for 15s, and a 60°C annealing for 1 min. Three types of controls aimed at detecting genomic DNA contamination in the RNA sample or during the RT or qrtPCR reactions were always included: a RT mixture without reverse transcriptase, a RT mixture including the enzyme but no RNA, negative control (reaction mixture without cDNA template). The data were collected and analyzed using OneStep Software (ABI). Relative quantification was performed using the comparative threshold (CT) method after determining the CT values for reference (*Gapdh*) and target (*sv2a, sv2b or sv2c, calb28 and Slc17a7*) genes in each sample sets according to the $2^{-\Delta\Delta Ct}$ method (ΔΔCT, delta-delta CT)[83,84] as described by the manufacturer (ABI; User Bulletin 2). Changes

in mRNA expression level were calculated after normalization to *Gapdh*. As calibrator sample we used cDNA from arbitrarily selected control rat. The ΔΔCT method provides a relative quantification ratio according to calibrator that allows statistical comparisons of gene expression among samples. Values of fold changes in the control sample versus the post-SE samples represent averages from triplicate measurements. Changes in gene expression were reported as fold changes relative to controls. Data were analyzed by analysis of variance (ANOVA) (followed by post-hoc analysis) or via paired *t*-test to check for statistically significant differences among the groups (significance *P* value was set at <0.05).

Our data indicate a significance change in **sv2a gene expression** among the different groups (ANOVA, p<0.05, **Figure 6**). Post-hoc analysis revealed that *in vivo* levetiracetam treatment reduced the expression of *sv2a* transcripts in control group (no *status epilepticus*) when compared to all the other groups (p<0.05). This was unexpected considering that in protein expression analysis this effect was not observed. In addition, unlike effect of chronic treatment with levetiracetam SV2A protein expression, sv2a transcripts were not upregulated in levetiracetam-treated *status epilepticus* group. Hence, levetiracetam-induced Sv2A up-regulation may be mediated by non-transcriptional mechanisms, but perhaps by slowing down SV2A protein degradation, etc. No significant changes were detected in **sv2b gene expression** among the groups. However, a significant change was observed for **sv2c gene expression** (ANOVA, p>0.0001, F=11.87) where *status epilepticus* induced a significant sv2c upregulation (SE-NT) when compared to saline-injected control group (C-NT) (post-hoc Tukey Honest, p<0.01). Interestingly, in contrast to SV2C protein expression, chronic treatment with levetiracetam induced a significant 33.8% and 11.7% reduction of sv2c levels in treated *status epilepticus* and control groups respectively when compared to saline-injected status epilepticus and control groups. These data indicate that levetiracetam treatment can reduce abnormally increased sv2c transcripts after *status epilepticus*. Changes were detected among groups for calbindin 28 expression. *Status epilepticus* induced a down-regulation of calbidin 28 (*calb28, calb1*) and chronic treatment with levetiracetam corrected (increased) expression of these transcripts compared to control levels (post hoc Tukey Honest, p<0.05). Significant changes were noticed among groups for expression of *Slc17a7* gene *(vGLUt1). Status epilepticus* induced a significant upregulation of VGluT1 when compared to control (Tukey Honest, p<0.01) that was not further modified after treatment. VGluT1 increased in both levetiracetam and saline-injected groups after *status epilepticus*.
The relevance of these findings is unclear as SV2C plays an unknown role in transmission release or in the pathogenesis of epilepsy. Our data indicate that SV2C may be also involved in the antiepileptic action of levetirecetam in chronically epileptic brain. However, there is a differential effect of seizures on SV2A and SV2C (down- and up-regulation respectively) while effect of levetiracetam partially restore these abnormalities.

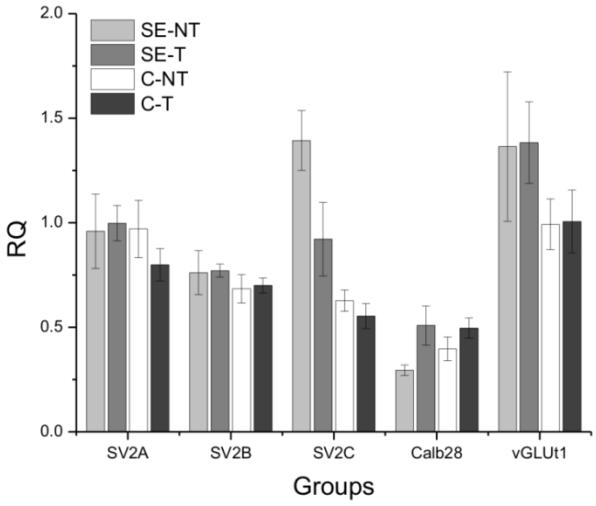

SE-NT *Status epilepticus* non treated group (saline injections) SE-T *Status epilepticus* levetiracetam-treated group
CN-T Control non-treated group (saline injections) CT-T Control levetiracetam-treated group

Figure 30. *Changes in gene expression after levetiracetam in vivo treatment in different groups of SpH mice*. Bar graphs represent percentage changes of triplicated results ± SE, and adjusted to the *Gapdh* gene (normalizing gene, housekeeping gene). Data was obtained using the TaqMan-based real-time quantitative PCR and delta-delta CT analysis. Levetiracetam treatment did not change expression of *sv2a* in epileptic brain but reduced transcripts in control group. No significant changes were detected for *sv2b* expression. S*v2c* expression was up-regulated after *status epilepticus but* chronic treatment with levetiracetam induced a reduction of *sv2c* expression, although *sv2c* levels remained above controls. Changes were detected among groups for calbindin 28 expression. *Status epilepticus* induced a down-regulation of calbidin 28 (*calb28*) and levetiracetam corrected (increased) expression of these transcripts compared to control levels (Post-hoc Tukey Honest, $p<0.05$). Significant changes were noticed among groups for expression of *Slc17a7* gene *(vGLUt1). Status epilepticus* induced a significant upregulation of vGLUt1 (*Slc17a7* gene) when compared to control (Post-hoc Tukey Honest, $p<0.01$) that was not further modified after treatment.

During the extension year, we repeat these experiments but including additional genes that were previously demonstrated to change during epilepsy. Specifically, in previous study we demonstrated that vesicular glutamate transporter type 1 (VGlut1) and metabotropic glutamate receptor type 2 (Grm2) are upregulated in dentate gyrus of pilocarpine-treated epileptic animals[11,12,19]. Moreover, calbindin 28K has been shown to be down-regulated in models of temporal lobe epilepsy[20]. We measure gene expression in several groups of mice treated and untreated with levetirecetam. Treatment with levetirecetam or saline vehicle was initiated 24h after SE. For this purpose intraperitoneal injections of drug 100mg/kg i.p was performed in alternate days during 4 weeks.

Description of methodology: Isolation of mRNA and real-time quantitative PCR analysis of gene expression.
For isolation of total RNA, control and experimental groups (as described above) of SpH mice were anaesthetized and sacrificed 1 months (endpoint) after the beginning of injection sections (saline or levetiracetam) . One hemisphere was used for protein isolation while the other hemisphere was used for total RNA isolation as previously reported[12,39-41,82]. Briefly, tissue was collected, weighed (about 20 mg), homogenized, and processed for total RNA isolation at 4°C using the RNAqueous-4PCR Kit (Foster City, California, USA), following manufacturer's instructions. The concentration and purity of total RNA for each sample was determined by the Quant-iT RNA Assay Kit and Q32857 Qubit fluorometer (Carlsbad, Invitrogen, California, USA) and confirmed by optical density measurements at 260 and 280nm using a BioMate 5 UV-visible spectrophotometer (Thermo Spectronic, Waltham, Massachusetts, USA). The integrity of the extracted RNA was confirmed by electrophoresis under denaturating condition. RNA samples from each set of control and epileptic rats were processed in parallel under the same conditions. RT were performed on an iCycler Thermal Cycler PCR System (Bio-Rad Laboratories, Hercules, California, USA), the High Capacity cDNA Reverse Transcription Kit (P/N: 4368814; Applied Biosystems, ABI, California, USA) for synthesis of single-stranded cDNA. The cDNA synthesis was carried out by following manufacturer's protocol using random primers for 1 µg of starting RNA. Each RT reaction contained 1000 ng of extracted total RNA template and RT reagents. The 20 µl reactions were incubated in the iCycler Thermocycler in thin-walled 0.2-µl PCR tubes for 10 min at 25°C, 120 min at 37°C, 5 s at 85°C, and then held at 4°C. The efficiency of the RT reaction and amount of input RNA template was determined by serial dilutions of input RNA. Each RNA concentration was reverse transcribed using the same RT reaction volume. The resulting cDNA template was subjected to quantitative real-time PCR (qrtPCR) real-time using Taqman-based Applied Biosystems gene expression assays, the TaqMan Fast Universal PCR Master Mix (ABI) and the StepOne Real-Time PCR System (ABI). Analysis of SV2A, SV2B and SV2C mRNA expression were carried out in a StepOne Real-Time PCR System using the validated TaqMan Gene Expression Assays for target genes. Gene expression analysis was performed using the TaqMan Gene Expression Assays Mm00486647_m1 for the target gene *Calb1* (RefSeq: NM_009788.4, amplicon size = 78 bp), Mm00812888_m1 for the target gene *Slc17a7* (RefSeq: NM_020309.3, amplicon size = 81 bp), Mm00491537_m1 for the target gene *Sv2a* (RefSeq: NM_022030.3, amplicon size = 79 bp), Mm00463805_m1 for the target gene *Sv2b* (RefSeq: NM_001109753.1, amplicon size = 88 bp), Mm01282622_m1 for the target gene *Sv2c* (RefSeq: NM_029210.1, amplicon size = 72 bp), and Mn01235831_m1 for the target gene mGluR2 (amplicon size 82 bp) and Mm99999915_g1 for the normalization gene glyceraldehyde-3-phosphate dehydrogenase *Gapdh* (RefSeq: NM_008084.2, amplicon size = 107 bp).

For qrtPCR analysis, each sample was run in triplicates. Each run included a no-template control to test for contamination of assay reagents. After a 94°C denaturation for 10 min, the reactions were cycled 40 times with a 94°C denaturation for 15s, and a 60°C annealing for 1 min. Three types of controls aimed at detecting genomic DNA contamination in the RNA sample or during the RT or qrtPCR reactions were always included: a RT mixture without reverse transcriptase, a RT mixture including the enzyme but no RNA, negative control (reaction mixture without cDNA template). The data were collected and analyzed using OneStep Software (ABI). Relative quantification was performed using the comparative threshold (CT) method after determining the CT values for reference (*Gapdh*) and target (*sv2a, sv2b or sv2c, calb28 and Slc17a7*) genes in each sample sets according to the $2^{-\Delta\Delta Ct}$ method (ΔΔCT, delta-delta CT)[83,84] as described by the manufacturer (ABI; User Bulletin 2). Changes in mRNA expression level were calculated after normalization to *Gapdh*. As calibrator sample we used cDNA from arbitrarily selected control rat. The ΔΔCT method provides a relative quantification ratio according to calibrator that allows statistical comparisons of gene expression among samples. Values of fold changes in the control sample versus the post-SE samples represent averages from triplicate measurements. Changes in gene expression were reported as percent changes relative to controls. Data were analyzed by one-way analysis of variance (ANOVA) (followed by post-hoc analysis) or via paired *t*-test to check for statistically significant differences among the groups (significance *P* value was set at <0.05).

Analysis of relative index of gene expression by TaqMan qPCR shows no significant differences in the expression of SV2A and SV2B between saline-injected controls (n=5) and SE-suffering mice (n=4) that were not treated with levetirecetam (0.97±0.13 vs 0.95±0.17 and 0.68±0.06 vs 0.76±0.1, for SV2A and SV2B respectively Fig. 31A). However, we detected a significant 122.24% increase in relative index for SV2C gene expression (F=11.87, p<0.0001 by One way ANOVA). Specifically, levels of SV2C increased from 0.63±0.05 in saline-injected group to 1.39±0.14 in mice suffering SE (p<0.001, Tukey post-hoc analysis). We also analyzed the expression of other genes that are known to be modified after SE including calbindin (calb28)[20,85], vesicular glutamate transporter type 1 (VGlut1)[11,19] and metabotropic glutamate receptor type 2 (Grm2)[12]. Our analysis revealed a no significant 25.8% reduction in expression of Calb28 between these two groups 1 month after SE (0.40±0.05 vs 0.29±0.02 , p>0.05). In addition, we detected a 37.4% increase in VGlut1 expression after SE (1.36±0.35) when compared to the control group (0.99±0.12) that was not statistically significant. Moreover, analysis of Grm2 revealed a significant 161.1% increase in animals that suffered SE (2.27±0.29) compared to controls (0.87±0.03, p<0.001 by Tukey post-hoc pairwise comparisons).

We then compared the changes in gene expression in animals treated with levetirecetam during 4 weeks after pilocarpine-induced SE. When compared to non-treated animals, treatment of saline-injected animals with levetirecetam induced non-significant 18% reduction in the expression of SV2A (0.80±0.07). Levetiracetam treatment of SE-suffering animals induced no significant changes in SV2A gene expression when compared to other groups (0.99±0.08). Analysis of variance using one way ANOVA for changes in SV2A expression revealed no significant changes among groups (F=0.56, p=0.64). Similarly, analysis of SV2B gene expression was not significant (F=0.45, p=0.72). Specifically, treatment with levetirecetam revealed no significant changes in saline-injected animals (0.69±0.03) or SE-suffering mice (0.77±0.03) when compared to non-treated saline-injected group (0.68+0.06) and SE-suffering group (0.76±0.10) (Figure 1A. In contrast, we detected a significant change in the expression of SV2C (F=11.8, p<0.001). In this case, post-hoc analysis indicate that treatment with levetirecetam did not significantly changed SV2C expression in saline-injected group (0.55±0.05) when compared to non-treated animals (0.62±0.05) (p>0.05), however, treatment of SE-suffering group for 4 weeks with levetirecetam induced a significant 33.8% down-regulation of originally increased levels of SV2C expression in non-treated groups (1.39±0.14) to 0.92±0.17 in levetirecetam-treated SE suffering mice (Tukey post-hoc analysis, p<0.05) (Figure 1a). However, when compared to saline-injected animals, levels of SV2C in levetirecetam-treated SE suffering mice remained elevated compared to non-treated and levetirecetam-treated saline-injected groups (0.62±0.05 and 0.55±0.05 respectively) (Figure 31, b and c).

No statistically significant changes were detected for gene expression of Calb28 (F=2.6, p=0.09) and VGlut1 (F=1.06, p=0.39) by one way ANOVA analysis despite a 25.5% reduction of Calb28 expression in SE-suffering animals (0.39±0.05) when compared to saline-injected controls (0.29±0.02) (Figure 31a). Treatment with levetirecetam did not significantly changed expression of Calb28 (0.49±0.04) in saline-injected or SE-suffering mice (0.50±0.09) when compared to respective non-treated controls above (Figure 1b and c). In the case of

VGluT1, there was a 37.4% increase in the expression of VGluT1 gene expression in SE group (1.36±0.12) when compared to saline-injected controls (0.99±0.35) (Figure 31a) but data was not significant in one way ANOVA. Treatment with levetirecetam did not induce significant changes in the levels of gene expression in saline-injected or SE suffering groups (1.0±0.15 *vs*. 1.38 ±0.19) (Figure 31d and e). In contrast, a significant change was detected for Grm2 gene expression (F=10.7, p<0.0001) among all groups. Specifically, induction of SE resulted in 161% upregulation of Grm2 1 month after pilocarpine injection (2.27±0.29) when compared to saline-injected group (0.87±0.03, Tukey honest test, p<0.001, Figure 31a). Treatment with levetiracetam induced a non-significant 19.5% increase in the level of Grm2 expression in saline-treated group (1.04±0.05) while non-significant 10.38% reduction was detected in SE group (2.04±0.38) (Figure 31).

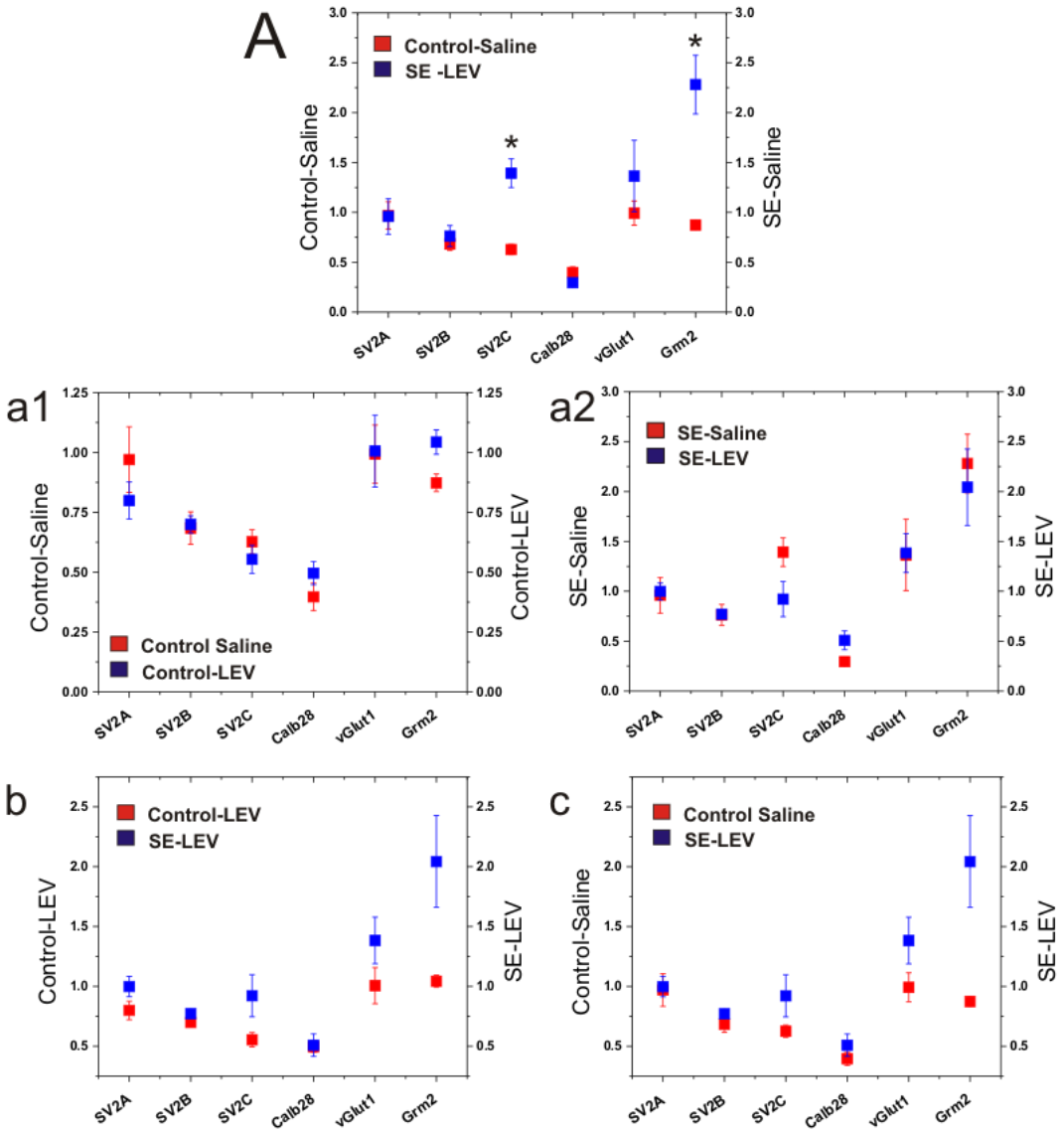

Figure 31. Graphs represent changes of relative quantification index of different transcripts by TaqMan qPCR assays in hippocampus of mice after *status epilepticus* (SE-Saline) compared to saline-injected control group (Control-Saline) and after the treatment of status epilepticus-suffering animals and saline-injected animals with levetirecetam (SE-LEV and control-LEV respectively).

Milestones: The following milestones were accomplished during year 3 and extension period.

We have shown that chronic treatment of animals with levetiracetam is effective in inhibiting abnormally enhanced presynaptic vesicle release of in mossy fibers of granule cells after *status epilepticus*.

In addition, we found that chronic treatment with levetiracetam increased protein expression of SV2A (levetiracetam targets) in mossy fiber pathway while reducing seizure-induced increases in SV2C (gene expression of sv2c by qrtPCR) in hippocampus after pilocarpine-induced *status epilepticus*. However, data real time PCR analysis of gene expression indicates that changes in SV2A and SV2C was not statistically significant.

Our data indicate that instead of SV2A which is the major target for levetirecetam, another synaptic protein SV2C is the one that robustly change (upregulation) after pilocarpine-induced status epilepticus. Status epilepticus induced upregulation of SV2C was ameliorated significantly by the treatment with levetirecetam indicating that these synaptic protein may play an important role in the pathogenesis of epilepsy and it can be a relevant target for development of new or improved antiepileptic drugs.

Our data indicate that levetiracetam is effective in counteracting pro-epileptogenic changes in transmitter release and presynaptic molecules if administered after the epileptogenic insult (status epilepticus).

KEY RESEARCH ACCOMPLISHMENTS:

Our results indicate that chronic treatment with the antiepileptic drug levetiracetam after *status epilepticus* can reduce abnormally enhanced presynaptic vesicle release of glutamatergic mossy fiber boutons in pilocarpine-treated SpH transgenic mice. In a previous study we reported a long-lasting abnormality of presynaptic structure and function in experimental epilepsy[7]. Specifically, multiphoton microscopy was used to directly measure prospective changes in vesicular recycling properties from hippocampal mossy fiber presynaptic boutons in control versus pilocarpine-treated chronic epileptic SpH21 transgenic mice expressing SpH preferentially at glutamatergic synapses. We detected significant increases in action potential-driven vesicular release at 1-2 months after pilocarpine-induced *status epilepticus*. Results from Year 3 of this proposal also indicate that levetiracetam may decrease exaggerated presynaptic vesicular release by affecting the presynaptic release machinery at excitatory pathways. Specifically, chronic treatment with levetiracetam increased deficient expression of SV2A in hippocampus (SV2A is a molecular target for levetirecetam) and reduced the abnormally increased levels of SV2C in similar pathway. Additional experiments are in progress to detect changes in another presynaptic protein mGluR2. Deciphering the mechanisms of levetiracetam-induced changes in presynaptic proteins may lead to a novel antiepileptic mechanism for this antiepileptic drug. In addition, additional studies are necessary to develop and assess the role of new antiepileptic drugs that target newly reported changes in presynaptic proteins, specifically SV2C.

These data indicate that presynaptically acting drugs such as levetiracetam reduces hyperexcitability and inhibit presynaptic transmission in mesial temporal lobe epilepsy. Preventive treatment with antiepileptic drug is a feasible strategy to reduce the development of epilepsy (specifically post-traumatic epilepsy). In our study, we investigate whether treatment with the drug levetiracetam immediately after pilocarpine-induced status epilepticus (epileptogenic insult) significantly reduced abnormally enhanced presynaptic vesicle release and reduce molecular abnormalities in presynaptic molecules (i.e. SV2A, SV2B, SV2C) in treated epileptic mice. Interestingly, we also detected that *status epilepticus* induced up-regulation of SV2C while producing down-regulation of SV2A in the mossy fiber pathways. In vivo treatment with levetiracetam partially corrected both protein and mRNA gene expression changes in SV2C while only partially restored deficient SV2A protein levels after *status epilepticus* indicating that SV2C may also play a role in the epileptogenic process. LEV is a novel antiepileptic drug that binds to presynaptic targets SV2A. Although SV2A has been identified as the main molecular target for levetiracetam[81,86,87], our data indicate that “pro-epileptic” changes in SV2C may become a novel antiepileptic

therapeutic target for new pharmacological drugs in order to modify presynaptic transmitter release and reduce hyperexcitability in epilepsy.

SV2 proteins are abundant synaptic vesicle integral membrane proteins expressed in two major (*SV2A* and SV2B) and one minor isoform (SV2C) whose membrane topology resembles that of transporter proteins [88,89]. Although SV2A is the major target of the antiepileptic drug levetiracetam, its function and partner molecules are still unknown [80,81,90,91]. Our study indicates that SV2C may play a role in the pathogenesis of epilepsy. We found that levels of SV2C transcripts increased after pilocarpine-induced *status epilepticus* consistent with previous studies in human epilepsy [77]. These authors reported that SV2C, which is weakly expressed or absent in the hippocampus of control cases, was overexpressed in 10/11 cases with classical MTS1A and mossy fibre sprouting but not in cases with other types of MTS. In our study, we demonstrated that changes in SV2C expression may start as early as 4 weeks after *status epilepticus*. Additional studies are necessary to determine the earlier time point fat which status epilepticus will induce an upregulation of SV2C. Interestingly, we also found that treatment with levetirecetam during 4 weeks after *status epilepticus* reduced the expression of SV2C significantly but still levels remained above controls. These findings indicate that SV2C expression is also dysregulated during epileptogenesis but levels can be partially restored with pharmacological treatment with antiepileptic drugs. The significance of these findings for the pathogenesis of epilepsy remains to be elucidated considering that despite a high degree of homology between SV2 isoforms SV2A is the known molecular target of levetirecetam[69,80,81,87,91]. It is known that levetiracetam failed to control convulsions/seizures in acute models of epilepsy while exerting a very potent antiepileptic effect in chronic models of epilepsy [79-81]. It is currently unknown whether seizures can induce levetirecetam-binding splice variants of SV2C. This will be a therapeutically relevant finding since upregulation of SV2C in epilepsy will allow for increased pharmacological targets for levetirecetam and consequentially improve the pharmacological action of this antiepileptic drug when compared to SV2A expression which has been found to be reduced in previous studies using animal models of epilepsy and tissue from epileptic patients [77,78]. Interestingly, in our study, we failed to demonstrate a significant down-regulation of SV2A after *status epilepticus*, neither a significant effect of levetiractam on SV2A transcript levels in animals that suffered *status epilepticus*. The role of SV2A on epilepsy has been established by 3 facts: (1) SV2A is the sole molecular target for the antiepileptic drug levetiracetam (LEV)[64,92,93], (2) SV2A knockout mice exhibit severe seizures[65,66,94], and (3) down-regulation of SV2A has been reported in epilepsy [77,78]. SV2A is consistently reduced in mossy fibers in experimental MTLE and epileptic patients. Despite these compelling findings, the exact function of SV2A remains unknown. Hence, the molecular cascades and pathways mediating the action of loevetiracetam deserve further investigation. A major problem is the lack of functional assays to probe how levetiracetam interacts with and modifies SV2A function. Moreover, the exact binding site of levetiracetam on the structure of SV2A has not been discovered yet.

4. Impact

It is important to highlight that LEV is a drug with a unique antiepileptic profile. LEV failed to block seizures in acute models of epilepsy while exhibited a potent antiepileptic effect in chronic experimental models of epilepsy as the kainate, kindling and pilocarpine models. This antiepileptic profile may be related to molecular changes that are specific for tissue undergoing epileptogenesis (i.*e.* abnormal binding sites for LEV, in addition to the already reported SV2A). This project will elucidate the presynaptic mechanisms of action of LEV and other antiepileptic drugs as a strategy to accelerate the development of novel antiepileptic drugs acting in presynapses. Understanding abnormalities of presynaptic terminals during epileptogenesis is critical to elucidate the pathogenesis of pharmacoresistant epilepsy.

LEV is a novel antiepileptic drug that binds to presynaptic targets. However, the presynaptic mechanisms are still unclear and innovative research paradigms need to be deployed to understand how this drug work in order to design similarly effective or better versions for the treatment of pharmaco-resistance epilepsy. We found that expression of LEV targts are down-regulated in epilepsy but expression of homologous protein SV2C is upregulated 10 days after status epilepticus and transcripts are upregulated during the chronic phase of the model. Sv2C my represent novel targets for LEV and similar drugs acting on presynaptic terminals to control release of glutamate. In this project will elucidate the presynaptic mechanisms of action of LEV and other antiepileptic drugs as a strategy to accelerate the development of novel antiepileptic drugs acting in presynapses.

In Year 3, we assessed if treatment with LEV can restore molecular deficiencies caused by epilepsy in this animal model of mesial temporal lobe epilepsy (including down-regulation of SV2A and mGluR2. Understanding abnormalities of presynaptic terminals during epileptogenesis is critical to elucidate the pathogenesis of pharmacoresistant epilepsy.

The expression of S2V isoforms in neurochemically-distinct neuronal subtypes is also different in hippocampus. Although both SV2A and SV2C are expressed in mossy fibers, the expression of SV2A is also found in GABAergic terminals while SV2C is predominantly expressed in glutamatergic terminals [69,88]. It is possible that levetirecetam can binds to both SV2A and spliced or upregulated SV2C. Regardless, increases in SV2C expression after status epilepticus may play a role in the pathogenesis of epilepsy as a contributing or a compensatory molecular event that needs to be elucidated.

Data in this project indicate that in addition to the known target of levetirecetam SV2A, SV2C may play an important role in the pathogenesis of epilepsy. SV2C can be a novel target for development of new and more efficient antiepileptic drugs considering that there will be a higher density of targets (SV2C) available during the disease process while SV2A is actually down-regulated.

5. Changes/Problems

6. Products

REPORTABLE OUTCOMES:

MANUSCRIPTS (APPENDIX 1)

1) A manuscript entitled was published in Brain (2012) (see Appendix) "Altered neurotransmitter release, vesicle recycling and presynaptic structure in the pilocarpine model of temporal lobe epilepsy." Upreti C, Otero R, Partida C, Skinner F, Thakker R, Pacheco LF, Zhou ZY, Maglakelidze G, Velíšková J, Velíšek L, Romanovicz D, Jones T, Stanton PK, **Garrido-Sanabria** ER. *Brain*. March 2012; 135 (Pt 3): 869-85, 2012. (See Appendix 1).

2) A manuscript entitled will be submitted to Neuroreport in 2015. "Abnormal expression of synaptic vesicle protein 2 (SV) isoforms after pilocarpine-induced status epilepticus". Luis F. Pacheco Otalora[1], Nuri Ruvalcaba, Jose Mario Rodriguez, Samantha Gomez, Aliya Sharif, Chirag Upreti, Patric Stanton, Emilio R. Garrido-Sanabria (See Appendix 2).

Other manuscripts with data from this grant are currently in preparation

NATIONAL MEETINGS (APPENDIX 2)

Data from this grant was presented or submitted to scientific meetings and conferences (below)

Year 1

Data from electrophysiological and pharmacological experiments was submitted to the Society for Neuroscience Meeting that will be held October 13 - 17, 2012, in New Orleans, LA. **E. G. Sanabria,** L. F. Pacheco, L. M. Rambo, J. M. Rodriguez, C. Upreti, P. K. Stanton. Levetiracetam inhibits excitatory drive onto dentate gyrus granule cells: Effects of SV2A gene dosage and pilocarpine-induced epilepsy. (see Abstract in Appendix 1).

Abnormal function and reorganization of presynaptic nanocomponents in experimental epilepsy: A multiphoton laser scanning confocal imaging and transmission electron microscopy study. Upreti C, Skinner F, Otero R, Thakker R, Rosas G, Partida C, Pacheco LF, Jones TA, Romanovicz D, Stanton PK and **Garrido-Sanabria** ER. *3rd Meeting of the American Society for Nanomedicine,* Rockville, MD, Nov 9-11, 2011.

Abnormalities in presynaptic vesicle pools of mossy fiber boutons in the pilocarpine model of mesial temporal lobe epilepsy. Upreti PK, Stanton E, **Garrido-Sanabria ER**. Poster. 779.10/Z13 *Society for Neuroscience Meeting*, Washington, Nov 16, 2011.

Abnormal functional and ultrastructural changes of synaptic vesicle pools at active zones in mossy fiber boutons in mesial temporal lobe epilepsy, (ID: 1149994), Upreti C, **Garrido-Sanabria ER**, Stanton PK, presented at the *65th America Epilepsy Society Annual Meeting*, Baltimore, December 2-6, 2011.

Abnormal Ultrastructure of Large Mossy Fiber Boutons-CA3 pyramidal Cell Synapses in Mesial Temporal Lobe Epilepsy. (ID: 1150094). **Garrido-Sanabria ER**, Otero R, Thakker R, Partida C, Skinner F, Jones T, Romanovicz D, Upreti C, Stanton PK., presented at the *65th America Epilepsy Society Annual Meeting*, Baltimore, December, 2011.

Year 2

Levetiracetam inhibits excitatory drive onto dentate gyrus granule cells: Effects of SV2A gene dosage and pilocarpine-induced epilepsy. **E. G. Sanabria,** L. F. Pacheco, L. M. Rambo, J. M. Rodriguez, C. Upreti, **P. K. Stanton**. Society for Neuroscience Meeting that will be held October 13 - 17, 2012, in New Orleans, LA.

Inhibitory action of levetiracetam on CA1 population spikes and dentate gyrus excitatory transmission in pilocarpine-treated chronic epileptic rats. **E. G. Sanabria**, L. Pacheco, J. Zavaleta, F. Shriver, L. M. Rambo, C. Upreti, **P. K. Stanton**. Society for Neuro9science Meeting that will be held in San Diego, CA, Nov 9-13, 2013.

Year 3 and non-cost extension period

Inhibitory action of levetiracetam on CA1 population spikes and dentate gyrus excitatory transmission in pilocarpine-treated chronic epileptic rats. **E. G. Sanabria**, L. Pacheco, J. Zavaleta, F. Shriver, L. M. Rambo, C. Upreti, **P. K. Stanton**. Society for Neuroscience Meeting in San Diego, CA, Nov 9-13, 2013

Synaptic Vesicle Protein Expression in Sprague-Dawley Rats Treated with the Pilocarpine Model for Mesial Temporal Lobe Epilepsy. Mayra Velazquez, L.F. Pacheco, **E. R. Garrido-Sanabria**. 25th Anniversary Conference, HENAAC Conference, October 3 - 5, 2013, New Orleans.

*Chronic treatment with levetiracetam upregulate SV2A and reduce abnormally augmented presynaptic vesicular release after pilocarpine-induced status epilepticus***.** Luis F. Pacheco, Vinicius Funck, Nuri Ruvalcaba, Jose M.

Rodriguez, Daniela Taylor, Rubi Garcia, Jason Zavaleta, Chirag Upreti, **Patric K. Stanton**, **Emilio R. Garrido-Sanabria,** the Military Health System Research Symposium, to be held on August 18-21, 2014.

*Treatment with levetiracetam ameliorates abnormal presynaptic vesicular release and altered presynaptic protein expression in a glutamatergic pathway after pilocarpine-induced status epilepticus***. Emilio R. Garrido-Sanabria,** Luis F. Pacheco, Vinicius Funck, Nuri Ruvalcaba, Jose M. Rodriguez, Daniela Taylor, Rubi Garcia, Jason Zavaleta, Chirag Upreti, **Patric K. Stanton**. This abstract will be submitted to the 68th Annual Meeting of the American Epilepsy Society, Dec 5-9, 2014, Seattle, Washington.

Abnormal upregulation of SV2C after pilocarpine-induced seizures is restored after treatment with antiepileptic drug levetirecetam. Luis F. Pacheco, Vinicius Funck, Nuri Ruvalcaba, Samantha Gomez, Aliya Sharif, Jose M. Rodriguez, Daniela Taylor, Rubi Garcia, Chirag Upreti, Patric K. Stanton, **Emilio R. Garrido-Sanabria,** the Military Health System Research Symposium, to be held on August, 2015.

7. Participants & Other Collaborating Organizations

Name:	*Emilio R. Garrido Sanabria, MD, PhD*
Project Role:	*Principal Investigator*
Researcher Identifier (e.g. ORCID ID):	*UTBID: Eg0213903*
Nearest person month worked:	*12*
Contribution to Project:	*Dr. Garrido has performed work in the area of electrophysiology, immunohistochemistry, data analysis*
Funding Support:	

Name:	*Luis F. Pacheco*
Project Role:	*Research*
Researcher Identifier (e.g. ORCID ID):	*UTBID LP0234778*
Nearest person month worked:	*12*
Contribution to Project:	*Dr. Pacheco has performed work in the area of electrophysiology, real-time PCR, immunohistochemistry and western blotting, imaging and data analysis.*

	Development of pilocarpine model of mesial temporal lobe epilepsy.
Funding Support:	

8. Special Reporting Requirements

Nothing to report

References

[1] Schauwecker PE. Strain differences in seizure-induced cell death following pilocarpine-induced status epilepticus. *Neurobiol Dis* 2012; **45**: 297-304.

[2] Turski WA, Cavalheiro EA, Bortolotto ZA, Mello LM, Schwarz M, Turski L. Seizures produced by pilocarpine in mice: a behavioral, electroencephalographic and morphological analysis. *Brain Res* 1984; **321**: 237-253.

[3] Muller CJ, Bankstahl M, Groticke I, Loscher W. Pilocarpine vs. lithium-pilocarpine for induction of status epilepticus in mice: development of spontaneous seizures, behavioral alterations and neuronal damage. *Eur J Pharmacol* 2009; **619**: 15-24.

[4] Burrone J, Li Z, Murthy VN. Studying vesicle cycling in presynaptic terminals using the genetically encoded probe synaptopHluorin. *Nat Protoc* 2006; **1**: 2970-2978.

[5] Li Z, Burrone J, Tyler WJ, Hartman KN, Albeanu DF, Murthy VN. Synaptic vesicle recycling studied in transgenic mice expressing synaptopHluorin. *Proc Natl Acad Sci U S A* 2005; **102**: 6131-6136.

[6] Mello LE, Cavalheiro EA, Tan AM, Kupfer WR, Pretorius JK, Babb TL *et al.* Circuit mechanisms of seizures in the pilocarpine model of chronic epilepsy: cell loss and mossy fiber sprouting. *Epilepsia* 1993; **34**: 985-995.

[7] Upreti C, Otero R, Partida C, Skinner F, Thakker R, Pacheco LF *et al.* Altered neurotransmitter release, vesicle recycling and presynaptic structure in the pilocarpine model of temporal lobe epilepsy. *Brain* 2012; **135**: 869-885.

[8] Boulland JL, Ferhat L, Tallak Solbu T, Ferrand N, Chaudhry FA, Storm-Mathisen J *et al.* Changes in vesicular transporters for gamma-aminobutyric acid and glutamate reveal vulnerability and reorganization of hippocampal neurons following pilocarpine-induced seizures. *J Comp Neurol* 2007; **503**: 466-485.

[9] Epsztein J, Represa A, Jorquera I, Ben-Ari Y, Crepel V. Recurrent mossy fibers establish aberrant kainate receptor-operated synapses on granule cells from epileptic rats. *J Neurosci* 2005; **25**: 8229-8239.

[10] Esclapez M, Hirsch JC, Ben-Ari Y, Bernard C. Newly formed excitatory pathways provide a substrate for hyperexcitability in experimental temporal lobe epilepsy. *J Comp Neurol* 1999; **408**: 449-460.

[11] Pacheco Otalora LF, Couoh J, Shigamoto R, Zarei MM, Garrido Sanabria ER. Abnormal mGluR2/3 expression in the perforant path termination zones and mossy fibers of chronically epileptic rats. *Brain Res* 2006; **1098**: 170-185.

[12] Ermolinsky B, Pacheco Otalora LF, Arshadmansab MF, Zarei MM, Garrido-Sanabria ER. Differential changes in mGlu2 and mGlu3 gene expression following pilocarpine-induced status epilepticus: a comparative real-time PCR analysis. *Brain Res* 2008; **1226**: 173-180.

[13] Garrido-Sanabria ER, Otalora LF, Arshadmansab MF, Herrera B, Francisco S, Ermolinsky BS. Impaired expression and function of group II metabotropic glutamate receptors in pilocarpine-treated chronically epileptic rats. *Brain Res* 2008; **1240**: 165-176.

[14] Winden KD, Karsten SL, Bragin A, Kudo LC, Gehman L, Ruidera J *et al.* A systems level, functional genomics analysis of chronic epilepsy. *PLoS One* 2011; **6**: e20763.

[15] Sills GJ. SV2A in epilepsy: the plot thickens. *Epilepsy Curr* 2010; **10**: 47-49.

[16] de Groot M, Toering ST, Boer K, Spliet WG, Heimans JJ, Aronica E *et al.* Expression of synaptic vesicle protein 2A in epilepsy-associated brain tumors and in the peritumoral cortex. *Neuro Oncol* 2010; **12**: 265-273.
[17] Feng G, Xiao F, Lu Y, Huang Z, Yuan J, Xiao Z *et al.* Down-regulation synaptic vesicle protein 2A in the anterior temporal neocortex of patients with intractable epilepsy. *Journal of molecular neuroscience : MN* 2009; **39**: 354-359.
[18] Kaminski RM, Gillard M, Leclercq K, Hanon E, Lorent G, Dassesse D *et al.* Proepileptic phenotype of SV2A-deficient mice is associated with reduced anticonvulsant efficacy of levetiracetam. *Epilepsia* 2009; **50**: 1729-1740.
[19] Pacheco Otalora LF, Hernandez EF, Arshadmansab MF, Francisco S, Willis M, Ermolinsky B *et al.* Down-regulation of BK channel expression in the pilocarpine model of temporal lobe epilepsy. *Brain Res* 2008; **1200**: 116-131.
[20] Carter DS, Harrison AJ, Falenski KW, Blair RE, DeLorenzo RJ. Long-term decrease in calbindin-D28K expression in the hippocampus of epileptic rats following pilocarpine-induced status epilepticus. *Epilepsy Res* 2008; **79**: 213-223.
[21] Hallermann S, Pawlu C, Jonas P, Heckmann M. A large pool of releasable vesicles in a cortical glutamatergic synapse. *Proc Natl Acad Sci U S A* 2003; **100**: 8975-8980.
[22] Blackstad TW, Brink K, Hem J, Jeune B. Distribution of hippocampal mossy fibers in the rat. An experimental study with silver impregnation methods. *J Comp Neurol* 1970; **138**: 433-449.
[23] Claiborne BJ, Amaral DG, Cowan WM. A light and electron microscopic analysis of the mossy fibers of the rat dentate gyrus. *J Comp Neurol* 1986; **246**: 435-458.
[24] Miesenbock G, De Angelis DA, Rothman JE. Visualizing secretion and synaptic transmission with pH-sensitive green fluorescent proteins. *Nature* 1998; **394**: 192-195.
[25] Bayazitov IT, Richardson RJ, Fricke RG, Zakharenko SS. Slow presynaptic and fast postsynaptic components of compound long-term potentiation. *J Neurosci* 2007; **27**: 11510-11521.
[26] Dobrunz LE, Stevens CF. Heterogeneity of release probability, facilitation, and depletion at central synapses. *Neuron* 1997; **18**: 995-1008.
[27] Murthy VN, Sejnowski TJ, Stevens CF. Heterogeneous release properties of visualized individual hippocampal synapses. *Neuron* 1997; **18**: 599-612.
[28] Matz J, Gilyan A, Kolar A, McCarvill T, Krueger SR. Rapid structural alterations of the active zone lead to sustained changes in neurotransmitter release. *Proc Natl Acad Sci U S A* 2010; **107**: 8836-8841.
[29] Schikorski T, Stevens CF. Quantitative ultrastructural analysis of hippocampal excitatory synapses. *J Neurosci* 1997; **17**: 5858-5867.
[30] Amaral DG, Dent JA. Development of the mossy fibers of the dentate gyrus: I. A light and electron microscopic study of the mossy fibers and their expansions. *J Comp Neurol* 1981; **195**: 51-86.
[31] Chicurel ME, Harris KM. Three-dimensional analysis of the structure and composition of CA3 branched dendritic spines and their synaptic relationships with mossy fiber boutons in the rat hippocampus. *J Comp Neurol* 1992; **325**: 169-182.
[32] Rollenhagen A, Satzler K, Rodriguez EP, Jonas P, Frotscher M, Lubke JH. Structural determinants of transmission at large hippocampal mossy fiber synapses. *J Neurosci* 2007; **27**: 10434-10444.
[33] Suyama S, Hikima T, Sakagami H, Ishizuka T, Yawo H. Synaptic vesicle dynamics in the mossy fiber-CA3 presynaptic terminals of mouse hippocampus. *Neurosci Res* 2007; **59**: 481-490.
[34] Patrylo PR, Dudek FE. Physiological unmasking of new glutamatergic pathways in the dentate gyrus of hippocampal slices from kainate-induced epileptic rats. *J Neurophysiol* 1998; **79**: 418-429.
[35] Dudek FE, Sutula TP. Epileptogenesis in the dentate gyrus: a critical perspective. *Prog Brain Res* 2007; **163**: 755-773.
[36] Sutula TP, Dudek FE. Unmasking recurrent excitation generated by mossy fiber sprouting in the epileptic dentate gyrus: an emergent property of a complex system. *Prog Brain Res* 2007; **163**: 541-563.
[37] Buckmaster PS, Zhang GF, Yamawaki R. Axon sprouting in a model of temporal lobe epilepsy creates a predominantly excitatory feedback circuit. *J Neurosci* 2002; **22**: 6650-6658.
[38] Pacheco Otalora LF, Skinner F, Oliveira MS, Farrell B, Arshadmansab MF, Pandari T *et al.* Chronic deficit in the expression of voltage-gated potassium channel Kv3.4 subunit in the hippocampus of pilocarpine-treated epileptic rats. *Brain research* 2011; **1368**: 308-316.

[39] Ermolinsky BS, Skinner F, Garcia I, Arshadmansab MF, Otalora LF, Zarei MM *et al.* Upregulation of STREX splice variant of the large conductance Ca2+-activated potassium (BK) channel in a rat model of mesial temporal lobe epilepsy. *Neurosci Res* 2011; **69**: 73-80.
[40] Oliveira MS, Skinner F, Arshadmansab MF, Garcia I, Mello CF, Knaus HG *et al.* Altered expression and function of small-conductance (SK) Ca(2+)-activated K+ channels in pilocarpine-treated epileptic rats. *Brain research* 2010; **1348**: 187-199.
[41] Ermolinsky B, Arshadmansab MF, Pacheco Otalora LF, Zarei MM, Garrido-Sanabria ER. Deficit of Kcnma1 mRNA expression in the dentate gyrus of epileptic rats. *Neuroreport* 2008; **19**: 1291-1294.
[42] Vogl C, Mochida S, Wolff C, Whalley BJ, Stephens GJ. The SV2A Ligand Levetiracetam Inhibits Presynaptic Ca2+ Channels Via an Intracellular Pathway. *Mol Pharmacol* 2012.
[43] Lee CY, Chen CC, Liou HH. Levetiracetam inhibits glutamate transmission through presynaptic P/Q-type calcium channels on the granule cells of the dentate gyrus. *Br J Pharmacol* 2009; **158**: 1753-1762.
[44] Fukuyama K, Tanahashi S, Nakagawa M, Yamamura S, Motomura E, Shiroyama T *et al.* Levetiracetam inhibits neurotransmitter release associated with CICR. *Neurosci Lett* 2012.
[45] Faught E. Efficacy of topiramate as adjunctive therapy in refractory partial seizures: United States trial experience. *Epilepsia* 1997; **38 Suppl 1**: S24-27.
[46] Faught E, Wilder BJ, Ramsay RE, Reife RA, Kramer LD, Pledger GW *et al.* Topiramate placebo-controlled dose-ranging trial in refractory partial epilepsy using 200-, 400-, and 600-mg daily dosages. Topiramate YD Study Group. *Neurology* 1996; **46**: 1684-1690.
[47] Gibbs JW, 3rd, Sombati S, DeLorenzo RJ, Coulter DA. Cellular actions of topiramate: blockade of kainate-evoked inward currents in cultured hippocampal neurons. *Epilepsia* 2000; **41 Suppl 1**: S10-16.
[48] Kaminski RM, Banerjee M, Rogawski MA. Topiramate selectively protects against seizures induced by ATPA, a GluR5 kainate receptor agonist. *Neuropharmacology* 2004; **46**: 1097-1104.
[49] Gryder DS, Rogawski MA. Selective antagonism of GluR5 kainate-receptor-mediated synaptic currents by topiramate in rat basolateral amygdala neurons. *J Neurosci* 2003; **23**: 7069-7074.
[50] Coulter DA, Sombati S, Delorenzo RJ. Selective effects of topiramate on sustained repetitive firing and spontaneous bursting in cultured hippocampal neurons. . *Epilepsia* 1993; **34**: S123.
[51] Rogawski MA, Porter RJ. Antiepileptic drugs: pharmacological mechanisms and clinical efficacy with consideration of promising developmental stage compounds. . *Pharmacol Rev* 1990; **42**: 223-286.
[52] Zona C, Ciotti MT, Avoli M. Topiramate attenuates voltage-gated sodium currents in rat cerebellar granule cells. *Neurosci Lett* 1997; **231**: 123-126.
[53] Wu SP, Tsai JJ, Gean PW. Frequency-dependent inhibition of neuronal activity by topiramate in rat hippocampal slices. *Br J Pharmacol* 1998; **125**: 826-832.
[54] McLean MJ, Bukhari AA, Wamil AW. Effects of topiramate on sodium-dependent action-potential firing by mouse spinal cord neurons in cell culture. *Epilepsia* 2000; **41 Suppl 1**: S21-24.
[55] Sitges M, Guarneros A, Nekrassov V. Effects of carbamazepine, phenytoin, valproic acid, oxcarbazepine, lamotrigine, topiramate and vinpocetine on the presynaptic Ca2+ channel-mediated release of [3H]glutamate: comparison with the Na+ channel-mediated release. *Neuropharmacology* 2007; **53**: 854-862.
[56] Dudek FE, Bramley JR. GluR5 Kainate Receptors and Topiramate: A New Site of Action for Antiepileptic Drugs? *Epilepsy Curr* 2004; **4**: 17.
[57] Macdonald RL, Kelly KM. Antiepileptic drug mechanisms of action. *Epilepsia* 1995; **36 Suppl 2**: S2-12.
[58] Macdonald RL, Kelly KM. Antiepileptic drug mechanisms of action. *Epilepsia* 1993; **34 Suppl 5**: S1-8.
[59] McLean MJ, Macdonald RL. Carbamazepine and 10,11-epoxycarbamazepine produce use- and voltage-dependent limitation of rapidly firing action potentials of mouse central neurons in cell culture. *J Pharmacol Exp Ther* 1986; **238**: 727-738.
[60] Meehan AL, Yang X, Yuan LL, Rothman SM. Levetiracetam has an activity-dependent effect on inhibitory transmission. *Epilepsia* 2012; **53**: 469-476.
[61] Muller CJ, Groticke I, Hoffmann K, Schughart K, Loscher W. Differences in sensitivity to the convulsant pilocarpine in substrains and sublines of C57BL/6 mice. *Genes Brain Behav* 2009; **8**: 481-492.
[62] Rush AM, Kilbride J, Rowan MJ, Anwyl R. Presynaptic group III mGluR modulation of short-term plasticity in the lateral perforant path of the dentate gyrus in vitro. *Brain Res* 2002; **952**: 38-43.
[63] Kilbride J, Rush AM, Rowan MJ, Anwyl R. Presynaptic group II mGluR inhibition of short-term depression in the medial perforant path of the dentate gyrus in vitro. *J Neurophysiol* 2001; **85**: 2509-2515.

[64] Lynch BA, Lambeng N, Nocka K, Kensel-Hammes P, Bajjalieh SM, Matagne A *et al.* The synaptic vesicle protein SV2A is the binding site for the antiepileptic drug levetiracetam. *Proc Natl Acad Sci U S A* 2004; **101**: 9861-9866.
[65] Custer KL, Austin NS, Sullivan JM, Bajjalieh SM. Synaptic vesicle protein 2 enhances release probability at quiescent synapses. *J Neurosci* 2006; **26**: 1303-1313.
[66] Crowder KM, Gunther JM, Jones TA, Hale BD, Zhang HZ, Peterson MR *et al.* Abnormal neurotransmission in mice lacking synaptic vesicle protein 2A (SV2A). *Proc Natl Acad Sci U S A* 1999; **96**: 15268-15273.
[67] Toering ST, Boer K, de Groot M, Troost D, Heimans JJ, Spliet WG *et al.* Expression patterns of synaptic vesicle protein 2A in focal cortical dysplasia and TSC-cortical tubers. *Epilepsia* 2009; **50**: 1409-1418.
[68] Crevecoeur J, Kaminski RM, Rogister B, Foerch P, Vandenplas C, Neveux M *et al.* Expression pattern of synaptic vesicle protein 2 (SV2) isoforms in patients with temporal lobe epilepsy and hippocampal sclerosis. *Neuropathol Appl Neurobiol* 2013.
[69] Bandala C, Miliar-Garcia A, Mejia-Barradas CM, Anaya-Ruiz M, Luna-Arias JP, Bazan-Mendez CI *et al.* Synaptic vesicle protein 2 (SV2) isoforms. *Asian Pac J Cancer Prev* 2012; **13**: 5063-5067.
[70] Schivell AE, Mochida S, Kensel-Hammes P, Custer KL, Bajjalieh SM. SV2A and SV2C contain a unique synaptotagmin-binding site. *Mol Cell Neurosci* 2005; **29**: 56-64.
[71] Janz R, Sudhof TC. SV2C is a synaptic vesicle protein with an unusually restricted localization: anatomy of a synaptic vesicle protein family. *Neuroscience* 1999; **94**: 1279-1290.
[72] Vogl C, Mochida S, Wolff C, Whalley BJ, Stephens GJ. The synaptic vesicle glycoprotein 2A ligand levetiracetam inhibits presynaptic Ca2+ channels through an intracellular pathway. *Mol Pharmacol* 2012; **82**: 199-208.
[73] Ozcan M, Ayar A. Modulation of action potential and calcium signaling by levetiracetam in rat sensory neurons. *J Recept Signal Transduct Res* 2012; **32**: 156-162.
[74] Marek GJ. Metabotropic glutamate 2/3 receptors as drug targets. *Curr Opin Pharmacol* 2004; **4**: 18-22.
[75] Flor PJ, Battaglia G, Nicoletti F, Gasparini F, Bruno V. Neuroprotective activity of metabotropic glutamate receptor ligands. *Adv Exp Med Biol* 2002; **513**: 197-223.
[76] Tang FR, Lee WL. Expression of the group II and III metabotropic glutamate receptors in the hippocampus of patients with mesial temporal lobe epilepsy. *J Neurocytol* 2001; **30**: 137-143.
[77] Crevecoeur J, Kaminski RM, Rogister B, Foerch P, Vandenplas C, Neveux M *et al.* Expression pattern of synaptic vesicle protein 2 (SV2) isoforms in patients with temporal lobe epilepsy and hippocampal sclerosis. *Neuropathol Appl Neurobiol* 2014; **40**: 191-204.
[78] van Vliet EA, Aronica E, Redeker S, Boer K, Gorter JA. Decreased expression of synaptic vesicle protein 2A, the binding site for levetiracetam, during epileptogenesis and chronic epilepsy. *Epilepsia* 2009; **50**: 422-433.
[79] Shetty AK. Prospects of Levetiracetam as a Neuroprotective Drug Against Status Epilepticus, Traumatic Brain Injury, and Stroke. *Front Neurol* 2013; **4**: 172.
[80] Kaminski RM, Gillard M, Klitgaard H. Targeting SV2A for Discovery of Antiepileptic Drugs. 2012.
[81] Abou-Khalil B. Levetiracetam in the treatment of epilepsy. *Neuropsychiatr Dis Treat* 2008; **4**: 507-523.
[82] Garrido-Sanabria ER, Perez-Cordova MG, Colom LV. Differential expression of voltage-gated K+ currents in medial septum/diagonal band complex neurons exhibiting distinct firing phenotypes. *Neurosci Res* 2011; **70**: 361-369.
[83] Pfaffl MW, Horgan GW, Dempfle L. Relative expression software tool (REST) for group-wise comparison and statistical analysis of relative expression results in real-time PCR. *Nucleic Acids Res* 2002; **30**: e36.
[84] Pfaffl MW. A new mathematical model for relative quantification in real-time RT-PCR. *Nucleic Acids Res* 2001; **29**: e45.
[85] Liu JX, Cao X, Liu Y, Tang FR. CCL28 in the mouse hippocampal CA1 area and the dentate gyrus during and after pilocarpine-induced status epilepticus. *Neurochem Int* 2012; **61**: 1094-1101.
[86] Frycia A, Starck JP, Jadot S, Lallemand B, Leclercq K, Lo Brutto P *et al.* Discovery of indolone acetamides as novel SV2A ligands with improved potency toward seizure suppression. *ChemMedChem* 2010; **5**: 200-205.
[87] Gillard M, Chatelain P, Fuks B. Binding characteristics of levetiracetam to synaptic vesicle protein 2A (SV2A) in human brain and in CHO cells expressing the human recombinant protein. *Eur J Pharmacol* 2006; **536**: 102-108.

[88] Bajjalieh SM, Frantz GD, Weimann JM, McConnell SK, Scheller RH. Differential expression of synaptic vesicle protein 2 (SV2) isoforms. *J Neurosci* 1994; **14**: 5223-5235.
[89] Bajjalieh SM, Peterson K, Shinghal R, Scheller RH. SV2, a brain synaptic vesicle protein homologous to bacterial transporters. *Science* 1992; **257**: 1271-1273.
[90] Krishna K, Raut AL, Gohel KH, Dave P. Levetiracetam. *J Assoc Physicians India* 2011; **59**: 656-658.
[91] Klitgaard H, Verdru P. Levetiracetam: the first SV2A ligand for the treatment of epilepsy. *Expert Opin Drug Discov* 2007; **2**: 1537-1545.
[92] Rogawski MA. Molecular targets versus models for new antiepileptic drug discovery. *Epilepsy Res* 2006; **68**: 22-28.
[93] Pitkanen A. SV2A: more than just a new target for AEDs. *Epilepsy Curr* 2005; **5**: 14-16.
[94] Janz R, Goda Y, Geppert M, Missler M, Sudhof TC. SV2A and SV2B function as redundant Ca2+ regulators in neurotransmitter release. *Neuron* 1999; **24**: 1003-1016.

8. Appendices

Appendix #1

Brain Advance Access published February 16, 2012

BRAIN
A JOURNAL OF NEUROLOGY

Altered neurotransmitter release, vesicle recycling and presynaptic structure in the pilocarpine model of temporal lobe epilepsy

Chirag Upreti,[1] Rafael Otero,[2] Carlos Partida,[2] Frank Skinner,[2] Ravi Thakker,[2] Luis F. Pacheco,[2] Zhen-yu Zhou,[1] Giorgi Maglakelidze,[1] Jana Velíšková,[1,3] Libor Velíšek,[1,4] Dwight Romanovicz,[5] Theresa Jones,[6] Patric K. Stanton[1,7] and Emilio R. Garrido-Sanabria[2]

1 Department of Cell Biology and Anatomy, New York Medical College, Valhalla, NY 10595, USA
2 Department of Biomedicine, University of Texas Brownsville, Brownsville, TX 78520, USA
3 Department of Obstetrics and Gynaecology, New York Medical College, Valhalla, NY 10595, USA
4 Department of Paediatrics, New York Medical College, Valhalla, NY 10595, USA
5 Institute for Cellular and Molecular Biology, University of Texas Austin, Austin, TX 78712, USA
6 Department of Psychology, Institute for Neuroscience, University of Texas Austin, Austin, TX 78712, USA
7 Department of Neurology, New York Medical College, Valhalla, NY 10595, USA

Correspondence to: Emilio R. Garrido-Sanabria, MD, PhD,
Epilepsy Research Laboratory,
Department of Biomedicine,
University of Texas Brownsville,
80 Fort Brown, BRHP 2117,
Brownsville,
TX 78520, USA
E-mail: emilio.garrido@utb.edu

In searching for persistent seizure-induced alterations in brain function that might be causally related to epilepsy, presynaptic transmitter release has relatively been neglected. To measure directly the long-term effects of pilocarpine-induced status epilepticus on vesicular release and recycling in hippocampal mossy fibre presynaptic boutons, we used (i) two-photon imaging of FM1-43 vesicular release in rat hippocampal slices; and (ii) transgenic mice expressing the genetically encoded pH-sensitive fluorescent reporter synaptopHluorin preferentially at glutamatergic synapses. In this study we found that, 1–2 months after pilocarpine-induced status epilepticus, there were significant increases in mossy fibre bouton size, faster rates of action potential-driven vesicular release and endocytosis. We also analysed the ultrastructure of rat mossy fibre boutons using transmission electron microscopy. Pilocarpine-induced status epilepticus led to a significant increase in the number of release sites, active zone length, postsynaptic density area and number of vesicles in the readily releasable and recycling pools, all correlated with increased release probability. Our data show that presynaptic release machinery is persistently altered in structure and function by status epilepticus, which could contribute to the development of the chronic epileptic state and may represent a potential new target for antiepileptic therapies.

Keywords: epilepsy; neurotransmitter release; hippocampus; synaptic vesicle recycling; mossy fibre terminals

Abbreviations: MFB = mossy fibre bouton; RRP = readily releasable pool; SpH = SynaptopHluorin

Received August 10, 2011. Revised October 4, 2011. Accepted November 8, 2011.

Introduction

Hippocampal mossy fibres exhibit complex structural rearrangements and abnormal synaptic function in mesial temporal lobe epilepsy (McNamara, 1994; Frotscher *et al.*, 2006; Dudek and Sutula, 2007; Danzer *et al.*, 2010). During epileptogenesis, axons of dentate gyrus granule cells sprout and establish abnormal excitatory synapses onto multiple targets, including granule cells, interneurons and CA3 pyramidal neurons (McNamara, 1994; Wenzel *et al.*, 2000; Frotscher *et al.*, 2006; Dudek and Sutula, 2007). While studies have shown alterations in postsynaptic function of excitatory and inhibitory circuits in mesial temporal lobe epilepsy (Coulter, 2000; Gorter *et al.*, 2002), far less attention has been paid to presynaptic dysfunction in the pathogenesis of epilepsy.

Large mossy fibre boutons (MFBs) have multiple release sites with substantial numbers of small and large clear synaptic vesicles containing glutamate (Chicurel and Harris, 1992; Rollenhagen *et al.*, 2007). Large synaptic vesicles are thought to mediate the monoquantal nature of 'giant' miniature excitatory postsynaptic currents onto CA3 pyramidal cells, allowing action potential invasion of presynaptic MFBs to trigger neurotransmitter release in amounts that reliably excite CA3 pyramidal neurons. During status epilepticus, excessive glutamate release from MFBs can be highly deleterious to survival of CA3 neurons and is thought to be responsible for the massive and sustained neuronal damage in the CA3 region (Zhang *et al.*, 2009).

Surprisingly little is known about the long-term effects of status epilepticus on vesicular release of transmitter from MFBs. Goussakov *et al.* (2000) found that, several weeks after kainic acid-induced status epilepticus, mossy fibre, but not associational-commissural, synapses exhibit impaired induction of long-term potentiation, markedly reduced paired-pulse facilitation and augmentation of burst induced mossy fibre-CA3 excitatory field potential (Goussakov *et al.*, 2000). These changes in activity-dependent plasticity were also associated with a significant increase in the size of the readily releasable pool (RRP) of vesicles, suggesting a persistent increase in release probability at mossy fibre–CA3 synapses (Goussakov *et al.*, 2000). Ultrastructural features and targets of abnormally sprouted MFBs in the inner molecular layer have been studied by electron microscopy in models of mesial temporal lobe epilepsy (Cavazos *et al.*, 2003; Frotscher *et al.*, 2006); indeed, redistribution of synaptic vesicles to a 'strategic position' in the vicinity of the synaptic cleft has been described after kindled seizures (Hovorka *et al.*, 1989), but these studies did not characterize the arrangement of active zones and morphological features of vesicle pools.

We used the cholinergic agonist pilocarpine to induce prolonged status epilepticus as a model of mesial temporal lobe epilepsy (Turski *et al.*, 1984; Curia *et al.*, 2008), to test the hypothesis that status epilepticus can result in long-term enhancement of vesicular release from MFBs. Assessing presynaptic release properties by patch-clamp electrophysiology in long-term epileptic animals is hampered by the CA3 pyramidal neurons being susceptible to cell death due to excitotoxicity, thus are not optimal to record from as biosensors of transmitter release. Here we utilized two different methods to directly image presynaptic vesicular release by using two-photon laser scanning microscopy of (i) the styryl dye FM1-43 (Pyle *et al.*, 1999), which selectively labels transmitter vesicles for direct visualization of destaining kinetics, in slices from control versus post-status epilepticus rats; and (ii) imaging exocytosis–endocytosis kinetics from individual MFBs in acute hippocampal slices from transgenic mice that selectively express the pH-sensitive vesicle fusion protein synaptopHluorin (SpH) (Li *et al.*, 2005). We also used transmission electron microscopy of rat hippocampus to investigate whether the post-status epilepticus period is associated with ultrastructural modifications at active zones of MFBs in the stratum lucidum correlated with functional changes in vesicular release (Dobrunz and Stevens, 1997; Murthy *et al.*, 1997; Schikorski and Stevens, 1997; Matz *et al.*, 2010).

By each of these measures, we found a persistent enhancement of vesicular release, vesicle endocytosis and ultrastructure reorganization of active zones in MFBs after status epilepticus. These changes are likely to add to observed changes in intrinsic excitability of granule cells and circuit plasticity to increase the excitatory drive from granule cells onto CA3 pyramidal neurons in MTLE.

Materials and methods

Experiments were performed in accordance with the National Institutes of Health Guidelines for the Care and Use of Laboratory Animals as approved by New York Medical College and University of Texas Brownsville Institutional Animal Care and Use Committees.

Pilocarpine-induced status epilepticus

Status epilepticus was induced by a single pilocarpine intraperitoneal injection (350 mg/kg in saline) to 30- to 35-day-old Sprague–Dawley rats (Taconic) or SpH21 mice (C57BL/6J background, kind gift from Dr Venkatesh Murthy, Harvard University) following standard procedures (Cavalheiro, 1995; Pacheco *et al.*, 2008). Animals received methylscopolamine nitrate (0.1 mg/kg in saline, subcutaneous) 30 min before pilocarpine to minimize peripheral effects of cholinergic stimulation (Turski *et al.*, 1984). Rats seized for 3 h, mice 1 h (Muller *et al.*, 2009), and motor seizures were terminated with one diazepam injection (10 mg/kg in saline, intraperitoneal). Only animals experiencing continuous status epilepticus during these periods were studied. Controls animals received methylscopolamine and saline instead of pilocarpine.

Hippocampal slice preparation and electrophysiological recordings

Rats and mice 1–2 months post-status epilepticus and age-matched controls were decapitated under deep isoflurane anaesthesia, their brains quickly removed, hemisected in ice-cold sucrose-based cutting solution (Bischofberger *et al.*, 2006) in mM: 87 NaCl, 25 $NaHCO_3$, 25 glucose, 75 sucrose, 2.5 KCl, 1.25 NaH_2PO_4, 0.5 $CaCl_2$ and 7 $MgCl_2$ (equilibrated with 95% O_2/5% CO_2), and 350–400 μm thick horizontal hippocampal slices cut with a vibratome (DSK model

DTK-1000). Slices were submerged in cutting solution at 32°C for 30 min, then transferred to a holding chamber in room temperature artificial CSF (in mM: 126 NaCl, 3 KCl, 1.25 NaH_2PO_4, 1.3 MgCl, 2.5 $CaCl_2$, 26 $NaHCO_3$, 10 glucose) saturated with 95% O_2/5% CO_2. Evoked field excitatory postsynaptic potentials were recorded in the proximal dendritic field in stratum lucidum for at least 15 min before starting an experiment.

Two-photon laser scanning microscopy

Fluorescence was visualized with a customized two-photon laser-scanning Olympus BX61WI microscope with a ×60/0.90 NA water immersion infrared objective lens and an Olympus multispectral confocal laser scan unit. The light source was a Mai-Tai^{TM} laser (Solid-State Laser Co.), tuned to 825 nm for exciting Alexa Fluor 594, and 890 nm for exciting SpH and FM1-43. Epifluorescence was detected with photomultiplier tubes of the confocal laser scan head with pinhole maximally open and emission spectral window optimized for signal over background. A 565-nm dichroic mirror (Chroma Technology) separated green and red fluorescence to eliminate transmitted or reflected excitation light. Depending on the fluorophore, HQ525/50 (SpH) or HQ605/50 (FM1-43 or Alexa Fluor 594) filters were placed in the 'green' pathways. Images were acquired with Fluoview FV300 software (Olympus America). Although there were no signs of photodamage, we used the lowest intensity needed for adequate signal-to-noise ratios. Pixel images (512 × 512) were acquired, 0.15 μm/pixel in $x-y$ axes and, in some cases, 8–10 μm steps of 0.5–1 μm in the z-axis. For imaging MFBs, glass microelectrodes with broken tips ($R < 1$ MΩ) were dipped in 1% Alexa Fluor 594 10-kDa dextran (Invitrogen) in distilled water until the tip filled by capillarity action, desiccated for 2–3 days until dye formed a crystal particle at the tip. During the experiment, dye coated tips (with sealed backends) were inserted ~50–100 μm into the dentate gyrus granule cell layer for 15–20 min, then slices were transferred to a holding chamber in artificial CSF at 32°C for 30 min, followed by room temperature for 1–1.5 h, before imaging. Using NIH ImageJ, greyscale images of Alexa Fluor 594 filled MFBs flanked by at least one axonal process were processed by automated Otsu thresholding to eliminate investigator bias (Lee *et al.*, 2011), and cross-sectional area of binary images measured. A total of 8–10 images were acquired in a z-axis stack in 0.2–0.5 μm steps for 3D reconstruction (Supplementary Video 3). For SpH fluorescence experiments, slices were perfused with 25 μM 6-cyano-7-nitroquinoxaline-2,3-dione (CNQX; Tocris) and 50 μM D-(-)-2-Amino-5-phosphonopentanoic acid (D-AP5; Tocris). A 600 stimulus 20-Hz train in the stratum lucidum evoked SpH fluorescence increases (imaged within 100 μm from stimulating electrode) in the proximal region (the first 100 μm) of CA3 apical dendrites and images were acquired every 30 s. While extracellular brain pH changes during seizures, first to alkaline and later to acidic (Xiong and Stringer, 2000), we use SpH as a pH-sensitive indicator of vesicular release in brain slices bathed in artificial CSF (containing 25 μM CNQX and 50 μM D-AP5 to prevent synaptically driven action potentials and epileptiform activity) in our recording chamber with pH maintained at or ~7.4. To calculate half-time of post-stimulus decay of SpH peak fluorescence intensity, ($t_{1/2}$) was calculated for each punctum by single exponential fits to destaining curves using the equation: $y_0 + A_1e^{(-x/t_1)}$, with t_1 the decay constant. Data were analysed with OriginPro and presented with KaleidaGraph (Synergy software).

FM1-43 loading and destaining of the readily releasable vesicle pool

FM1-43 was loaded into the RRP as previously described (Stanton *et al.*, 2003, 2005). After recording a 15 min stable baseline field excitatory postsynaptic potential (~50% of maximum amplitude), 25 μM CNQX and 50 μM D-AP5 were bath applied to prevent synaptically driven action potentials and epileptiform activity from accelerating dye release or inducing synaptic plasticity. Presynaptic boutons were loaded by 5-min bath applied 5 μM FM1-43 in normal artificial CSF, followed by hypertonic artificial CSF (800 mOsm) for 30 s to load the RRP, returned to normal artificial CSF with 5 μm FM1-43 for 1 min, then washed out with dye-free artificial CSF (Supplementary Fig. 2). Stimulus-induced destaining was evoked by a 50 stimulus 20-Hz train each 30 s, and measured after 30 min in dye-free artificial CSF plus 100 μM ADVASEP-7 to scavenge and remove extracellular FM1-43. To measure spontaneous release, after FM1-43 loading, slices were continuously bathed in 1 μM tetrodotoxin, 25 μm CNQX and 50 μM D-AP5 and extracellular [K^+] raised to 15 mM [K^+]o (*High[K+]o)* to facilitate action potential-independent release (Axmacher *et al.*, 2004). For some slices, 8–10 images were acquired in 0.5–1 μm in the z-axis at each time point, maximal intensity z-axis projections were made for this subset of the final stack. Circular regions of interest were selected around centres of bright, punctate fluorescence spots at least 2 μm in diameter within 100 μm of the CA3 pyramidal cell body layer. Activity-dependent destaining time courses were generated by correcting for bleaching, subtracting background fluorescence and normalizing each region of interest to pre-stimulus intensity as previously reported (Stanton *et al.*, 2003, 2005; Tyler *et al.*, 2006). Vertical bars show SEMs for all normalized and corrected boutons.

Tissue preparation for immunohistochemistry

Age-matched control and epileptic SpH mice (<6 months post-status epilepticus) were anaesthetized with 100 mg/kg ketamine, the brain removed and immersed for 48 h in 4% formaldehyde in 0.1 M sodium phosphate buffer (pH 7.4) plus 0.9% NaCl (phosphate-buffered saline). After a phosphate-buffered saline wash, brains were cryoprotected in 30% sucrose in phosphate-buffered saline for ~48 h at 4°C, frozen in Optimum Cutting Temperature Compound (EMS Co.) at −20°C, and 40 μm thick coronal sections sliced with a cryostat (HM500 Microm, Zeiss) and stored in 150 mM Tris plus 150 mM NaCl (Tris-buffered saline; pH 7.4) and 0.1% NaN_3. Several sections were Nissl-stained to assess seizure-mediated neuronal loss and cyto-architectonic boundaries. Free-floating sections from controls and post-status epilepticus were processed simultaneously for VGluT1 and NeuN immunofluorescence as described (Pacheco *et al.*, 2008). The extent of cell loss in the CA3 subfield was assessed at ×400 magnification by using grid morphometric techniques (Gorter *et al.*, 2003). A 240 × 240 μm box was placed over the region of interest (CA3 area) and NeuN-labelled cells in the pyramidal layer, presumed neurons, were counted by an observer masked to experimental group/condition. Counts of three sections per animal were averaged. Final neuron counts were calculated as the density of neurons per 0.1 mm^2. It should be noted that this technique provides a relative estimate and not absolute calculation of the number of neurons in a region. Statistical differences in the number of neurons per square millimetre between control and pilocarpine-treated epileptic groups were

determined by Student's *t*-test with significance set at $P < 0.05$. The cross-sectional diameter of SpH-positive VGluT1-labelled puncta in the granule cell layer and supragranular region was measured in three confocal images of dentate gyrus per animal per group using the measuring tool of Fluoview (Olympus).

Fixation and embedding for transmission electron microscopy

Tissue was prepared for transmission electron microscopy using standard methods (Miranda *et al.*, 2011). Seven post-status epilepticus and six age-matched Sprague–Dawley rats were anaesthetized with ketamine (50 mg/kg, intraperitoneal injection), transcardially perfused with saline followed by fixative (2% paraformaldehyde, 2% glutaraldehyde, 0.002% $CaCl_2$ in 0.1 M cacodylate and Hank's buffered salt solution; pH 7.3–7.4), and their brains were removed, sliced in 5-mm thick slabs, and post-fixed in fresh fixative overnight at room temperature. Serial 250-μm thick sections were cut with a vibratome in Hank's buffered salt solution (1000 Plus, Vibratome Co.), and the hippocampus and surrounding cortex dissected away. Samples were osmicated in 2% buffered osmium tetroxide, a 50:50 mixture of 4% osmium tetroxide and 4% potassium ferrocyanide in 0.2 M cacodylate buffer (EMS Co.), then contrasted in 1% aqueous uranyl acetate. Tissue was flat-embedded in 50:50 Spurr/Epon (EMS Co.) and polymerized at 60°C for 24 h before resin blocks were pseudo-randomly selected and trimmed to ~1 mm^3 trapezoids containing the CA3 pyramidal cell layer and stratum lucidum. To identify field CA3, 1–2 μm sections were stained with 0.1% cresyl violet acetate solution and viewed on a transmitted light scope. Ultrathin sections (55 ± 5 nm) were cut through stratum lucidum of CA3 with a Leica Ultracut ultramicrotome and collected on Formvar-coated copper slotted grids.

Transmission electron microscopy inspection and identification of mossy fibre boutons

Images 26 000× (FEI Tecnai) were used to identify regions of interest in field CA3 containing cross-sectioned or parallel bundles of axons and large MFBs (1–5 μm diameter) with numerous synaptic vesicles. For blind analysis of morphometry, coded images were imported into NIH ImageJ. Active zones were distinguished by the following criteria: (i) synaptic vesicles in close proximity to a presynaptic density; (ii) asymmetry between pre- and postsynaptic densities; and (iii) widening of the synaptic cleft (Rollenhagen *et al.*, 2007). Asymmetric (excitatory) non-perforated synapses with well-defined presynaptic compartments, clear synaptic clefts and postsynaptic density were analysed. Perforated synapses refer to a presumably more efficacious synapse subtype found in the CNS characterized by a discontinuous postsynaptic density (Calverley and Jones, 1987; Itarat and Jones, 1992; Adkins *et al.*, 2008). The number of perforated and non-perforated synapses was compared between groups

Active zone length was measured by a continuous line following the contour of presynaptic membrane on the synaptic cleft. Synaptic cleft width was averaged from three measures of distance between pre- and postsynaptic membranes (centre and ~20 nm from cleft ends). Postsynaptic density area was measured as the contour around electron-dense aggregates and postsynaptic membrane. The active zone length and quantification of synaptic vesicles was performed in single ultrathin sections using a modified 2D cross-sectional method as described previously (Miranda *et al.*, 2011) using NIH ImageJ.

The RRP was defined as the number of synaptic vesicles <60 nm from the presynaptic membrane, and the releasable pool of vesicles 60–200 nm from the presynaptic membrane (Rollenhagen *et al.*, 2007). Docked synaptic vesicles consisted of vesicles immediately adjacent to or fused to the active zone presynaptic membrane. Perimeter and mean area of synaptic vesicles were also measured, and number of active zones exhibiting ultrastructural signs of bulk endocytosis indicative of intense synaptic activity (Meunier *et al.*, 2010).

Differences in vesicle pool size were assessed by non-parametric Kolmogorov–Smirnov two-sample test (MiniAnalysis, Synaptosoft), and differences in means of normally distributed measurements were evaluated using two-tailed Student's *t*-test. Significance level was preset to $P < 0.05$. Correlation analysis between parameters was performed with non-parametric Spearman analysis, since most parameters were not normally distributed. Correlations were classified as weak [Spearman rho (r) value < 0.40], moderate ($0.4 < r < 0.7$) and strong ($r > 0.7$).

Results

Two-photon laser scanning microscopy imaging of large mossy fibre boutons of synaptopHluorin-expressing transgenic mice in acute hippocampal slices

SpH is a fusion protein that consists of a pH-sensitive pHluorin fused to the C-terminus luminal domain of the vesicle SNARE protein synaptobrevin (Miesenbock *et al.*, 1998). Under resting conditions, the luminal pH of the synaptic vesicle is acidic (pH ~5.5), resulting in proton dependent quenching of SpH fluorescence. When vesicle exocytosis is triggered and glutamate released, the lumen of the vesicle is exposed to the more alkaline pH of the extracellular space (pH ~7.2), resulting in a 20-fold increase in SpH fluorescence. When the vesicle membrane is retrieved by endocytosis and the vesicle reformed, it undergoes rapid reacidification by the vesicular ATPase, which returns SpH to its quenched state. The SpH21 transgenic mice line we used in this study expresses SpH preferentially at glutamatergic synapses (Li *et al.*, 2005; Burrone *et al.*, 2006; Bayazitov *et al.*, 2007). A representative two-photon laser scanning image of the CA3 region of an acute hippocampal slice from this mouse (Fig. 1A) contains bright GFP-positive boutons >2 μm in diameter, proximal to CA3 pyramidal cell bodies in the region innervated by mossy fibre axons of dentate granule cells (Blackstad *et al.*, 1970; Claiborne *et al.*, 1986). Associational-commissural CA3 synapses were significantly smaller (<1 μm in diameter) and more distal to our region of interest (rectangular box, Fig. 1A).

To independently confirm that large SpH expressing boutons were mossy fibre terminals, we used anterograde, bulk labelling of mossy fibres with Alexa Fluor 594 dextran introduced into the granule cell layer of the dentate gyrus (Fig. 1B). During a 1.5- to 2-h incubation, Alexa Fluor 594 dextran was taken up by granule cells and transported anterogradely to label mossy fibre axons and presynaptic boutons (Fig. 1C, Supplementary Fig. 1A and Supplementary Video 3). Figure 1E and F illustrate that some

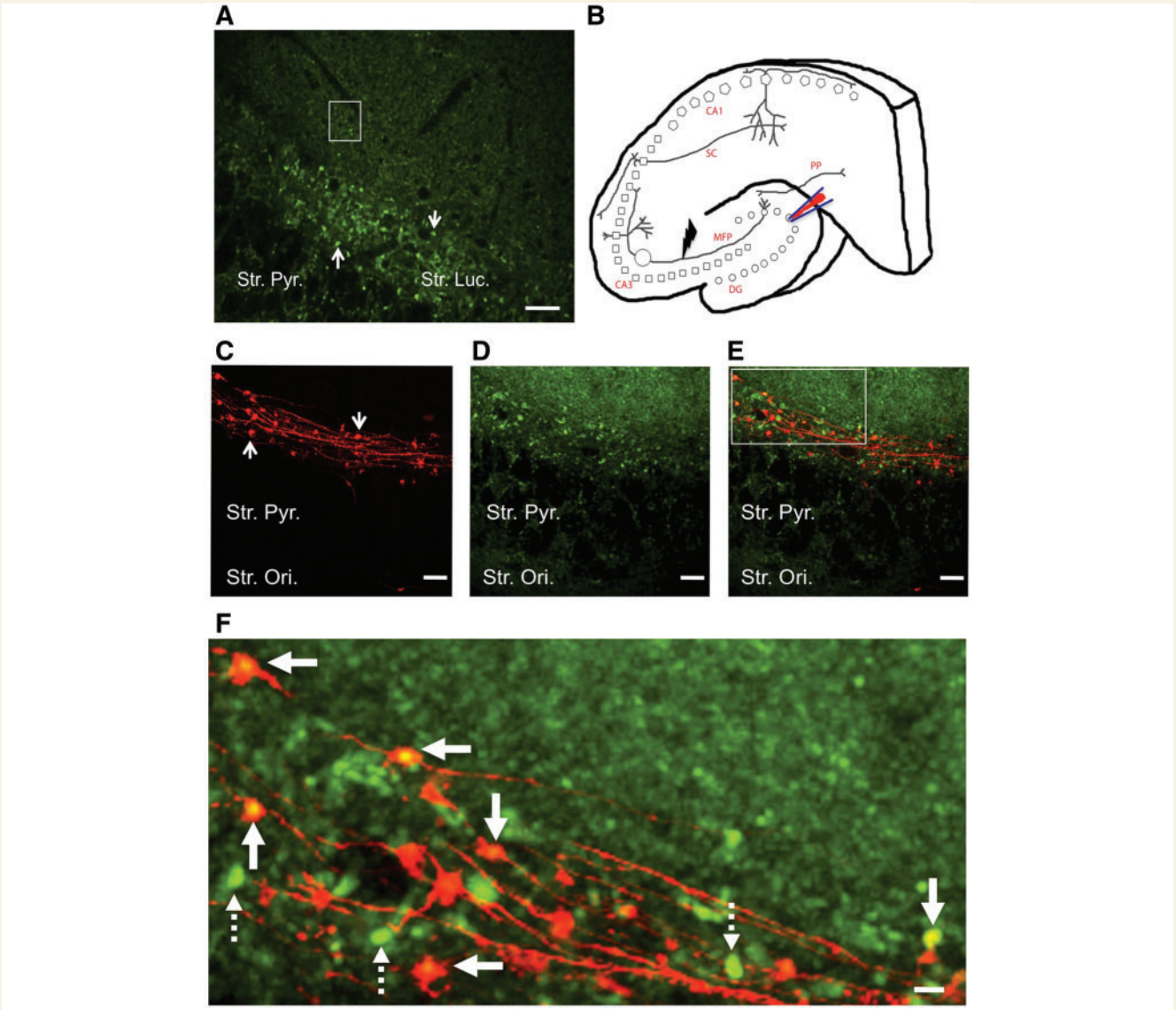

Figure 1 Visualizing MFBs in acute hippocampal slices from SpH21 transgenic mice. (**A**) Live cell two-photon laser scanning image of field CA3 of SpH-expressing glutamatergic terminals in a control hippocampal slice (post natal 60 days of age). The arrows depict representative fluorescence puncta (~4–5 μm in diameter) in the proximal (stratum lucidum, Str. Luc.) region of CA3 pyramidal cells (seen here as a ghost layer) that are likely to be giant MFBs. Distal puncta shown within the rectangular box are notably smaller in size and likely represent associational-commissural synapses in stratum radiatum. (**B**) Schematic representing hippocampal circuitry with the circle in the mossy fibre pathway (MFP) depicting the area of imaging Lightning symbol depicts the area of local stimulation and the pipette in the dentate granule cell layer (DG) showing the area of Alexa Fluor 594 dextra containing pipette insertion. Squares and pentagons depict CA3 and CA1 pyramidal cell layers, respectively. (**C**) Alexa Fluor 594 dextran filled mossy fibre axons and giant MFBs (arrows) showing characteristic *en-passant* arrangement along the axonal projections, visualized using 825 nm excitation. (**D**) Same region as (**C**) but visualized with 890-nm excitation to see SpH native fluorescence. CA3 pyramidal cell bodies can be seen as ghost cells in stratum pyramidal, and bright giant MFBs in stratum lucidum. (**E–F**) Merged images of (**C**) and (**D**) showing co-localization (**F**: arrows) between SpH and Alexa Fluor 594 dextran-labelled puncta. (**F**) Digital zoom of image from the inset box in (**E**). Note not all SpH-positive puncta co-localize with Alexa Fluor 594 puncta (broken arrows). PP = perforant path; SC = Schaffer collaterals; Str. Ori. = stratum oriens; Str. Pyr. = stratum pyramidale. Scale bars: **A** = 20 μm; **C–E** = 20 μm; and **F** = 4 μm.

(solid arrows) but not all (broken arrows) SpH and Alexa Fluor 594-positive boutons were co-labelled confirming that the large (>2 μm in diameter) SpH fluorescent puncta within the proximal 60 μm of the CA3 cell body are excitatory MFBs (Fig. 1D). Incomplete co-localization is likely because Alexa Fluor 594 labelled a subset of mossy fibre axons in stratum lucidum, along with sparse SpH expression in the excitatory terminals (Li *et al.*, 2005; Burrone *et al.*, 2006).

Pilocarpine-induced status epilepticus causes disorganization of dentate gyrus and CA3 cytoarchitecture in synaptopHluorin-expressing transgenic mice

In the hippocampal CA3 region of both control and post-status epilepticus mice (Fig. 2A), immunostaining for the presynaptic glutamate transporter VGluT1 was intense in the mossy fibre projection area in stratum lucidum, where it co-localized with native SpH fluorescence, consistent with the glutamatergic nature of presynaptic terminals expressing SpH in SpH21 mice (Li *et al.*, 2005; Burrone *et al.*, 2006). There was also ~51% reduction in CA3 stratum pyramidale of post-status epilepticus mice in the density of neurons (117.9 ± 35.4 cells/0.1 mm^2, $n = 6$, Student's *t*-test, $P < 0.01$, Fig. 2A), consistent with seizure-induced loss of CA3 pyramidal neurons following pilocarpine-induced status epilepticus reported previously (Mello *et al.*, 1993; Schauwecker, 2012).

In the dentate gyrus, we detected robust SpH fluorescence in the inner molecular layer and hilus of both control and post-status epilepticus mice (Fig. 2B), closely co-localized with VGluT1 immunofluorescence (Fig. 2B). VGluT1 puncta positive for SpH fluorescence in the inner molecular layer exhibited 39.5% larger cross-sectional diameters (Fig. 2B, 1.84 ± 0.54 µm, Student's *t*-test, $P < 0.001$) and 47.5% higher normalized mean fluorescence intensity (Fig. 2B, post-status epilepticus: VGluT1) relative to background-subtracted baseline intensity [204.8 ± 35.5 arbitrary units (a.u), $n = 29$, Student's *t*-test, $P < 0.0001$] in pilocarpine-treated post-status epilepticus mice compared with controls (Fig. 2B, control: VGluT1 138.8 ± 32.2 a.u and mean diameter of puncta: 1.31 ± 0.37 µm, $n = 29$). Interestingly, SpH puncta in granule cell somata in the control dentate gyri exhibited little immunostaining for VGluT1, whereas the granule cell layers of post-status epilepticus hippocampi showed strong co-immunolabelling for VGluT1 (Fig. 2B), suggesting either a possible upregulation of VGluT1 expression in existing terminals or neo-synaptogenesis manifested by the appearance of ectopic glutamatergic (VGluT1 positive) terminals in both inner molecular and granule cell layers during epileptogenesis, as previously reported in animal models of MTLE (Mello *et al.*, 1993; Esclapez *et al.*, 1999; Epsztein *et al.*, 2005; Pacheco *et al.*, 2006; Boulland *et al.*, 2007).

Pilocarpine-induced status epilepticus persistently increases size and vesicular release rate of mossy fibre boutons in synaptopHluorin-expressing mice

Live cell imaging of MFBs in acute hippocampal slices was done by bulk loading a group of granule cells and their axons with Alexa Fluor 594-dextran. Dye-filled excrescences (Fig. 1B) were classified as the main body of giant MFBs if they had at least a 4 µm^2 cross-sectional area (Claiborne *et al.*, 1986; Acsady *et al.*, 1998; Danzer *et al.*, 2010). The mean area of MFBs 1–2 months after pilocarpine induced-status epilepticus was significantly enhanced (~21.09%, Fig. 3C, $P = 0.008$, Mann–Whitney U-test, $n = 7$) compared with aged matched controls ($n = 7$). A frequency distribution histogram of individual MFBs from epileptic animals revealed a significant rightward shift in the curves (Fig. 3B; $P < 0.05$, Kolmogorov–Smirnov test), consistent with increased MFB volumes.

To determine whether post-status epilepticus leads to functional differences in transmitter release from excitatory MFBs, we utilized two-photon live cell imaging in slices from SpH21 mice. To trigger vesicular release from MFBs in CA3 stratum lucidum (Fig. 1B–F), granule cell axons in slices from control and post-status epilepticus animals were stimulated with a single, continuous train of 600 stimuli at 20 Hz (Fig. 1B and Supplementary Video 4A and B, respectively), a paradigm that recruits both the RRP and rapidly recycling vesicle pools (Li *et al.*, 2005). Representative time-lapse images (Fig. 4A) of control and post-status epilepticus SpH-expressing MFBs showed robust, cumulative increases in SpH fluorescence intensity during the stimulus train, followed by return of fluorescence to baseline levels ~40 s after stimulus termination. Figure 4C plots the normalized mean SpH fluorescence responses in control versus post-status epilepticus animals, which showed significantly larger stimulus-evoked rises in SpH fluorescence (2.02 ± 0.15, red circles, $n = 8$, $P < 0.05$, Student's *t*-test) compared with controls (1.47 ± 0.03, black circles, $n = 10$).

This result could be due to either a general increase in release probability of existing MFBs or appearance of a distinct sub-population of terminals with higher release probabilities. To resolve this distinction, we plotted a distribution histogram (Fig. 4D) of the normalized peak SpH fluorescence values, which is a function of the total number of vesicles released during the stimulus train. Control and post-status epilepticus distributions of peak SpH fluorescence for all individual MFBs indicate the appearance of a new sub-population of ~3-fold higher release rate MFBs in the post-status epilepticus animals. The cumulative probability distribution (Fig. 4D inset) showed a significant increase in peak SpH fluorescence attained for the post-status epilepticus MFBs compared with controls ($P < 0.001$, Kolmogorov–Smirnov test).

Taken together, these results suggest that, in the first 1–2 months post-status epilepticus, morphological changes develop in the MFB cytoarchitecture, correlated with both an increase in vesicular release rate of MFBs and appearance of a high release rate sub-population of terminals.

Pilocarpine-induced status epilepticus persistently enhances vesicular endocytosis in mossy fibre boutons of synaptopHluorin-expressing mice

To determine whether there are changes in rate of vesicle endocytosis in MFBs, we used the decay kinetics of SpH fluorescence after the end of the stimulus train. Since vesicle endocytosis is the rate-limiting step for decay in vesicle fluorescence (Sankaranarayanan and Ryan, 2000), determining the decay constant (τ) of this fluorescence gives an estimate of the rate of

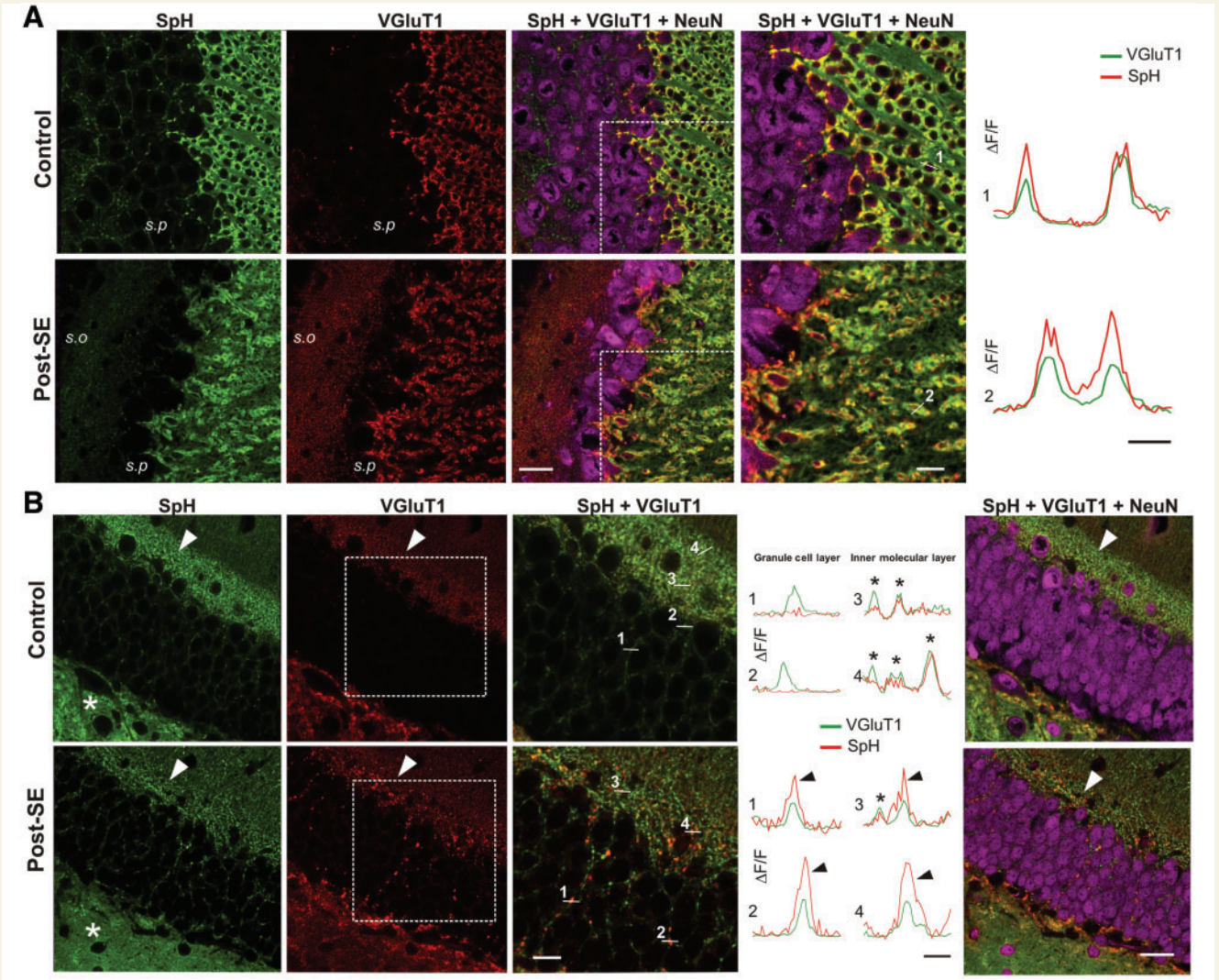

Figure 2 Confocal images of SpH, VGluT1 and NeuN expression in CA3 (**A**) and dentate granule cell (**B**) layers of control and post-status epilepticus (SE) SpH transgenic mice. (**A**) Native SpH fluorescence image (green), VGluT1 immunofluorescence image (red) and NeuN immunofluorescence image (purple) in control and post-status epilepticus mice showing co-localization of SpH with VgluT1 labelling in MFBs. A dramatic loss of cells was noticed in CA3 stratum pyramidale by NeuN staining (SpH + VGluT1 + NeuN, column 3) and SpH and VGluT1-positive terminals appear disorganized in stratum lucidum of post-status epilepticus compared with controls (SpH + VGluT1 + NeuN, column 4). Punctate SpH signals were also scattered through the pyramidal cell layer (s.p) surrounding cell somata that were stained with NeuN antibody. The column on the *right* (column 4) shows fluorescence intensity profile and co-localization along line scans (1: control and 2: post-status epilepticus) through single MFBs indicated in the respective ×2 magnification images (scale bar = 25 μm) of the rectangular boxes seen in column 3 (scale bar = 50 μm). Scale bar for line scans = 2 μm. (**B**) In the dentate granule cell layer of control and post-status epilepticus, (NeuN labelling), SpH fluorescence (green) and VGluT1 immunofluorescence (red) were intense in the hilus (asterisk) and in the inner molecular layer (arrow head). In the control (**B,** *top* row) SpH-positive puncta around putative granule cell somata were devoid of VGluT1 expression (line plots: lines 1 and 2), while SpH and VGluT1 signals co-localized in the inner molecular layer (line plots: lines 3 and 4), as shown by respective line scans of fluorescence intensity through puncta in the granule cell layer (1 and 2) versus the inner molecular layer (3 and 4). In post-status epilepticus (**B,** *bottom* row) SpH and VGluT1 co-localize in both the dentate granule cell layer (SpH + VGluT1) and inner molecular layer. NeuN immunofluorescence illustrates a lack of marked granule cell loss in post-status epilepticus dentate gyrus (SpH + VGluT1 + NeuN). Stratum oriens scale bar = 2 μm.

vesicle endocytosis. We first normalized the mean peak stimulus-evoked SpH fluorescence increases to 1.0 for control and post-status epilepticus slices, to compare directly the time courses of decay. As shown in Fig. 4E, the mean rate of decay of SpH fluorescence from peak to baseline for epileptic slices was significantly faster (red circles) compared with control slices (black circles, $P < 0.05$, Student's *t*-test), indicating an enhanced speed of endocytosis. We also fit single exponential decay functions to curves for individual MFBs to determine the decay time constants in post-status epilepticus vs. control MFBs. As shown in the Fig. 4E inset, chronic post-status epilepticus led to a significant decrease in decay time constants [red bar, $\tau = 7.23 \pm 0.32$ s versus

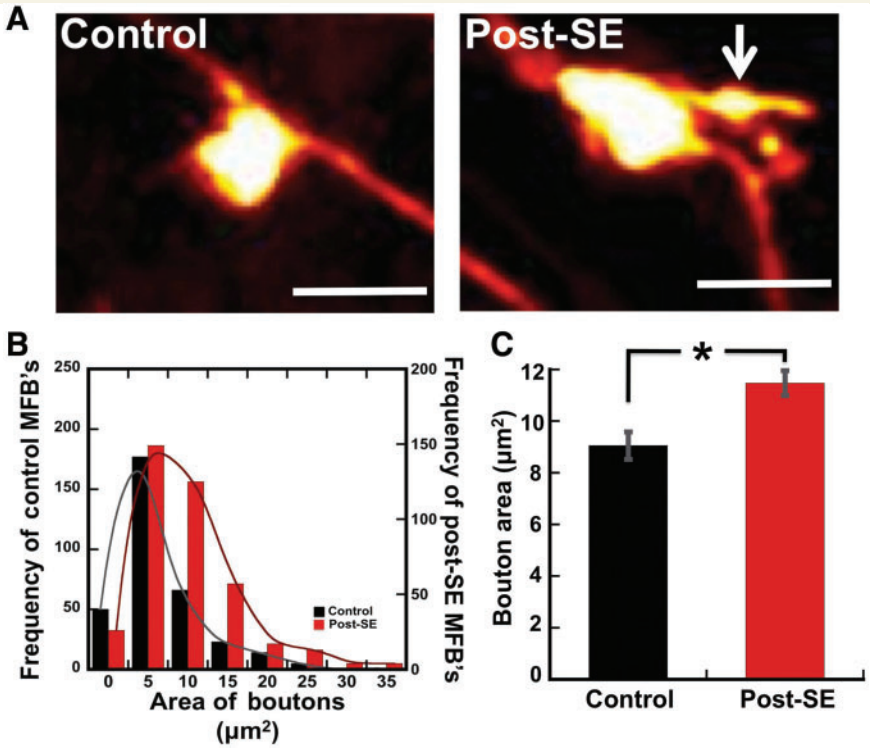

Figure 3 Pilocarpine-induced status epilepticus (SE) leads to persistent increases in dentate gyrus giant MFB area. (**A**) Live cell two-photon images of Alexa Fluor 594 dextran-loaded giant mossy fibre terminals from field CA3 of acute hippocampal slices from control and post-status epilepticus mice. The arrow shows a filopodia-like projection arising from the giant MFB. (**B**) Frequency distribution histogram of individual MFB areas from control (black columns, total of 336 boutons, $n = 7$) vs. 1–2 months post-SE mice (red columns, 394 boutons, $n = 7$). (**C**) Mean MFB area for control (black column, $9.05 \pm 0.52\ \mu m^2$) and epileptic (red column, $11.47 \pm 0.48\ \mu m^2$) mice. Data plotted as mean ± SEM, $^*P < 0.05$, Mann–Whitney U-test. Scale bar **A** = 5 μm.

control slices (black bar), $\tau = 10.4 \pm 0.77$ s, $P < 0.05$; Student's *t*-test] also consistent with acceleration in the rate of vesicle retrieval.

FM1-43 measurement of changes in vesicular release from the rat mossy fibre bouton readily releasable pool at early and late time points post-status epilepticus

As a second, independent measure of vesicular release, we estimated the time course of neurotransmitter release in slices from post-status epilepticus Sprague–Dawley rats using two-photon imaging of stimulus-evoked release of the styryl dye FM1-43 as described previously (Stanton *et al.*, 2003, 2005; Zakharenko *et al.*, 2003; Winterer *et al.*, 2006; Bailey *et al.*, 2008). We loaded FM1-43 selectively into vesicles of the RRP with a 30-s hypertonic shock (Supplementary Fig. 2) and similar to SpH fluorescence, we visualized bright puncta in the proximal region of field CA3 > 2 μm in diameter (Fig. 5A), presumed MFBs (Galimberti *et al.*, 2006). More distal puncta that took up FM1-43 were much smaller in size, consistent with associational-commissural synaptic terminals. Dye release was triggered by repetitive bursts of 50 mossy fibre stimuli at a frequency of 20 Hz, spaced 30 s apart (Fig. 5B and Supplementary Fig. 2), to allow binding and clearance by the scavenger ADVASEP-7 (100 μm) (Zakharenko *et al.*, 2003) and minimize potential movement artefacts.

Figure 5C shows that mean time courses of RRP loaded stimulus-evoked FM1-43 destaining from MFBs in slices up to 2 months post-status epilepticus was associated with a significantly enhanced release of FM1-43 (~64% from pre-stimulus baseline), when compared with age matched controls (~51% from pre-stimulus baseline, $P < 0.05$, Student's *t*-test). Interestingly, 11 months post-status epilepticus rats showed a substantial slowing in MFBs release rate in the epileptic group (~21% from pre-stimulus baseline) versus aged matched controls (~37% of baseline, $P < 0.05$, Student's *t*-test).

Action potential-independent release of FM1-43 from the mossy fibre bouton readily releasable pool is not persistently altered by pilocarpine-induced status epilepticus in rats

The above data suggest changes in stimulus evoked, but not necessarily spontaneous release rate post-status epilepticus.

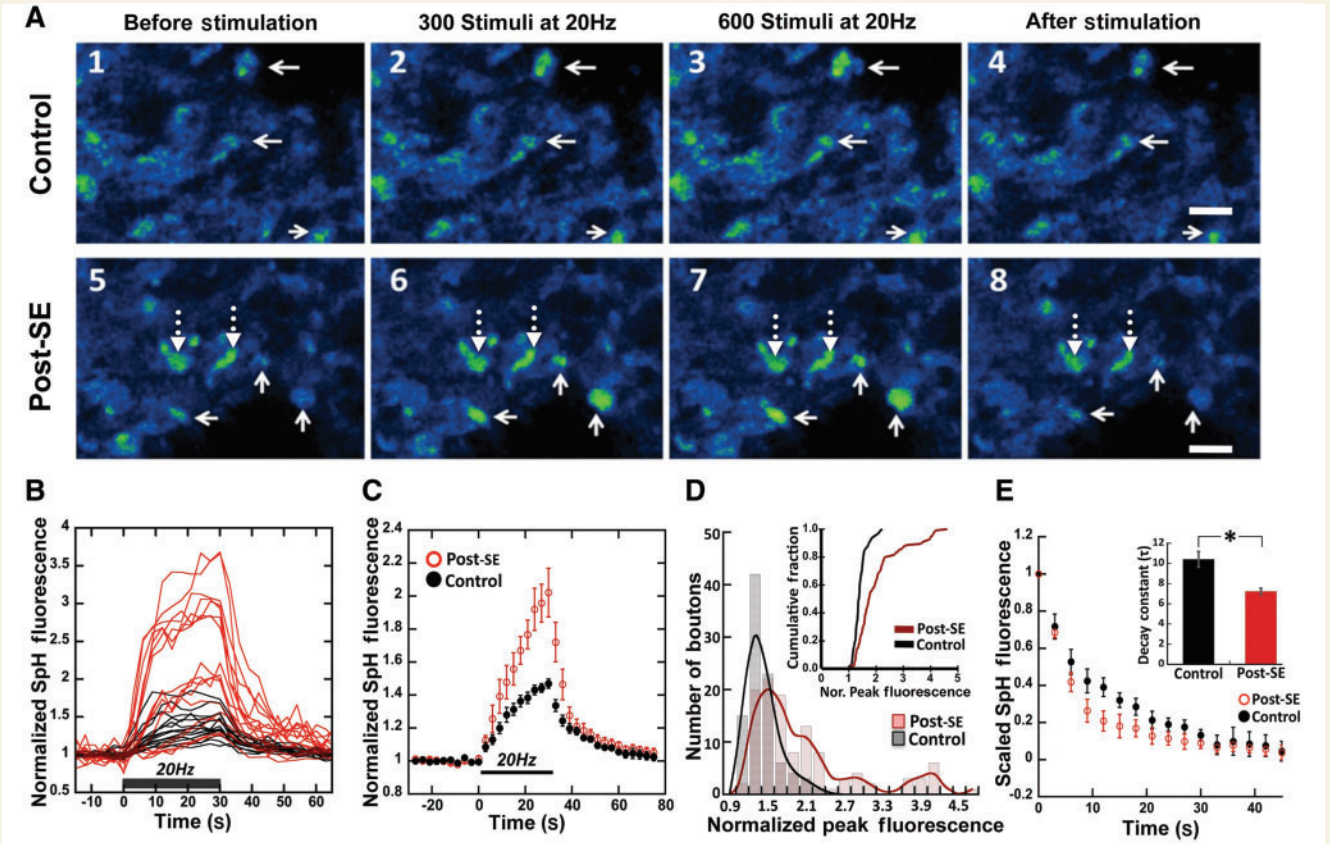

Figure 4 Pilocarpine-induced status epilepticus (SE) enhances vesicular release and endocytosis at mossy fibre terminals in CA3 stratum lucidum. (**A**) Time-lapse two-photon images from control and post-status epilepticus SpH-expressing MFBs in the proximal apical dendritic region of field CA3. Solid arrows indicate puncta that showed activity-dependent fluorescence changes during a 600 pulse/20 Hz stimulus train. The broken arrows in (**A**, *bottom* row) show there were some slowly fluorescing boutons in the epileptic slices. (**B**) Representative time course of normalized fluorescence intensity of individual boutons from a control (black traces) and a post-status epilepticus (red traces) slice in response to the 600 pulse/20 Hz mossy fibre stimulation (black bar shows duration of the train). (**C**) Normalized, evoked SpH fluorescence increases in response to a 600 pulse/20 Hz mossy fibre stimulus train, in MFBs from control (filled black circles, $F_{peak} = 1.47 \pm 0.03$, $n = 10$) versus post-status epilepticus (open red circles, $F_{peak} = 2.02 \pm 0.15$, $n = 8$) slices. F_{peak} was significantly increased in post-status epilepticus slices ($P < 0.05$, Student's *t*-test; all values mean ± SEM). (**D**) Frequency distribution histogram of normalized peak SpH fluorescence for all MFBs in post-status epilepticus ($F_{peak} = 1.76 \pm 0.04$, 100/115 puncta and 3.89 ± 0.10, 15/115 puncta) versus control slices ($F_{peak} = 1.41 \pm 0.025$, 93 puncta). Inset is a cumulative histogram of normalized peak SpH fluorescence, $P < 0.001$, Kolmogorov–Smirnov test. (**E**) Mean fluorescence values of scaled SpH fluorescence decay (data normalized to respective peak fluorescence values from (**C**) after cessation of stimulation, control (filled black circles) and post-status epilepticus (open red circles). Inset represents mean ± SEM of individual decay constants derived by a single exponential fit to the SpH fluorescence decay curve. Control (black bar), $\tau = 10.4 \pm 0.77$ s, $n = 67$ and post-status epilepticus (red bar), $\tau = 7.23 \pm 0.32$ s, $n = 133$ (*$P < 0.05$, Student's *t*-test). Scale bar: **A** = 5 μm.

To measure presynaptic spontaneous release from the RRP, we loaded FM1-43 by hypertonic shock (800 mOsm/20 s), followed by bath application of tetrodotoxin (1 μM), and extracellular [K^+] raised to 15 mM [K^+]o (*High[K+]o*) to facilitate action potential-independent release (Axmacher *et al.*, 2004). To mark the early phase of action potential-independent release, we monitored the magnitude of FM1-43 destaining within the first 4.5 min of *High[K+]o* application (Fig. 5D), which showed no significant difference between control (~15%) and post-status epilepticus (~20%) MFBs ($P > 0.20$, Student's *t*-test). To determine whether steady-state spontaneous release was altered, we examined the late phase of spontaneous release 10–25 min after application of *High[K+]o* (Fig. 5E). As in the early phase, there was no significant difference between the two groups after 25 min of *High[K+]o*, indicating action potential dependent and independent vesicular release from the RRP are differentially regulated in the post-status epilepticus state.

Status epilepticus elicits long-term ultrastructural reorganization of active zones in rat mossy fibre boutons

Previous literature has shown clear correlations between release probability and synapse morphological parameters such as sizes of the RRP (Dobrunz and Stevens, 1997) and rapidly-recycling

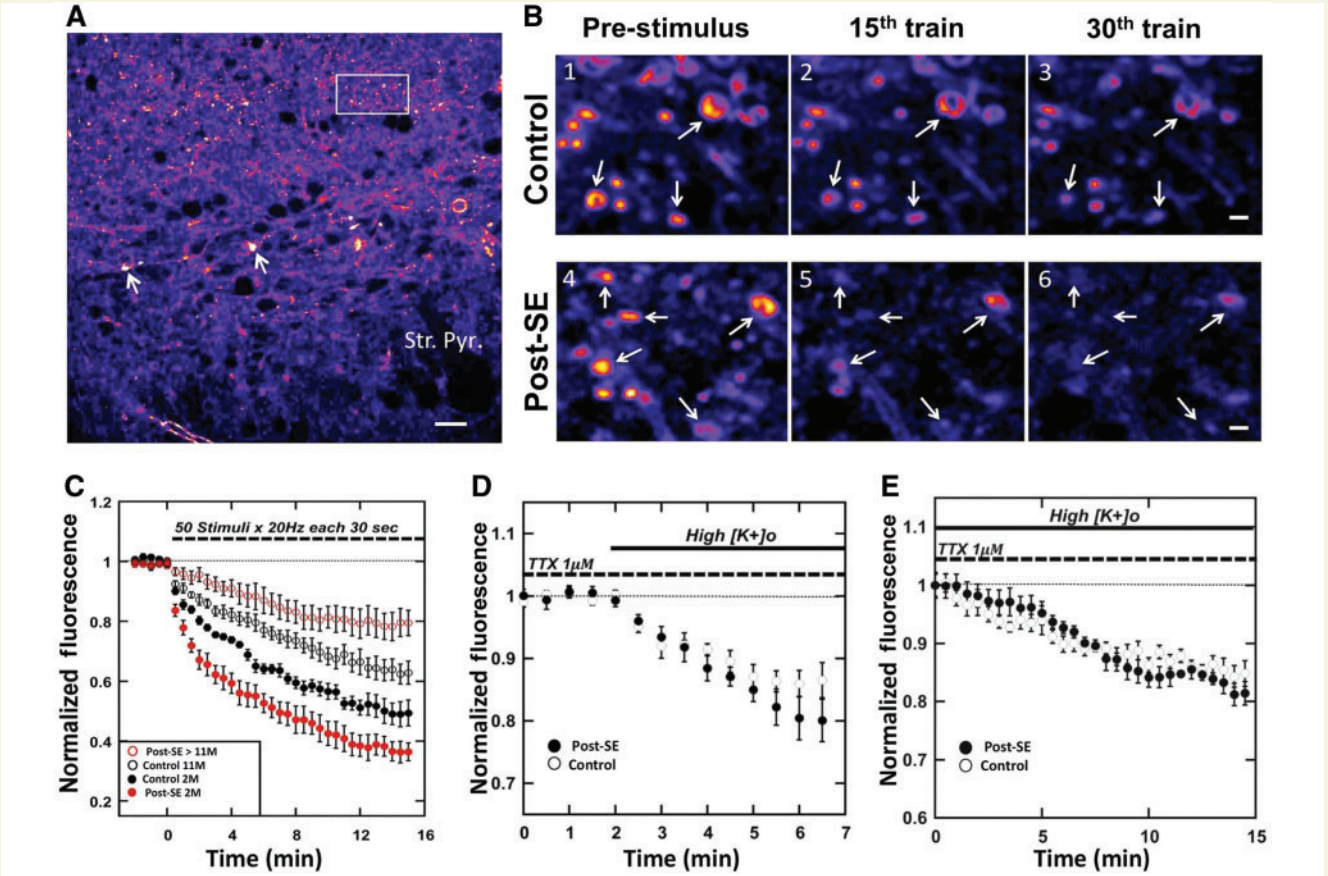

Figure 5 Pilocarpine-induced status epilepticus (SE) enhances evoked, but not action potential independent, presynaptic vesicular release of FM1-43 from the RRP in MFBs. (**A**) Two-photon image of a control field CA3 showing FM1-43 loaded RRP of MFBs. The solid arrows show staining of giant mossy fibre terminals in the proximal region of CA3 stratum lucidum. The rectangular box outlines FM1-43 staining of puncta distal to the CA3 pyramidal cell bodies and much smaller in size, likely to be associational-commissural synapses. (**B**) Representative time-lapse images of FM1-43 destaining from the RRP using repetitive mossy fibre stimulus bursts (50 stimuli/20 Hz each 30 s) to evoke release from MFBs in control and 2-month post-SE slices, respectively. [**B** (1 and 4)] Pre-stimulus baseline fluorescence, [(**B** (2 and 5)] fluorescence intensity after 15 trains, and [**B** (3 and 6)] fluorescence intensity after 30 trains of mossy fibre stimulation. Solid arrows indicate regions of interest $>2\,\mu m$ in diameter that showed robust stimulus dependent FM1-43 destaining. (**C**) Time course of FM1-43 destaining of MFBs in 1–2 months (2 M) post-SE slices (filled red circles, 0.36 ± 0.03, $n = 6$), aged-matched controls (filled black circles, 0.49 ± 0.04, $n = 5$), >11 month (11 M) post-SE slices (open red circles, 0.79 ± 0.04, $n = 5$) and aged-matched controls (open black circles, 0.62 ± 0.04, $n = 6$). All points are mean ± SEM of normalized fluorescence decay at 30th stimulus burst. $P < 0.05$, Student's *t*-test. (**D**) Time course of first 4.5 min of action potential independent FM1-43 destaining in presence of tetrodotoxin (TTX; 1 μm) and 15 mM [K+]o from the RRP in MFBs of 1–2 months post-SE slices (filled circles, $n = 4$) and aged matched control (open circles, $n = 5$) slices (all points are mean ± SEM). Decay after 4.5 min in *High[K+]o*: Control = 0.86 ± 0.028 (~14% of pre-stimulus baseline) and post-SE = 0.80 ± 0.034 (~20% of pre-stimulus baseline; $P > 0.20$, Student's *t*-test). (**E**) Late phase of spontaneous release. Time course of renormalized spontaneous FM1-43 destaining after 10–25 min in *High[K+]o*. Control normalized destaining = 0.85 ± 0.02 and post-SE destaining = 0.81 ± 0.02 ($P > 0.20$, Student's *t*-test, all points are mean ± SEM). Scale bars: **A** = 20 μm; **B** = 10 μm.

pools (Murthy *et al.*, 1997), active zone size (Schikorski and Stevens, 1997; Matz *et al.*, 2010) also known as 'release sites', postsynaptic density (Schikorski and Stevens, 1997) and presynaptic bouton size (Matz *et al.*, 2010). Since we found increased release probability post-status epilepticus as measured by both SpH (Fig. 4C) and FM1-43 destaining (Fig. 5C), we examined possible ultrastructural rearrangements in MFBs in CA3 stratum lucidum in post-status epilepticus and age-matched control Sprague–Dawley rats (Fig. 6A).

Transmission electron microscopy shows that large MFBs (2–5 μm in diameter) had multiple active zones facing postsynaptic densities, contained mitochondria of various sizes, and were filled with numerous small and large clear synaptic vesicles distributed throughout the terminal (Fig. 6A), as described previously (Amaral and Dent, 1981; Chicurel and Harris, 1992; Rollenhagen *et al.*, 2007). Asymmetric active zones were distinguished at MFBs synapses by the dense accumulation of synaptic vesicles in close proximity to the presynaptic density and characteristic widening of the synaptic cleft.

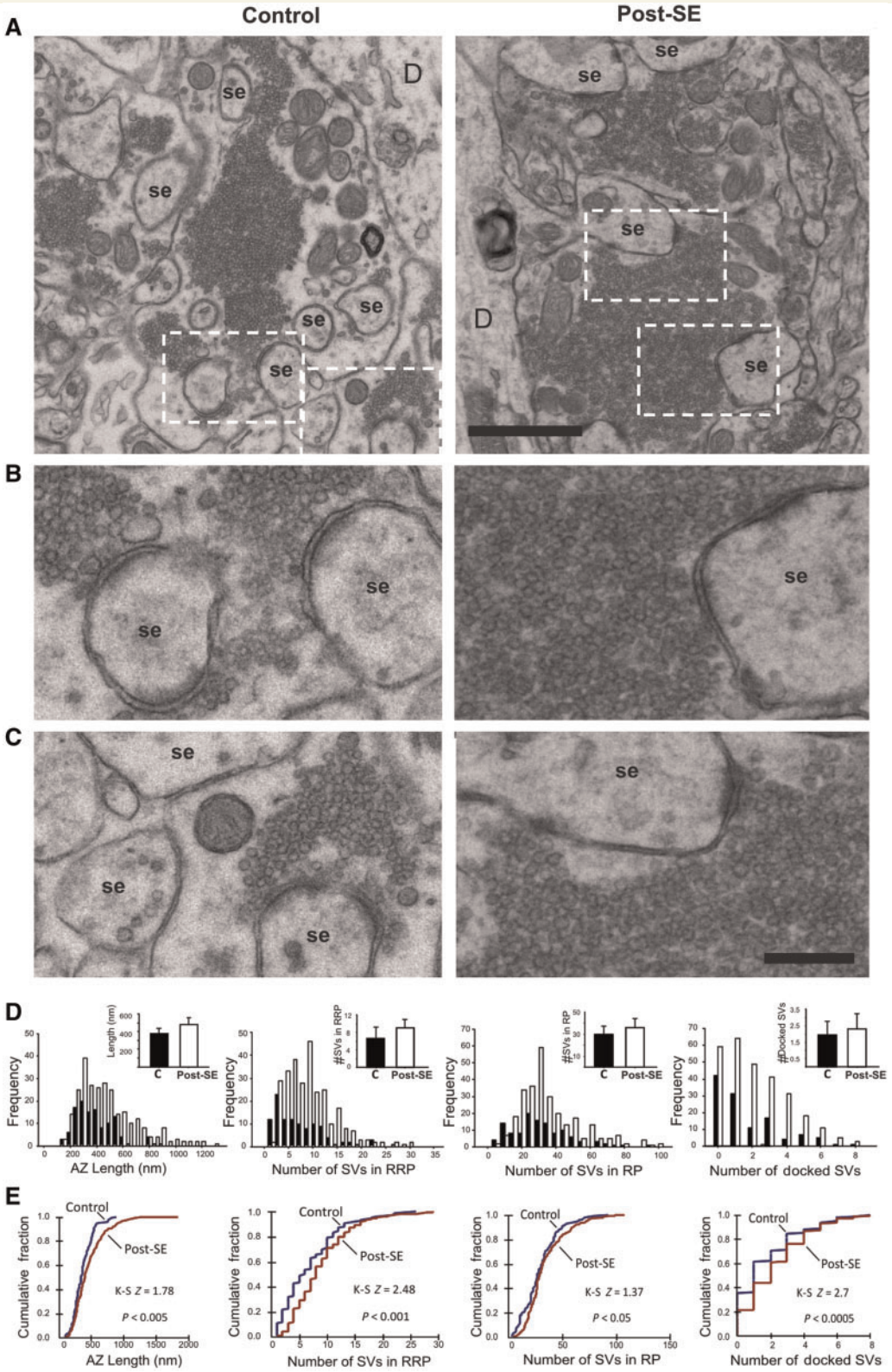

Figure 6 Transmission electron microscopy of active zones (AZ) in MFBs of control and post-status epilepticus (SE) rats. (**A**) Representative transmission electron microscopy images of control (*left*) and post-SE (*right*) MFBs illustrating active zones on synaptic excrescences (se) showing an apparent increase in synaptic vesicle density in post-SE MFBs. Boxed areas are depicted at higher magnification ($\times 4$) in images (**B** and **C**), showing arrangement of vesicles in the active zones of control and post-SE MFBs. Notice the larger density of vesicles and length of active zones in post-SE MFBs. (**D**) Frequency histograms and bar graph representation of data for active zone length, number of synaptic vesicles (SV) in RRP and releasable vesicle pool (RP), and number of docked synaptic vesicles. Notice appearance of increased number of active zones exhibiting larger lengths post-SE (>800 nm). (**E**) Cumulative histograms for these variables in control versus post-SE groups revealed significant rightward shifts toward larger sizes (Kolmogorov–Smirnov (K–S) two-sample test). Scale bars: **A** = 2 μm; **B–E** = 500 nm. D = dendrite.

Table 1 Summary of quantitative analysis of structural variables in active zones of MFBs

	Control, Mean ± SD	Post-status epilepticus, Mean ± SD	Percentage of control	K–S, *P*
Active zone ultrastructural variables				
Length of active zone (nm)	364.91 ± 44.81	485.27 ± 59.63	133.5	*<0.005*
Length of synaptic cleft (nm)	26.93 ± 3.91	29.95 ± 2.46	107.4	*0.31*
PSD area (mm^2)	12.31 ± 3.03	16.90 ± 3.31	136.9	*<0.005*
Number of SVs in RRP	7.43 ± 3.12	8.94 ± 1.78	120.3	*<0.001*
Number of SVs in the releasable pool	31.07 ± 6.05	33.44 ± 7.13	107.6	*<0.05*
Number of docked SVs per active zone	1.96 ± 0.68	2.63 ± 0.56	134.2	*<0.0005*
Docked SVs per active zone length (SV/mm)	5.48 ± 1.75	5.88 ± 0.90	108.9	*<0.05*
Percentage of docked SVs of RRP	27.92 ± 6.45	29.56 ± 3.24	105.85	*0.59*

Measurements were obtained from analysis of active zone variables in MFBs. Statistical comparisons were made using the Kolmogorov–Smirnov (K–S) two-sample test, with statistical significance set at $P < 0.05$. Values are presented as means ± SEM.
PSD = postsynaptic density; SV = synaptic vesicle.

There was a significant increase in number of active zones per MFB in post-status epilepticus rats (130 active zones in six control rats, 5.1 ± 1.36 active zones per MFB; 286 active zones in seven post-status epilepticus rats, 7.7 ± 3.05 active zones per MFB, Student's *t*-test, $P < 0.05$). The number of perforated synapses was also significantly increased in MFBs from post-status epilepticus animals (46 of 286, 16.1%) compared to controls (12 of 130, 9.2%, Student's *t*-test, $P < 0.05$). The majority of electron microscopy variables failed to follow normal distributions, necessitating use of a non-parametric Kolmogorov–Smirnov two-sample test to assess between group differences in distributions. As reported previously (Chicurel and Harris, 1992; Rollenhagen *et al.*, 2007), individual active zones varied substantially in shape and size; both large and small active zones were found in control (104–887 nm) and post-status epilepticus (105–1837 nm) hippocampus. Frequency distributions revealed the presence of a distinct group of synapses of larger length in epileptic animals that was absent in controls (Fig. 6D). A cumulative histogram indicated a significant leftward shift towards larger individual active zone lengths in MFBs post-status epilepticus (Fig. 6E), compared with controls (Table 1, Kolmogorov–Smirnov test, $P < 0.005$). There was also a significant increase in mean postsynaptic density area in the post-status epilepticus group (Table 1) compared to controls (Table 1, Kolmogorov–Smirnov test $P < 0.005$, ~37% increase). In contrast, no significant changes were detected in average synaptic cleft width between control and post-status epilepticus active zones (Table 1).

It has been previously suggested that a rapid refilling of the RRP from a larger releasable vesicle pool is a key mechanism in ensuring fidelity of mossy fibre-CA3 pyramidal cell neurotransmission (Suyama *et al.*, 2007). To determine whether ultrastructural organization of synaptic vesicle pools is altered post-status epilepticus, we measured the number of vesicles docked, within 60 nm of the active zone, 60–200 nm from an active zone, and >200 nm from an active zone, in MFBs of control versus epileptic animals. The RRP was defined as the sum of docked vesicles and those within 60 nm of the active zone, while the releasable pool was defined as vesicles 60–200 nm away from an active zone (Suyama *et al.*, 2007). Compared with controls, post-status epilepticus increased number of docked (+34.2%), RRP (+20.3%), and releasable pool (+7.6%) synaptic vesicles (Fig. 6D and Table 1). A significant difference was detected in the analysis of the cumulative distributions of these variables by Kolmogorov–Smirnov test (Fig. 6E and Table 1). Although the percentage of docked vesicles relative to RRP size was not significantly different (Table 1), the average number of docked vesicles per length of active zone was significantly higher for post-status epilepticus (+8.9%, Table 1). Additionally, the number of synaptic vesicles in each of these pools was significantly correlated with the length of individual active zones in both control (RRP: $r = 0.33$, $P < 0.001$ and releasable pool: $r = 0.41$, $P < 0.001$) and post-status epilepticus MFBs (RRP: $r = 0.57$, $P < 0.001$ and releasable pool: $r = 0.55$, $P < 0.001$, Supplementary Fig. 3).

In order to assess endocytosis, we measured the number and percent of clathrin-coated vesicles 0–200 nm from an active zone (Fig. 7A) and the area of membranous regions apparently internalized at the active zone, indicative of 'bulk endocytosis' (Fig. 7B), in MFBs of control and post-status epilepticus. There were no statistical differences in percent of synapses exhibiting one or two putative clathrin-coated vesicles at active zones between control (22.7 ± 10.1%) and post-status epilepticus (22.0 ± 7.1%, Fig. 7C) animals, or percent synapses exhibiting bulk endocytosis (control: 48.7 ± 13.1%, epileptic: 40.7 ± 15.8%). In contrast, the area of large elliptical or irregular membranous structures at the active zone was significantly higher at MFB synapses post-status epilepticus (5662 ± 385 nm^2) compared with controls (2917 ± 287 nm^2, Kolmogorov–Smirnov test, $P < 0.001$, Fig. 7D), suggesting increased rate of endocytosis.

Taken together, our electron microscopy data show pilocarpine-induced status epilepticus leads to a profound and long-lasting rearrangement of MFB transmitter release sites, resulting in significant increases in number of release sites per MFB, length of individual release sites, and RRP and releasable pool vesicle pools sizes that may underlie persistent increases in functional transmitter vesicular release rates, magnitude and recycling properties.

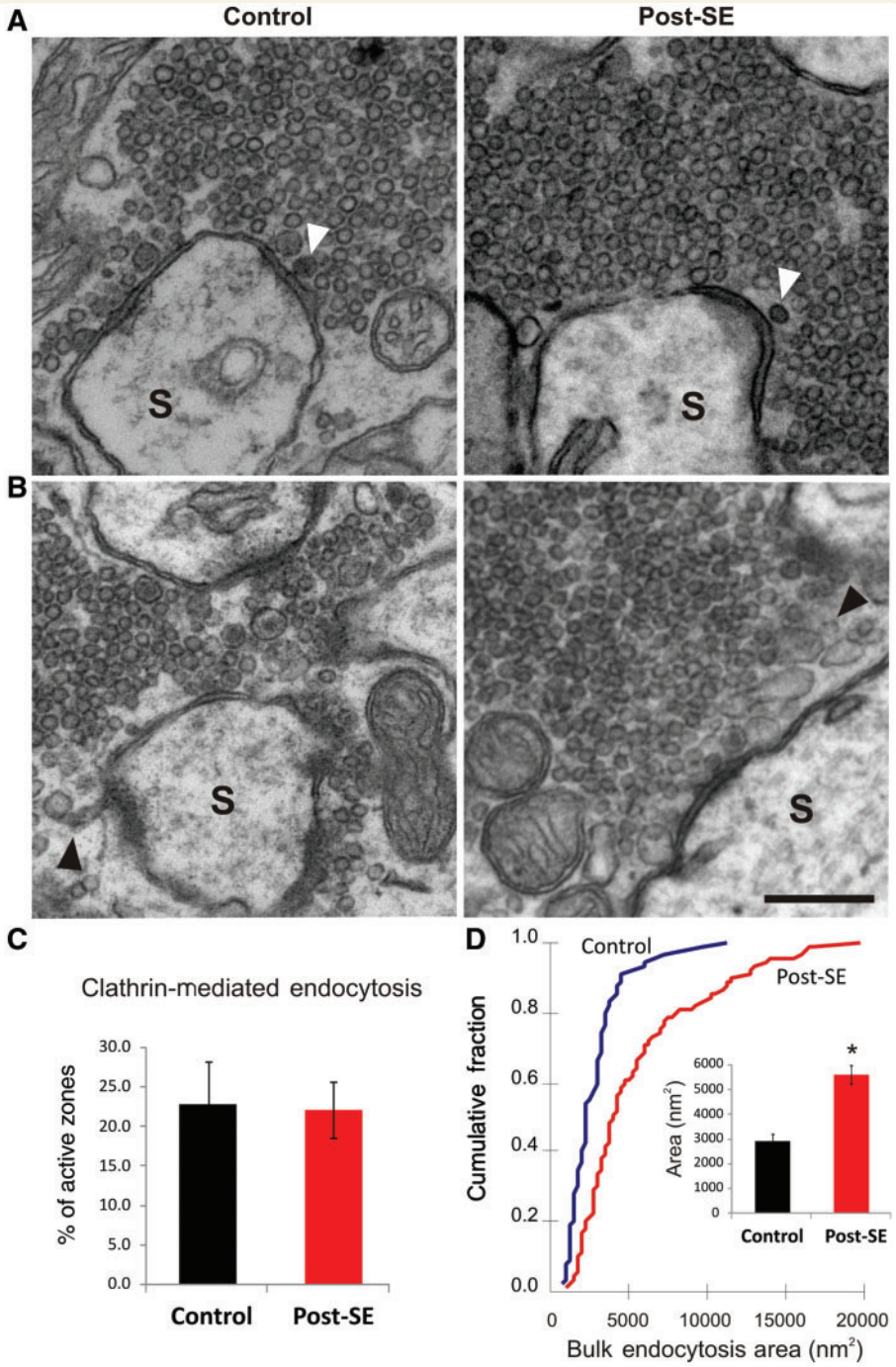

Figure 7 Representative transmission electron microscopy images of active zones in MFBs exhibiting structural signs of clathrin-mediated endocytosis and 'bulk endocytosis' in control versus epileptic rats. (**A**) Putative clathrin-coated (dark) vesicles (white arrowheads) located proximal to presynaptic membrane active zones synapsing on spines (S) of control and post-status epilepticus (SE) MFBs. (**B**) Irregular membranous structures (black arrowheads) near active zones on spines were observed in both control and post-SE MFBs. Note these structures were larger in post-SE rats. (**C**) Mean ± SEM% active zones positive for clathrin-coated vesicles, showing no difference in control versus post-SE rats ($P > 0.20$, Student's *t*-test). (**D**) Cumulative histogram plot of bulk endocytosis area showing a significant rightward shift on the size distribution towards larger values in post-SE MFBs (red) compared with controls (blue, $P < 0.001$, Kolmogorov–Smirnov test). Inset: mean area of bulk endocytosis in control (black) versus post-status epilepticus (red) rats (*$P < 0.05$, Student's *t*-test. Scale bars: **A**, **B** = 500 nm.

Discussion

We describe here a set of long-term alterations in presynaptic morphology and synaptic vesicle recycling at mossy fibre-CA3 terminals of rats and mice subjected to pilocarpine-induced status epilepticus, a model of temporal lobe epilepsy that results in spontaneous recurrent seizures within 2 months in ~97% of rats (Leite *et al.*, 1990; Cavalheiro *et al.*, 1991; Mello *et al.*, 1993; Priel *et al.*, 1996) and mice (Cavalheiro *et al.*, 1996; Muller *et al.*, 2009). In rats, the latent period ranges between 1 and 6 weeks (Curia *et al.*, 2008), with the mean latent period between 15–18 days (Leite *et al.*, 1990; Priel *et al.*, 1996), and depends on the duration of status epilepticus, where a 2-h status epilepticus corresponds to about a 7-day long latent period (Goffin *et al.*, 2007). In mice, the latent period is ~14 days (Cavalheiro *et al.*, 1996), therefore, an overwhelming majority of our animals likely developed spontaneous seizures prior to experiments. Observed presynaptic changes include increases in (i) MFB size; (ii) number of release sites per MFB; (iii) number of vesicles in the RRP and releasable pool; (iv) active zone length; (v) action potential-driven vesicular release rate measured with either FM1-43 or in SpH-expressing transgenic mice; and (vi) enhanced vesicle endocytosis. These alterations persisted for at least 1 month following a single sustained status epilepticus.

Functional enhancement in vesicular transmitter release from MFBs correlates well with previously reported structural changes (number of docked synaptic vesicles or the RRP, area of postsynaptic density, active zone length) that track vesicle release probability (Schikorski and Stevens, 1997; Matz *et al.*, 2010), suggesting that the morphological changes are probably components of the response to hyperactivation that underlie enhanced transmitter release. This agrees with a previous report that kainic acid-induced seizures lead to an increase in glutamate release from the RRP and loss of paired pulse facilitation (Goussakov *et al.*, 2000), suggesting that seizures of a variety of causes may lead to persistent increases in basal release probability.

The significant increase we observed in FM1-43 destaining post-status epilepticus and the correlated increase of vesicle pool sizes measured by transmission electron microscopy suggest an increase in both initial release probability and size of the readily releasable and rapidly recycling vesicle pools. Previous reports suggest that the size of the recycling pool is an important determinant of sustainability of release with prolonged activation (Suyama *et al.*, 2007), consistent with the increases we observed post-status epilepticus. While our transmission electron microscopy SpH and Alexa Fluor 594-dextran loading data all indicate that MFBs show increased size and larger numbers of synaptic vesicles for months after status epilepticus; the new population of terminals, with significantly larger size and faster release rate, could be from modification of existing terminals, ectopic MFBs, or both, and remains to be determined. Also, since individual MFBs contain multiple active zones (Hallermann *et al.*, 2003), we cannot tell whether increased release probability at MFBs (Figs 4D and 5C) occurs at the level of individual active zones switching to a high release state, or whether there is a uniform increase in release probability across all active zones. Additional changes such as increases in the number of active zones per bouton and size of the RRP and releasable pool in individual active zones also suggest persistent increase in glutamate release that could be a key contributor to death of CA3 pyramidal neurons characteristic of hippocampal sclerosis. Increases in the density of perforated synapses have been associated with synaptogenesis and post-lesional compensatory plasticity (Itarat and Jones, 1992; Luke *et al.*, 2004; Adkins *et al.*, 2008). Increased incidence of perforated mossy fibre synapses after status epilepticus suggest that synaptic connectivity undergoes structural remodelling favouring synapses, with potentially higher transmission efficiency during the process of epileptogenesis.

Using SpH fluorescence, we derived a decay constant of 10.4 ± 0.77 s for control boutons (Fig. 4E), similar to previous reports of an endocytic time constant of 9.0 ± 5.5 s estimated using capacitance recordings at MFBs (Hallermann *et al.*, 2003). Our observations of accelerated recovery of stimulus-evoked SpH fluorescence in slices from post-status epilepticus mice, but lack of differences between the number of clathrin-coated vesicles in electromicrographs between the post-status epilepticus and control groups, could be due to an enhanced rate of endocytosis that may or may not depend on clathrin, increased local recycling of vesicles to the RRP (Stanton *et al.*, 2003) or to the recycling pool after exocytosis (Wu and Wu, 2009), increase in bulk endocytosis (retrieval of larger membrane area, Table 1) or combinations of the above. Also, tissues used for electromicrographs were not electrically stimulated prior to fixation, and thus do not necessarily reflect activity-dependent endocytic events but, more likely, the steady-state of the presynaptic bouton ultrastructure.

The 1–2 month time point post-status epilepticus used in our experiments corresponds to the period of occurrence of spontaneous seizures in both rats (Leite *et al.*, 1990; Cavalheiro *et al.*, 1991; Priel *et al.*, 1996; Dudek and Sutula, 2007) and mice (Cavalheiro *et al.*, 1996; Muller *et al.*, 2009; Schauwecker, 2012). Interestingly, in contrast to the early increase in MFB release probability, we found that, at very long survival periods post-status epilepticus (11–12 months), rates of MFB release were markedly reduced. The reduced transmitter release from the RRP in these animals could either reflect long-term compensatory changes or dysfunction of presynaptic release machinery. Our observation that action potential independent RRP release rate in tetrodotoxin (1 μm) was not altered by pilocarpine seizures indicates that action potential dependent and independent regulation of the RRP is very different, perhaps due to potentially distinct pools of vesicles and mechanisms between evoked and spontaneous release (Fredj and Burrone, 2009; Chung *et al.*, 2010). We cannot rule out the possibility that new vesicle pools may contribute to action potential independent release of glutamate post-status epilepticus.

Our functional data demonstrating that post-status epilepticus state leads to increased vesicular release and endocytotic rates, and electron microscope data showing increased presynaptic active zone length, membrane invaginations, clathrin-coated vesicles and vesicle pool sizes, are all consistent with the conclusion that post-status epilepticus state is associated with long-term increases in transmitter release from MFBs, and perhaps other glutamatergic terminals. Since brain-derived neurotrophic factor

is highly expressed in presynaptic MFBs (Danzer and McNamara, 2004) and can elicit long-term enhancements in both transmitter release and size of the RRP (Zakharenko *et al.*, 2003; Tyler *et al.*, 2006), neurotrophins seem a likely candidate mediator of these presynaptic alterations.

Whether increase in stimulus evoked release following-status epilepticus results from alterations in Ca^{2+} influx, release of Ca^{2+} from internal stores *per se*, or whether there are downstream changes in SNARE protein sensitivity to Ca^{2+} is not known. A recent study (Pacheco *et al.*, 2008) found that pilocarpine seizures also cause downregulation of large conductance calcium-activated potassium (BK) channels in MFBs, reductions that could slow hyperpolarization and increase terminal Ca^{2+} influx. Levels of the Ca^{2+} buffer calbindin D-28K are also lowered in MFBs after pilocarpine seizures (Carter *et al.*, 2008), a change that could further increase presynaptic Ca^{2+} influx, dysregulate Ca^{2+} homeostasis and promote multivesicular release (Hallermann *et al.*, 2003).

In summary, our study is the first, to our knowledge, using the pilocarpine model of temporal lobe epilepsy in SpH-expressing transgenic mice, a new tool to investigate presynaptic alterations in epilepsy with potential application for other CNS diseases that may involve presynaptic dysfunction. Our studies indicate that the early phase of the pilocarpine model of temporal lobe epilepsy is associated with persistent structural changes in mossy fibre presynaptic terminal size, vesicle pools and active zones that are correlated with functional increases in rates of action potential-driven vesicular release and associated endocytotic recycling. The time course and mechanisms underlying these changes suggests the presynaptic terminal as a novel target for new therapeutics to treat epilepsy, especially temporal lope epilepsy.

Acknowledgements

The authors would like to thank Dr Venkatesh Murthy for providing us with the SpH21 transgenic mice line, Dr Kenichi Miyazaki for help with Alexa Fluor 594 dextran experiments, Mohini Rawat for technical assistance, Dr Pravin Sehgal and Jason Lee for discussions on Otsu thresholding and Dr Xiao-Lei Zhang and John Sullivan for additional helpful discussions.

Funding

National Institutes of Health (grants GM081109, P20 MD001091-06 and NS063950); Department of Defense (grant PR100534 to E.R.G.S.); National Institute of Neurological Diseases and Stroke (grants NS056093 to J.V., NS072966 to L.V. and NS044421 to P.K.S.); Department of Defense (grant PR100534P1 to P.K.S.).

Supplementary material

Supplementary material is available at *Brain* online.

References

Acsady L, Kamondi A, Sik A, Freund T, Buzsaki G. GABAergic cells are the major postsynaptic targets of mossy fibers in the rat hippocampus. J Neurosci 1998; 18: 3386–403.

Adkins DL, Hsu JE, Jones TA. Motor cortical stimulation promotes synaptic plasticity and behavioral improvements following sensorimotor cortex lesions. Exp Neurol 2008; 212: 14–28.

Amaral DG, Dent JA. Development of the mossy fibers of the dentate gyrus: I. A light and electron microscopic study of the mossy fibers and their expansions. J Comp Neurol 1981; 195: 51–86.

Axmacher N, Winterer J, Stanton PK, Draguhn A, Muller W. Two-photon imaging of spontaneous vesicular release in acute brain slices and its modulation by presynaptic GABAA receptors. Neuroimage 2004; 22: 1014–21.

Bailey CP, Nicholls RE, Zhang XL, Zhou ZY, Muller W, Kandel ER, et al. Galpha(i2) inhibition of adenylate cyclase regulates presynaptic activity and unmasks cGMP-dependent long-term depression at Schaffer collateral-CA1 hippocampal synapses. Learn Mem 2008; 15: 261–70.

Bayazitov IT, Richardson RJ, Fricke RG, Zakharenko SS. Slow presynaptic and fast postsynaptic components of compound long-term potentiation. J Neurosci 2007; 27: 11510–21.

Bischofberger J, Engel D, Li L, Geiger JR, Jonas P. Patch-clamp recording from mossy fiber terminals in hippocampal slices. Nat Protoc 2006; 1: 2075–81.

Blackstad TW, Brink K, Hem J, Jeune B. Distribution of hippocampal mossy fibers in the rat. An experimental study with silver impregnation methods. J Comp Neurol 1970; 138: 433–49.

Boulland JL, Ferhat L, Tallak Solbu T, Ferrand N, Chaudhry FA, Storm-Mathisen J, et al. Changes in vesicular transporters for gamma-aminobutyric acid and glutamate reveal vulnerability and reorganization of hippocampal neurons following pilocarpine-induced seizures. J Comp Neurol 2007; 503: 466–85.

Burrone J, Li Z, Murthy VN. Studying vesicle cycling in presynaptic terminals using the genetically encoded probe synaptopHluorin. Nat Protoc 2006; 1: 2970–8.

Calverley RK, Jones DG. Determination of the numerical density of perforated synapses in rat neocortex. Cell Tissue Res 1987; 248: 399–407.

Carter DS, Harrison AJ, Falenski KW, Blair RE, DeLorenzo RJ. Long-term decrease in calbindin-D28K expression in the hippocampus of epileptic rats following pilocarpine-induced status epilepticus. Epilepsy Res 2008; 79: 213–23.

Cavalheiro EA. The pilocarpine model of epilepsy. Ital J Neurol Sci 1995; 16: 33–7.

Cavalheiro EA, Leite JP, Bortolotto ZA, Turski WA, Ikonomidou C, Turski L. Long-term effects of pilocarpine in rats: structural damage of the brain triggers kindling and spontaneous recurrent seizures. Epilepsia 1991; 32: 778–82.

Cavalheiro EA, Santos NF, Priel MR. The pilocarpine model of epilepsy in mice. Epilepsia 1996; 37: 1015–9.

Cavazos JE, Zhang P, Qazi R, Sutula TP. Ultrastructural features of sprouted mossy fiber synapses in kindled and kainic acid-treated rats. J Comp Neurol 2003; 458: 272–92.

Chicurel ME, Harris KM. Three-dimensional analysis of the structure and composition of CA3 branched dendritic spines and their synaptic relationships with mossy fiber boutons in the rat hippocampus. J Comp Neurol 1992; 325: 169–82.

Chung C, Barylko B, Leitz J, Liu X, Kavalali ET. Acute dynamin inhibition dissects synaptic vesicle recycling pathways that drive spontaneous and evoked neurotransmission. J Neurosci 2010; 30: 1363–76.

Claiborne BJ, Amaral DG, Cowan WM. A light and electron microscopic analysis of the mossy fibers of the rat dentate gyrus. J Comp Neurol 1986; 246: 435–58.

Coulter DA. Mossy fiber zinc and temporal lobe epilepsy: pathological association with altered "epileptic" gamma-aminobutyric acid A receptors in dentate granule cells. Epilepsia 2000; 41 (Suppl 6): S96–9.

Curia G, Longo D, Biagini G, Jones RS, Avoli M. The pilocarpine model of temporal lobe epilepsy. J Neurosci Methods 2008; 172: 143–57.

Danzer SC, He X, Loepke AW, McNamara JO. Structural plasticity of dentate granule cell mossy fibers during the development of limbic epilepsy. Hippocampus 2010; 20: 113–24.

Danzer SC, McNamara JO. Localization of brain-derived neurotrophic factor to distinct terminals of mossy fiber axons implies regulation of both excitation and feedforward inhibition of CA3 pyramidal cells. J Neurosci 2004; 24: 11346–55.

Dobrunz LE, Stevens CF. Heterogeneity of release probability, facilitation, and depletion at central synapses. Neuron 1997; 18: 995–1008.

Dudek FE, Sutula TP. Epileptogenesis in the dentate gyrus: a critical perspective. Prog Brain Res 2007; 163: 755–73.

Epsztein J, Represa A, Jorquera I, Ben-Ari Y, Crepel V. Recurrent mossy fibers establish aberrant kainate receptor-operated synapses on granule cells from epileptic rats. J Neurosci 2005; 25: 8229–39.

Esclapez M, Hirsch JC, Ben-Ari Y, Bernard C. Newly formed excitatory pathways provide a substrate for hyperexcitability in experimental temporal lobe epilepsy. J Comp Neurol 1999; 408: 449–60.

Fredj NB, Burrone J. A resting pool of vesicles is responsible for spontaneous vesicle fusion at the synapse. Nat Neurosci 2009; 12: 751–8.

Frotscher M, Jonas P, Sloviter RS. Synapses formed by normal and abnormal hippocampal mossy fibers. Cell Tissue Res 2006; 326: 361–7.

Galimberti I, Gogolla N, Alberi S, Santos AF, Muller D, Caroni P. Long-term rearrangements of hippocampal mossy fiber terminal connectivity in the adult regulated by experience. Neuron 2006; 50: 749–63.

Goffin K, Nissinen J, Van Laere K, Pitkanen A. Cyclicity of spontaneous recurrent seizures in pilocarpine model of temporal lobe epilepsy in rat. Exp Neurol 2007; 205: 501–5.

Gorter JA, Goncalves Pereira PM, van Vliet EA, Aronica E, Lopes da Silva FH, Lucassen PJ. Neuronal cell death in a rat model for mesial temporal lobe epilepsy is induced by the initial status epilepticus and not by later repeated spontaneous seizures. Epilepsia 2003; 44: 647–58.

Gorter JA, Van Vliet EA, Proper EA, De Graan PN, Ghijsen WE, Lopes Da Silva FH, et al. Glutamate transporter alterations in the reorganizing dentate gyrus are associated with progressive seizure activity in chronic epileptic rats. J Comp Neurol 2002; 442: 365–77.

Goussakov IV, Fink K, Elger CE, Beck H. Metaplasticity of mossy fiber synaptic transmission involves altered release probability. J Neurosci 2000; 20: 3434–41.

Hallermann S, Pawlu C, Jonas P, Heckmann M. A large pool of releasable vesicles in a cortical glutamatergic synapse. Proc Natl Acad Sci USA 2003; 100: 8975–80.

Hovorka J, Langmeier M, Mares P. Are there morphological changes in presynaptic terminals of kindled rats? Neurosci Lett 1989; 107: 179–83.

Itarat W, Jones DG. Perforated synapses are present during synaptogenesis in rat neocortex. Synapse 1992; 11: 279–86.

Lee JE, Patel K, Almodovar S, Tuder RM, Flores SC, Sehgal PB. Dependence of Golgi apparatus integrity on nitric oxide in vascular cells: implications in pulmonary arterial hypertension. Am J Physiol Heart Circ Physiol 2011; 300: H1141–58.

Leite JP, Bortolotto ZA, Cavalheiro EA. Spontaneous recurrent seizures in rats: an experimental model of partial epilepsy. Neurosci Biobehav Rev 1990; 14: 511–7.

Li Z, Burrone J, Tyler WJ, Hartman KN, Albeanu DF, Murthy VN. Synaptic vesicle recycling studied in transgenic mice expressing synaptopHluorin. Proc Natl Acad Sci USA 2005; 102: 6131–6.

Luke LM, Allred RP, Jones TA. Unilateral ischemic sensorimotor cortical damage induces contralesional synaptogenesis and enhances skilled reaching with the ipsilateral forelimb in adult male rats. Synapse 2004; 54: 187–99.

Matz J, Gilyan A, Kolar A, McCarvill T, Krueger SR. Rapid structural alterations of the active zone lead to sustained changes in neurotransmitter release. Proc Natl Acad Sci USA 2010; 107: 8836–41.

McNamara JO. Cellular and molecular basis of epilepsy. J Neurosci 1994; 14: 3413–25.

Mello LE, Cavalheiro EA, Tan AM, Kupfer WR, Pretorius JK, Babb TL, et al. Circuit mechanisms of seizures in the pilocarpine model of chronic epilepsy: cell loss and mossy fiber sprouting. Epilepsia 1993; 34: 985–95.

Meunier FA, Nguyen TH, Colasante C, Luo F, Sullivan RK, Lavidis NA, et al. Sustained synaptic-vesicle recycling by bulk endocytosis contributes to the maintenance of high-rate neurotransmitter release stimulated by glycerotoxin. J Cell Sci 2010; 123 (Pt 7): 1131–40.

Miesenbock G, De Angelis DA, Rothman JE. Visualizing secretion and synaptic transmission with pH-sensitive green fluorescent proteins. Nature 1998; 394: 192–5.

Miranda R, Nudel U, Laroche S, Vaillend C. Altered presynaptic ultrastructure in excitatory hippocampal synapses of mice lacking dystrophins Dp427 or Dp71. Neurobiol Dis 2011; 43: 134–41.

Muller CJ, Bankstahl M, Groticke I, Loscher W. Pilocarpine vs. lithium-pilocarpine for induction of status epilepticus in mice: development of spontaneous seizures, behavioral alterations and neuronal damage. Eur J Pharmacol 2009; 619: 15–24.

Murthy VN, Sejnowski TJ, Stevens CF. Heterogeneous release properties of visualized individual hippocampal synapses. Neuron 1997; 18: 599–612.

Pacheco Otalora LF, Couoh J, Shigamoto R, Zarei MM, Garrido Sanabria ER. Abnormal mGluR2/3 expression in the perforant path termination zones and mossy fibers of chronically epileptic rats. Brain Res 2006; 1098: 170–85.

Pacheco Otalora LF, Hernandez EF, Arshadmansab MF, Francisco S, Willis M, Ermolinsky B, et al. Down-regulation of BK channel expression in the pilocarpine model of temporal lobe epilepsy. Brain Res 2008; 1200: 116–31.

Priel MR, dos Santos NF, Cavalheiro EA. Developmental aspects of the pilocarpine model of epilepsy. Epilepsy Res 1996; 26: 115–21.

Pyle JL, Kavalali ET, Choi S, Tsien RW. Visualization of synaptic activity in hippocampal slices with FM1-43 enabled by fluorescence quenching. Neuron 1999; 24: 803–8.

Rollenhagen A, Satzler K, Rodriguez EP, Jonas P, Frotscher M, Lubke JH. Structural determinants of transmission at large hippocampal mossy fiber synapses. J Neurosci 2007; 27: 10434–44.

Sankaranarayanan S, Ryan TA. Real-time measurements of vesicle-SNARE recycling in synapses of the central nervous system. Nat Cell Biol 2000; 2: 197–204.

Schauwecker PE. Strain differences in seizure-induced cell death following pilocarpine-induced status epilepticus. Neurobiol Dis 2012; 45: 297–304.

Schikorski T, Stevens CF. Quantitative ultrastructural analysis of hippocampal excitatory synapses. J Neurosci 1997; 17: 5858–67.

Stanton PK, Winterer J, Bailey CP, Kyrozis A, Raginov I, Laube G, et al. Long-term depression of presynaptic release from the readily releasable vesicle pool induced by NMDA receptor-dependent retrograde nitric oxide. J Neurosci 2003; 23: 5936–44.

Stanton PK, Winterer J, Zhang XL, Muller W. Imaging LTP of presynaptic release of FM1-43 from the rapidly recycling vesicle pool of Schaffer collateral-CA1 synapses in rat hippocampal slices. Eur J Neurosci 2005; 22: 2451–61.

Suyama S, Hikima T, Sakagami H, Ishizuka T, Yawo H. Synaptic vesicle dynamics in the mossy fiber-CA3 presynaptic terminals of mouse hippocampus. Neurosci Res 2007; 59: 481–90.

Turski WA, Cavalheiro EA, Bortolotto ZA, Mello LM, Schwarz M, Turski L. Seizures produced by pilocarpine in mice: a behavioral, electroencephalographic and morphological analysis. Brain Res 1984; 321: 237–53.

Tyler WJ, Zhang XL, Hartman K, Winterer J, Muller W, Stanton PK, et al. BDNF increases release probability and the size of a rapidly recycling vesicle pool within rat hippocampal excitatory synapses. J Physiol 2006; 574 (Pt 3): 787–803.

Wenzel HJ, Woolley CS, Robbins CA, Schwartzkroin PA. Kainic acid-induced mossy fiber sprouting and synapse formation in the dentate gyrus of rats. Hippocampus 2000; 10: 244–60.

Winterer J, Stanton PK, Muller W. Direct monitoring of vesicular release and uptake in brain slices by multiphoton excitation of the styryl dye FM 1-43. Biotechniques 2006; 40: 343–51.

Wu XS, Wu LG. Rapid endocytosis does not recycle vesicles within the readily releasable pool. J Neurosci 2009; 29: 11038–42.

Xiong ZQ, Stringer JL. Extracellular pH responses in CA1 and the dentate gyrus during electrical stimulation, seizure discharges, and spreading depression. J Neurophysiol 2000; 83: 3519–24.

Zakharenko SS, Patterson SL, Dragatsis I, Zeitlin SO, Siegelbaum SA, Kandel ER, et al. Presynaptic BDNF required for a presynaptic but not postsynaptic component of LTP at hippocampal CA1-CA3 synapses. Neuron 2003; 39: 975–90.

Zhang S, Khanna S, Tang FR. Patterns of hippocampal neuronal loss and axon reorganization of the dentate gyrus in the mouse pilocarpine model of temporal lobe epilepsy. J Neurosci Res 2009; 87: 1135–49.

Abnormal expression of synaptic vesicle protein 2 (SV) isoforms after pilocarpine-induced status epilepticus

Luis F. Pacheco Otalora[1], Nuri Ruvalcaba[1], Jose Mario Rodriguez[1], Samantha Gomez[1], Aliya Sharif1, Chirag Upreti[2], Patric Stanton[2], Emilio R. Garrido-Sanabria[1*]

[1]Department of Biomedicine at the University of Texas at Brownsville and Center for Biomedical Studies, One W. University Blvd, Brownsville, Texas 78520 USA.

[2]Department of Cell Biology & Anatomy and Department of Neurology, New York Medical College, Basic Sciences Bldg, Rm 217, Valhalla, NY 10595.

Corresponding author:

Emilio R. Garrido Sanabria, MD, PhD

Department of Biomedicine, 1 W. University Blvd, Brownsville Texas 78520

Phone: (956) 882-5053, Fax: (956) 882-5043, E-mail: emilio.garrido@utb.edu

Abbreviations:

CA1	Corpus Ammonis Area 1
CT	Cycle Threshold
ΔΔCT	Delta-delta Cycle Threshold method of comparative real time PCR
DG	Dentate gyrus
qPCR	Quantitative real time polymerase chain reaction
mGluR2	Metabotropic glutamate receptor type 2
MTLE	Mesial Temporal Lobe Epilepsy
PBS	Phosphate-buffered saline
PCR	Polymerase Chain Reaction
PVDF	Polyvinylidene difluoride
RIPA	Radioimmunoprecipitation assay
RQ	Relative quantification index
SE	*Status epilepticus*
SV2	Synaptic vesicle protein type 2
SV2A	Synaptic vesicle protein type 2 isoform A
SV2B	Synaptic vesicle protein type 2 isoform B
SV2C	Synaptic vesicle protein type 2 isoform C

Abstract

Synaptic vesicle protein 2A (SV2A) is the putative molecular target of the antiepileptic drug levetirecetam. Previous studies indicate that the expression pattern of SV2 isoforms (SV2A, SV2B, and SV2C) is altered in patients with temporal lobe epilepsy. In this study, we investigate whether the expression of these isoforms is disturbed after pilocarpine induced *status epilepticus* and whether treatment with levetirecetam can restore epilepsy-induced changes in SV2A, SV2B and SV2C expression. For this purpose, expression of synaptic vesicle proteins was assessed using western blotting and gene expression assays. Gene expression was analyzed using TaqMan-based probes and the quantitative real-time polymerase chain reaction (qPCR) comparative method delta-delta cycle threshold (□□CT) in samples extracted from control and pilocarpine-treated mice that were treated with levetirecetam and compared to untreated groups. Our findings indicate no changes in protein and transcript expression of SV2A and SV2B 30 after pilocarpine-insuded *status epilepticus*. However, we detected a significant increase in the expression of SV2C protein and transcripts. Treatment with levetiracetam for 4 weeks significantly reduced the expression of SV2C in both treated and untreated groups with minimal effect on SV2A and SV2C. These data indicate an abnormal expression of SV2C and differential effect of levetirecetam treatment in the expression of SV2 isoforms in the pilocarpine model of MTLE. It remains unclear whether in epileptic tissue SV2C or SV2C spliced isoforms can play a role in the action of levetirecetam.

Keywords: pilocarpine, epilepsy, hippocampus, synaptic vesicle proteins, *status epilepticus*

Introduction

Synaptic vesicle proteins (SV2A, SV2B and SV2C) are thought to play a role in presynaptic transmitter release. Attention to these synaptic vesicle proteins has increased after the discovery that the antiepileptic drug levetirecetam binds to SV2A [1-3]. However, the exact mechanism of action of levetirecetam remains unclear [3-5]. SV2A is expressed in both glutamatergic and GABAergic neurons in the central nervous system. However, SV2B is selectively expressed in GABAeric neurons and SV2C is selectively expressed in glutamatergic neurons [6-10]. Previous studies in epileptic patients indicate that SV2A is down-regulated during epilepsy [11]. However, it is not clear if similar changes occur in animal models of epilepsy. In the hippocampus, SV2A is selectively expressed in mossy fibers projecting to the CA3 area [10,12,13]. Similar but weaker expression in mossy fiber has been described for SV2C. In a recent study, expression of Sv2C was upregulated in mossy fibers of patients suffering mesial temporal lobe epilepsy [12]. Hence, in study, we investigated the effect of status epilepticus on the expression of synaptic vesicle isoforms and whether treatment with levetirecetam will affect *status epilepticus*-induced altered expression of these proteins.

Experimental Procedure

Animals and rat model of chronic epilepsy

Experiments were developed in accordance with the National Institutes of Health *Guidelines for the Care and Use of Laboratory Animals* and with the approval of The University of Texas at Brownsville Institutional Animal Care and Use Committee (Protocol# 2011-001-IACUC). Sprague Dawley rats were kept in IACUC-approved *vivarium* with water and food *ad libitum*. Mice were subjected to pilocarpine-induced *status epilepticus* following described procedures [14,15]. At the time of performing the model of epilepsy, animals were approximately 35-45 days old (130-200g). A total of 35 animals were used in our experiments. All animals received same dose of 1% methyl-scopolamine nitrate (0.1 mg/kg in saline, s.c.) (Sigma-Aldrich, St. Louis, MO) thirty minutes before pilocarpine administration to minimize the peripheral effects of cholinergic stimulation [16]. Animals were then injected with 4% pilocarpine hydrochloride (Sigma-Aldrich) (320 mg/kg in saline, i.p.). Controls included (a) animals that received methyl-scopolamine but were injected with saline, instead of pilocarpine and (b) saline-injected control animals. Pilocarpine administration induced *status epilepticus* (SE) in about 70% of injected mice. SE consisted of continuous tremor, rearing, myoclonic jerks, clonic forearms and head movements with eventual side fallings and tonic seizures. Mortality rate of the procedure was reduced by administering diazepam (10 mg/kg, *i.p.*) 3 hours after SE onset to quell behavioral seizures [15,17,18]. All animals that received pilocarpine were given fresh apples and water in an easily-reachable container inside the recovery cage for 48 hr after SE induction. Subcutaneous injections of 20 ml Ringer-lactate were administered to compensate for any liquid lost (*i.e.* salivation, urination) 1 hr after diazepam injection and the following morning after induction of the pilocarpine-mediated SE. SE induction protocol was lethal in about 20% of pilocarpine-treated mice and another 10% of the animals did not enter into SE. Treatment with levetirecetam

or saline vehicle was initiated 24h after SE. For this purpose intraperitoneal injections of drug 100mg/kg i.p was performed in alternate days during 4 weeks.

Isolation of mRNA and real-time quantitative PCR analysis of gene expression.

For isolation of total RNA, control and experimental groups (as described above) of SpH mice were anaesthetized and sacrificed 1 months (endpoint) after the beginning of injection sections (saline or levetiracetam) . One hemisphere was used for protein isolation while the other hemisphere was used for total RNA isolation as previously reported[19-23]. Briefly, tissue was collected, weighed (about 20 mg), homogenized, and processed for total RNA isolation at 4°C using the RNAqueous-4PCR Kit (Foster City, California, USA), following manufacturer's instructions. The concentration and purity of total RNA for each sample was determined by the Quant-iT RNA Assay Kit and Q32857 Qubit fluorometer (Carlsbad, Invitrogen, California, USA) and confirmed by optical density measurements at 260 and 280nm using a BioMate 5 UV-visible spectrophotometer (Thermo Spectronic, Waltham, Massachusetts, USA). The integrity of the extracted RNA was confirmed by electrophoresis under denaturating condition. RNA samples from each set of control and epileptic rats were processed in parallel under the same conditions. RT were performed on an iCycler Thermal Cycler PCR System (Bio-Rad Laboratories, Hercules, California, USA), the High Capacity cDNA Reverse Transcription Kit (P/N: 4368814; Applied Biosystems, ABI, California, USA) for synthesis of single-stranded cDNA. The cDNA synthesis was carried out by following manufacturer's protocol using random primers for 1 µg of starting RNA. Each RT reaction contained 1000 ng of extracted total RNA template and RT reagents. The 20 µl reactions were incubated in the iCycler Thermocycler in

thin-walled 0.2-µl PCR tubes for 10 min at 25°C, 120 min at 37°C, 5 s at 85°C, and then held at 4°C. The efficiency of the RT reaction and amount of input RNA template was determined by serial dilutions of input RNA. Each RNA concentration was reverse transcribed using the same RT reaction volume. The resulting cDNA template was subjected to quantitative real-time PCR (qrtPCR) real-time using Taqman-based Applied Biosystems gene expression assays, the TaqMan Fast Universal PCR Master Mix (ABI) and the StepOne Real-Time PCR System (ABI). Analysis of SV2A, SV2B and SV2C mRNA expression were carried out in a StepOne Real-Time PCR System using the validated TaqMan Gene Expression Assays for target genes. Gene expression analysis was performed using the TaqMan Gene Expression Assays Mm00486647_m1 for the target gene *Calb1* (RefSeq: NM_009788.4, amplicon size = 78 bp), Mm00812888_m1 for the target gene *Slc17a7* (RefSeq: NM_020309.3, amplicon size = 81 bp), Mm00491537_m1 for the target gene *Sv2a* (RefSeq: NM_022030.3, amplicon size = 79 bp), Mm00463805_m1 for the target gene *Sv2b* (RefSeq: NM_001109753.1, amplicon size = 88 bp), Mm01282622_m1 for the target gene *Sv2c* (RefSeq: NM_029210.1, amplicon size = 72 bp), and Mn01235831_m1 for the target gene mGluR2 (amplicon size 82 bp) and Mm99999915_g1 for the normalization gene glyceraldehyde-3-phosphate dehydrogenase *Gapdh* (RefSeq: NM_008084.2, amplicon size = 107 bp).

For qrtPCR analysis, each sample was run in triplicates. Each run included a no-template control to test for contamination of assay reagents. After a 94°C denaturation for 10 min, the reactions were cycled 40 times with a 94°C denaturation for 15s, and a 60°C annealing for 1 min. Three

types of controls aimed at detecting genomic DNA contamination in the RNA sample or during the RT or qrtPCR reactions were always included: a RT mixture without reverse transcriptase, a RT mixture including the enzyme but no RNA, negative control (reaction mixture without cDNA template). The data were collected and analyzed using OneStep Software (ABI). Relative quantification was performed using the comparative threshold (CT) method after determining the CT values for reference (*Gapdh*) and target (*sv2a, sv2b or sv2c, calb28 and Slc17a7*) genes in each sample sets according to the $2^{-\Delta\Delta Ct}$ method (ΔΔCT, delta-delta CT)[24,25] as described by the manufacturer (ABI; User Bulletin 2). Changes in mRNA expression level were calculated after normalization to *Gapdh*. As calibrator sample we used cDNA from arbitrarily selected control rat. The ΔΔCT method provides a relative quantification ratio according to calibrator that allows statistical comparisons of gene expression among samples. Values of fold changes in the control sample versus the post-SE samples represent averages from triplicate measurements. Changes in gene expression were reported as percent changes relative to controls. Data were analyzed by one-way analysis of variance (ANOVA) (followed by post-hoc analysis) or via paired *t*-test to check for statistically significant differences among the groups (significance *P* value was set at <0.05).

Results

Analysis of relative index of gene expression by TaqMan qPCR shows no significant differences in the expression of SV2A and SV2B between saline-injected controls (n=5) and SE-suffering mice (n=4) that were not treated with levetirecetam (0.97±0.13 vs 0.95±0.17 and 0.68±0.06 vs 0.76±0.1, for SV2A and SV2B respectively Fig. 1A). However, we detected a significant

122.24% increase in relative index for SV2C gene expression ($F=11.87$, $p<0.0001$ by One way ANOVA). Specifically, levels of SV2C increased from 0.63±0.05 in saline-injected group to 1.39±0.14 in mice suffering SE ($p<0.001$, Tukey post-hoc analysis). We also analyzed the expression of other genes that are known to be modified after SE including calbindin (calb28)[26,27], vesicular glutamate transporter type 1 (VGlut1)[18,28] and metabotropic glutamate receptor type 2 (Grm2)[22]. Our analysis revealed a no significant 25.8% reduction in expression of Calb28 between these two groups 1 month after SE (0.40±0.05 vs 0.29±0.02 , $p>0.05$). In addition, we detected a 37.4% increase in VGlut1 expression after SE (1.36±0.35) when compared to the control group (0.99±0.12) that was not statistically significant. Moreover, analysis of Grm2 revealed a significant 161.1% increase in animals that suffered SE (2.27±0.29) compared to controls (0.87±0.03, $p<0.001$ by Tukey post-hoc pairwise comparisons).

We then compared the changes in gene expression in animals treated with levetirecetam during 4 weeks after pilocarpine-induced SE. When compared to non-treated animals, treatment of saline-injected animals with levetirecetam induced non-significant 18% reduction in the expression of SV2A (0.80±0.07). Levetiracetam treatment of SE-suffering animals induced no significant changes in SV2A gene expression when compared to other groups (0.99±0.08). Analysis of variance using one way ANOVA for changes in SV2A expression revealed no significant changes among groups ($F=0.56$, $p=0.64$). Similarly, analysis of SV2B gene expression was not significant ($F=0.45$, $p=0.72$). Specifically, treatment with levetirecetam revealed no significant changes in saline-injected animals (0.69±0.03) or SE-suffering mice (0.77±0.03) when compared to non-treated saline-injected group (0.68+0.06) and SE-suffering group (0.76±0.10) (Figure 1A. In contrast, we detected a significant change in the expression of SV2C ($F=11.8$, $p<0.001$). In this case, post-hoc analysis indicate that treatment with levetirecetam did not significantly

changed SV2C expression in saline-injected group (0.55±0.05) when compared to non-treated animals (0.62±0.05) ($p>0.05$), however, treatment of SE-suffering group for 4 weeks with levetirecetam induced a significant 33.8% down-regulation of originally increased levels of SV2C expression in non-treated groups (1.39±0.14) to 0.92±0.17 in levetirecetam-treated SE suffering mice (Tukey post-hoc analysis, $p<0.05$) (Figure 1a). However, when compared to saline-injected animals, levels of SV2C in levetirecetam-treated SE suffering mice remained elevated compared to non-treated and levetirecetam-treated saline-injected groups (0.62±0.05 and 0.55±0.05 respectively) (Figure 1, b and c).

No statistically significant changes were detected for gene expression of Calb28 ($F=2.6$, $p=0.09$) and VGlut1 ($F=1.06$, $p=0.39$) by one way ANOVA analysis despite a 25.5% reduction of Calb28 expression in SE-suffering animals (0.39±0.05) when compared to saline-injected controls (0.29±0.02) (Figure 1a). Treatment with levetirecetam did not significantly changed expression of Calb28 (0.49±0.04) in saline-injected or SE-suffering mice (0.50±0.09) when compared to respective non-treated controls above (Figure 1b and c). In the case of VGluT1, there was a 37.4% increase in the expression of VGluT1 gene expression in SE group (1.36±0.12) when compared to saline-injected controls (0.99±0.35) (Figure 1a) but data was not significant in one way ANOVA. Treatment with levetirecetam did not induce significant changes in the levels of gene expression in saline-injected or SE suffering groups (1.0±0.15 *vs*. 1.38 ±0.19) (Figure 1d and e). In contrast, a significant change was detected for Grm2 gene expression ($F=10.7$, $p<0.0001$) among all groups. Specifically, induction of SE resulted in 161% upregulation of Grm2 1 month after pilocarpine injection (2.27±0.29) when compared to saline-injected group (0.87±0.03, Tukey honest test, $p<0.001$, Figure 1a). Treatment with levetiracetam induced a non-

significant 19.5% increase in the level of Grm2 expression in saline-treated group (1.04±0.05) while non-significant 10.38% reduction was detected in SE group (2.04±0.38) (Figure 1).

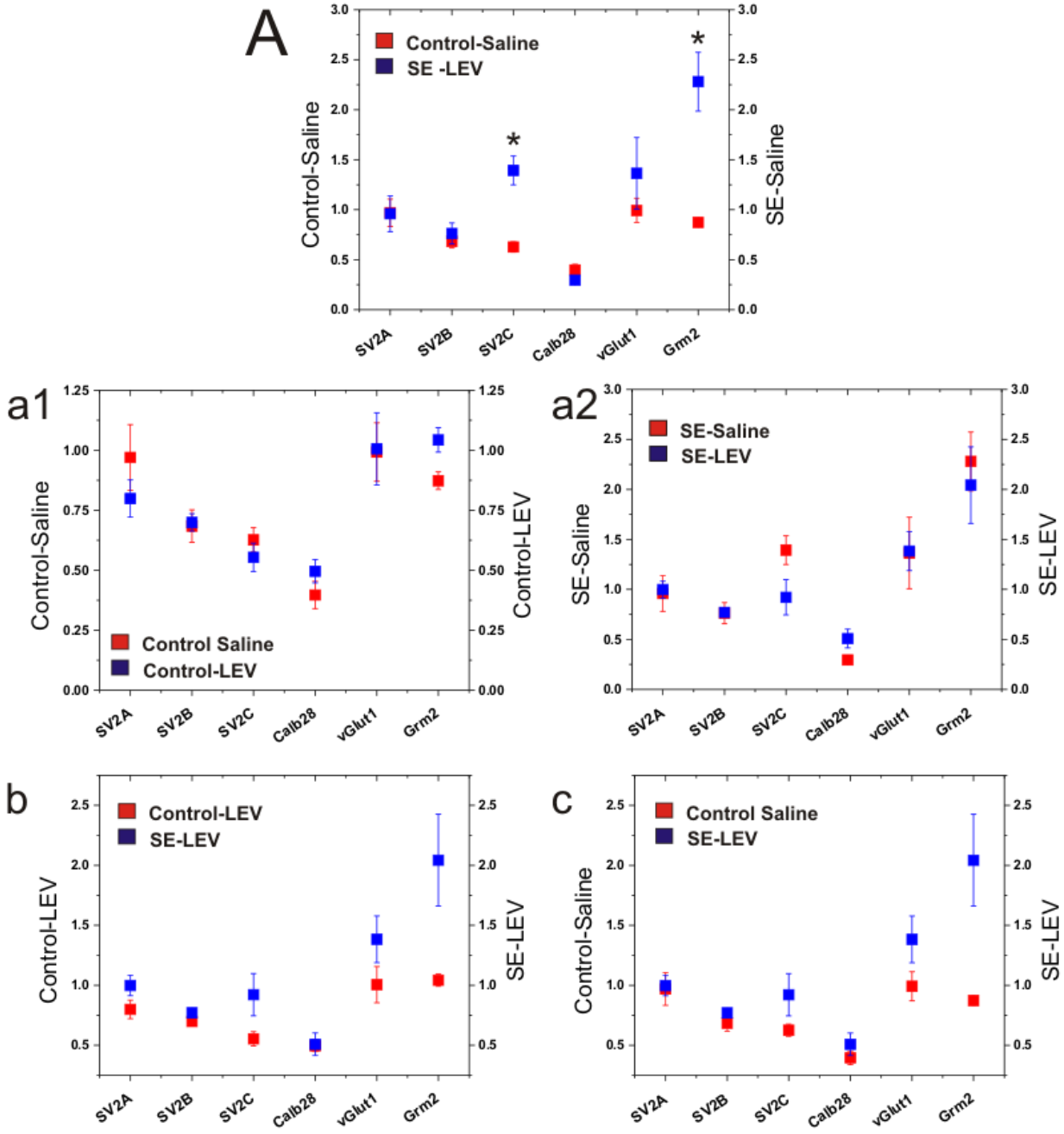

Figure 1. Graphs represent changes of relative quantification index of different transcripts by TaqMan qPCR assays in hippocampus of mice after *status epilepticus* (SE-Saline) compared to saline-injected control group (Control-Saline) and after the treatment of status epilepticus-suffering animals and saline-injected animals with levetirecetam (SE-LEV and control-LEV respectively).

Discussion

SV2 proteins are abundant synaptic vesicle integral membrane proteins expressed in two major (*SV2A* and SV2B) and one minor isoform (SV2C) whose membrane topology resembles that of transporter proteins [6,7]. Although SV2A is the major target of the antiepileptic drug levetiracetam, its function and partner molecules are still unknown [3,4,29,30]. Our study indicates that SV2C may play a role in the pathogenesis of epilepsy. We found that levels of SV2C transcripts increased after pilocarpine-induced *status epilepticus* consistent with previous studies in human epilepsy [12]. These authors reported that SV2C, which is weakly expressed or absent in the hippocampus of control cases, was overexpressed in 10/11 cases with classical MTS1A and mossy fibre sprouting but not in cases with other types of MTS. In our study, we demonstrated that changes in SV2C expression may start as early as 4 weeks after *status epilepticus*. Additional studies are necessary to determine the earlier time point fat which status epilepticus will induce an upregulation of SV2C. Interestingly, we also found that treatment with

levetirecetam during 4 weeks after *status epilepticus* reduced the expression of SV2C significantly but still levels remained above controls. These findings indicate that SV2C expression is also dysregulated during epileptogenesis but levels can be partially restored with pharmacological treatment with antiepileptic drugs. The significance of these findings for the pathogenesis of epilepsy remains to be elucidated considering that despite a high degree of homology between SV2 isoforms SV2A is the known molecular target of levetirecetam[2,3,8,29,30]. It is known that levetiracetam failed to control convulsions/seizures in acute models of epilepsy while exerting a very potent antiepileptic effect in chronic models of epilepsy [29-31]. It is currently unknown whether seizures can induce levetirecetam-binding splice variants of SV2C. This will be a therapeutically relevant finding since upregulation of SV2C in epilepsy will allow for increased pharmacological targets for levetirecetam and consequentially improve the pharmacological action of this antiepileptic drug when compared to SV2A expression which has been found to be reduced in previous studies using animal models of epilepsy and tissue from epileptic patients [10,12]. Interestingly, in our study, we failed to demonstrate a significant down-regulation of SV2A after *status epilepticus*, neither a significant effect of levetiractam on SV2A transcript levels in animals that suffered *status epilepticus*. The role of SV2A on epilepsy has been established by 3 facts: (1) SV2A is the sole molecular target for the antiepileptic drug levetiracetam (LEV)[1,32,33], (2) SV2A knockout mice exhibit severe seizures[34-36], and (3) down-regulation of SV2A has been reported in epilepsy [10,12]. SV2A is consistently reduced in mossy fibers in experimental MTLE and epileptic patients. Despite these compelling findings, the exact function of SV2A remains unknown. Hence, the molecular cascades and pathways mediating the action of loevetiracetam deserve further investigation. A major problem is the lack of functional assays to probe how levetiracetam interacts with and

modifies SV2A function. Moreover, the exact binding site of levetiracetam on the structure of SV2A has not been discovered yet.

The expression of S2V isoforms in neurochemically-distinct neuronal subtypes is also different in hippocampus. Although both SV2A and SV2C are expressed in mossy fibers, the expression of SV2A is also found in GABAergic terminals while SV2C is predominantly expressed in glutamatergic terminals [6,8]. It is possible that levetirecetam can binds to both SV2A and spliced or upregulated SV2C. Regardless, increases in SV2C expression after status epilepticus may play a role in the pathogenesis of epilepsy as a contributing or a compensatory molecular event that needs to be elucidated.

Acknowledgments

This work was supported by Department of Defense grants to E.R.G.S (Award W81XWH-11-1-0) and P.K. Stanton (Award W81XWH-11-1-0)

References

[1] Lynch BA, Lambeng N, Nocka K, Kensel-Hammes P, Bajjalieh SM, Matagne A *et al.* The synaptic vesicle protein SV2A is the binding site for the antiepileptic drug levetiracetam. *Proc Natl Acad Sci U S A* 2004; **101**: 9861-9866.

[2] Gillard M, Chatelain P, Fuks B. Binding characteristics of levetiracetam to synaptic vesicle protein 2A (SV2A) in human brain and in CHO cells expressing the human recombinant protein. *Eur J Pharmacol* 2006; **536**: 102-108.

[3] Klitgaard H, Verdru P. Levetiracetam: the first SV2A ligand for the treatment of epilepsy. *Expert Opin Drug Discov* 2007; **2**: 1537-1545.

[4] Krishna K, Raut AL, Gohel KH, Dave P. Levetiracetam. *J Assoc Physicians India* 2011; **59**: 656-658.

[5] Lynch JM, Tate SK, Kinirons P, Weale ME, Cavalleri GL, Depondt C *et al.* No major role of common SV2A variation for predisposition or levetiracetam response in epilepsy. *Epilepsy Res* 2009; **83**: 44-51.

[6] Bajjalieh SM, Frantz GD, Weimann JM, McConnell SK, Scheller RH. Differential expression of synaptic vesicle protein 2 (SV2) isoforms. *J Neurosci* 1994; **14**: 5223-5235.

[7] Bajjalieh SM, Peterson K, Shinghal R, Scheller RH. SV2, a brain synaptic vesicle protein homologous to bacterial transporters. *Science* 1992; **257**: 1271-1273.

[8] Bandala C, Miliar-Garcia A, Mejia-Barradas CM, Anaya-Ruiz M, Luna-Arias JP, Bazan-Mendez CI *et al.* Synaptic vesicle protein 2 (SV2) isoforms. *Asian Pac J Cancer Prev* 2012; **13**: 5063-5067.

[9] Dardou D, Dassesse D, Cuvelier L, Deprez T, De Ryck M, Schiffmann SN. Distribution of SV2C mRNA and protein expression in the mouse brain with a particular emphasis on the basal ganglia system. *Brain Res* 2011; **1367**: 130-145.

[10] van Vliet EA, Aronica E, Redeker S, Boer K, Gorter JA. Decreased expression of synaptic vesicle protein 2A, the binding site for levetiracetam, during epileptogenesis and chronic epilepsy. *Epilepsia* 2009; **50**: 422-433.

[11] Feng G, Xiao F, Lu Y, Huang Z, Yuan J, Xiao Z *et al.* Down-regulation synaptic vesicle protein 2A in the anterior temporal neocortex of patients with intractable epilepsy. *J Mol Neurosci* 2009; **39**: 354-359.

[12] Crevecoeur J, Kaminski RM, Rogister B, Foerch P, Vandenplas C, Neveux M *et al.* Expression pattern of synaptic vesicle protein 2 (SV2) isoforms in patients with temporal lobe epilepsy and hippocampal sclerosis. *Neuropathol Appl Neurobiol* 2014; **40**: 191-204.

[13] Upreti C, Otero R, Partida C, Skinner F, Thakker R, Pacheco LF *et al.* Altered neurotransmitter release, vesicle recycling and presynaptic structure in the pilocarpine model of temporal lobe epilepsy. *Brain* 2012; **135**: 869-885.

[14] Cavalheiro EA. The pilocarpine model of epilepsy. *Ital J Neurol Sci* 1995; **16**: 33-37.

[15] Mello LE, Cavalheiro EA, Tan AM, Kupfer WR, Pretorius JK, Babb TL *et al.* Circuit mechanisms of seizures in the pilocarpine model of chronic epilepsy: cell loss and mossy fiber sprouting. *Epilepsia* 1993; **34**: 985-995.

[16] Turski WA, Cavalheiro EA, Bortolotto ZA, Mello LM, Schwarz M, Turski L. Seizures produced by pilocarpine in mice: a behavioral, electroencephalographic and morphological analysis. *Brain Res* 1984; **321**: 237-253.

[17] Danzer SC, McNamara JO. Localization of brain-derived neurotrophic factor to distinct terminals of mossy fiber axons implies regulation of both excitation and feedforward inhibition of CA3 pyramidal cells. *J Neurosci* 2004; **24**: 11346-11355.

[18] Pacheco Otalora LF, Couoh J, Shigamoto R, Zarei MM, Garrido Sanabria ER. Abnormal mGluR2/3 expression in the perforant path termination zones and mossy fibers of chronically epileptic rats. *Brain Res* 2006; **1098**: 170-185.

[19] Garrido-Sanabria ER, Perez-Cordova MG, Colom LV. Differential expression of voltage-gated K+ currents in medial septum/diagonal band complex neurons exhibiting distinct firing phenotypes. *Neurosci Res* 2011; **70**: 361-369.

[20] Ermolinsky BS, Skinner F, Garcia I, Arshadmansab MF, Otalora LF, Zarei MM *et al.* Upregulation of STREX splice variant of the large conductance Ca2+-activated potassium (BK) channel in a rat model of mesial temporal lobe epilepsy. *Neurosci Res* 2011; **69**: 73-80.

[21] Oliveira MS, Skinner F, Arshadmansab MF, Garcia I, Mello CF, Knaus HG *et al.* Altered expression and function of small-conductance (SK) Ca(2+)-activated K+ channels in pilocarpine-treated epileptic rats. *Brain Res* 2010; **1348**: 187-199.

[22] Ermolinsky B, Pacheco Otalora LF, Arshadmansab MF, Zarei MM, Garrido-Sanabria ER. Differential changes in mGlu2 and mGlu3 gene expression following pilocarpine-induced status epilepticus: a comparative real-time PCR analysis. *Brain Res* 2008; **1226**: 173-180.

[23] Ermolinsky B, Arshadmansab MF, Pacheco Otalora LF, Zarei MM, Garrido-Sanabria ER. Deficit of Kcnma1 mRNA expression in the dentate gyrus of epileptic rats. *Neuroreport* 2008; **19**: 1291-1294.

[24] Pfaffl MW, Horgan GW, Dempfle L. Relative expression software tool (REST) for group-wise comparison and statistical analysis of relative expression results in real-time PCR. *Nucleic Acids Res* 2002; **30**: e36.

[25] Pfaffl MW. A new mathematical model for relative quantification in real-time RT-PCR. *Nucleic Acids Res* 2001; **29**: e45.

[26] Liu JX, Cao X, Liu Y, Tang FR. CCL28 in the mouse hippocampal CA1 area and the dentate gyrus during and after pilocarpine-induced status epilepticus. *Neurochem Int* 2012; **61**: 1094-1101.

[27] Carter DS, Harrison AJ, Falenski KW, Blair RE, DeLorenzo RJ. Long-term decrease in calbindin-D28K expression in the hippocampus of epileptic rats following pilocarpine-induced status epilepticus. *Epilepsy Res* 2008; **79**: 213-223.

[28] Pacheco Otalora LF, Hernandez EF, Arshadmansab MF, Francisco S, Willis M, Ermolinsky B *et al.* Down-regulation of BK channel expression in the pilocarpine model of temporal lobe epilepsy. *Brain Res* 2008; **1200**: 116-131.

[29] Kaminski RM, Gillard M, Klitgaard H. Targeting SV2A for Discovery of Antiepileptic Drugs. 2012.

[30] Abou-Khalil B. Levetiracetam in the treatment of epilepsy. *Neuropsychiatr Dis Treat* 2008; **4**: 507-523.

[31] Shetty AK. Prospects of Levetiracetam as a Neuroprotective Drug Against Status Epilepticus, Traumatic Brain Injury, and Stroke. *Front Neurol* 2013; **4**: 172.

[32] Rogawski MA. Molecular targets versus models for new antiepileptic drug discovery. *Epilepsy Res* 2006; **68**: 22-28.

[33] Pitkanen A. SV2A: more than just a new target for AEDs. *Epilepsy Curr* 2005; **5**: 14-16.

[34] Custer KL, Austin NS, Sullivan JM, Bajjalieh SM. Synaptic vesicle protein 2 enhances release probability at quiescent synapses. *J Neurosci* 2006; **26**: 1303-1313.

[35] Crowder KM, Gunther JM, Jones TA, Hale BD, Zhang HZ, Peterson MR *et al.* Abnormal neurotransmission in mice lacking synaptic vesicle protein 2A (SV2A). *Proc Natl Acad Sci U S A* 1999; **96**: 15268-15273.

[36] Janz R, Goda Y, Geppert M, Missler M, Sudhof TC. SV2A and SV2B function as redundant Ca2+ regulators in neurotransmitter release. *Neuron* 1999; **24**: 1003-1016.

Appendix #2

NEUROSCIENCE 2012

Print this Page for Your Records Close Window

Control/Tracking Number: 2012-S-11204-SfN
Activity: Scientific Abstract
Current Date/Time: 5/10/2012 12:59:34 AM

Levetiracetam inhibits excitatory drive onto dentate gyrus granule cells: Effects of SV2A gene dosage and mesial temporal lobe epilepsy.

AUTHOR BLOCK: *E. G. SANABRIA[1], L. F. PACHECO[2], L. M. RAMBO[2], J. M. RODRIGUEZ[2], C. UPRETI[3], P. K. STANTON[4];
[1]Biomedicine, Univ. of Texas Brownsville, BROWNSVILLE, TX; [2]Biomedicine, Univ. of Texas at Brownsville, Brownsville, TX; [3]Dept. of Cell Biol. & Anat., [4]Cell Biol. & Anat. and Dept. of Neurol., New York Med. Col., Valhalla, NY

Abstract:
Levetiracetam (LEV) is a new type of antiepileptic drug (AED) exhibiting selective seizure protection in chronic animal models of epilepsy. LEV binds to the synaptic vesicle protein SV2A indicating a presynaptic site of action to counter hyperexcitability. In this study, we evaluated the in vitro effects of LEV on excitatory synaptic transmission in the pilocarpine model of mesial temporal lobe epilepsy (MTLE). It has been reported that expression levels of SV2A decline during the course of human epilepsy and in experimental MTLE. We hypothesized that LEV action may be differentially affected during epileptogenesis and in transgenic mice with altered SV2A expression. For this purpose, we assessed LEV effects on excitatory synaptic transmission in slices from pilocarpine-treated epileptic and control mice with different SV2A genotypes. AMPA receptor-mediated miniature excitatory postsynaptic currents (mEPSCs) were recorded in dentate granule cells using the whole cell patch-clamp configuration. Different concentrations of LEV (5, 50 and 100 microM) were bath applied to evaluate effects on mEPSC frequency and amplitude. Double SV2A/SV2B knockout (KO) mice were not included in this study due to early life mortality. 14% of SV2A heterozygous mice exhibited spontaneous seizures (epileptic). LEV induced a significant decrease of mEPSC frequency in granule cells from SV2A wild-type (26% reduction) and heterozygous mice (37% reduction) when compared to pre-drug baseline. LEV (100 microM) failed to modify mEPSC frequency in ~ 60% of the slices from SV2A KO/SV2B wild control mice while a paradoxical increase of mEPSC frequency was detected in the rest of the slices. In addition, LEV induced a significant decrease of mEPSC frequency (51.7% reduction, Paired T-test, $P<0.05$) in slices from SV2A/SV2B (wild-type) mice sacrificed 2-4 months after status epilepticus. LEV exerted no significant effects on mEPSC amplitude in all experimental groups. Our findings indicate that LEV acts presynaptically to inhibit the glutamatergic drive onto dentate granule cells in control and chronically epileptic mice but this effect was more pronounced in epileptic slices. Lack of SV2A expression (SV2A KO) occluded the inhibitory effect of LEV on excitatory transmission in a subset of animals while a paradoxical increase of glutamate release was detected in another group. Although LEV selectively binds SV2A in normal brain, it is possible that compensatory changes (i.e. abnormal splicing) of remaining SV2B and

SV2C proteins may provide additional non-SV2A LEV binding sites in SV2A KO and in epileptic mice with significant implications for the development of novel LEV-like AEDs.

:

Presentation Preference (Complete): Poster Only
Linking Group (Complete): None selected
Nanosymposium Information (Complete):
Theme and Topic (Complete): C.07.k. Anticonvulsant and antiepileptic therapies ; C.07.e. Synaptic mechanisms
Keyword (Complete): EPILEPSY ; SYNAPTIC TRANSMISSION ; PRESYNAPTIC
Support (Complete):
Support: Yes
Grant/Other Support: : DoD Grant PR100534
Grant/Other Support: : DoD Grant PR100534P1
Grant/Other Support: : NIH Grant NS063950
Grant/Other Support: : NIH Grant GM081109

Special Requests (Complete):
Is the first (presenting) author of this abstract a high school or undergraduate student?: None

Religious Conflict?: No Religious Conflict
Additional Conflict?: No

Status: Complete

ABSTRACT:

Levetiracetam modify synaptic vesicle protein expression and reduce abnormally augmented presynaptic vesicular release after pilocarpine-induced status epilepticus.

Emilio R. Garrido-Sanabria, Luis F. Pacheco, Vinicius Funck, Nuri Ruvalcaba, Jose M. Rodriguez, Daniela Taylor, Rubi Garcia, Jose Carlos Martinez, Cecilia Castro, Chirag Upreti, Patric K. Stanton,

Epilepsy is a neurological disorder affecting 2% of the population. Levetiracetam (LEV) is a new antiepileptic drug that binds to presynaptic vesicular protein SV2A; however, the mechanism of action remains unknown. Abnormal presynaptic release of glutamate has been considered one of the seizure-induced alterations in epilepsy. Previous studies have shown abnormally enhanced vesicular release in hippocampal presynaptic boutons in epilepsy. Here, we investigate if chronic treatment with LEV will modify abnormal presynaptic vesicle release and synaptic vesicle proteins (SV2A, SV2B, and SV2C) and transcripts expression after pilocarpine-induced *status epilepticus*. Different groups of control and epileptic mice were treated with LEV (experimental) or saline solution (control). To induce chronic epilepsy, the pilocarpine model of temporal lobe epilepsy was developed in synaptopHluorin (SpH)-expressing transgenic mice. Protein samples were extracted and immoblottings were developed to assess expression of SV2A, SV2B, and SV2C. Gene expression was analyzed using TaqMan real time quantitative PCR assays. Imaging of electrically-evoked release was performed by confocal imaging in brain slices. Time-lapsed images were obtained from the CA3 stratum lucidum in hippocampus. For this analysis, we included 92 synaptic boutons from 7 slices in the control non-treated group, 148 boutons from 12 slices in control (treated with LEV), 115 boutons from 7 slices in epileptic (non-treated group) and 100 boutons from 6 slices in epileptic group chronically treated with LEV. As previously reported, epileptic SpH mice exhibited an increase in vesicular release when compared to control group. In contrast, LEV-treated SpH epileptic mice exhibited a reduction in release when compared to control animals treated with same. SV2A protein expression was down-regulated 22.9% in epileptic mice but after treatment with LEV SV2A expression increased 40% above controls. In contrast, sv2a transcripts were not upregulated in LEV-treated *status epilepticus* group. No significant changes were detected in sv2b gene expression among the groups. However, a significant change was observed for sv2c gene expression (ANOVA, $p>0.0001$, $F=11.87$) where *status epilepticus* induced a significant sv2c upregulation when compared to saline injected control group. Interestingly, in contrast to SV2C protein expression, chronic treatment with LEV induced a significant 33.8% and 11.7% reduction of sv2c levels in treated *status epilepticus* and control groups respectively when compared to saline-injected status epilepticus and control groups. Levetiracetam partially corrected abnormal SV2A and SV2C expression and inhibited abnormally enhanced vesicular release in epileptic SpH mice indicating that the anti-epileptic action and effectiveness in chronically epileptic tissue may be associated with changes in the presynaptic vesicular release machinery and its own pharmacological targets.

Abstract submitted to the Society for Neuroscience Meeting that will be held in Nov 9-13,

San Diego, California

Inhibitory action of levetiracetam on CA1 population spikes and dentate gyrus excitatory transmission in pilocarpine-treated chronic epileptic rats. **E. G. SANABRIA**[1], L. PACHECO[1], J. ZAVALETA[1], F. SHRIVER[1], L. M. RAMBO[2], C. UPRETI[3], **P. K. STANTON**[3];

Control/Tracking Number: 2013-S-12910-SfN
Activity: Scientific Abstract
Current Date/Time: May 9, 2013 12:07:38 PM EDT

Inhibitory action of levetiracetam on CA1 population spikes and dentate gyrus excitatory transmission in pilocarpine-treated chronic epileptic rats.

E. G. SANABRIA[1], L. PACHECO[1], J. ZAVALETA[1], F. SHRIVER[1], L. M. RAMBO[2], C. UPRETI[3], **P. K. STANTON**[3];
[1]Biomedicine, Univ. of Texas Brownsville, BROWNSVILLE, TX; [2]Dept. de Fisiologia e Farmacologia, Univ.

Federal de Santa Maria, Santa Maria, Brazil; [3]Cell Biol. & Anatatomy, Dept. Neurol., New York Med. Col., Valhalla, NY

Abstract:

The presynaptic target for Levetiracetam (LEV) has been identified as synaptic vesicle SV2A proteins in presynaptic terminals; however, the mechanisms of LEV's antiepileptic action remain unclear. Previous studies have shown a reduction of SV2A expression in both animal models and human suffering mesial temporal lobe epilepsy (MTLE). However, in vivo treatment with LEV appears to be still effective in those conditions in ameliorating seizures. In this study, we evaluated the in vitro effects of LEV on excitability and excitatory synaptic transmission in the pilocarpine model of mesial temporal lobe epilepsy (MTLE). In this study, we investigated the action of LEV on (a) population spikes recorded in CA1 area and (b) excitatory synaptic transmission onto dentate gyrus of control versus chronically epileptic rats obtained by the pilocarpine model of MTLE. For this purpose, we used extracellular potential recordings in acutely dissociated slices. Slices were pre-incubated in 300 microM of LEV for 3 hours prior recordings. LEV was also applied in the bath during recording sections. Field excitatory postsynaptic potentials (fEPSP) were evoked by different paradigms of repetitive stimuli of perforant path (e.g. 10@20Hz). Pre-incubation with LEV induced a 20% and 10% reduction in amplitude of CA1 population spikes in slices from control and epileptic rats respectively relative to non-treated slices. LEV induced a 37.2% and 49% significant reduction in the amplitude of the summated fEPSPs in a 20Hz train evoked by perforant path stimulations in both control and epileptic groups respectively ($df=9$, $p< 0.0001$ by paired T-test) compare to baseline. Significant changes were also detected in the first four fEPSP responses in the train with a non-significant reduction of remaining 6 fEPSPs (ANOVA repetitive Test, $p<0.01$ for both groups followed by pairwise Tukey post-hoc test). These results indicate that LEV is effective in reducing in vitro excitability and excitatory synaptic transmission in both control and epileptic groups (despite possible changes in SV2A expression). Further studies are in progress to determine presynaptic mechanisms involved in this inhibitory effect.

Presentation Preference (Complete): Poster Only

Theme and Topic (Complete): C.08.k. Anticonvulsant and antipileptic therapies; C.08.e. Synaptic mechanisms

Keyword (Complete): EPILEPSY ; SYNAPTIC TRANSMISSION ; HYPEREXCITABILITY

Grant/Other Support: DoD W81XWH-11-1-0356

Grant/Other Support: DoD W81XWH-11-1-0357

Anat., [4]Cell Biol. & Anat. Dept. of Neurol., New York Med. Col., Valhalla, NY

Abstract: Levetiracetam (LEV) is a new type of antiepileptic drug (AED) exhibiting selective seizure protection in chronic animal models of epilepsy. LEV binds selectively to the synaptic vesicle protein SV2A, indicating a presynaptic site of action to counter hyperexcitability. In this study, we evaluated the in vitro effects of LEV on excitatory synaptic transmission in the pilocarpine model of mesial temporal lobe epilepsy (MTLE). It has been reported that expression levels of SV2A decline during the course of human epilepsy and in experimental MTLE. We hypothesized that LEV action may be differentially affected during epileptogenesis and in transgenic mice with altered SV2A expression. For this purpose, we assessed LEV effects on excitatory synaptic transmission in slices from pilocarpine-treated epileptic and control mice with different SV2A genotypes, by recording AMPA receptor-mediated miniature excitatory postsynaptic currents (mEPSCs) in dentate granule cells using whole cell patch-clamp recording. Different concentrations of LEV (5, 50 and 100 microM) were bath applied to evaluate effects on mEPSC frequency and amplitude. Double SV2A/SV2B knockout (KO) mice were not included in this study due to early life mortality. 14% of SV2A heterozygous KO mice exhibited spontaneous seizures (epileptic). LEV induced a significant decrease of mEPSC frequency in granule cells from SV2A wild-type (26% reduction) and heterozygous mice (37% reduction) when compared to pre-drug baseline. LEV (100 μM) failed to modify mEPSC frequency in ~ 60% of slices from SV2A KO mice, while a paradoxical increase of mEPSC frequency was detected in the rest of the slices. LEV still induced a significant decrease of mEPSC frequency (51.7% reduction, paired t-test, $P<0.05$) in slices from SV2A/SV2B (wild-type) mice sacrificed 2-4 months after status epilepticus. LEV exerted no significant effects on mEPSC amplitude in any group. Our findings indicate that LEV acts presynaptically to inhibit glutamatergic drive onto dentate granule cells in control and chronically epileptic mice, but that this effect is more pronounced in epileptic slices. Lack of SV2A expression occluded the inhibitory effect of LEV on excitatory transmission in a subset of animals, while a paradoxical increase of glutamate release was detected in the rest. Although LEV selectively binds SV2A in normal brain, it is possible that compensatory changes (i.e. abnormal splicing) of remaining SV2B and SV2C proteins may provide additional non-SV2A LEV binding sites in SV2A KO and in epileptic mice with significant implications for the development of novel LEV-like AEDs.

Support: DoD Grant PR100534

DoD Grant PR100534P1

poster hall. Failure to comply may make your abstract ineligible for a poster in the future. We look forward to your participation in what promises to be a very successful meeting!

Sincerely,

2014 AES Scientific Program Committee

Activity: Scientific Abstract
Current Date/Time: May 9, 2013 12:07:38 PM EDT

Inhibitory action of levetiracetam on CA1 population spikes and dentate gyrus excitatory transmission in pilocarpine-treated chronic epileptic rats.

E. G. SANABRIA[1], L. PACHECO[1], J. ZAVALETA[1], F. SHRIVER[1], L. M. RAMBO[2], C. UPRETI[3], **P. K. STANTON**[3];
[1]Biomedicine, Univ. of Texas Brownsville, BROWNSVILLE, TX; [2]Dept. de Fisiologia e Farmacologia, Univ. Federal de Santa Maria, Santa Maria, Brazil; [3]Cell Biol. & Anatatomy, Dept. Neurol., New York Med. Col., Valhalla, NY

Abstract:
The presynaptic target for Levetiracetam (LEV) has been identified as synaptic vesicle SV2A proteins in presynaptic terminals; however, the mechanisms of LEV's antiepileptic action remain unclear. Previous studies have shown a reduction of SV2A expression in both animal models and human suffering mesial temporal lobe epilepsy (MTLE). However, in vivo treatment with LEV appears to be still effective in those conditions in ameliorating seizures. In this study, we evaluated the in vitro effects of LEV on excitability and excitatory synaptic transmission in the pilocarpine model of mesial temporal lobe epilepsy (MTLE). In this study, we investigated the action of LEV on (a) population spikes recorded in CA1 area and (b) excitatory synaptic transmission onto dentate gyrus of control versus chronically epileptic rats obtained by the pilocarpine model of MTLE. For this purpose, we used extracellular potential recordings in acutely dissociated slices. Slices were pre-incubated in 300 microM of LEV for 3 hours prior recordings. LEV was also applied in the bath during recording sections. Field excitatory postsynaptic potentials (fEPSP) were evoked by different paradigms of repetitive stimuli of perforant path (e.g. 10@20Hz). Pre-incubation with LEV induced a 20% and 10% reduction in amplitude of CA1 population spikes in slices from control and epileptic rats respectively relative to non-treated slices. LEV induced a 37.2% and 49% significant reduction in the amplitude of the summated fEPSPs in a 20Hz train evoked by perforant path stimulations in both control and epileptic groups respectively ($df=9$, $p< 0.0001$ by paired T-test) compare to baseline. Significant changes were also detected in the first four fEPSP responses in the train with a non-significant reduction of remaining 6 fEPSPs (ANOVA repetitive Test, $p<0.01$ for both groups followed by pairwise Tukey post-hoc test). These results indicate that LEV is effective in reducing in vitro excitability and excitatory synaptic transmission in both control and epileptic groups (despite possible changes in SV2A expression). Further studies are in progress to determine presynaptic mechanisms involved in this inhibitory effect.

Presentation Preference (Complete): Poster Only
Theme and Topic (Complete): C.08.k. Anticonvulsant and antipileptic therapies; C.08.e. Synaptic mechanisms
Keyword (Complete): EPILEPSY ; SYNAPTIC TRANSMISSION ; HYPEREXCITABILITY
Grant/Other Support: DoD W81XWH-11-1-0356
Grant/Other Support: DoD W81XWH-11-1-0357

Program#/Poster#: 656.26/N11

Presentation Title: Levetiracetam inhibits excitatory drive onto dentate gyrus granule cells: Effects of SV2A gene dosage and mesial temporal lobe epilepsy.

Presentation time: Tuesday, Oct 16, 2012, 2:00 PM - 3:00 PM

Authors: *E. G. SANABRIA[1], L. F. PACHECO[2], L. M. RAMBO[2], J. M. RODRIGUEZ[2], C. UPRETI[3], P. K. STANTON[4];
[1]Biomedicine, Univ. of Texas Brownsville, BROWNSVILLE, TX; [2]Biomedicine, Univ. of Texas at Brownsville, BROWNSVILLE, TX; [3]Dept. of Cell Biol. & Anat., [4]Cell Biol. & Anat. Dept. of Neurol., New York Med. Col., Valhalla, NY

Abstract: Levetiracetam (LEV) is a new type of antiepileptic drug (AED) exhibiting selective seizure protection in chronic animal models of epilepsy. LEV binds selectively to the synaptic vesicle protein SV2A, indicating a presynaptic site of action to counter hyperexcitability. In this study, we evaluated the in vitro effects of LEV on excitatory synaptic transmission in the pilocarpine model of mesial temporal lobe epilepsy (MTLE). It has been reported that expression levels of SV2A decline during the course of human epilepsy and in experimental MTLE. We hypothesized that LEV action may be differentially affected during epileptogenesis and in transgenic mice with altered SV2A expression. For this purpose, we assessed LEV effects on excitatory synaptic transmission in slices from pilocarpine-treated epileptic and control mice with different SV2A genotypes, by recording AMPA receptor-mediated miniature excitatory postsynaptic currents (mEPSCs) in dentate granule cells using whole cell patch-clamp recording. Different concentrations of LEV (5, 50 and 100 microM) were bath applied to evaluate effects on mEPSC frequency and amplitude. Double SV2A/SV2B knockout (KO) mice were not included in this study due to early life mortality. 14% of SV2A heterozygous KO mice exhibited spontaneous seizures (epileptic). LEV induced a significant decrease of mEPSC frequency in granule cells from SV2A wild-type (26% reduction) and heterozygous mice (37% reduction) when compared to pre-drug baseline. LEV (100 μM) failed to modify mEPSC frequency in ~ 60% of slices from SV2A KO mice, while a paradoxical increase of mEPSC frequency was detected in the rest of the slices. LEV still induced a significant decrease of mEPSC frequency (51.7% reduction, paired t-test, $P<0.05$) in slices from SV2A/SV2B (wild-type) mice sacrificed 2-4 months after status epilepticus. LEV exerted no significant effects on mEPSC amplitude in any group. Our findings indicate that LEV acts presynaptically to inhibit glutamatergic drive onto dentate granule cells in control and chronically epileptic mice, but that this effect is more pronounced in epileptic slices. Lack of SV2A expression occluded the inhibitory effect of LEV on excitatory transmission in a subset of animals, while a paradoxical increase of glutamate release was detected in the rest. Although LEV selectively binds SV2A in normal brain, it is possible that compensatory changes (i.e. abnormal splicing) of remaining SV2B and SV2C proteins may provide additional non-SV2A LEV binding sites in SV2A KO and in epileptic mice with significant implications for the development of novel LEV-like AEDs.

Support: DoD Grant PR100534

DoD Grant PR100534P1

Emilio Garrido Sanabria

From: cjohansson@aesnet.org
Sent: Wednesday, August 20, 2014 12:55 PM
To: Emilio Garrido Sanabria
Subject: AES 2014: Poster Notice

Dear Emilio Garrido,

We are pleased to inform you that your abstract, control ID # 2031171, has been accepted for a poster presentation at the 2014 Annual Meeting of the American Epilepsy Society. The meeting will be held December 5 - 9 in Seattle, Washington at the Washington State Convention Center. Poster Sessions are scheduled on Saturday, Sunday and Monday, December 6 - 8 at the Convention Center in Hall 4B, Level Four.

Below is your poster presentation assignment. Your poster session number reflects the poster session you are scheduled for (i.e., 1.001 is in Poster Session 1). Please also inform your co-authors of this acceptance. You should plan on being at your poster during the assigned author present time. If you are not able to do so, please make arrangements with a co-author to attend the session.

Title: Levetiracetam modify synaptic vesicle protein expression and reduce abnormally augmented presynaptic vesicular release after pilocarpine-induced status epilepticus.

Date: December 6, 2014

Poster Session #: 1.295

Tables beneath the poster board will not be available. We suggest you bring a plastic sleeve in which to place any handouts you may have. You may then tack this sleeve to the board so the handouts are readily available.

QR codes that link to pharmaceutical company websites are prohibited on the posters in the poster hall.

Poster tours will be held again this year. Please note that your poster may be included on a tour. These are small groups led by selected tour leaders.

You may upload your poster as a PDF file to be viewed on the AES website. Accept the poster invite and you will see where you can upload a PDF of your poster. This ePoster upload is optional and is not required. Please click on the "view invitation link" below to upload your ePoster.

View invitation

For further details about poster set up and presentation times, and to access the Annual Meeting Brochure, visit the Annual Meeting page on the AES website www.aesnet.org

All presenters are required to register for the Annual Meeting and no one will be admitted to the poster sessions without a badge. Registration details are also available on the Annual Meeting page on the AES website www.aesnet.org.

If for any reason you need to withdraw your poster, please notify Cindy Johansson at the AES Office immediately via email at cjohansson@aesnet.org. Please note that empty poster boards are unwelcome in the

poster hall. Failure to comply may make your abstract ineligible for a poster in the future. We look forward to your participation in what promises to be a very successful meeting!

Sincerely,

2014 AES Scientific Program Committee

ABSTRACT:

Levetiracetam modify synaptic vesicle protein expression and reduce abnormally augmented presynaptic vesicular release after pilocarpine-induced status epilepticus.

Emilio R. Garrido-Sanabria, Luis F. Pacheco, Vinicius Funck, Nuri Ruvalcaba, Jose M. Rodriguez, Daniela Taylor, Rubi Garcia, Jose Carlos Martinez, Cecilia Castro, Chirag Upreti, Patric K. Stanton,

Epilepsy is a neurological disorder affecting 2% of the population. Levetiracetam (LEV) is a new antiepileptic drug that binds to presynaptic vesicular protein SV2A; however, the mechanism of action remains unknown. Abnormal presynaptic release of glutamate has been considered one of the seizure-induced alterations in epilepsy. Previous studies have shown abnormally enhanced vesicular release in hippocampal presynaptic boutons in epilepsy. Here, we investigate if chronic treatment with LEV will modify abnormal presynaptic vesicle release and synaptic vesicle proteins (SV2A, SV2B, and SV2C) and transcripts expression after pilocarpine-induced *status epilepticus*. Different groups of control and epileptic mice were treated with LEV (experimental) or saline solution (control). To induce chronic epilepsy, the pilocarpine model of temporal lobe epilepsy was developed in synaptopHluorin (SpH)-expressing transgenic mice. Protein samples were extracted and immoblottings were developed to assess expression of SV2A, SV2B, and SV2C. Gene expression was analyzed using TaqMan real time quantitative PCR assays. Imaging of electrically-evoked release was performed by confocal imaging in brain slices. Time-lapsed images were obtained from the CA3 stratum lucidum in hippocampus. For this analysis, we included 92 synaptic boutons from 7 slices in the control non-treated group, 148 boutons from 12 slices in control (treated with LEV), 115 boutons from 7 slices in epileptic (non-treated group) and 100 boutons from 6 slices in epileptic group chronically treated with LEV. As previously reported, epileptic SpH mice exhibited an increase in vesicular release when compared to control group. In contrast, LEV-treated SpH epileptic mice exhibited a reduction in release when compared to control animals treated with same. SV2A protein expression was down-regulated 22.9% in epileptic mice but after treatment with LEV SV2A expression increased 40% above controls. In contrast, sv2a transcripts were not upregulated in LEV-treated *status epilepticus* group. No significant changes were detected in sv2b gene expression among the groups. However, a significant change was observed for sv2c gene expression (ANOVA, $p>0.0001$, $F=11.87$) where *status epilepticus* induced a significant sv2c upregulation when compared to saline injected control group. Interestingly, in contrast to SV2C protein expression, chronic treatment with LEV induced a significant 33.8% and 11.7% reduction of sv2c levels in treated *status epilepticus* and control groups respectively when compared to saline-injected status epilepticus and control groups. Levetiracetam partially corrected abnormal SV2A and SV2C expression and inhibited abnormally enhanced vesicular release in epileptic SpH mice indicating that the anti-epileptic action and effectiveness in chronically epileptic tissue may be associated with changes in the presynaptic vesicular release machinery and its own pharmacological targets.

Conference Portal › AbstractsForm: MHSRS-15-1061

2015 MHSRS Abstract Submission Form

Close

Abstract ID: MHSRS-15-1061 * Required Field

Submitter	**Affiliation:** *	ACADEMIA		
	Status: *	Civilian		
	Salutation: *	Dr.		
	First Name: *	Emilio	**Last Name:** *	Garrido Sanabria
	Email: *	ergs2009@gmail.com		
	Alt. Email:	ergs2009@gmail.com		
	Phone: *	9568825053		
	Country: *	United States		
	Organization: *	University of Texas at Brownsville		
	City: *	Brownsville, TX		
	State/Province:	TX	**Zip Code:**	78521
	Presentation Author Same as Submitter? Yes			
Presentation Author	**Affiliation:** *	ACADEMIA		
	Status: *	Civilian		
	Salutation: *	Dr.		
	First Name: *	Emilio	**Last Name:** *	Garrido Sanabria
	Email: *	emilio.garrido@utb.edu		
	Alternate Email:	emilio.garrido@utb.edu		
	Phone: *	9568825053		
	Country: *	United States		
	Organization: *	University of Texas at Brownsville		
	City: *	Brownsville		
	State/Province:	TX	**Zip Code:**	78520

Co-Authors

Luis F. Pacheco, PhD[1], Vinicius Funck, PhD[1], Nuri Ruvalcaba[1], Samantha Gomez[1], Aliya Sharif[1], Jose M. Rodriguez[1], Daniela Taylor[1], Rubi Garcia[1], Chirag Upreti[2], Patric K. Stanton[2], Emilio R. Garrido-Sanabria[1]

[1]University of Texas at Brownsville

[2]New York Medical College

Research Topic Area *

Neurotrauma/Brain Injury

Young Investigator Competition? No

Abstract Category *

Poster Only

Title of Abstract *

Abnormal upregulation of SV2C after pilocarpine-induced seizures is restored after treatment with antiepileptic drug levetirecetam.

Abstract *

(Abstract must contain background, methods, results, and conclusion section)

May we publish your abstract? Yes

Background, Temporal lobe epilepsy is a devastating neurological condition. Seizures can affect the expression of numerous molecules that participate in the pathogenesis of epilepsy. In this study, we investigate whether status epilepticus affect the expression of synaptic proteins and the effect of chronic levetirecetam treatment on status epilepticus-induced synaptic vesicle protein abnormalities. Methods: For this purpose, the pilocarpine model of epilepsy was developed in mice. The groups consisted of control (no status epilepticus) animals treated with saline (I) and animal suffering status epilepticus injected with saline (II), control (no status epilepticus) animals treated with levetirecetam for 30 days and animal suffering status epilepticus treated with levetirecetam for 30 days. After treatment, animals were sacrificed and proteins and mRNA was isolated for Western blotting and TaqMan-based real-time PCR assays to detect relative changes in protein and transcript expression of synaptic vesicle protein subtypes SV2A, SV2B, SV2C and vesicular Glutamate transporter type 1 among the different groups. Results: No significant changes were found for the expression of SV2A and SV2B among groups, however, status epilepticus induced a significant (p<0.01) up regulation of 122.24% in the expression of SV2C compared to saline-injected controls. Treatment with levetiracetam 100 ul/g resulted in a decrease in the expression of SV2C in both control and status epilepticus-suffering mice. Expression of SV2C was significantly reduced 88.34% compared to saline-treated status epilepticus group. Conclusion: SV2A is the binding site of levetiracetam and has been proposed as the molecular target in the mechanism of action of this antiepileptic drug. While the mechanism of action of levetirecetam has been associated with SV2A, our results indicate that another synaptic vesicle protein SV2C that is specifically

expressed in glutamatergic terminals may be involved in the pathogenesis of epilepsy and the antiepileptic action of levetieracetam. Status epilepticus upregulate the expression of SV2C while chronic treatment with levetirecetam restore levels of this target indicating that this may be an antiepileptic mechanisms of action of this drug that will reduce presynaptic release of neurotransmitters like glutamate and hippocampal hyperexcitability in epilepsy.

Learning Objectives *
(What should the attendee learn from this presentations? Enter at least 2, but no more than 3 learning objectives).

***1.** Epilepsy affect expresison of synaptic vesicle proteins

***2.** Antiepileptic drug levetiracetam restored affected levels of expression for a selective synaptic vesicle protein SV2C

3.

Media Communications
(Provide an organizational point of contact for any media/public affairs questions related to your abstract/follow-on presentation)

Salutation: Dr.

First Name: Emilio **Last Name:** Garrido

Email: ergs2009@gmail.com

Close

Version: 2.0
Created at 4/7/2015 3:54 PM by Emilio Garrido
Last modified at 4/7/2015 3:54 PM by Emilio Garrido

Appendix #3

RAT - SE #7 DOB 02.07.2012 – Pilo 03.12.2012

Cell#1 CBZ – 04.09.2012 – mEPSC (x20)

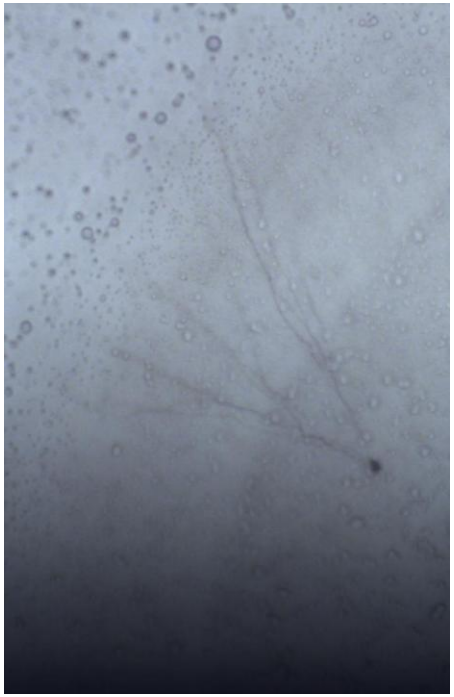

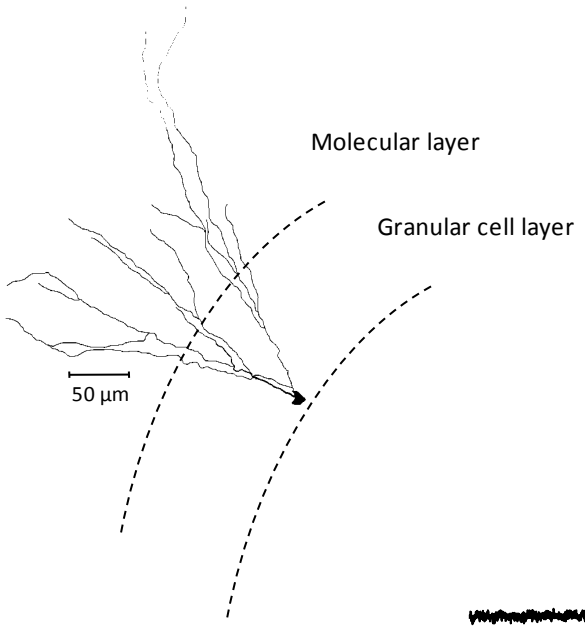

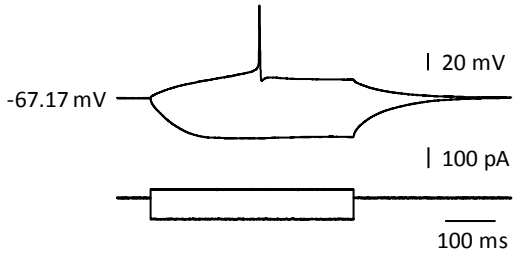

RAT - SE #7 DOB 02.07.2012 – Pilo 03.12.2012

Cell#2 CBZ – 04.09.2012 – mEPSC (x20)

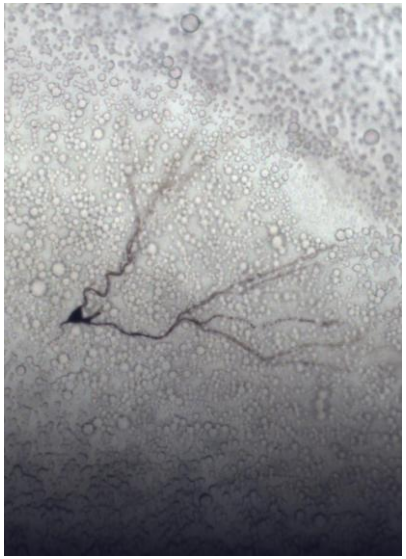

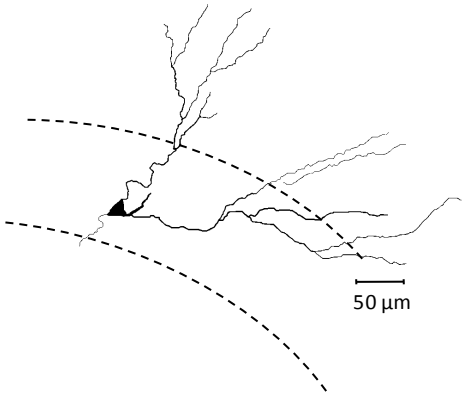

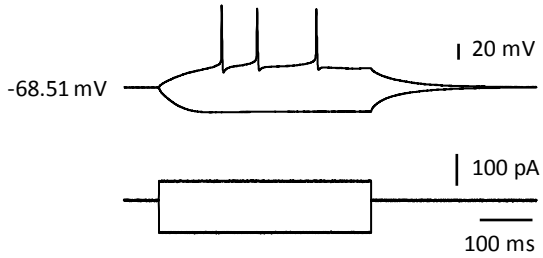

RAT - SE #7 DOB 02.07.2012 – Pilo 03.12.2012

Cell#3 CBZ – 04.09.2012 – mEPSC (x20)

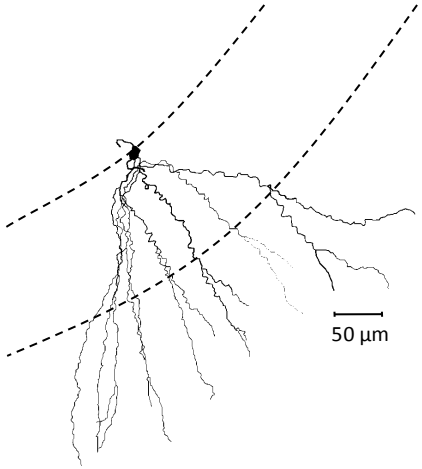

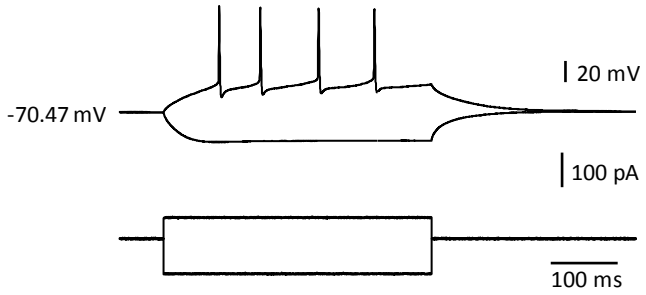

RAT - SE #7 DOB 02.07.2012 – Pilo 03.12.2012

Cell#4 CBZ – 04.09.2012 – mEPSC (x20)

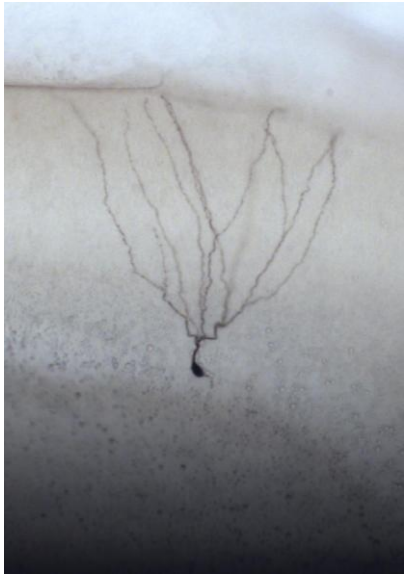

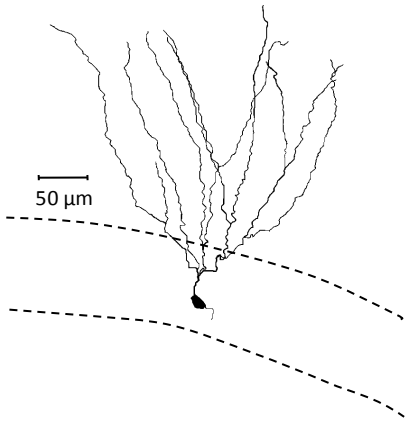

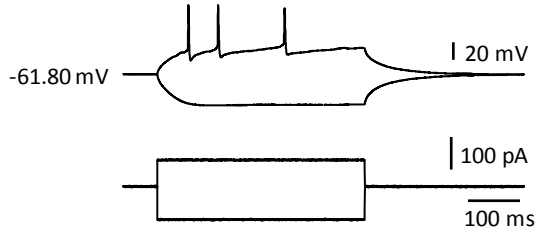

RAT - SE #2 DOB 02.08.2012 – Pilo 03.12.2012

Cell#5 CBZ – 04.11.2012 – mEPSC (x20)

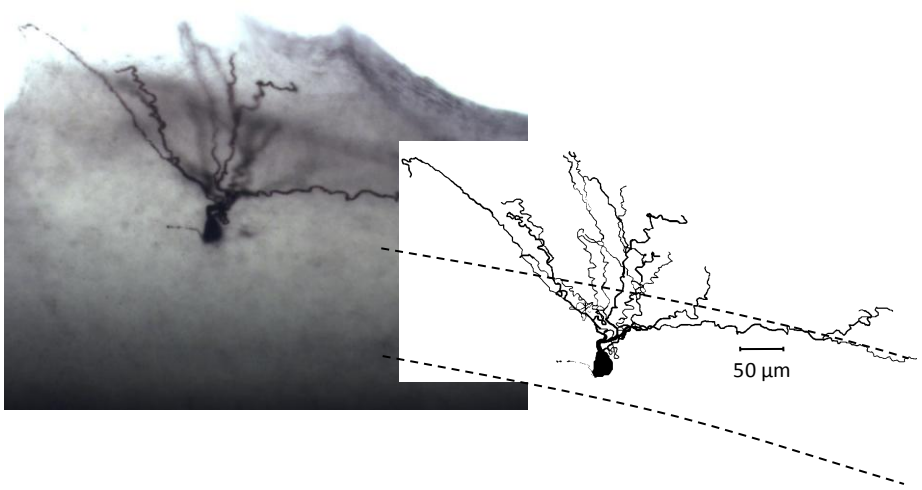

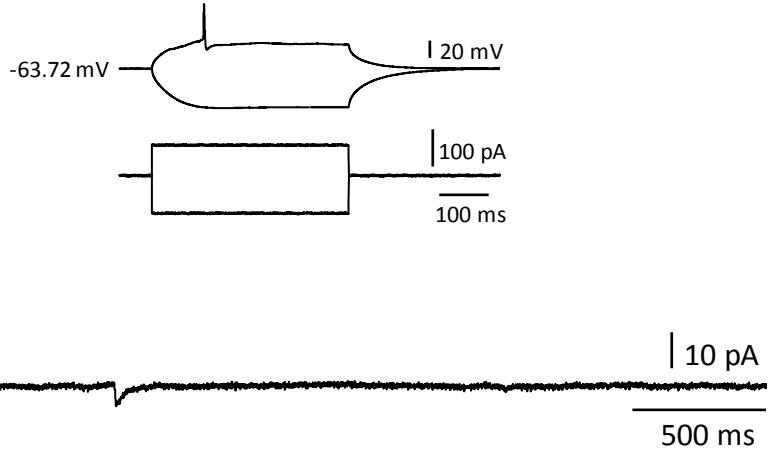

RAT - SE #2 DOB 02.08.2012 – Pilo 03.12.2012

Cell#6 CBZ – 04.11.2012 – mEPSC (x20)

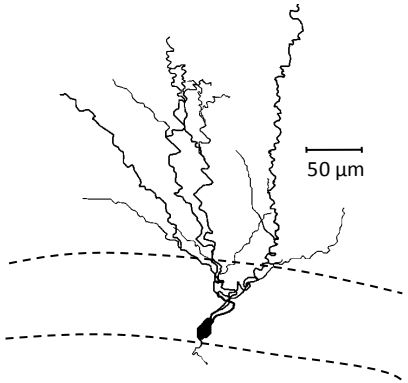

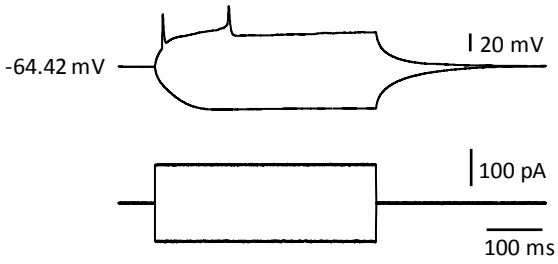

RAT - SE #2 DOB 02.08.2012 – Pilo 03.12.2012

Cell#8 CBZ – 04.11.2012 – mEPSC (x20)

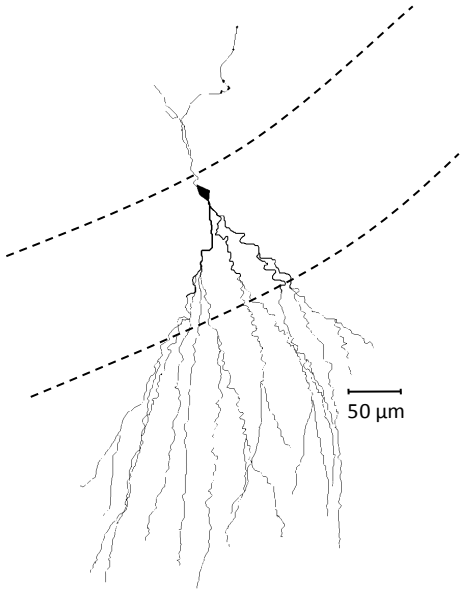

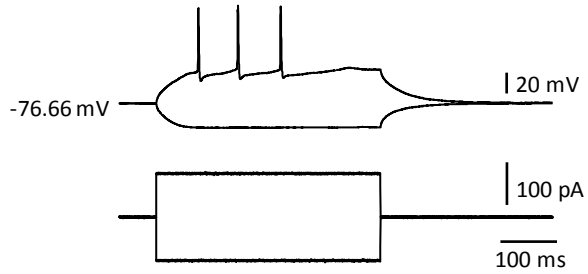

RAT - SE #2 DOB 02.08.2012 – Pilo 03.12.2012

Cell#9 CBZ – 04.11.2012 – mEPSC (x20)

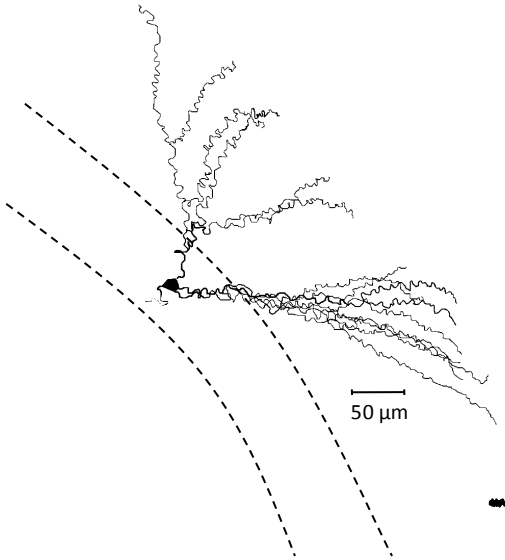

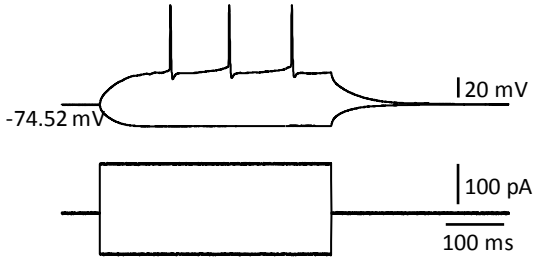

RAT - Control – F DOB – 02.24.12 #37

Cell#11 baseline – 04.12.2012 – mEPSC (x20)

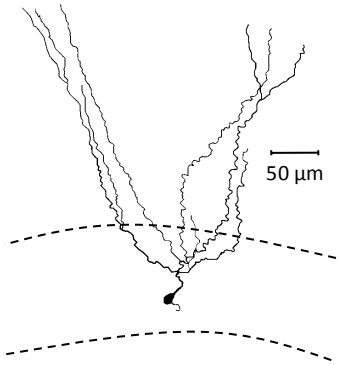

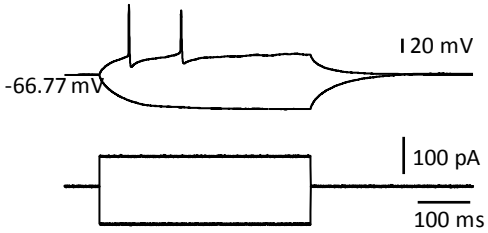

RAT - Control – F DOB – 02.24.12 #37

Cell#12 DC GIV – 04.12.2012 – mEPSC (x20)

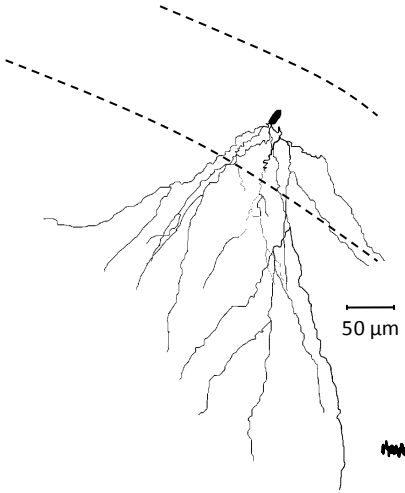

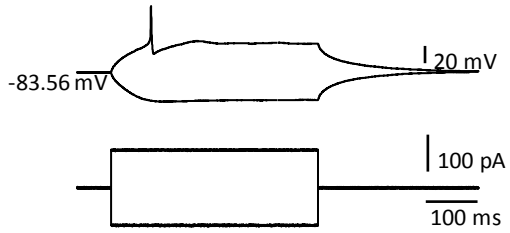

MOUSE - Control – F – 04.16.12 (8 month old)

Cell#14 - Keppra – 04.16.2012 – mEPSC (x20)

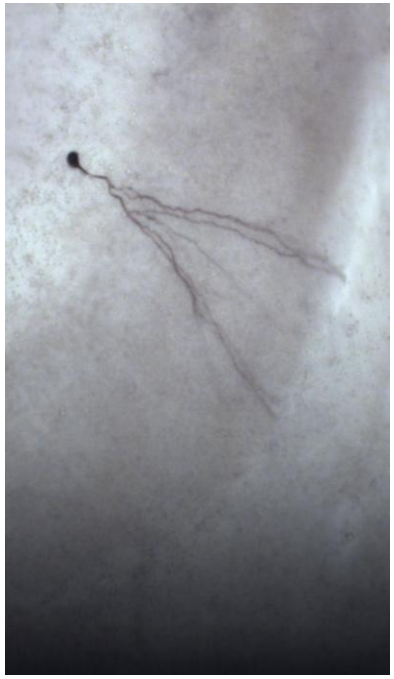

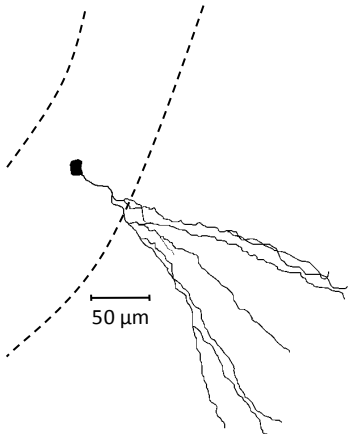

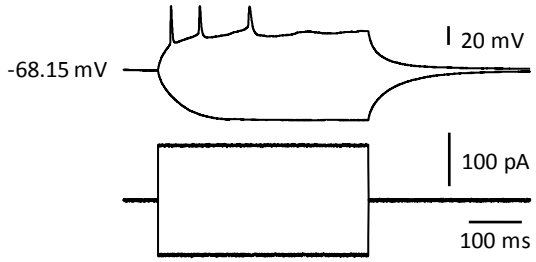

MOUSE - Control – F – 04.17.12 (8 month old)

Cell#20 - Keppra – 04.17.2012 – mEPSC (x20)

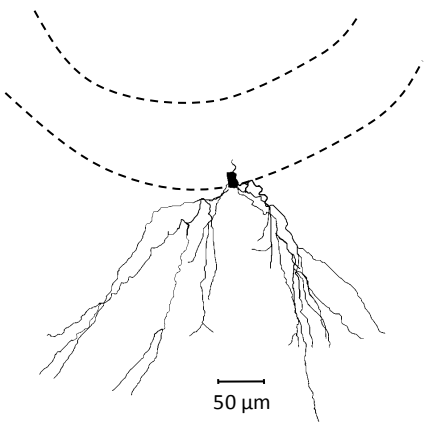

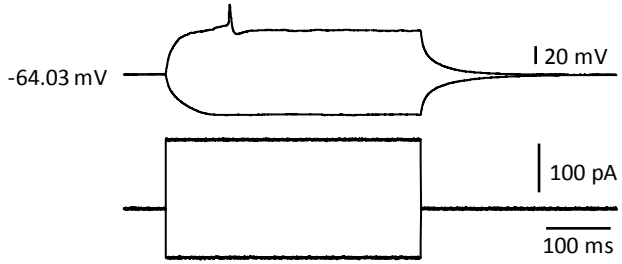

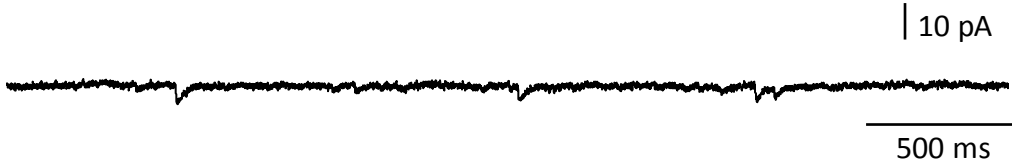

MOUSE - Control – F – 04.17.12 (8 month old)

Cell#22 - Keppra – 04.17.2012 – mEPSC (x20)

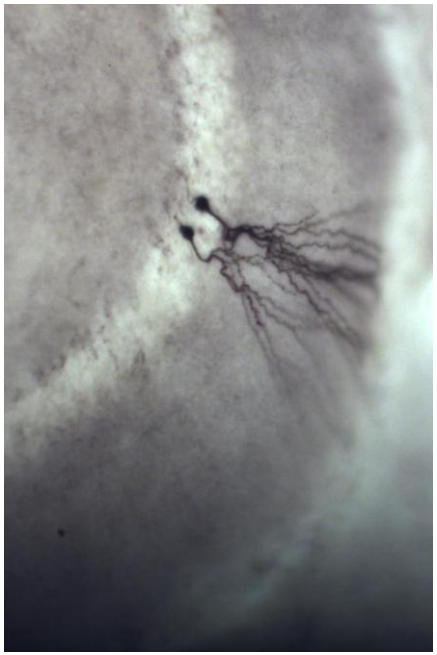

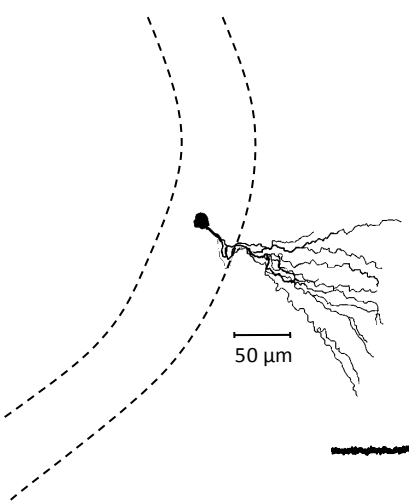

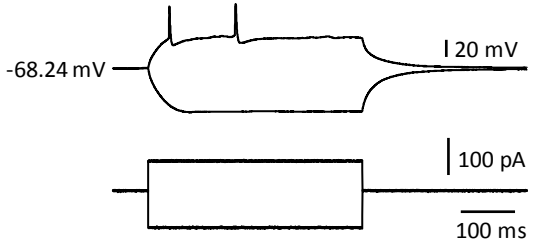

MOUSE – SE, EPSC TAG #155 - 04.23.12

Cell#2 Keppra 50 μM – mEPSC (x20)

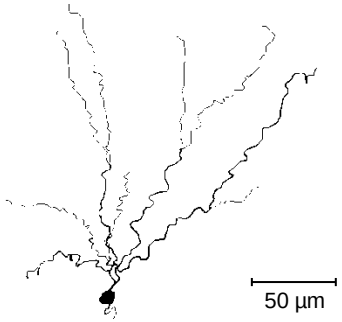

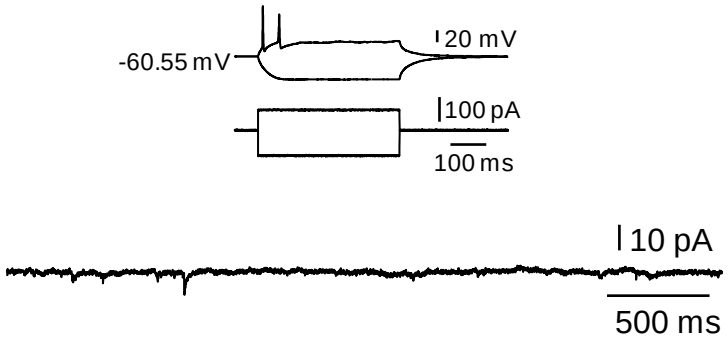

MOUSE KO - SE, EPSC - 04.24.12

Cell#9 Lev. – mEPSC (x20)

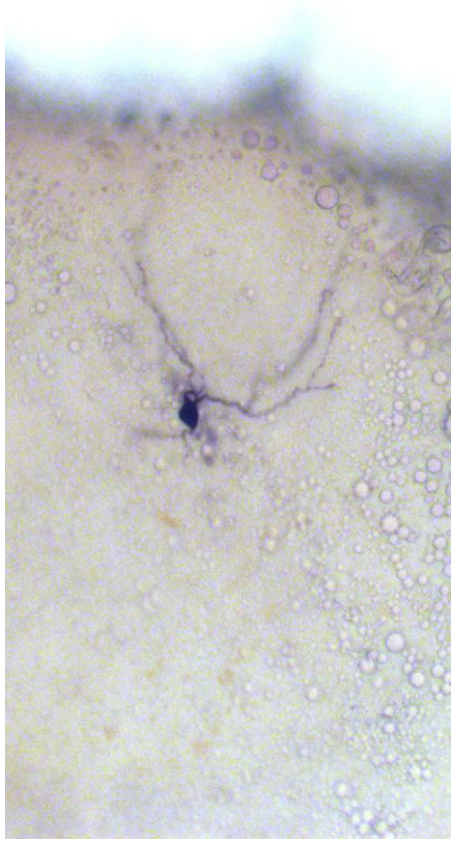

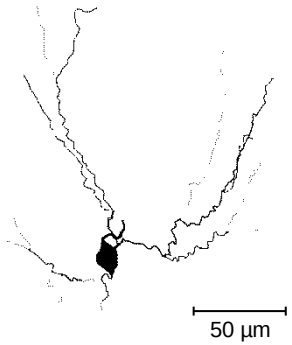

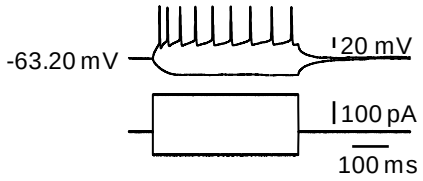

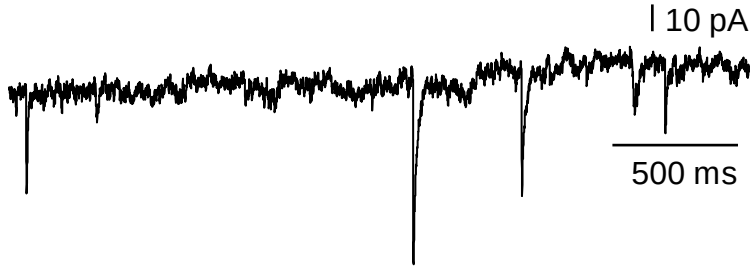

MOUSE C - EPSC – 04.30.12

Cell#14 Keppra 100 μM – mEPSC (x20)

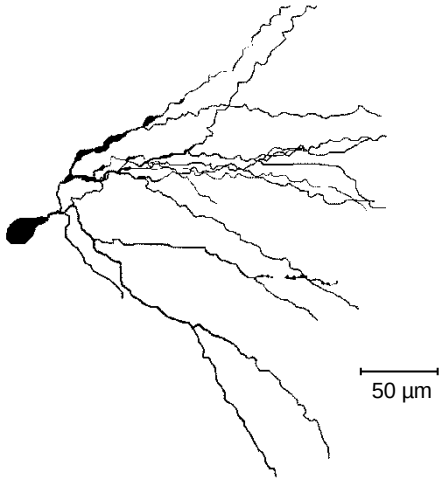

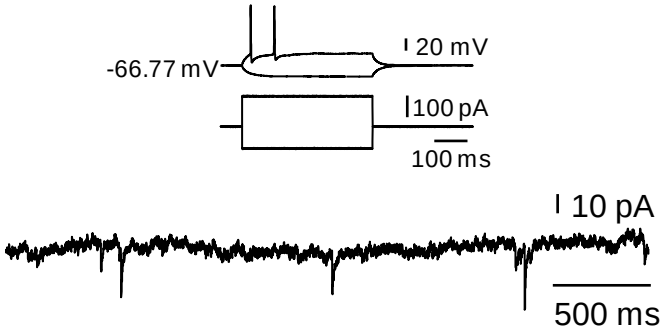

MOUSE C - EPSC – 04.30.12

Cell#15 Keppra 100 μM – mEPSC (x20)

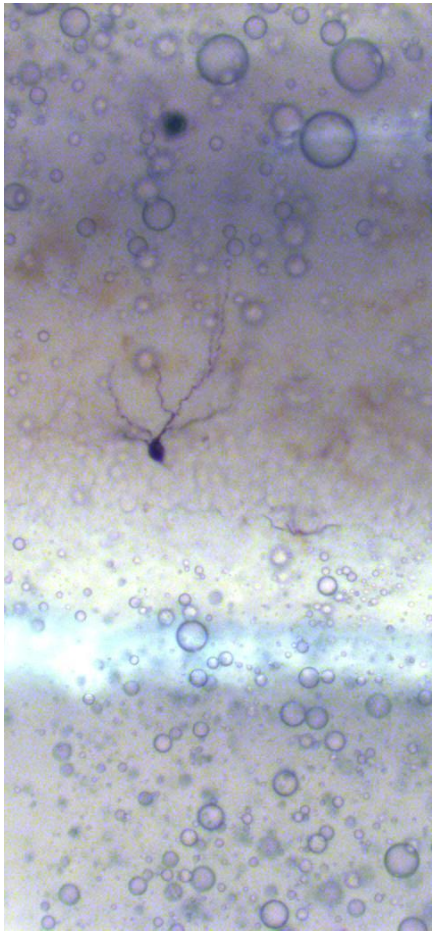

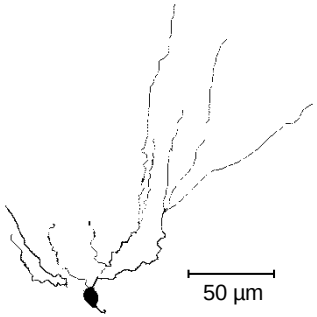

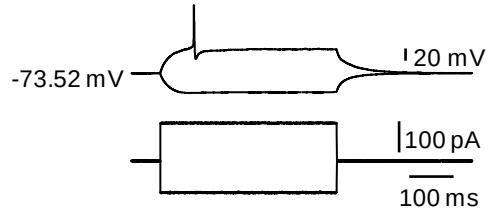

SV2A +/+ EPSC – 04.25.12

Cell#16 SV2A +/+ – mEPSC (x20)